CHARACTERIZATION OF γ-GLUTAMYL TRANSPEPTIDASE AND ELUCIDATING ITS ROLES IN THE PATHOGENESIS OF *HELICOBACTER PYLORI*

LING SHI MIN, SAMANTHA

(B.Sc. (Hons.), NUS)

A THESIS SUBMITTED

FOR THE DEGREE OF DOCTOR OF PHILOSOPHY

DEPARTMENT OF MICROBIOLOGY

NATIONAL UNIVERSITY OF SINGAPORE

2012

ACKNOWLEDGEMENTS

First and foremost, I would like to express my heartfelt gratitude to my supervisor A/P Ho Bow for his patient guidance, encouragement and invaluable support throughout this project. Over these years, he has taught me how to think like a scientist and how to form the right questions to do good science. Without him, this dissertation would definitely not have been possible.

I must also acknowledge Han Chong, my lab officer, for his technical support and friendship throughout my time in this lab as a PhD student. Special thanks also go to Gong Min, Shuxian and Meiling for all their help and invaluable suggestions especially when I just started out on this project. Appreciation goes out to all my fellow postgraduate students in the *Helicobacter pylori* Research Lab (both past and present), including Yan Wing, Yunshan, Mun Fai, Ammar, Vinod and Jin Huei. Thank you for all the help and assistance provided in one way or another. I would also like to specially thank my fiancé and also my best lab mate, Alvin, for always being there for me and for providing me with his continuous support.

I am also grateful to my wonderful family for their love, encouragement and support throughout this time.

Finally, I recognize that this research would not have been possible if not for the financial, academic and technical support of the National University of Singapore, particularly in the award of the NUS Research Scholarship that provided the necessary financial support for this research.

CONTENTS **PAGE**

SUMMARY

Helicobacter pylori is a major etiological agent of various gastroduodenal diseases. Of the known virulence factors of *H. pylori*, γ-glutamyl transpeptidase (GGT) is reported to induce apoptosis in host cells. However, its role in *H. pylori* pathogenesis is still not well characterized.

H. pylori GGT is a heterodimer consisting of a large and small subunit. Cloning, expression and purification of recombinant full length GGT (rGGT), large subunit (rGGTL) and small subunit (rGGTS) were carried out. Monoclonal antibodies raised against rGGT inhibited the enzymatic activity of *H. pylori* GGT by up to 93%. The neutralizing epitope was identified as 428-GNPNLYG-434 and spans a Tyrosine-433 containing loop previously reported to be important for catalysis.

Purified native GGT (nGGT) was found to generate H_2O_2 through thiol-dependent iron reduction as treatment with desferrioxamine (an Fe^{3+} chelator) significantly inhibited this effect. GGT was further found to activate NF-κB and induce interleukin-8 (IL-8) generation in various cell types including primary human gastric cells and macrophages, suggesting a pro-inflammatory effect.

Intriguingly, GGT was discovered to localize in host cell nuclei as observed by transmission electron microscopy, confocal laser scanning microscopy and western blot analysis. The internalization of GGT by AGS cells was identified to occur via the clathrin-mediated endocytosis pathway. GGT was also demonstrated to co-immunoprecipitate with importin β1, suggesting that nuclear import of GGT may be mediated by importin β1. Indeed, siRNA knockdown of importin β1 significantly inhibited the nuclear import of GGT, confirming our hypothesis. Interestingly, nuclear localization of GGT coincided with a decrease in the levels of glutathione in the nucleus, indicative of a role of GGT in causing redox imbalance in host cells.

H. pylori has been reported to cause cellular vacuolation in host cells, a phenomenon attributed to vacuolating cytotoxin and the presence of weak bases. In this study, the process of vacuolation was recorded over 24 hours using real-time microscopy and it was observed that Δ*ggt* induced less vacuolation in AGS cells as compared to the parental strain. Vacuolating ability of wild type was also significantly reduced in the absence of glutamine while exogenous ammonium chloride rescued the ability of Δ*ggt* to induce vacuolation as determined by neutral red assay. Hence, this indicates that ammonia generated by GGT through glutamine hydrolysis is an important contributory factor to vacuolation.

rGGT was also shown to exhibit potential as a diagnostic marker for *H. pylori* infection as significantly higher anti-GGT antibody levels ($P<0.01$) were detected in *H. pylori*-positive subjects (n=58) compared to *H. pylori*-negative controls (n=65). This suggests that GGT is capable of provoking an immune response in the host.

In conclusion, this study has demonstrated the capability of GGT in generating H_2O_2, activating NF-κB and upregulating IL-8 in host cells. Furthermore, GGT is endocytosed by gastric cells and subsequently transported into the cell nucleus where it depletes nuclear glutathione. In addition, GGT also strongly potentiates vacuolation by generating ammonia from glutamine hydrolysis. Taken together, GGT has been shown to be a potent virulence factor that ignites multiple pathways leading to host cell damage.

LIST OF TABLES **PAGE**

LIST OF FIGURES **PAGE**

LIST OF VIDEOS **PAGE**

LIST OF ABBREVIATIONS

BabA	Blood group antigen binding adhesin
BHI	Brain heart infusion
BSA	Bovine serum albumin
CagA	Cytotoxin-associated gene A
*cag*PAI	Cytotoxin-associated gene pathogenicity island
CBA	Chocolate blood agar
CFU	Colony-forming unit
CLIC	Clathrin- and dynamin-independent carrier
CLSM	Confocal laser scanning microscopy
CMFDA	5-chloromethylfluorescein diacetate
Co-IP	Co-immunoprecipitation
CPZ	Chlorpromazine
DFO	Desferrioxamine
DON	6-diazo-5-oxo-L-norleucine
DTT	Dithiothreitol
EGFR	Epidermal growth factor receptor
ELISA	Enzyme-linked immunosorbent assay
ER	Endoplasmic reticulum
GEEC	GPI-AP enriched early endosomal compartment
GGT	γ-glutamyl transpeptidase
GPI-AP	glycosylphosphatidylinositol-anchored protein
GSH	Glutathione
H_2O_2	Hydrogen peroxide
HPLC	High performance liquid chromatography

IκB	Inhibitor of NF-κB
IceA	Induced by contact with epithelium antigen
IL	Interleukin
IPTG	Isopropyl-β-D-thiogalactopyranoside
LB	Luria-Bertani
Le	Lewis
LPS	Lipopolysaccharide
MALDI-TOF	Matrix-assisted laser desorption/ionization time-of-flight
miR	microRNA
MOI	Multiplicity of infection
MTT	3-(4, 5- dimethylthiazolyl-2)-2, 5-diphenyltetrazolium bromide
NAC	N-acetylcysteine
NF-κB	Nuclear factor kappa B
nGGT	Native GGT
NLS	Nuclear localization signal
Nod1	Nucleotide-binding oligomerization domain protein
NPC	Nuclear pore complex
NYS	Nystatin
OD	Optical density
OipA	Outer inflammatory protein A
PBS	Phosphate-buffered saline
PBS-T	Phosphate-buffered saline-Tween 20
PCR	Polymerase chain reaction
PI	Propidium iodide
PVDF	Polyvinylidene fluoride

rGGT	Recombinant full length GGT
rGGTL	Recombinant large subunit of GGT
rGGTS	Recombinant small subunit of GGT
ROS	Reactive oxygen species
RPMI	Roswell Park Memorial Institute
RPTP	Receptor protein tyrosine phosphatase
SabA	Sialic acid binding adhesin
SBC	Serine-borate complex
SD	Standard deviation
SDS-PAGE	Sodium dodecyl sulphate-polyacrylamide gel electrophoresis
siRNA	Small interfering RNA
sLe	sialyl-Lewis
T4SS	Type IV secretion system
TAE	Tris acetate EDTA
TE	Tris-EDTA
TEM	Transmission electron microscopy
Tipα	TNF-α inducing protein
TLR	Toll-like receptor
TMB	Tetramethylbenzidine
TNF-α	Tumour necrosis factor alpha
VacA	Vacuolating cytotoxin A
V-ATPase	Vacuolar-type ATPase
X-gal	5-bromo-4-chloro-indolyl-β-D- galactopyranoside

LIST OF PUBLICATIONS

I. JOURNALS

1. Gong, M.*, **Ling, S.S.M.***, Lui, S.Y., Yeoh, K.G., and Ho, B. (2010). *Helicobacter pylori* γ-glutamyl transpeptidase is a pathogenic factor in the development of peptic ulcer disease. Gastroenterology *139*, 564-573.

   *co-first authors

2. **Ling, S.S.M.**, Khoo, L.H.B., Hwang, L.A., Yeoh, K.G., and Ho, B. *Helicobacter pylori* γ-glutamyl transpeptidase is a potentiator of VacA-dependent vacuolation. (Submitted).

3. **Ling, S.S.M.**, and Ho, B. Role of *Helicobacter pylori* γ-glutamyl transpeptidase in depleting nuclear glutathione. (In preparation).

II. CONFERENCES

1. **S.S.M. LING**, L.H.B. Khoo, L.A. Hwang and B. Ho. (2011). Neutralizing monoclonal antibodies are effective against *Helicobacter pylori* γ-glutamyl transpeptidase. XXIV International Workshop on Helicobacter and Related Bacteria in Chronic Digestive Inflammation and Gastric Cancer. Dublin, Ireland, September 11-13, 2011. Helicobacter *16*(Suppl 1), 101. (Poster; Abstract no.: P03.13)

2. **S.S.M. LING**, M. Gong, K.G. Yeoh, S.Y. Lui and B. Ho. (2010). *H. pylori* gamma-glutamyl transpeptidase (GGT) causes cell damage. XXIII International Workshop on Helicobacter and Related Bacteria in Chronic Digestive Inflammation and Gastric Cancer. Rotterdam, Netherlands, September 16-18, 2010. Helicobacter *15*(4), 319. (Oral; Abstract no.: W3.1)

3. **LING S.S.M.**, Khoo H.B.L., Hwang L.A. and Ho B. (2009). Monoclonal antibodies against *Helicobacter pylori* γ-glutamyl transpeptidase display neutralizing activity. 15th International Workshop on Campylobacter, Helicobacter, and Related Organisms. Niigata, Japan, September 2-5, 2009. (Poster; Abstract no.: P-141)

4. **LING S.S.M.**, Gong M. and Ho B. (2007). Apoptosis-inducing abilities of *Helicobacter pylori* and its γ-glutamyl transpeptidase isogenic mutants. National Healthcare Group Annual Scientific Congress. Singapore, November 10-11, 2007. Ann. Acad. Med. Singapore *36* Suppl. (11), S38. (Poster; Abstract no.: BAS 001)

5. **LING S.S.M.**, Gong M. and Ho B. (2007). Construction of *H. pylori* γ-glutamyl transpeptidase isogenic mutants. European Helicobacter Study Group. XX International Workshop on Helicobacter and Related Bacteria in Chronic Digestive Inflammation. Istanbul, September 20-22, 2007. Helicobacter *12*(4), 415. (Poster; Abstract no.: P026)

INTRODUCTION

1.1 Association of *Helicobacter pylori* and gastroduodenal diseases

Helicobacter pylori was first isolated in 1983 from human gastric biopsy specimens of patients with active chronic gastritis (Warren and Marshall, 1983). This landmark discovery initiated a major revolution in the field of gastroenterology during a time when stomach ulcers and gastritis were thought to be caused by excessive acid production in the stomach due to stress or the intake of spicy food (Marshall and Warren, 1984). Also, it was believed that no bacterium could survive for long in the acidic environment of the stomach. Further research then found *H. pylori* infection to be strongly associated with the development of a range of gastroduodenal diseases such as peptic ulcer disease (Peterson, 1991), chronic gastritis (Cover and Blaser, 1992a), mucosa-associated lymphoid tissue lymphomas (Parsonnet *et al.*, 1994) and even gastric cancer (De Koster *et al.*, 1994). In 1994, *H. pylori* was classified as a type I carcinogen for gastric cancer by the International Agency for Research on Cancer (IARC, 1994). This knowledge led to a major change in the clinical management of these diseases where antibiotics were subsequently added into the treatment regimen, along with histamine H2 receptor antagonists and proton pump inhibitors (Veldhuyzen van Zanten and Sherman, 1994).

1.2 Virulence factors of *H. pylori*

Approximately half of the world's population is reported to be infected with *H. pylori* (Covacci *et al.*, 1999; Linz *et al.*, 2007). Among these, approximately 10% develop peptic ulcer disease while 1-3% eventually develop gastric adenocarcinoma (Wroblewski *et al.*, 2010).

Disease progression largely depends on the virulence of the infecting *H. pylori* strain although host and environmental factors have also been reported to affect

clinical outcomes (Shanks and El-Omar, 2009). *H. pylori* is a highly heterogeneous bacterium (Linz *et al.*, 2007; Moodley *et al.*, 2009), having co-evolved with humans ever since they migrated out of Africa about 58000 years ago (Moodley and Linz, 2009). As a result, the virulence of the pathogen has also diverged and bacterial virulence factors are likely to play a major role in determining the outcome of *H. pylori* infection. One of the more extensively studied pathogenic factors is cytotoxin-associated gene A (CagA) where in western countries, individuals infected with *cagA*-positive *H. pylori* strains have a higher risk of developing more severe gastroduodenal diseases compared to those infected with *cagA*-negative strains (Covacci *et al.*, 1993; van Doorn *et al.*, 1998). However, in East Asia, where majority of *H. pylori* strains are *cagA*-positive, the presence or absence of *cagA* cannot fully account for differences in clinical pathologies (Maeda *et al.*, 1998; Zheng *et al.*, 2000).

The second most extensively studied virulence factor is vacuolating cytotoxin A (VacA). Differences in *vacA* gene structure can be found at the signal (s) region (namely s1 and s2), the middle (m) region (m1 and m2) (Atherton *et al.*, 1995) and the more recently identified intermediate (i) region which is located between the s and m regions (Rhead *et al.*, 2007). Similar to *cagA*, *vacA* s1/m1 alleles have been strongly associated with peptic ulcer disease and gastric cancer in western populations (Atherton *et al.*, 1997; Miehlke *et al.*, 2000) but in East Asia, where strains are mostly *vacA* s1/m1, such correlations were not observed (Yamaoka *et al.*, 1999).

From these studies, it can be inferred that CagA and VacA are probably not the only factors contributing to *H. pylori* pathogenesis. To date, many other virulent determinants have also been identified. Some examples include urease which helps neutralize the acidic environment of the stomach (Eaton *et al.*, 1991), flagella which confers motility to the organism (Ottemann and Lowenthal, 2002), and various

adhesins such as blood group antigen binding adhesin (BabA) (Ilver *et al.*, 1998), outer inflammatory protein A (OipA) (Yamaoka *et al.*, 2000) and sialic acid binding adhesin (SabA) (Yamaoka, 2008). This study focuses on another important virulence factor of *H. pylori* known as γ-glutamyl transpeptidase (GGT) [EC. E.3.2.2] (McGovern *et al.*, 2001).

1.3 γ-glutamyl transpeptidase (GGT)

GGT is fairly ubiquitous and can be found across several kingdoms such as bacteria (Xu and Strauch, 1996; Wada *et al.*, 2008), plants (Martin and Slovin, 2000; Martin *et al.*, 2007) and animals (Chikhi *et al.*, 1999). In mammalian tissues, GGT is embedded in the plasma membrane and plays an important role in glutathione (GSH, L-γ-glutamyl-L-cysteinylglycine) metabolism (Tate and Meister, 1981). It catalyzes reactions in which a γ-glutamyl moiety is transferred from γ-glutamyl compounds, such as GSH, to amino acids (transpeptidation) or water (hydrolysis) (Keillor *et al.*, 2005).

1.3.1 *H. pylori* GGT

GGT in *H. pylori* is synthesized as a 60 kDa pro-enzyme and is subsequently autoprocessed into a heterodimer comprising a large and small subunit with masses of about 40 and 20 kDa respectively. It is a secreted protein (Bumann *et al.*, 2002) that is highly conserved within the *H. pylori* species and has been reported to be expressed in all *H. pylori* strains (Chevalier *et al.*, 1999).

1.3.2 GGT and *H. pylori* pathogenesis

H. pylori GGT was found to confer a colonizing advantage to the bacteria in both mice and gnotobiotic piglet animal models (Chevalier *et al.*, 1999; McGovern *et al.*, 2001). In addition, *H. pylori* GGT has been reported to induce apoptosis in gastric epithelial cells (Shibayama *et al.*, 2003) via the mitochondrial pathway (Kim *et al.*, 2007). It has also been shown to upregulate cyclooxygenase-2 and epidermal growth factor-related peptide expression (Busiello *et al.*, 2004), inhibit T-cell proliferation (Schmees *et al.*, 2007), induce cell cycle arrest (Kim *et al.*, 2010) as well as upregulate microRNA-155 (miR-155) expression in T cells (Fassi Fehri *et al.*, 2010). In addition, it was earlier found in our laboratory by Dr. Gong M. (2006) that purified *H. pylori* native GGT (nGGT) induces production of hydrogen peroxide (H_2O_2) leading to nuclear factor kappa B (NF-κB) activation and interleukin-8 (IL-8) generation in gastric cancer cells. Furthermore, in the same study, *H. pylori* GGT was also shown to be associated with the development of peptic ulcer disease.

1.4 Objectives of the study

Despite many studies describing the effects of *H. pylori* GGT on the host, the underlying mechanisms are relatively unknown. Hence, this work aims to further characterize *H. pylori* GGT and its pathogenic effects, as well as to determine the mechanism(s) behind its actions. To address this, the study will focus on the following objectives:

- Cloning of *ggt* gene (full length and individual large and small subunits) from *H. pylori* and expressing the recombinant proteins in *E. coli*
- Raising and characterizing specific polyclonal and monoclonal antibodies against GGT
- Determining the subcellular localization of GGT in *H. pylori*
- Investigating the mechanism by which GGT produces reactive oxygen species (ROS)
- Assessing the ability of GGT in inducing IL-8 generation in various cell types
- Analyzing GGT entry into host cells and its probable downstream effects
- Examining the role of GGT in vacuolation induction
- Exploring the potential of GGT as a diagnostic marker for *H. pylori* infections

LITERATURE SURVEY

2.1 *Helicobacter pylori* – the organism

2.1.1 History

Gastric spiral microorganisms were first described in the 19th century by Giulio Bizzozero who observed them in the stomach of dogs (Bizzozero, 1893). Soon after, similar spiral bacteria were also seen in the human stomach (Doenges, 1938; Freedberg and Baron, 1940). However, the microbes did not gain much attention until the 1970s when spirals were observed, using transmission electron microscopy (TEM), on the surface of epithelial cells in gastric biopsies from gastric ulcer patients (Steer, 1975). Eight years later, Warren and Marshall successfully isolated a spiral *Campylobacter*-like organism from human gastric biopsy specimens (Warren and Marshall, 1983). Self-ingestion of a pure culture of *H. pylori* by Marshall and Morris on separate occasions later demonstrated that these bacteria were capable of colonizing the human stomach and inducing inflammation of the gastric mucosa (Marshall *et al.*, 1985; Morris and Nicholson, 1987), thus fulfilling Koch's postulates.

When first isolated, the organism was described as *Campylobacter*-like (Warren and Marshall, 1983). A year later, it was subsequently renamed formally as *Campylobacter pyloridis* (Marshall *et al*., 1984) and changed again to *Campylobacter pylori* in 1987 (Marshall and Goodwin, 1987). However, due to taxonomic differences such as in ultrastructure features (Goodwin *et al.*, 1985) and ribonucleic sequences (Romaniuk *et al.*, 1987) from the *Campylobacter* genus, coupled with its helical morphology, the genus *Helicobacter* was created and the organism was then renamed as *Helicobacter pylori* (Goodwin *et al.*, 1989). The discovery of *H. pylori* fuelled further research over the next 30 years and it is now considered the most common etiologic agent of various gastroduodenal diseases including chronic gastritis, peptic ulcer disease, gastric lymphoma and gastric adenocarcinoma (Ernst and Gold, 2000;

Atherton, 2006). For their groundbreaking work on the discovery of *H. pylori* and its role in peptic ulcer disease, Warren and Marshall were subsequently awarded the Nobel Prize in Physiology or Medicine in 2005.

2.1.2 Characteristics of *H. pylori*

H. pylori is a Gram-negative bacterium that selectively colonizes the human gastric mucosa. The spiral-shaped microorganism measures 2-4 μm in length and approximately 0.5 μm in width. On culture plates, *H. pylori* forms small translucent colonies of about 0.5-2 mm in diameter after 2 to 3 days.

2.1.2.1 Morphological forms

H. pylori exists in two morphological forms, namely spiral and coccoid. The spiral form is considered to be the active form where the organism is viable, culturable, virulent and able to colonize experimental animals (Eaton *et al.*, 1995; Cole *et al.*, 1997). Conversion from the actively dividing spiral form to the non-culturable coccoid form can occur after prolonged *in vitro* culture (Hua and Ho, 1996) or under unfavourable conditions such as antibiotic treatment (Berry *et al.*, 1995; Kusters *et al.*, 1997) or increased oxygen tension (Catrenich and Makin, 1991). The role of the coccoid form in *H. pylori* pathogenesis has been controversial. It has been suggested that the coccoid form of *H. pylori* is a degenerate nonviable phase which is non-virulent (Eaton *et al.*, 1995; Kusters *et al.*, 1997) while others have presented evidence that the coccoid form is metabolically active, hence likely to be viable although non-culturable (Zheng *et al.*, 1999; Willen *et al.*, 2000) and may be involved in transmission and infection (Shahamat *et al.*, 1993; Vijayakumari *et al.*, 1995; Ng *et al.*, 2003).

2.1.2.2 Growth requirements

H. pylori is a microaerophile, requiring between 2-5% O_2 levels and 5-10% CO_2 for optimal growth. The organism is able to grow at temperatures between 33-40°C, with 37°C being the most ideal (Owen, 1995). Although *H. pylori* will survive brief exposures to pH < 4.0, growth occurs only between pH 5.5-8.5 with good growth between pH 6.9 and 8.0, hence classifying it as a neutralophile (Owen, 1995; Scott *et al.*, 2002).

Being a fastidious microorganism, *H. pylori* requires complex media which are often supplemented with blood or serum. Commonly used solid media include Columbia or Brucella agar supplemented with 7-10% lysed horse or sheep blood (Andersen and Wadström, 2001). Chocolate blood agar (containing 5% lysed horse blood) has also been frequently used (Xia *et al.*, 1996; Hua *et al.*, 2000). High humidity and moist plates are important for its growth (Marshall and Warren, 1984). Liquid media can also be used to culture *H. pylori* and these include Mueller-Hinton broth, Columbia broth, brucella broth or brain heart infusion broth supplemented with 10% horse serum (Shahamat *et al.*, 1991; Ho and Vijayakumari, 1993).

2.2 Epidemiology of *H. pylori* infections

2.2.1 Prevalence of *H. pylori*

H. pylori has been reported to chronically infect at least half of the world's population (Covacci *et al.*, 1999; Linz *et al.*, 2007). The prevalence of *H. pylori* infection, however, exhibits large geographical variations. In various developing countries, infection rates are high such that more than 80% of the population are positive for *H. pylori.* In contrast, the rate of infection in developed countries generally remains under 40% (Perez-Perez *et al.*, 2004). Within geographical areas,

socioeconomic status (defined by occupation, family income level and living conditions) has been shown to be inversely related to *H. pylori* prevalence (Graham *et al.*, 1991; Dattoli *et al.*, 2010; Bauer *et al.*, 2011). Other factors which have also been statistically associated with *H. pylori* prevalence include ethnicity (Graham *et al.*, 1991; Zaterka *et al.*, 2007) and increasing age (Dube *et al.*, 2009; Jackson *et al.*, 2009).

In Singapore, prevalence of *H. pylori* has been found to increase with age, from 3% of children below the age of five to 71% of adults above 65 years (Epidemiological News Bulletin, 1996). Interestingly, distinct racial patterns have also been observed where *H. pylori* seroprevalence was found to be consistently higher in Indians and Chinese compared to Malays who displayed unusually low prevalence (Epidemiological News Bulletin, 1996; Kang *et al.*, 1997; Goh and Parasakthi, 2001), suggesting that environmental factors (e.g. diet, culture, etc) and genetic predisposition may play a role in *H. pylori* infection.

2.2.2 Routes of transmission

The route of transmission for *H. pylori* is still not completely understood. *H. pylori* has a narrow host range where it has been found almost exclusively in humans (Megraud and Broutet, 2000) and in some cases, non-human primates (Dubois *et al.*, 1995; Solnick *et al.*, 2003) and domestic cats (Handt *et al.*, 1994). New infections, including vertical transmission (Ng *et al*., 2001), however, are thought to occur via direct human-to-human transmission by gastro-oral, oral-oral and fecal-oral routes. *H. pylori* has been successfully isolated from fecal samples (Thomas *et al.*, 1992), saliva (Ferguson *et al.*, 1993) and vomitus (Leung *et al.*, 1999) but none of these have been conclusively proven to be the predominant vehicle of transmission. There is also

evidence that transmission of *H. pylori* may be waterborne and this could be particularly important in areas with poor sanitation (Klein *et al.*, 1991; Mazari-Hiriart *et al.*, 2001). However, most of these studies have only detected the presence of *H. pylori* DNA in water sources by molecular techniques and not by direct culture with the exception of a few reports (Lu *et al.*, 2002; Al-Sulami *et al.*, 2010). Water as a route of transmission would also require *H. pylori* to remain viable in the extragastric environment and this has faced much controversy given the fastidious nature of the organism in terms of oxygen sensitivity, nutrient availability and temperature range. Hence, the transmission of *H. pylori* is still a largely inconclusive area of study.

2.3 *H. pylori*-associated diseases

Gastric colonization with *H. pylori* causes chronic gastric inflammation in virtually all infected individuals although majority remain asymptomatic (Peek and Blaser, 2002). However, long-term carriage of the pathogen significantly increases the risk of various gastroduodenal diseases. For instance, the lifetime risk of developing peptic ulcer disease (including gastric and duodenal ulcers) in *H. pylori*-positive subjects is estimated to be 10-20% (Kuipers *et al.*, 1995) which is 3-4 fold higher than in non-infected individuals (Nomura *et al.*, 1994). It has not been clearly established as to how *H. pylori* causes peptic ulcers but there is evidence indicating that *H. pylori* infection elevates gastrin levels which plays an important role in the regulation of gastric acid secretion (Calam *et al.*, 1997). Elevated gastric acid secretion predisposes patients to duodenal ulcers while low acid secretion has been associated with gastric ulcers (Kuipers *et al.*, 1995).

Apart from peptic ulcer development, *H. pylori* infection has also been strongly associated with an increased risk of developing gastric adenocarcinoma – the

second highest cause of cancer deaths worldwide (Uemura *et al.*, 2001; Atherton, 2006). Approximately 1-3% of infected individuals eventually develop gastric cancer and less than 0.1% develop mucosa-associated lymphoid tissue lymphoma (Wroblewski *et al.*, 2010). It is believed that *H. pylori* causes gastric cancer both directly (through induction of protein modulation and gene mutation) as well as indirectly (through induction of chronic inflammation) (Chiba *et al.*, 2008). The progression of gastric carcinogenesis has been well described by the Correa pathway (Correa, 1988). However, the exact mechanism involved is still not completely understood.

Non-ulcer dyspepsia has also been linked to *H. pylori* infection although the relationship remains controversial (Armstrong, 1996). Non-ulcer dyspepsia is defined as persistent or recurrent pain or discomfort centred in the upper abdomen without any definite structural explanation for the symptoms (Talley and Xia, 1998). Prevalence of *H. pylori* in non-ulcer dyspepsia patients have been found to be as high as 50% but a causal relationship remains to be established (Talley and Quan, 2002). Symptom improvement after eradication of *H. pylori* in non-ulcer dyspepsia patients has also yielded conflicting results where some groups have reported a small but significant improvement (Moayyedi *et al.*, 2006) while others did not find any significant difference (Laine *et al.*, 2001).

2.4 Virulent determinants of *H. pylori* pathogenesis

2.4.1 Cell surface factors

2.4.1.1 Flagella

In addition to its spiral shape, *H. pylori* possesses 2-6 unipolar sheathed flagella, about 3-5 μm in length. Often, a club-shaped terminal structure or bulb is

seen at the end of the filament (Geis *et al.*, 1989). The flagella give the organism strong motility for burrowing into the viscous stomach mucus to reach the gastric epithelium (Hazell *et al.*, 1986). It also enables it to overcome peristaltic flushing (Dubois, 1995) and has been reported to be important for colonization of the gastric mucosa in the gnotobiotic piglet model (Eaton *et al.*, 1992).

2.4.1.2 Adhesins and outer membrane proteins

Adherence of *H. pylori* to the gastric epithelium is important for initial colonization and persistence as it protects the organism from clearance mechanisms such as peristaltic movements and liquid flow. *H. pylori* possesses several adhesins to aid in its adhesion to host cell receptors where approximately 4% of its genome encodes for outer membrane proteins (Yamaoka, 2010). The role of three such proteins will be described here and they include BabA, SabA and OipA (Magalhaes and Reis, 2010).

BabA is a 78 kDa protein encoded by the *babA* gene and mediates binding to fucosylated Lewis b (Le^b) blood group antigens on human host cells (Ilver *et al.*, 1998). There are two distinct *babA* alleles, namely *babA1* and *babA2*, but only *babA2* encodes active BabA. Strains possessing the *babA2* gene have been found to be strongly associated with increased epithelial proliferation and inflammation as well as an increased risk for peptic ulcer and gastric adenocarcinoma (Gerhard *et al.*, 1999; Yu *et al.*, 2002).

SabA has been found to mediate binding to sialyl-Lewis x/a antigens (sLe^x and sLe^a) (Mahdavi *et al.*, 2002). This is important as *H. pylori*-induced gastric inflammation and gastric carcinoma have been reported to be associated with the replacement of non-sialylated Lewis antigens by sLe^x and sLe^a (Sakamoto *et al.*,

1989; Ota *et al.*, 1998). Clinically, SabA has also been associated with severe intestinal metaplasia, gastric atrophy and the development of gastric cancer (Yamaoka *et al.*, 2006). As such it has been proposed that *H. pylori* adherence during chronic infection may occur via two separate receptor-ligand interactions, one of which occurs by Le^b-mediated adherence through BabA and the other through the weaker sLe^x/sLe^a-mediated adherence by SabA (Mahdavi *et al*., 2002).

OipA is a 34 kDa phase-variable outer membrane protein of *H. pylori* which was originally identified as a proinflammatory response-inducing protein (Yamaoka *et al.*, 2000). The *oipA* gene is present in all strains but expression of the protein is regulated by a variable number of CT dinucleotide repeats in the 5' region of the gene, leading to either an "on" or "off" status (Yamaoka *et al.*, 2000). *In vitro*, OipA has been shown to facilitate attachment of *H. pylori* to gastric epithelial cells (Dossumbekova *et al.*, 2006). It has also been reported to play a role in *H. pylori* colonization of the gastric mucosa in both the mice and Mongolian gerbil animal models (Akanuma *et al.*, 2002; Yamaoka *et al.*, 2002b). Clinically, an *oipA*-positive status has been significantly associated with duodenal ulcers and gastric cancer (Yamaoka *et al.*, 2006). However, as the *oipA* "on" status is closely linked to other virulence factors such as functional *vacA*, *babA* and *cagA* (Dossumbekova *et al.*, 2006), *oipA* may be linked to gastroduodenal diseases because of this association.

2.4.1.3 Lipopolysaccharides (LPS)

Similar to other Gram-negative bacteria, the cell envelope of *H. pylori* consists of an inner membrane, periplasm with peptidoglycan and an outer membrane. The outer membrane is made up of phospholipids and LPS. The latter comprises the core oligosaccharide, an O antigen side chain and lipid A. Unlike the lipid A moiety of

other Gram-negative bacteria, the LPS of *H. pylori* has low endotoxic activity (Muotiala *et al.*, 1992). In addition, the O antigen side chain of *H. pylori* can be post-translationally fucosylated to generate Le antigens which are also found on human blood erythrocytes and epithelial cells (Nilsson *et al.*, 2006), including those found in the gastric mucosa (Appelmelk *et al.*, 1996). This molecular mimicry is thought to help the pathogen evade the host immune system and allow persistance of infection (Vandenbroucke-Grauls and Appelmelk, 1998).

2.4.2 Cytotoxin-associated gene pathogenicity island (*cag*PAI)

The *cag*PAI is a genomic region of about 40 kb that contains between 27 to 31 genes (Censini *et al.*, 1996; Akopyants *et al.*, 1998). A subset of these genes have been found to encode for multiple structural components of a bacterial type IV secretion system (T4SS) which forms a syringe-like structure responsible for the translocation of various effector molecules from the bacteria into host gastric epithelial cells (Busler *et al.*, 2006). To date, two bacterial molecules have been shown to be selectively translocated into host cells via the T4SS, namely CagA (Backert *et al.*, 2000) and peptidoglycan (Viala *et al.*, 2004). The latter, upon translocation, is recognized by a cytosolic pathogen recognition molecule known as nucleotide-binding oligomerization domain protein (Nod1), leading to a cascade effect resulting in NF-κB activation and induction of IL-8 secretion by epithelial cells (Viala *et al.*, 2004). Importantly, infection with *cag*PAI-positive *H. pylori* strains has been shown to be associated with more severe disease outcome compared to *cag*PAI-negative strains in humans (Nilsson *et al.*, 2003). A long-term infection study (2-64 weeks) has also been conducted in Mongolian gerbils (Wiedemann *et al.*, 2009). In their study, it was found that the T4SS is essential for inducing severe corpus

inflammation, increase in proinflammatory cytokines as well as mucous gland metaplasia in the first 4-8 weeks of infection. Similarly, at later time points, only those animals infected with wild type *H. pylori* possessing T4SS developed hypochlorhydria and hypergastrinemia in parallel to gastric ulcers and focal dysplesia. These results strongly suggest the important role of *cag*PAI in triggering the events leading to gastric carcinogenesis which is also a multistep process in humans.

2.4.3 Cytotoxin-associated gene A (CagA)

CagA, a 120-140 kDa immunodominant protein, is arguably the most extensively studied virulence factor of *H. pylori*. In the West, numerous reports have found that *H. pylori* strains harbouring CagA are more commonly associated with peptic ulceration and gastric adenocarcinoma as compared to strains which lack the oncoprotein, suggesting its clinical importance in *H. pylori* infections (Blaser *et al.*, 1995; Nomura *et al.*, 2002). However this may only be true for the Western population as studies conducted in the East - where almost all strains are CagA-positive - have not observed such correlations between *cagA* status and clinical outcome (Maeda *et al.*, 1998; Zheng *et al.*, 2000).

CagA is encoded by the *cagA* gene which is found within the *cag*PAI and is the only known protein to date that is translocated into host epithelial cells by the T4SS of *H. pylori* (Odenbreit *et al.*, 2000). Upon translocation into host cells, CagA is phosphorylated by host cell Src and Abl family kinases on tyrosine residues within conserved Glu-Pro-Ile-Tyr-Ala (EPIYA) sequence motifs which are found at the C-terminus of the protein (Selbach *et al.*, 2002; Tammer *et al.*, 2007). Phosphorylated CagA then interacts with the Src homology 2 domains of several eukaryotic signalling proteins including SHP-2, a host cytoplasmic tyrosine phosphatase (Higashi *et al.*,

2002). Subsequent conformational change in SHP-2 leads to inhibition of its phosphatase activity which in turn induces gastric cells cultured *in vitro* to elongate and develop long processes termed the hummingbird phenotype (Segal *et al.*, 1999). Another major effect of phosphorylated CagA is the stimulation of transcription factors such as c-Fos and c-Jun (through increased Erk MAP kinase activation) which in turn leads to a deregulation of epithelial cell proliferation (Meyer-ter-Vehn *et al.*, 2000).

Effects of CagA independent of its phosphorylation status have also been reported. These include disruption of cell-cell junctions, loss of cell polarity and induction of proinflammatory and mitogenic responses (Backert and Selbach, 2008). Such diverse effects are due to the interaction of unphosphorylated CagA with various host proteins. For example, CagA binds to the adaptor protein Grb2 which can then lead to a cascade of signalling events resulting in the stimulation of the Raf/Mek/Erk pathway and subsequent cell scattering (Mimuro *et al.*, 2002). Unphosphorylated CagA can also bind to Par1b (a central regulator of cell polarity) and inhibit its kinase activity, resulting in the eventual loss of cell polarity (Hatakeyama, 2008). Injected CagA also complexes with various tight junction proteins such as zona occludens-1 and junctional adhesion molecule which can result in an ectopic assembly of tight-junction components, leading to loss of function of both tight and adherens junctions (Amieva *et al.*, 2003).

2.4.4 Vacuolating cytotoxin A (VacA)

Another extensively studied virulence factor of *H. pylori* is VacA, a secreted cytoxin that induces cytotoxic vacuolation in cells (Leunk *et al.*, 1988). Unlike the *cag*PAI, the *vacA* gene is present in virtually all strains of *H. pylori* (Atherton *et al.*,

1995). The gene codes for a 140 kDa protoxin which subsequently undergoes proteolytic cleavage during secretion to produce a 90 kDa toxin (Papini *et al.*, 2001). Secreted VacA is then further processed into an N-terminal fragment of 33 kDa (p33) and a C-terminal fragment of 55 kDa (p55) which remain covalently attached (Telford *et al.*, 1994). The p55 domain is responsible for host cell binding (Reyrat *et al.*, 1999) while the p33 domain exhibits pore-forming activity required for the formation of vacuoles in cells (McClain *et al.*, 2003). Several cell receptors for VacA have been identified and these include receptor protein tyrosine phosphatases α and β (RPTPα and β) (Yahiro *et al.*, 1999 and 2003), epidermal growth factor receptor (EGFR) (Seto *et al.*, 1998) as well as sphingomyelin (Gupta *et al.*, 2008). Upon binding to a specific receptor, oligomerization of monomeric VacA occurs and VacA is subsequently endocytosed into the cells via a clathrin-independent pathway.

After internalization, VacA can induce several multiple cellular activities including disruption of endosomal and lysosomal functions (Montecucco and de Bernard, 2003), induction of apoptosis via a mitochondria-dependent pathway (Yamasaki *et al.*, 2006) as well as immunomodulation by inhibiting T and B cell proliferation (Torres *et al.*, 2007). The best studied and most prominent feature of VacA, however, is its ability to induce massive vacuolation in cells, a phenomenon observed both *in vitro* (Cover and Blaser, 1992b) and *in vivo* (Tricottet *et al.*, 1986; Telford *et al.*, 1994). Vacuolating activity, however, varies between different *H. pylori* strains (Cover and Blaser, 1992b). This is primarily due to polymorphism in the *vacA* gene at the signal (s) and middle (m) regions (Atherton *et al.*, 1995). Signal region types include s1 and s2 while mid-region types include m1 and m2. *In vitro* experiments have shown that s1/m1 strains are more cytotoxic than s1/m2 strains while s2/m2 strains are non-toxic and s2/m1 strains are rarely found (Atherton *et al.*,

1995; Letley *et al.*, 1999). Clinically, strains with s1/m1 genotype are also typically associated with more severe gastroduodenal diseases (Sugimoto *et al.*, 2009; Sugimoto and Yamaoka, 2009).

2.4.5 Enzymes

2.4.5.1 Urease

H. pylori produces abundant urease, an enzyme which hydrolyzes urea to generate ammonia and carbon dioxide (Mobley, 2001). The ammonia produced forms a protective microenvironment around the organism and protects it from the acidity of the stomach (Mobley, 1996). Urease is a cytoplasmic enzyme but has also been found on the outside surface of the bacteria due to lysis of a subset of the cell population (Marcus and Scott, 2001). It is a nickel-containing enzyme that consists of UreA and UreB subunits which are encoded in an operon containing the *ureA* and *ureB* genes (Dunn *et al.*, 1990). The effective urease activity is dependent on the availability of urea, its substrate, whose transport into the bacterium is controlled by the proton-gated urea channel UreI (Weeks *et al.*, 2000). Although urease is not essential for *in vitro* viability, it has been reported to be an essential colonization factor in the gnotobiotic piglet model (Eaton *et al.*, 1991). In addition, urease has also been implicated in the dysregulation of tight junctions in gastric epithelial cells through myosin regulatory light chain phosphorylation and occludin internalization (Wroblewski *et al.*, 2009).

2.4.5.2 Catalase

Similar to catalase of other organisms, *H. pylori* catalase catalyzes the decomposition of H_2O_2 into water and oxygen to protect itself against oxygen-

dependent killing mechanisms (Hazell *et al.*, 1991). Although catalase is not required for *in vitro* viability of *H. pylori* (Odenbreit *et al.*, 1996), it is important for survival against the presence of extracellular ROS produced by professional phagocytes (Ramarao *et al.*, 2000) and within the phagosomes of macrophages upon phagocytosis (Basu *et al.*, 2004). Using the *H. pylori* SS1 mouse model, it was also shown that *H. pylori* mutants deficient in catalase had a reduced ability to maintain long-term colonization in the gastric mucosa of the mice compared to the wild type strain, indicating the importance of catalase in the chronic persistence of *H. pylori* (Harris *et al.*, 2003).

2.4.5.3 Phospholipase A

H. pylori produces phospholipase A, an enzyme that targets the phospholipidic components of the gastric mucosa and is thus believed to damage the protective gastric mucosal barrier (Figura, 1997). Phospholipase A has also been shown to hydrolyze phospholipids to generate lysolecithin and fatty acids which are cytotoxic and may act as precursors to ulcerogenic components (Langton and Cesareo, 1992). Additionally, the role of phospholipase A in colonization of the gastric mucosa has been studied where it was found that *H. pylori* isogenic mutants lacking phospholipase A were unable to colonize mice (Dorrell *et al.*, 1999).

2.5 Effects of *H. pylori* infection on host

H. pylori has been strongly associated with the development of several gastroduodenal diseases and has also been linked to gastric cancer progression (Ernst and Gold, 2000). Thus, understanding the mechanisms underlying *H. pylori* pathogenesis has been a major research target. Several possible mechanisms

describing how *H. pylori* could induce epithelial damage have been proposed and some of these are discussed below.

2.5.1 Oxidative stress

The term oxidative stress refers to the state of a cell that is characterized by the presence of excessively high levels of ROS and/or the lack of antioxidant defences (Franco *et al.*, 2008).

2.5.1.1 *H. pylori* and reactive oxygen species (ROS) generation

ROS are chemically reactive molecules that include hypochlorite ions (ClO^-), hydroxyl radicals (·OH), superoxide anions (O_2^-) and H_2O_2. Excessive generation of ROS could potentially damage various host cellular components such as proteins, lipids and nucleic acids (Valko *et al.*, 2007). It has been widely established that oxidative stress can increase DNA mutation rates which could lead to permanent modification of genetic material and initiate tumour development (Franco *et al.*, 2008; Kryston *et al.*, 2011). Apart from inducing DNA damage, ROS has also been reported to activate NF-κB (Schreck *et al.*, 1991; Takada *et al.*, 2003), a transcription factor that controls the expression of various pro-inflammatory genes. Some of these include cytokines such as IL-6 (Zhang *et al.*, 2001) and IL-8 (Roebuck, 1999a), both of which have also been implicated in gastric carcinogenesis (Crabtree and Lindley, 1994; Kai *et al.*, 2005). Additionally, ROS has also been documented to induce gastric mucosa injury which could potentially predispose host tissue to ulcer formation (Davies *et al.*, 1992).

Interestingly, high levels of ROS production have been reported in *H. pylori*-infected gastric mucosa (Davies *et al.*, 1994; Suzuki *et al.*, 1996). Possible sources of

ROS may derive from infiltrating neutrophils, vascular endothelial cells, gastric mucosa and epithelial cells and the bacterium itself (Handa *et al.*, 2010). Although neutrophils are believed to be the main contributor to ROS (Naito and Yoshikawa, 2002), it has been reported that *H. pylori* itself can produce ROS (Nagata *et al.*, 1998). Moreover, reduced intracellular GSH levels and DNA damage have also been reported in *H. pylori*-infected gastric cell lines (Beil *et al.*, 2000; Obst *et al.*, 2000), further supporting the ability of the bacterium in directly synthesizing ROS. Despite this, the exact mechanism and the possible bacterial factors which contribute to ROS generation have not been clearly established.

2.5.1.2 *H. pylori* decreases antioxidant levels

Antioxidants scavenge ROS and hence protect cells against the damaging effects of free radicals. Several cellular antioxidant defences exist to prevent the accumulation of ROS and they may be either enzymatic or non-enzymatic in nature. Superoxide disumutase, glutathione peroxidase and catalase are the three major classes of enzymatic antioxidants (Mates *et al.*, 1999) while non-enzymatic antioxidants include Vitamin C, Vitamin E, carotenoids and thiol antioxidants such as GSH (Valko *et al.*, 2006).

The GSH antioxidant system is one of the major protective mechanisms of the cell (Bounous and Molson, 2003). GSH (L-γ-glutamyl-L-cysteinylglycine) is highly abundant in the cytosol, nuclei and mitochondria, and it quenches ROS by donating the hydrogen atom required for their reduction (Valko *et al.*, 2006). A deficiency in GSH puts the cell at risk for oxidative damage as GSH has been shown to be involved in the repair of oxidative DNA lesions (Lenton *et al.*, 1999), supporting its role in protecting against mutagenesis and transformation. Apart from neutralizing ROS,

GSH is also a co-factor of many cellular enzymes (Townsend *et al.*, 2003) and helps regulate the activity of redox-sensitive enzymes such as protein-tyrosine kinases and phosphatases by maintaining their active sites in a reduced state (Staal *et al.*, 1994).

It has been reported in several studies that gastric mucosa harbouring *H. pylori* have significantly decreased levels of GSH as compared to *H. pylori*-negative mucosa (Beil *et al.*, 2000; Jung *et al.*, 2001; Shirin *et al.*, 2001), suggesting a possible role of *H. pylori* in the depletion of this important antioxidant. In addition, it has also been shown that *H. pylori* directly metabolizes extracellular GSH as a source of glutamate for its own amino acid metabolism (Shibayama *et al.*, 2007). Thus the observed decrease of GSH is probably not merely due to an increase in ROS levels but a more direct effect of the bacterium. Taken together, a decrease in GSH level, along with an increase in ROS generation as discussed in section 2.5.1.1 would lead to a redox imbalance in cells and may explain the onset of carcinogenesis in *H. pylori* infections.

2.5.2 *H. pylori* and inflammation

All *H. pylori*-infected subjects develop an inflammatory and immune response towards the pathogen. However, this response is ineffective in clearing the bacteria and results in chronic gastric inflammation which may eventually lead to pathogenesis (Robinson *et al.*, 2007). *H. pylori* produces several virulence factors which have been associated with inflammation. Some of these include the *cag*PAI (Wiedemann *et al.*, 2009), OipA (Yamaoka *et al.*, 2002a) and the induced by contact with epithelium antigen (IceA) (Peek *et al.*, 1998). *iceA* exists as two mutually exclusive genotypes, *iceA1* or *iceA2*, and it is *iceA1* which has been associated with gastric inflammation (Nishiya *et al.*, 2000; Sheu *et al.*, 2002).

Apart from causing direct cell damage through bacterial factors, *H. pylori* may also indirectly induce mucosal damage as a consequence of the persistent inflammatory response. Histologically, chronic *H. pylori* infection is characterized by infiltration of the mucosa by polymorphonuclear and mononuclear leukocytes, as well as neutrophils which are important components of the inflammatory response (Dundon *et al.*, 2002).

2.5.2.1 Interleukin-8 (IL-8) generation

Numerous proinflammatory cytokines including IL-1β, IL-6, IL-8 and tumour necrosis factor alpha (TNF-α) have been reported to be upregulated in the gastric mucosa during *H. pylori* infection (Crabtree *et al.*, 1991 and 1994; Noach *et al.*, 1994a). Of these, special interest has been focused on the chemokine IL-8 which is a potent neutrophil recruitment factor thought to play a pivotal role in the immunopathogenesis of *H. pylori* infection (Yamaoka *et al.*, 1996).

A major source of IL-8 in the gastric mucosa is the epithelium (O'Hara *et al.*, 2006) and whole genome profiling of *H. pylori*-infected gastric epithelial cells has revealed IL-8 to be the most significantly upregulated gene (Eftang *et al.*, 2012). Indeed, numerous studies have shown that *in vitro* co-culture of *H. pylori* with gastric epithelial cells stimulates significant IL-8 secretion (Crabtree *et al.*, 1995a; Sharma *et al.*, 1995). *In vivo*, gastric mucosal IL-8 levels have also been found to correlate strongly with histological severity of *H. pylori*-induced gastritis (Ando *et al.*, 1996) and gastric ulcers (Shimizu *et al.*, 2000). Several virulence factors of *H. pylori* have been reported to induce IL-8 production including OipA (Yamaoka *et al.*, 2002a), urease (Beswick *et al.*, 2006) and CagA (Kim *et al.*, 2006).

Expression of IL-8 is regulated primarily at the transcriptional level (Roebuck, 1999b). In gastric epithelial cells, several transcription factors have been found to be involved in *H. pylori*-induced IL-8 promoter activation, including NF-κB (Keates *et al.*, 1997) and to a lesser extent, activator protein-1 (Chu *et al.*, 2003). NF-κB is an inducible transcription factor sequestered in the cytoplasm by association with proteins of the inhibitor of NF-κB (IκB) family (Jacobs and Harrison, 1998). In unstimulated cells, IκB proteins bind to and mask the nuclear localization signals (NLS) of NF-κB, preventing the latter from entering into the nucleus (Beg *et al.*, 1992). On exposure to external stimuli such as ROS (Schreck *et al.*, 1992) or TNF-α (Fitzgerald *et al.*, 2007), IκB is phosphorylated by IκB kinase which targets it for proteosome degradation, hence liberating NF-κB to migrate into the nucleus to regulate gene expression (Mercurio *et al.*, 1997). Various studies have shown that *H. pylori* infection activates NF-κB in gastric epithelial cells both *in vitro* and *in vivo* (Keates *et al.*, 1997; Ferrero *et al.*, 2008), possibly through an upstream mitogen-activated protein kinase pathway (Seo *et al.*, 2004). In addition, it has also been reported that *H. pylori* can induce Toll-like receptor (TLR) and Nod-like receptor (NLR) activation in host cells (Smith *et al*., 2003; Viala *et al*., 2004), leading to the expression of several pro-inflammatory genes including IL-8 (Torok *et al*., 2005).

2.5.3 Cellular vacuolation

Intracellular vacuolation has been observed by ultrastructural microscopy in the gastric epithelial cells of patients infected with *H. pylori* (Chen *et al.*, 1986; Fiocca *et al.*, 1989). *In vitro*, broth culture supernatants of *H. pylori* have also been reported to induce vacuolation in primary human gastric epithelial cells (Smoot *et al.*, 1996), indicating that *H. pylori* induces a cytopathic effect on the host. Cellular

vacuolation has been attributed to a cytotoxin secreted by *H. pylori* known as VacA (Cover and Blaser, 1992b).

2.5.3.1 Role of VacA in vacuolation

The unique function of VacA in inducing cellular vacuolation has been widely reported and studied (Leunk *et al.*, 1988; Papini *et al.*, 1994). VacA is able to induce vacuolation in several cell types although cell line sensitivity may differ (de Bernard *et al.*, 1998). The membranes of VacA-induced vacuoles contain both late endosomal and lysosomal markers, in particular Rab7, lysosomal-associated membrane protein 1 and lysosomal glycoprotein 110 (Papini *et al.*, 1994; Molinari *et al.*, 1997), indicating that VacA may disrupt normal membrane trafficking at the late endosomal stage (Montecucco and de Bernard, 2003). Vacuolation not only depends on VacA, but also requires the presence of permeant weak bases, such as ammonia, in the extracellular medium (Cover *et al.*, 1992). In addition, several enzymes required for vacuole formation have been identified and these include vacuolar-type ATPase (V-ATPase) (Cover *et al.*, 1993), and the small GTPases Rab7 (Papini *et al.*, 1997) and Rac1 (Hotchin *et al.*, 2000).

A current model outlining the mechanism by which VacA induces vacuolation is illustrated in Figure 1. In this model, it is proposed that after binding to receptors on the cell surface, VacA is internalized and forms anion-selective channels in the membranes of late endosomes and lysosomes (Cover and Blanke, 2005). These VacA channels conduct anions (e.g. chloride) into the endosomal compartment which in turn stimulates V-ATPase activity. To compensate for the increase in anion concentration, V-ATPase activity increases and an influx of protons occurs which then reduces the intralumenal pH. Membrane permeant weak bases such as ammonia

then diffuse into the acidified endosome, become protonated and are trapped in these compartments. Subsequently, osmotic swelling of these endosomes results in the formation of massive vacuoles in the cells.

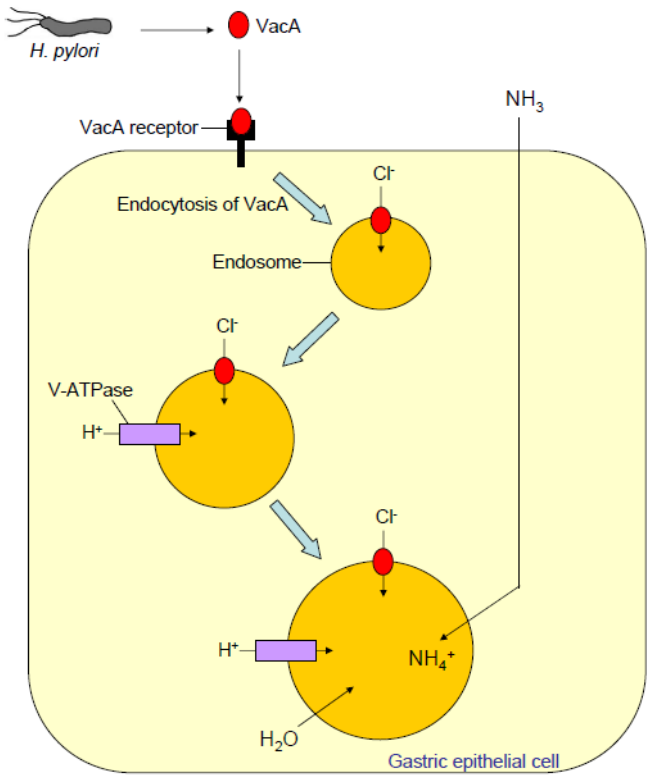

Figure 1. Schematic illustration of a model depicting how VacA induces cellular vacuolation.

2.5.3.2 Role of urease and ammonia in vacuolation

Based on the model as described above, it is apparent that the presence of weak bases (e.g. ammonia) in the extracellular medium is necessary for vacuolation to occur (Cover *et al.*, 1992). Previous studies have attributed the source of ammonia required for vacuolation to come from the hydrolysis of urea by urease as it was observed that ammonia generated from urease greatly potentiated VacA-induced vacuolation (Cover *et al.*, 1991). However, it was also reported in the same study that in the absence of urea, supernatant from a urease deficient mutant induced vacuolation to a similar extent as compared to the wild type strain. In addition,

acetohydroxamic acid (a urease inhibitor) failed to inhibit vacuolation induction by *H. pylori* supernatants. These observations indicate that urease is probably not the only factor contributing to ammonia required for VacA-induced vacuolation.

2.6 GGT

2.6.1 Human GGT

2.6.1.1 Properties and catalytic action

Human GGT, a member of the N-terminal nucleophile hydrolase family, is first synthesized as an inactive 569-amino acid single propeptide which undergoes post-translational autocleavage to produce the mature heterodimeric enzyme consisting of a large and small subunit (West *et al.*, 2011). The large subunit consists of an aminoterminal sequence which is intracellular, a single transmembrane domain, as well as an extracellular component that binds the small subunit (Whitfield, 2001). The active site of the enzyme faces the external side of the plasma membrane and is found in the small subunit (Taniguchi and Ikeda, 1998). Human GGT is also heavily N-glycosylated and this has been found to be important for the proper folding and autocatalytic cleavage of the proenzyme (West *et al.*, 2011).

GGT catalyzes the cleavage of the γ-glutamyl amide bond found in γ-glutamyl compounds (e.g. GSH) where the γ-glutamyl moiety is transferred to an acceptor either through a transpeptidation or hydrolysis reaction (Lieberman *et al.*, 1995). A general formula illustrating the catalytic action of GGT is shown below (Hanigan, 1998) where R represents any chemical group and the acceptor can be amino acids, peptides or water:

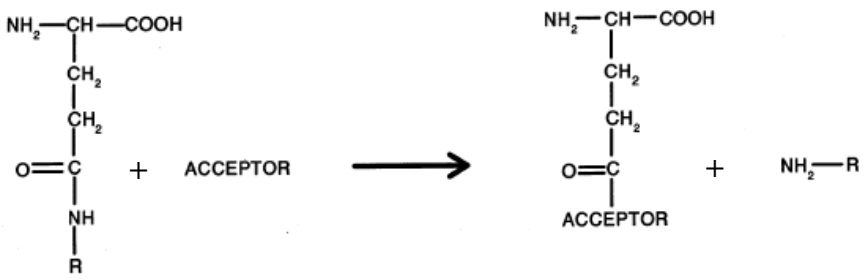

The first step is the cleavage of the γ-glutamyl bond of the substrate and the formation of a transient enzyme-glutamyl substrate complex (Wickham *et al.*, 2011). The γ-glutamyl group then forms a transient acyl bond with the enzyme while the remainder of the substrate is released (Tate and Meister, 1974). In the transpeptidation reaction, the γ-glutamyl moiety is transferred to the amine of an acceptor (e.g. an amino acid or dipeptide) to form new γ-glutamyl compounds (Thompson and Meister, 1976). In the hydrolysis reaction - the predominant reaction catalyzed by GGT *in vivo* (Wickham *et al.*, 2011) - water hydrolyzes the acyl bond between the substrate and the nucleophilic residue, leading to the release of glutamate and the free enzyme (Keillor *et al.*, 2005). Physiologically, the most abundant substrates of GGT are GSH and GSH-conjugated compounds (Hanigan, 1998) although a wide variety of γ-glutamyl compounds can also be used as substrates (Magnan *et al.*, 1982).

The catalytic activity of GGT can be effectively inhibited by L-serine in the presence of borate buffer (Tate and Meister, 1978). This occurs because L-serine binds to the γ-glutamyl binding site of the enzyme by interacting with the α-carboxyl and α-amino binding groups in a competitive manner (Thompson and Meister, 1977). Binding is further enhanced by complex formation between the serine hydroxyl group, borate and a hydroxyl group at the active center of GGT which is thought to mimic the tetrahedral transition state intermediate formed during the normal catalytic

reaction, thus making the serine-borate complex (SBC) an inhibitory transition-state analog (Tate and Meister, 1978).

Apart from SBC, other inhibitors of GGT that have been used include 6-diazo-5-oxo-L-norleucine (DON) (Tate and Meister, 1981) and acivicin (Meister and Anderson, 1983). Both DON and acivicin are potent non-reversible inhibitors that bind covalently to the small subunit of GGT (Tate and Meister, 1977; Smith *et al.*, 1995). However, although extremely effective in inhibiting GGT, DON and acivicin are also glutamine antagonists that inhibit many glutamine-dependent amidotransferases involved in purine biosynthesis, rendering them cytotoxic to cells (Lyons *et al.*, 1990). Furthermore, acivicin has also been demonstrated to induce apoptosis independently of GGT activity in the V79 cell line (Aberkane *et al.*, 2001).

2.6.1.2 Physiological function

The physiological role of GGT relating to GSH has been studied extensively. As exported GSH cannot be reabsorbed by cells in the tripeptide form, GGT initiates the cleavage of extracellular GSH to release the γ-glutamyl group from cysteinylglycine. The latter is then hydrolyzed into cysteine and glycine by dipeptidases present on the cell surface (McIntyre and Curthoys, 1982). The constituent amino acids of GSH (i.e. glutamate, cysteine and glycine) can then be readily absorbed and used for resynthesis of GSH intracellularly (Hanigan and Ricketts, 1993). This cyclic process is known as the γ-glutamyl cycle and is illustrated in Figure 2. As GGT is the only enzyme known to cleave intact GSH, it thus plays a key role in this cycle (Hanigan, 1998).

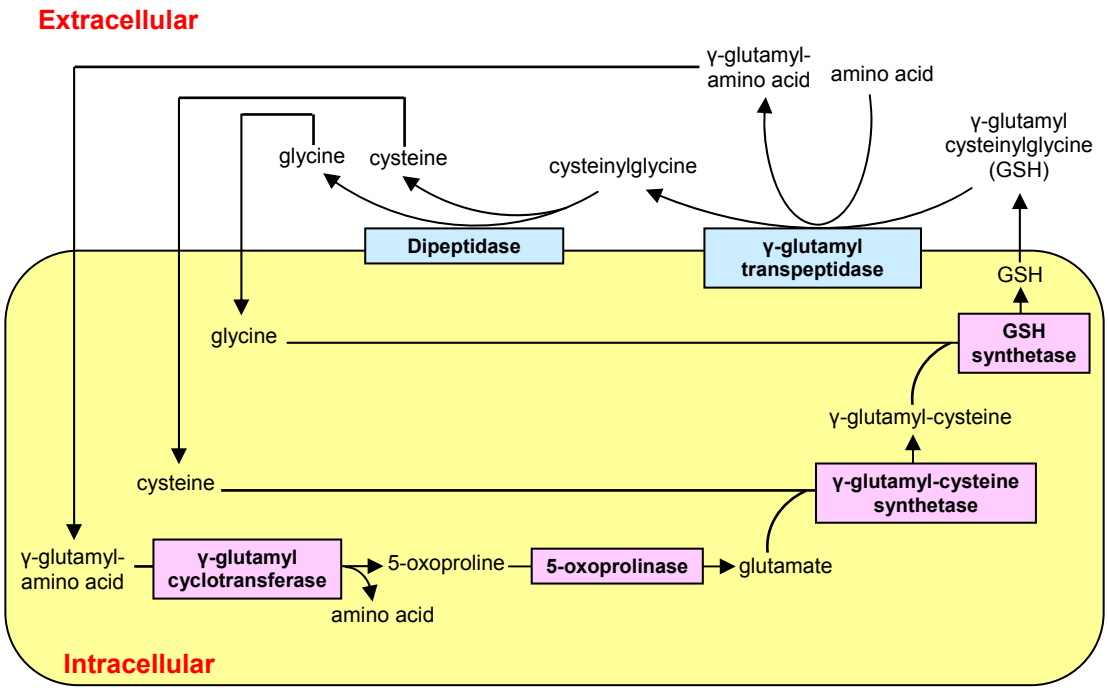

Figure 2. The γ-glutamyl cycle.

2.6.1.3 Cellular expression

GGT is most prominently expressed on luminal surfaces of cells that align ducts and glands throughout the body (West *et al.*, 2011) and the highest concentration can be found on the luminal surface of renal proximal tubules in the kidney (Hanigan, 1998). Additionally, the presence of GGT has also been observed on hepatic bile canaliculi, pancreatic acini, intestinal crypts, salivary gland ducts and testicular tubules among many others (Hanigan and Frierson, 1996). It is believed that GGT functions to retain the constitutive amino acids of GSH (especially cysteine) in these tissues to maintain intracellular levels of GSH (Lieberman *et al.*, 1995).

2.6.2 *H. pylori* GGT

2.6.2.1 Properties of GGT

H. pylori GGT is a highly conserved 60 kDa polypeptide encoded by a single gene (HP1118) that is located far from both the *vac*A gene and the *cag*PAI (Shibayama *et al.*, 2003). The *ggt* gene of 1704 bp codes for a protein consisting of 567 amino acids and is translated in a single-chain precursor form which is inactive (Boanca *et al.*, 2006). Following secretion into the periplasmic space, the pre-proenzyme is first cleaved of its N-terminal signal peptide at the site between alanine 26 and alanine 27 (Chevalier *et al.*, 1999). Subsequently, intramolecular autocatalytic cleavage of the proenzyme then occurs (between asparagine 379 and threonine 380), resulting in a fully active heterodimer comprising a 40 kDa and 20 kDa subunit which remain non-covalently associated (Shibayama *et al.*, 2003). The new N-terminal residue (threonine 380) has been demonstrated to serve as a catalytic nucleophile in both the autoprocessing and enzymatic reactions (Boanca *et al.*, 2007).

2.6.2.2 Comparison between *H. pylori* GGT and human GGT

H. pylori GGT shares 22% amino acid sequence similarity with human GGT, suggesting a certain degree of conservation in their overall structure and function (Boanca *et al.*, 2007). Indeed, *H. pylori* GGT is also capable of metabolizing γ-glutamyl substrates such as GSH and glutamine in the extracellular medium (Shibayama *et al.*, 2007). However, several differences do exist. For example, human GGT is membrane-bound and heavily N-glycosylated while *H. pylori* GGT is a soluble protein and is not glycosylated (Boanca *et al.*, 2006). In addition, *H. pylori ggt* gene also lacks the GY residues at the C-terminal end which are present on mammalian homologues, including human *ggt* (Chevalier *et al.*, 1999). The

significance of this difference, however, is still unclear. Catalytic differences have also been observed between *H. pylori* GGT and human GGT. For instance, human GGT is >100 fold more effective than *H. pylori* GGT in catalyzing the transpeptidation reaction (Boanca *et al.*, 2006), suggesting considerable structural differences in their catalytic sites. Hydrolysis rates, on the other hand, are comparable between the two (Boanca *et al.*, 2007).

2.6.2.3 Physiological role of GGT in *H. pylori*

GGT is highly conserved, constitutively expressed and common in all *H. pylori* strains (Chevalier *et al.*, 1999), suggesting its importance in the physiology of the bacterium. As reported by Shibayama *et al.* (2007), one of the main physiological functions of *H. pylori* GGT is to enable the bacterium to utilize extracellular GSH and glutamine as a source of glutamate for its own metabolism. This is because *H. pylori* is unable to take up GSH or glutamine directly, thus GGT functions to hydrolyze these substrates extracellularly to glutamate which is then transported into the bacterium in a Na^+-dependent manner. In the same study, it was further demonstrated that the transported glutamate was subsequently incorporated into the tricarboxylic acid cycle and also used as a substrate for glutamine synthesis in the cytosol of *H. pylori*. Hence, GGT has been shown to be an important metabolic enzyme of *H. pylori*.

2.6.2.4 Effects of *H. pylori* GGT on the host

H. pylori GGT was first described as an essential colonization factor in a study done on Swiss specific pathogen-free mice (Chevalier *et al.*, 1999). However, a later study using two different animal models (C57/BL/6 mice and gnotobiotic piglets)

demonstrated that GGT was not essential for colonization but did contribute to the virulence of the pathogen (McGovern *et al.*, 2001). Subsequently, GGT was found to induce apoptosis in gastric epithelial cells (Shibayama *et al.*, 2003) via the mitochondria-mediated pathway (Kim *et al.*, 2007). In addition, GGT also induces cell cycle arrest at the G1-S phase transition (Kim *et al.*, 2010). On the other hand, it was also demonstrated that GGT upregulates cyclooxygenase-2 and epidermal growth factor-related peptides in gastric epithelial cells which are events that inhibit apoptosis (Busiello *et al.*, 2004). Interestingly, it has been postulated that the ability of *H. pylori* to both stimulate and inhibit apoptosis may increase the risk of gastric carcinogenesis as mutations of apoptosis-regulating genes may occur more frequently (Peek and Blaser, 2002). Hence, it has been speculated that GGT may play an important role in promoting *H. pylori*-mediated gastric adenocarcinoma (Shibayama *et al.*, 2003).

Apart from gastric epithelial cells, *H. pylori* GGT has also been found to affect cells of the immune system, in particular T cells (Schmees *et al.*, 2007). In their study, it was demonstrated that GGT inhibited the proliferation of human T lymphocytes by inducing G1 arrest through an apoptosis-independent mechanism. The authors hence suggested a contributory role of GGT in immune evasion by *H. pylori* through the inhibition of immune effector cells. Recently, it has also been reported that GGT is an inducer of miR-155 expression in human lymphocytes (Fassi Fehri *et al.*, 2010). Interestingly, miR-155 is one of the key regulators of the immune system and overexpression of miR-155 has been linked to carcinogenesis (Tili *et al.*, 2011).

As described in the previous section 2.6.2.3, one of the physiological roles of GGT is to utilize extracellular GSH and glutamine as a source of glutamate for the bacterium. However, the depletion of these important nutrients inevitably also damages the host in several ways. Firstly, excessive hydrolysis of GSH (an important

antioxidant) may impair the redox balance in the host and secondly, compensatory GSH synthesis by the host incurs excessive energy consumption on the cell and may subsequently affect its viability (Shibayama *et al.*, 2007). Taken together, it is evident that GGT is a formidable virulence factor of *H. pylori* whose actions cannot be underestimated.

2.7 Host internalization of *H. pylori* proteins

Several virulence factors of *H. pylori* have been reported to be internalized by host cells. One of the best studied is that of the oncogenic CagA, which is delivered from the bacterium into the host via the T4SS where it then hijacks the host cell signalling system (Odenbreit *et al.*, 2000). In addition, peptidoglycan is another polymer that has been described to be transported through the T4SS into the host (Viala *et al.*, 2004). Apart from CagA and peptidoglycan, however, there have been no other reports to date describing other effectors which are translocated through the T4SS (Fischer, 2011).

Other *H. pylori* factors that have been reported to be taken up by host cells include VacA (Gauthier *et al.*, 2005) and TNF-α inducing protein (Tipα) (Watanabe *et al.*, 2010). These proteins are not mediated through the *H. pylori* T4SS but rather are secreted by the bacterium and subsequently taken up by the host cell via various pathways of endocytosis. Internalized VacA induces several cellular effects (previously discussed in section 2.4.4) including vacuolation induction (Isomoto *et al.*, 2010). Interestingly, Tipα has been found to subsequently localize to host cell nuclei where it is postulated to regulate the expression of genes such as TNF-α, resulting in tumour development (Suganuma *et al.*, 2006). Another route which *H. pylori* utilizes to deliver proteins into host cells is through the shedding of outer

membrane vesicles (OMVs) which have been shown to be subsequently taken up by gastric epithelial cells (Parker *et al*., 2010). Importantly, these vesicles contain a range of virulence-associated factors including CagA, VacA and GGT (Olofsson *et al*., 2010). Given that most *H. pylori* do not adhere directly to the gastric epithelium during an infection (Hessey *et al.*, 1990), it is believed that internalization of some of its secreted virulence factors plays an important role in its pathogenesis.

2.7.1 Endocytosis pathways

The plasma membrane of a cell is a dynamic and complex structure which serves to physically segregate intracellular contents from the extracellular environment. Passage of molecules into and out of the cell is tightly regulated and only some small molecules (e.g. CO_2, O_2, water, etc) are able to diffuse freely across the membrane. Macromolecules, on the other hand, cannot traverse the membrane on their own and must be brought into the cell via membrane-bound vesicles that are pinched off from the plasma membrane, a process known as endocytosis (Conner and Schmid, 2003). Endocytosis occurs by multiple mechanisms and these can be classified into two main categories, namely phagocytosis (uptake of large particles) and pinocytosis (uptake of fluid and solutes) (Soldati and Schliwa, 2006). These various pathways are illustrated in Figure 3 and further described in the subsequent sections.

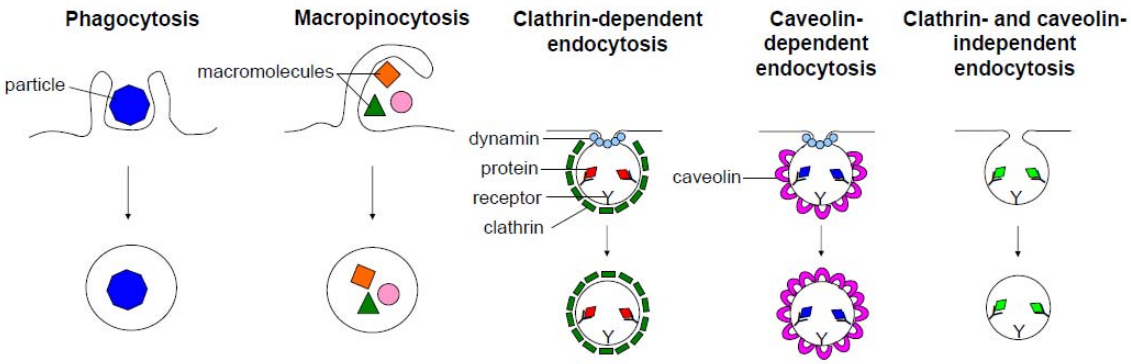

Figure 3. Different pathways of endocytosis.

2.7.1.1 Phagocytosis

Phagocytosis is generally restricted to specialized mammalian cells such as macrophages, monocytes and neutrophils (Conner and Schmid, 2003) and is a major mechanism used by the immune system to remove pathogens (Stuart and Ezekowitz, 2008). The process involves the cell-surface recognition of specific particles (e.g. bacteria, apoptotic cells, etc), their engulfment through a cup-shaped membrane distortion encircling the object and the subsequent formation of internalized phagosomes (Kumari *et al.*, 2010). Once formed, phagosomes undergo maturation to become acidic and hydrolytic, ultimately resulting in the degradation of the cargo (Stuart and Ezekowitz, 2008).

2.7.1.2 Pinocytosis

2.7.1.2.1 Macropinocytosis

Macropinocytosis is the bulk engulfment of extracellular fluid that mediates the non-selective uptake of solute macromolecules (Swanson and Watts, 1995). It involves actin-mediated plasma membrane ruffling where a subset of the lamellipodia formed fold back onto themselves, fuse at the base of the membrane and trap solutes in macropinosomes (Lim and Gleeson, 2011). Macropinosomes are heterogeneous in

size and can range from 0.2 μm to 10 μm in diameter (Swanson, 2008). The process is constitutively activated in immune cells such as dendritic cells and macrophages (Norbury *et al.*, 1997; Krysko *et al.*, 2006) while in other cells types (e.g. epithelial cells), macropinocytosis can be activated by growth factor stimulation (Haigler *et al.*, 1979).

2.7.1.2.2 Clathrin-dependent endocytosis

Clathrin-mediated endocytosis occurs constitutively in all mammalian cells (Conner and Schmid, 2003) and is the best understood among all the known pinocytic pathways. It typically involves the concentration of receptor-ligand complexes into clathrin-coated pits on the plasma membrane that invaginate and pinch off to form endocytic vesicles, thus bringing cargo molecules into the cell (Kumari *et al.*, 2010). The large GTPase dynamin is responsible for scission of the clathrin-coated vesicle from the plasma membrane (van der Bliek *et al.*, 1993). Unlike the sizes of phagosomes and macropinosomes, clathrin-coated vesicles are only ~100 nm in diameter (Traub, 2011). Some examples of pathogens that enter into the cell via clathrin-mediated endocytosis include Ebola virus (Bhattacharyya *et al.*, 2010) and severe acute respiratory syndrome coronavirus (Inoue *et al.*, 2007).

2.7.1.2.3 Caveolin-mediated endocytosis

Caveolin-mediated endocytosis, on the other hand, is less well-characterized. It generally involves formation of flask-shaped invaginations (termed caveolae) at the cell surface lined by caveolin which are integral membrane proteins that bind to membrane cholesterol (Kumari *et al.*, 2010). Formation of caveolae is dependent on cholesterol and loss of membrane cholesterol results in their disassembly (Hailstones

et al., 1998). Binding of specific cargoes to receptors within the caveolae then stimulates the endocytosis of these caveolae into the cell. Similar to clathrin-mediated endocytosis, severing of caveolin-coated vesicles is also dependent on dynamin (Henley *et al.*, 1998). Caveolae can be found in various cell types but are most abundantly expressed on endothelial cells, smooth-muscle cells, fibroblasts and adipocytes (Parton *et al.*, 1994). Examples of cargoes endocytosed by this pathway include Simian virus 40 (Norkin *et al.*, 2002) and cholera toxin (Parton *et al.*, 1994).

2.7.1.2.4 Clathrin- and caveolin-independent endocytosis

The mechanisms underlying clathrin and caveolin-independent endocytosis remain poorly understood. These pathways involve the internalization of non-coated vesicles which may or may not be dependent on fission by dynamin. In addition, in the case of endocytosis of glycosylphosphatidylinositol-anchored proteins (GPI-APs), they are delivered to the early endosome via intermediate structures known as clathrin- and dynamin-independent carriers (CLICs) and GPI-AP enriched early endosomal compartments (GEECs) (Sabharanjak *et al.*, 2002). Other cargoes known to be endocytosed in a clathrin and cavelin-independent manner include IL-2 receptor (Lamaze *et al.*, 2001) and human papillomavirus type 16 (Spoden *et al.*, 2008).

2.7.2 Mechanisms of nuclear import

2.7.2.1 Classical pathway

Nuclear import is tightly regulated and is an energy-requiring process (Kohler *et al.*, 1999). Proteins targeted for the nucleus have to be ferried through the nuclear pore complex (NPC) by transport carriers called importins although small molecules (< ~20 kDa) may passively diffuse through the pore (Chook and Blobel, 2001). The

primary determinant of nuclear localization is the nuclear targeting signal and the best characterized nuclear import signal to date is the classical NLS. Classical NLSs are highly basic consensus sequences that are usually rich in lysines and can either be monopartite (consisting of a single cluster of 5-7 amino acids) or bipartite (having two clusters of basic amino acids separated by a linker of 10-12 amino acids) (Kosugi *et al.*, 2009). Transport substrates are recognized through their classical NLSs by importin α which serves as an adaptor protein by binding both NLS-containing cargoes and importin β1 to form a trimeric protein complex (Lange *et al.*, 2007). This complex then docks on the NPC via importin β1 and is subsequently imported into the nucleus through the NPC. Once inside the nucleus, the complex is dissociated by Ran GTP and importins α and β are recycled back into the cytoplasm. This pathway is known as the classical nuclear import pathway and is illustrated in Figure 4.

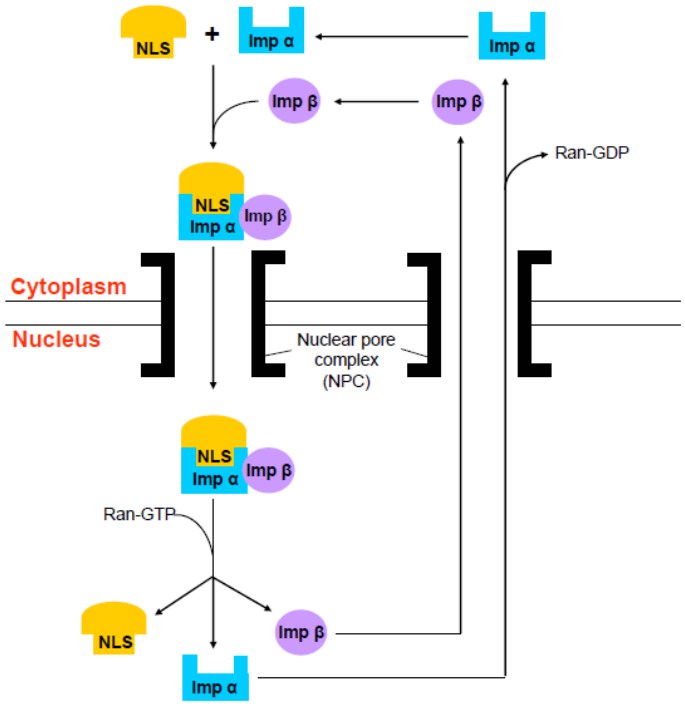

Figure 4. The classical nuclear import cycle.

2.7.2.2 Alternative pathways

Apart from the classical nuclear import pathway, alternative pathways have also been described. For instance, several proteins are imported through direct

interactions with importin β1without the need for the adaptor importin α (Takizawa *et al.*, 1999; Forwood *et al.*, 2001). The NLSs recognized directly by importin β1, however, are less well-defined. They are generally longer than classical NLSs and are rich in arginine (Palmeri and Malim, 1999) although non-arginine rich NLSs have also been identified (Lam *et al.*, 2001). Interestingly, direct importin β-cargo transport was found to be faster and more efficient than that mediated by the importin α-importin β complex although the latter pathway may exist to control nuclear import rates (Riddick and Macara, 2007).

Importin β2 is another relatively well-described nuclear import carrier that binds directly to cargoes and transports them across the NPC. Unlike the well-defined classical NLSs, the NLSs that importin β2 recognize are diverse in sequence and structure. However, although they do not have a consensus sequence, they do have some common characteristics such as being structurally disordered, having an overall basic character and possessing a set of weakly conserved sequence motifs (Lee *et al.*, 2006). Accordingly, these atypical NLSs have been categorized in a new class termed as PY-NLS.

Apart from importins β1 and β2, several other importins have also been described to import cargoes into the human nucleus (Mosammaparast and Pemberton, 2004). However, few cargoes have been identified. This is because most of their import signals have not been determined. Furthermore, many nuclear proteins do not have a recognizable NLS and several also contain import signals that do not resemble previously described NLSs (Christophe *et al.*, 2000), thus making nuclear localization difficult to predict.

MATERIALS AND METHODS

3.1 *H. pylori* strains used in the study

H. pylori strain 88-3887 (kindly provided by Prof. Berg D.E., Washington University School Medicine, St Louis, USA) was the predominant strain used in this study. This strain is a pig-passaged motile variant of 26695 with an ability to colonize mice (Hoffman *et al.*, 2003). Different isogenic *H. pylori* mutants (Δ*ggt*, Δ*vacA*, Δ*vacA*/*ggt*, Δ*cagA*, Δ*cagA*/*ggt*, Δ*ureAB*, Δ*ureAB*/*ggt* and Δ*cag*PAI) were constructed from the wild type strain 88-3887 and used in the study. In addition, three other standard *H. pylori* strains: 26695, SS1 and NCTC11637 were also utilized. A total of seven clinical strains isolated from biopsies obtained from the gastric antrum within 2 cm of the pylorus (Lui *et al.*, 2003) in patients who underwent upper gastrointestinal endoscopy at the National University Hospital in Singapore were also used in this study. Informed consent was obtained from all patients for gastroscopy and biopsies.

3.1.1 Growth conditions

All standard and clinical *H. pylori* strains were cultured on non-selective chocolate blood agar (CBA) plates containing Blood Agar base No. 2 (Oxoid) and supplemented with 5% lysed horse blood (Quad Five) (Appendix 1). Isogenic mutants were cultured on selective CBA plates supplemented with kanamycin (20 μg/ml) or chloramphenicol (15 μg/ml) (Appendix 2) according to the respective antibiotic resistance cassette inserted (Table 1). All cultures were incubated at 37°C in an atmosphere of 5% CO_2 in a humidified incubator (Forma, Scientific) for 3 days.

Table 1. Antibiotic resistance of constructed *H. pylori* mutants.

***H. pylori* mutant**	**Antibiotic resistance**
Δ*ggt*	kanamycin
Δ*vacA*	chloramphenicol
Δ*vacA*/*ggt*	chloramphenicol and kanamycin
Δ*cagA*	chloramphenicol
Δ*cagA*/*ggt*	chloramphenicol and kanamycin
Δ*ureAB*	chloramphenicol
Δ*ureAB*/*ggt*	chloramphenicol and kanamycin
Δ*cag*PAI	kanamycin

3.1.2 Maintenance of *H. pylori* cultures

Confluent growth of *H. pylori* cultures were harvested from 2 CBA plates using sterile cotton swabs (Copan). The bacteria were then resuspended in a cryotube (Nunc) containing 1 ml of brain heart infusion (BHI) broth (Oxoid) supplemented with 10% horse serum and 20% glycerol (Appendix 3). The cultures were stored at -80°C until use.

3.2 Genotyping of *H. pylori* virulence genes

3.2.1 Genomic DNA extraction

Bacterial cells from CBA plates were harvested and transferred to microfuge tubes containing 1.5 ml Tris-EDTA (TE) buffer (Appendix 4). The bacterial suspension was centrifuged at 8000 × g for 5 minutes at room temperature and the pellet washed once with TE buffer. Thereafter, chromosomal DNA was extracted by silica-membrane-based nucleic acid purification using the QIAamp DNA Mini Kit (Qiagen) according to the manufacturer's protocol. The amount of extracted DNA was measured spectrophotometrically at wavelength 260 nm using NanoDrop™ 1000 Spectrophotometer (Thermo Scientific).

3.2.2 Polymerase Chain Reaction (PCR)

PCR was carried out to determine the presence of various virulence genes, namely *cagA*, *vacA*, *iceA1*, *iceA2* and *babA2*, in the chromosomal DNA of *H. pylori* strain 88-3887. The PCR reaction was carried out in an amplification thermal cycler (Bio-Rad) according to the method as described by Zheng *et al.* (2000). To amplify *cagA*, *vacA*, *iceA1* and *iceA2*, a 50 µl reaction mixture consisting of 50 ng genomic DNA, 1 × incubation buffer, 50 pmol primers (forward and reverse) (Table 2), 1 unit of *Taq* DNA polymerase (DynaZyme), 200 µM each of dNTPs (dATP, dGTP, dTTP and dCTP) and sterile distilled water (Appendix 5) was used. For the amplification of *babA2*, a 50 µl reaction mixture consisting of 40 ng genomic DNA, 1 × incubation buffer, 10 pmol primers (forward and reverse) (Table 2), 1 unit of *Taq* DNA polymerase (DynaZyme), 200 µM each of dNTPs (dATP, dGTP, dTTP and dCTP) and sterile distilled water was prepared.

The amplification reaction included an initial denaturation at 94°C for 5 minutes, annealing at 50°C for 1 minute and elongation at 72°C for 1 minute. This was followed by 39 cycles of denaturation at 94°C for 1 minute, annealing at 50°C for 1 minute and elongation at 72°C for 1 minute. In the final cycle, the reaction comprised denaturation at 94°C for 1 minute, annealing at 50°C for 1 minute and elongation at 72°C for 5 minutes. At the end of the PCR process, the reaction temperature was brought down to and held at 4°C. The PCR products were stored at -20°C until use. For *babA2*, all amplification steps were similar except that annealing was carried out at 52°C instead of 50°C.

Table 2. Primers used to amplify various virulence genes of *H. pylori.*

Primer name	Primer Sequence (5' → 3')	T_a (°C)	Length of fragment (bp)
*cagA*F	AATACACCAACGCCTCCAAG	50	400
*cagA*R	TTGTTGCCGCTTTGCTCTC		
*vacA*F	GCTTCTCTTACCACCAATGC	50	1160
*vacA*R	TGTCAGGGTTGTTCACCATG		
*iceA1*F	GTGTTTTTAACCAAAGTATC	50	246
*iceA1*R	CTATAGCCAGTCTCTTTGCA		
*iceA2*F	GTTGGGTATATCACAATTTAT	50	229/334
*iceA2*R	TTGCCCTATTTTCTAGAGGT		
*babA2*F	AATCCAAAAAGGAGAAAAAGTATGAAA	52	831
*babA2*R	TGTTAGTGATTTCGGTGTAGGACA		

F: Forward primer; R: Reverse primer; T_a : annealing temperature.

3.2.3 Agarose gel electrophoresis

An aliquot of 10 µl of PCR product was mixed with 2 µl of 6 × loading buffer (Appendix 6) and electrophoresed in a 1% horizontal agarose (Seakem) gel containing ethidium bromide (Appendix 7) for 1-2 hours at 80 V in 1 × Tris acetate EDTA (TAE) buffer (Appendix 8). Molecular weight markers (100 bp ladder) (Fermentas) were also included in the run to enable easy identification of the band sizes of the PCR products. At the end of each electrophoresis gel run, the ethidium bromide-stained gel was photographed with filtered ultraviolet illumination under the Electrophoresis Documentation and Analysis System 290 (Kodak).

3.3 Bradford protein assay

Bradford protein assay was used to determine the amount of protein in samples. The protocol was carried out according to the manufacturer's instructions (Bio-Rad). A standard curve was constructed using different known concentrations (0.2 – 1 mg/ml) of bovine serum albumin (BSA; Merck). Determination of protein content in samples was carried out by adding 1 µl of each sample in 0.1 ml dye

reaction solution. The dye reaction solution was earlier prepared by mixing 1 part of concentrated Bio-Rad dye solution with 4 parts of deionized water and filtered through Whatman filter paper. The mixture was vortexed and incubated at room temperature for 15 minutes. The optical density (OD) was measured at 595 nm in a microplate reader (Bio-Rad). The protein concentration of samples was calculated based on the standard curve.

3.4 Sodium dodecyl sulphate – polyacrylamide gel electrophoresis (SDS-PAGE)

3.4.1 Preparation of SDS-polyacrylamide gel

Vertical minislab gels (1 mm) comprising 12% resolving gel and 4% stacking gel (Appendix 9) were cast using the Mini-protean II system (Bio-Rad). The two-gel system (stacking and resolving gel) significantly enhances the sharpness of the bands within the gel.

3.4.2 Sample preparation and electrophoretic gel run

Protein samples (10 µl) were mixed with 3 µl of 5 × SDS loading buffer (Appendix 10) and boiled for 5 minutes before being loaded into the wells of the gel slab placed in a mini-PROTEAN 3 vertical electrophoresis system (Bio-Rad). Electrophoresis was performed in running buffer (Appendix 11) at 0.03A/gel at room temperature with Power Pac 250 (Bio-Rad) until the dye front reached the bottom of the gel. Prestained Protein Ladder (Bio-Rad) was used as the molecular marker.

3.4.3 Gel staining and visualization of protein bands

Gels were stained with Coomassie blue solution R-250 (Appendix 12) with gentle shaking for 30 minutes. Following which, the gels were destained with destaining solution (Appendix 13) until the background became clear.

3.5 Cloning and expression of recombinant full length GGT (rGGT), large subunit (rGGTL) and small subunit of GGT (rGGTS)

3.5.1 Construction of pRSET-*ggt*, pRSET-*ggtl* and pRSET-*ggts*

3.5.1.1 Cloning strategy

pRSET-A expression vector (Invitrogen) was used for the cloning of full length *ggt* excluding the signal peptide (*ggt*; 79^{th}-1704^{th} bp), the *ggt* gene fragment encoding the large (*ggtl*: 79^{th}-1137^{th}) and small subunit of GGT (*ggts*; 1138^{th}-1704^{th} bp). Inserts *ggt* (red), *ggtl* (green) and *ggts* (blue) were ligated separately into the plasmid vector at *Pst*I and *Hin*dIII restriction sites (Figure 5).

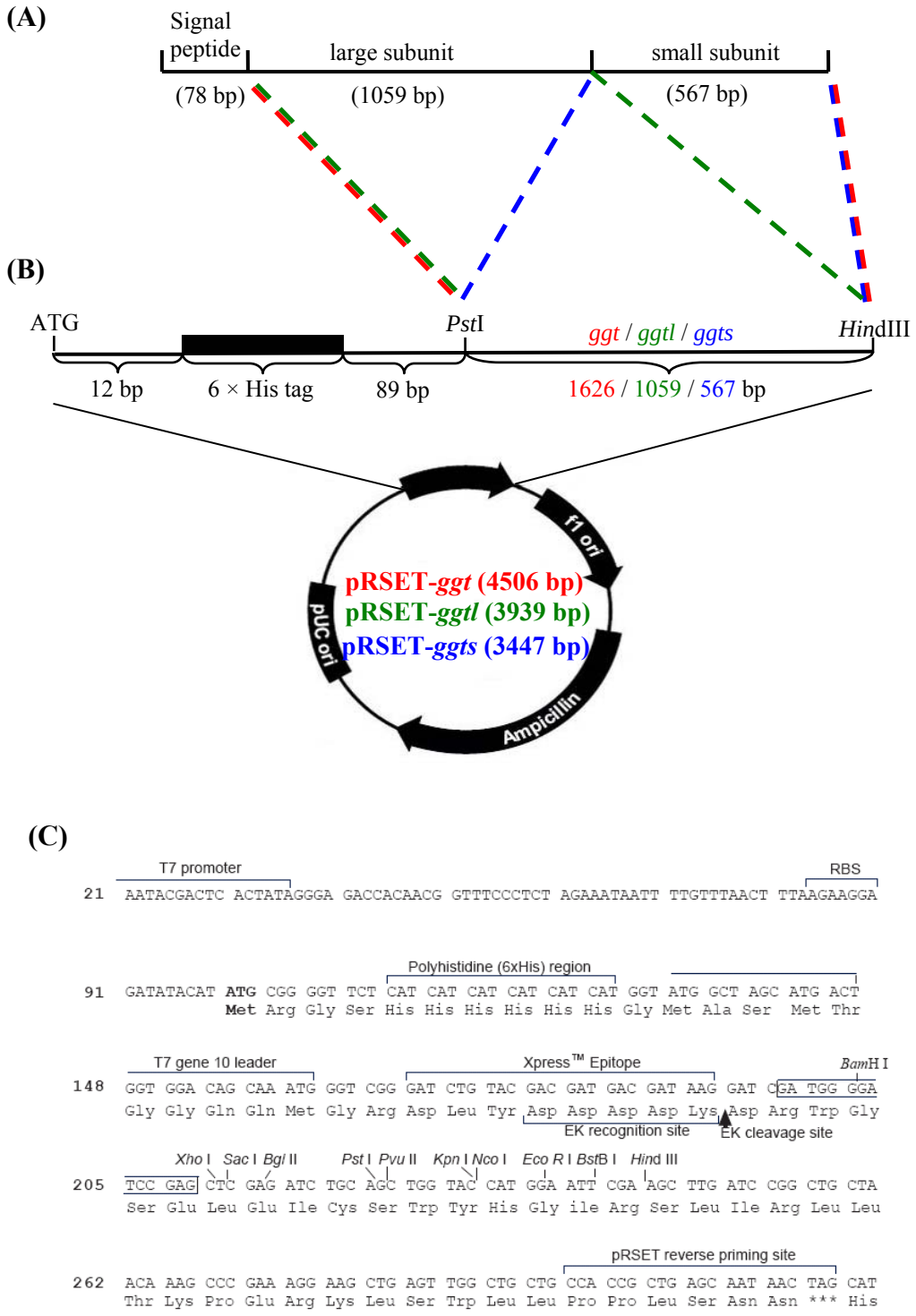

Figure 5. Schematic construction of pRSET-*ggt*, pRSET-*ggtl* and pRSET-*ggts* recombinant expression vector. (A) Diagrammatical representation of *H. pylori* full length *ggt* gene (1704 bp). (B) Physical map of pRSET-*ggt* (red), pRSET-*ggtl* (green) and pRSET-*ggts* (blue) recombinant expression vectors. (C) Multiple cloning site of pRSET-A vector.

3.5.1.2 PCR amplification of *ggt*, *ggtl* and *ggts*

H. pylori strain 88-3887 genomic DNA was used as the template. Primers were designed according to the genomic sequence of *H. pylori* strain 26695 (Tomb *et al*., 1997). Primer sequences are illustrated in Table 3. *Pst*I and *Hin*dIII restriction sites (underlined) were introduced in the 5' and 3' ends respectively for insertion into the expression vector downstream of Histidine-tag. The PCR amplification condition was set as 30 cycles of denaturation at 94°C for 1 minute, annealing at 50°C for 45 seconds and elongation at 72°C for 2 minutes. The PCR cycles were carried out in an amplification thermal cycler (Bio-Rad) and the amplified gene products were purified using QIAquick PCR Purification Kit (Qiagen) according to the manufacturer's protocol.

Table 3. **Sequences of primers used to amplify *ggt*, *ggtl* and *ggts*.**

Target	Primer	Primer sequence (5' → 3')	Length (bp)
ggt	ggtF	GCCGCTGCAGCGCGAGTTACCCCCCCATTAAA	1626
	ggtR	GCCGAAGCTTTTAAAATTCTTTCCTTGGATCCGTT	
ggtl	ggtlF	GCCGCTGCAGCGCGAGTTACCCCCCCATTAAA	1059
	ggtlR	GCCGAAGCTTATTGCTCCCCTCATGCAACTG	
ggts	ggtsF	GCCGCTGCAGCACCACGCATTATTCTGTAGCGGAC	567
	ggtR	GCCGAAGCTTTTAAAATTCTTTCCTTGGATCCGTT	

*Pst*I (CTACAG) and *Hind*III (AAGCTT) restriction sites are underlined.

3.5.1.3 Restriction enzyme digestion

Restriction enzyme digestion of the plasmid vector pRSET-A and the respective PCR products (from section 3.5.1.2) was carried out using *Pst*I and *Hin*dIII (Promega) simultaneously at 37°C for 4 hours. Buffers compatible to both enzymes were used for this double digest. Respective restriction enzymes were used to digest 0.5 to 1.0 μg of DNA sample. After digestion, restriction enzymes were heat-inactivated at 65°C for 20 minutes.

3.5.1.4 Extraction and purification of insert and plasmid vector

The products from the restriction enzyme reactions were analyzed by agarose gel electrophoresis as described in section 3.2.3. The desired DNA bands were excised from the agarose gel with a clean surgical blade. QIAquick Gel Extraction Kit (Qiagen) was used to purify the excised bands as recommended by the manufacturer. Purified DNA samples were stored at -20°C until use.

3.5.1.5 Ligation of insert into expression vector pRSET-A

The amount of DNA from the purified digested inserts and pRSET-A was measured spectrophotometrically as described in section 3.2.1. The molar ratio of insert DNA to vector DNA used was 3:1. Ligation reaction (10 µl) containing ligase buffer, insert DNA, plasmid vector and T4 DNA ligase (Promega) was carried out at 4°C overnight.

3.5.2 Transformation of *Escherichia coli*

3.5.2.1 *E. coli* strains

E. coli Top10 was used as a host for cloning and maintenance of plasmids as it gives high transformation efficiency and good plasmid yield. *E. coli* BL21 (DE3) pLysS (Novagen) was used as an expression host because it contains a chromosomal copy of the gene for T7 polymerase which facilitates the production of recombinant protein upon induction with isopropyl-β-D-thiogalactopyranoside (IPTG).

E. coli Top10 and BL21 (DE3) pLysS were grown in Luria-Bertani (LB) broth (Appendix 14) or on LB agar plates (Appendix 15) at 37°C. Plasmid-transformed *E. coli* was grown at 37°C on LB agar plates supplemented with 50 µg/ml ampicillin (Appendix 16).

3.5.2.2 Preparation of competent *E. coli*

Competent cells were prepared as previously described (Sambrook *et al.*, 1989). Briefly, a single bacterial colony of *E. coli* was inoculated into 5 ml LB broth and incubated overnight at 37°C on a shaker incubator (Certomat) at 200 rpm. From the overnight bacterial culture, 1 ml was transferred into 100 ml LB broth and incubated at 37°C on a shaker incubator at 200 rpm for 2-4 hours. The growth of the bacteria was monitored periodically by measuring at OD_{600} using a spectrophotometer (Beckman Coulter) . The cells were harvested when OD_{600} reached approximately 0.3. Thereafter, 30 ml of bacterial culture was transferred into a sterile 50 ml centrifuge tube (Falcon) and cooled on ice for 10 minutes before centrifuging at 6000 × g for 5 minutes at 4°C to obtain a cell pellet. The supernatant was discarded and the tube was inverted to drain off excess liquid. The cell pellet was resuspended in 15 ml of ice-cold 0.1 M $CaCl_2$ (Appendix 17) and placed on ice for 30 minutes. The $CaCl_2$-treated cells were centrifuged at 6000 × g for 5 minutes at 4°C. The supernatant was discarded and the tube was inverted to remove excess fluid. The cell pellet was then resuspended in 2 ml ice-cold 0.1 M $CaCl_2$ containing 20% glycerol. Aliquots of 200 µl were stored in microfuge tubes at -80°C until use.

3.5.2.3 Transformation and selection of positive clones

The ligated products (from section 3.5.1.5) were added into 200 µl of thawed *E. coli* Top10 competent cells and gently mixed by tapping. The suspension was incubated on ice for 30 minutes and then heat-shocked at 42°C in a water bath for 90 seconds without shaking. The suspension was quickly transferred on ice for 2 minutes. An aliquot of 800 µl of LB broth was then added into the DNA-cell suspension and incubated at 37°C for 1.5 hours with gentle shaking at 90 rpm. From

the suspension, 200 µl was spread onto LB agar plates containing 50 µg/ml ampicillin, IPTG and 5-bromo-4-chloro-indolyl-β-D-galactopyranoside (X-Gal) (Appendix 18) and incubated overnight at 37°C for a maximum of 20 hours. Blue-white selection was used to screen for *E. coli* transformed with plasmid vector and insert.

3.5.3 Purification and identification of recombinant plasmid

A single white colony of *E. coli* grown on LB agar plate (supplemented with ampicillin, IPTG and X-Gal) was inoculated into 5 ml LB broth containing 50 µg/ml ampicillin and incubated overnight at 37°C on a shaker incubator at 200 rpm. Plasmid DNA was extracted using MiniPrep Kit (Qiagen) according to the manufacturer's instructions.

Extracted plasmids were digested with *Pst*I and *Hin*dIII to screen for positive pRSET-*ggt*, pRSET-*ggtl* and pRSET-*ggts* clones as described in section 3.5.1.3. PCR was also carried out using the primers as recorded in Table 3 to screen for the presence of the respective gene fragments in the extracted plasmids.

3.5.3.1 DNA sequencing

DNA sequencing was performed using the ABIPRISM BigDye^{TM} Terminator sequencing kit (Applied Biosystems). A total of 4 primers, T7 and T7R (specific to sequence on the pRSET-A vector upstream and downstream of the multiple cloning site respectively), F2 and F3 (specific to regions on *ggt* gene) were used (Table 4). The sequencing reaction included 25 cycles of 96°C for 10 seconds, 50°C for 5 seconds and 60°C for 4 minutes. After the reaction was completed, ethanol precipitation was used to remove excess terminators and primers. Precipitated

products were sequenced using ABI 100 model 377 DNA sequencer (Applied Biosystems).

Table 4. Primers for DNA sequencing of *ggt, ggtl* and *ggts* gene inserts cloned into pRSET-A vector.

Primer name	Sequence (5' → 3')	Position on *ggt* gene
T7	TAATACGACTCACTATAGGG	-
T7R	TATGCTAGTTATTGCTCAG	-
F2	GCGATTTCACAAAGACAAGC	511-531
F3	ATGGGGCAGTTGCATGAG	1111-1129

3.5.4 Expression of rGGT, rGGTL and rGGTS

3.5.4.1 Induction of target proteins

The recombinant proteins (rGGT, rGGTL or rGGTS) were induced as recommended by the manufacturer (Invitrogen). The constructed recombinant expression vector pRSET-*ggt*, pRSET-*ggtl* or pRSET-*ggts* was transformed into *E. coli* expression strain BL21 (DE3) pLysS by the method described in section 3.5.2.3. To optimize the conditions for induction, a single colony of transformed *E. coli* BL21 (DE3) pLysS was picked and inoculated into 5 ml of LB medium supplemented with 50 µg/ml ampicillin. The culture was shaken overnight vigorously in a 37°C shaking incubator at 200 rpm. An aliquot of 100 µl of overnight culture was inoculated into 5 ml LB medium supplemented with 50 µg/ml ampicillin and the cultures were shaken vigourously at 200 rpm at 37°C until an OD_{600} of 0.5 was reached. Cultures were then supplemented with IPTG (ranging from 0.2 mM to 0.8 mM final concentration) and shaking was continued. Induced cells were collected after 3 hours of incubation. Uninduced cells served as the negative control. After centrifugation at 6000 × g for 5 minutes, cell pellets were thoroughly resuspended in 50 µl of SDS loading buffer and subjected to SDS-PAGE analysis as described in section 3.4. The large scale

expression of rGGT, rGGTL and rGGTS was subsequently carried out in 100 ml LB medium according to the respective optimized conditions for induction.

3.5.4.2 Localization of target proteins

Induction of respective *E. coli* clones in 5 ml LB medium was carried out under the optimized conditions (rGGT: 0.4 mM IPTG; rGGTL: 0.2 mM IPTG; rGGTS: 0.2 mM IPTG) as described in section 3.5.4.1. Cells were then centrifuged at 6000 × g for 10 minutes at 4°C. The supernatant was collected and the pellet was resuspended in 0.5 ml of phosphate-buffered saline (PBS) (Appendix 19). This cell suspension was sonicated on ice at 10 MHz for 10 seconds with 10 seconds rest for 20 cycles using a Soniprep 150 sonicator (Sanyo). The whole cell lysate was then centrifuged at 8000 × g for 10 minutes at 4°C. The supernatant and pellet obtained served as the soluble and insoluble fraction respectively. The pellet was resuspended in SDS loading buffer and all fractions were subjected to SDS-PAGE as described in section 3.4.

3.5.5 Purification of rGGT, rGGTL and rGGTS

3.5.5.1 Preparation of cell extracts

Induction of respective *E. coli* clones in 100 ml LB medium was carried out. Cells were harvested at 6000 × g at 4°C for 5 minutes, resuspended in binding buffer (Appendix 20A) and sonicated on ice 20 times for 10 seconds at 10 MHz amplitude with 10 seconds rest using a Soniprep 150 sonicator (Sanyo). The whole cell lysate was then centrifuged at 8000 × g for 10 minutes at 4°C to separate the soluble and insoluble fractions. As rGGT was found to be substantially present in both the soluble and insoluble fractions, the soluble fraction was used in the downstream purification

process as insolubility generally indicates misfolding of the protein (Fahnert *et al.*, 2004). The solution was filtered through a 0.45 μm syringe filter (Millipore) before purification. On the other hand, rGGTL and rGGTS were exclusively found in the insoluble fraction. Hence, purification of rGGTL and rGGTS was carried out under denaturing conditions. After centrifugation of the whole cell lysate, the pellet was resuspended in binding buffer containing 6 M urea for 2 hours at 4°C with gentle shaking to completely dissolve the protein. The remaining insoluble content was removed by centrifugation at 6000 × g for 10 minutes while the supernatant was filtered through a 0.45 μm syringe filter (Millipore).

3.5.5.2 His-Tag affinity chromatography

Purification of rGGT was carried out using affinity chromatography through a nickel chelating column (GE Healthcare) according to the manufacturer's instructions. The column was first washed with distilled water and subsequently charged with 1 × charge buffer (Appendix 20B). The column was then equilibrated with 1 × binding buffer (Appendix 20A). Following which, the sample (from section 3.5.5.1) was loaded onto the column and washed with 1 × binding buffer to remove unbound proteins. The column was then washed again with 6 volumes of 1 × wash buffer (Appendix 20C). The target protein was eluted with an ascending gradient of imidazole ranging from 0.1 – 1 M using 6 column volumes of 1 × elute buffer (Appendix 20D). After elution, the column was stripped with 1 × strip buffer (Appendix 20E). All fractions collected throughout the purification procedures were subjected to SDS-PAGE as described in section 3.4 and protein concentration was measured by Bradford protein assay (as described in section 3.3). Purification of

rGGTL and rGGTS was subjected to the same procedures except that binding, wash and elute buffers loaded onto the column contained 6 M urea.

3.5.5.3 Dialysis of purified recombinant proteins

The eluted rGGT protein was dialyzed against three changes of PBS at 4°C for 10-12 hours each. For rGGTL and rGGTS, the proteins were first diluted to a concentration of 50 µg/ml. Following which, step-wise dialysis against three changes of PBS buffer containing decreasing concentrations of urea (4 M – 0 M) was carried out at 4°C for 10-12 hours each. Concentration of the recombinant proteins was carried out using PEG 35000 (Merck).

3.5.5.4 Mass spectrometry

Purified recombinant proteins were subjected to SDS-PAGE and the coomassie blue-stained protein bands of interest were individually excised. In-gel trypsin digestion was then carried out according to the method as described by Shevchenko *et al.* (1996). All reagents used were of high performance liquid chromatography (HPLC) grade. The target protein bands were excised from the gel with a clean blade and grinded into small pieces in a microcentrifuge tube. The gel pieces were immersed in 100 µl of 100 mM ammonium bicarbonate/50% (v/v) acetonitrile (Merck), vortexed and left to stand for 5 minutes at room temperature. The solution was removed and the step was repeated 2-3 times until the gel washings came out colourless. The white and opaque gel pieces were then treated with 50 µl acetonitrile for 5 minutes. After removal of the acetonitrile, the gel pieces were dried in a vacuum centrifuge (Thermo Electron Corporation).

Reduction of the protein sample was carried out by adding a fresh solution of 10 mM dithiothreitol (DTT) in 100 mM ammonium bicarbonate with a volume enough to cover the gel fully. The sample was incubated at 57°C for 60 minutes. Afterwhich, the excess DTT was aspirated and the protein samples were alkylated with 55 mM iodoacetamide solution in 100 mM ammonium bicarbonate. The reaction was carried out in the dark and left at room temperature for 60 minutes. After alkylation, the gel pieces were washed thrice with 100 µl of 100 mM ammonium bicarbonate solution and dehydrated twice with 100 µl acetonitrile. Washing and dehydration steps were repeated twice before drying to completion with a vacuum centrifuge.

The dried gel pieces were incubated with 12.5 ng/µl modified sequencing grade trypsin (Promega) in 50 mM ammonium bicarbonate (15-30 µl, depending on the size of the gel pieces) for 30 minutes at 4°C. Excess trypsin solution was then removed and 15 µl of 50 mM ammonium bicarbonate solution was added. The digestion was continued overnight at 37°C, afterwhich the digested gel pieces were centrifuged at 6000 × g for 10 minutes and the supernatant transferred to a fresh microcentrifuge tube. The gel pieces were then further treated with 20 mM ammonium bicarbonate and the supernatant was again saved after centrifugation. Finally, the gel pieces were treated with 5% formic acid in 50% aqueous acetonitrile (10-25 µl) for 5-10 minutes at room temperature before centrifugation. All three supernatants containing the digested peptides were pooled and dried in a vacuum centrifuge to completion. The peptides were subsequently purified and concentrated using Zip Tip C_{18} (Millipore) before being sent for identification by mass spectrometry. Peptide mass fingerprints and sequence were obtained using a matrix-assisted laser desorption/ionization-time of flight (MALDI-TOF) mass spectrometer

(Micromass Q-Tof Tandem Mass Spectrometer; Applied Biosystems). Mass spectrometry was performed at the Protein and Proteomics Centre, National University of Singapore and the data was analyzed using NCBI database search (www.matrixscience.com) to determine the identity of the proteins.

3.5.5.5 GGT activity assay

GGT activity was assayed according to the method described by Gong and Ho (2004). γ-glutamyl-ρ-nitroanilide (Sigma-Aldrich) was used as a donor substrate and glycyl-glycine (Sigma-Aldrich) was used as the glutamate acceptor for the transpeptidation reaction. Briefly, purified rGGT was incubated at 37°C for 30 minutes in 1 ml of 100 mM Tris-HCl (pH 8.0) in the presence of 1 mM γ-glutamyl-ρ-nitroanilide and 20 mM glycyl-glycine (Appendix 21). The production of free ρ-nitroanilide released in the incubation medium was determined by spectrophotometry at 405 nm. One unit of GGT activity was defined as the quantity of enzyme that releases 1 μmol ρ-nitroaniline per minute per mg of protein at 37°C. Bovine GGT (Sigma-Aldrich) served as control.

3.6 Raising antibody against rGGTS and rGGT

3.6.1 Raising polyclonal antibody in rabbits using rGGTS

Polyclonal antibodies were generated against rGGTS as the small subunit of GGT is more conserved than the large subunit (Chevalier *et al*., 1999). These antibodies were later used to detect for the presence of GGT in gastric epithelial cells by western blot analysis.

3.6.1.1 Immunization procedure

Antibody against rGGTS was raised in rabbits according to the method as described (Coligan and Current Protocols Online., 1992) with slight modifications. The study was approved by the Institutional Animal Care and Use Committee, National University of Singapore. After refolding, the mixture of purified rGGTS (150 μg) and Complete Freund's adjuvant (Sigma-Aldrich) was injected into a New Zealand white rabbit (~1.2 kg) subcutaneously at 7-8 different spots. Two boosters (consisting of 150 μg rGGTS and Incomplete Freund's adjuvant) were given on days 28 and 42 after the first immunization respectively. Blood (~15 ml) was drawn from the rabbit's ear before each booster and subsequently on days 56, 71 and 85 after the first immunization. The rabbit was sacrificed after the final bleed on day 85. Serum was separated from whole blood by centrifugation at 1500 × g for 10 minutes.

3.6.1.2 Enzyme-linked immunosorbent assay (ELISA)

Antibody production profile was determined by indirect ELISA method as previously described (Delves, 1995). In brief, *H. pylori* wild type or Δ*ggt* were first lysed in lysis buffer (Appendix 22). The total cell lysate was then diluted in carbonate coating buffer (Appendix 23) to a concentration of 100 ng/ml. An aliquot of 100 μl of the diluted antigen was coated onto each well of a microtitre plate (Nunc) and incubated overnight at 4°C. The coated plate was washed 3 times with 0.05% PBS-Tween buffer (PBS-T; Appendix 24) and blocked with 2% BSA-PBS (w/v) at room temperature for 2 hours. Aliquots of 100 μl of rabbit sera diluted in 2% BSA-PBS (1:400) were then added in triplicates and incubated at room temperature for 2 hours. The plates were then washed thrice with 0.05% PBS-T before 100 μl of horseradish-peroxidase-conjugated goat anti-rabbit secondary antibody (1:2000)

(DakoCytomation) was added to each well and incubated for another 2 hours at room temperature. The plate was then washed thrice with 0.05% PBS-T. Substrate solution consisting of tetramethylbenzidine (TMB) and H_2O_2 (BD Pharmingen) was added to each well (100 µl/well) and incubated in the dark for 30 minutes. The reaction was stopped using 2N H_2SO_4 (50 µl/well). Absorbance was read at OD_{450} with substraction of background OD_{570} using a microplate reader (Bio-Rad).

3.6.1.3 Purification of anti-rGGTS antibody

Protein A sepharose CL-4B (Amersham Biosciences) affinity column was used to purify IgG from antiserum (Coligan and Current Protocols Online., 1992) according to the manufacturer's protocol. The serum was diluted with 4 volumes of 50 mM Tris-Cl buffer (pH 7.0) and loaded into the equilibrated column. The specific IgG was eluted with 0.1 M glycine-Cl buffer (pH 3.0) and neutralized with 1 M Tris-Cl (pH 9.0; 50-100 µl/ml fraction) immediately after elution. All buffers used were kept on ice during the purification process. The purified IgG was analyzed by SDS-PAGE (as described in section 3.4) and protein concentration was measured by Bradford protein assay (as described in section 3.3). The purified IgG was stored at -80°C until use.

3.6.1.4 Characterization of antibody by western blot analysis

Purified IgG was characterized on its binding specificity using Western blot analysis. *H. pylori* wild type and Δ*ggt* whole cell lysates (10 µg) were run on SDS-PAGE (as described in section 3.4) and transferred onto a polyvinylidene fluoride (PVDF) membrane (ImmobilionP, Millipore) by semi-dry blotting using Trans-Blot® SD Semi-Dry Transfer Cell (Bio-Rad) for 1 hour at 150 mA (Appendix 25). The non-

specific binding sites of the membrane were blocked overnight with 2% BSA-PBS with slight rotation at 4°C. The membrane was then incubated with the purified IgG against rGGTS in 2% BSA-PBS (1:4000 dilution) for 2 hours at 4°C on a belly dancer (Stovall Life Sciences, Inc). Following which, the membrane was washed with 0.1% PBS-T five times for 5 minutes each and incubated with horseradish-peroxidase-conjugated goat anti-mouse secondary antibody (1:2000 dilution; DakoCytomation) for 2 hours at room temperature with slight agitation. The membrane was washed again in 0.1% PBS-T for five times. Signals were detected using enhanced chemiluminescence detection kit (Pierce) according to the manufacturer's protocol.

3.6.2 Raising monoclonal antibody (MAb) in mice using rGGT

3.6.2.1 Immunization, fusion and ascites production

MAb production was done in collaboration with Dr. Hwang Le-Ann (Monoclonal Antibody Unit, Institute of Molecular & Cell Biology, Singapore). Briefly, five BALB/c female mice, aged 8 weeks old were immunized with 100 μg of purified rGGT emulsified in Complete Freund's Adjuvant (Sigma-Aldrich) by intraperitoneal injection. Booster injections were administered 4 times in the same manner using Incomplete Freund's Adjuvant (Sigma-Aldrich) at 3-week intervals. Prior to hybridoma fusion, GGT-specific antibodies in the serum of immunized mice were tested by ELISA and Western blot assays as described in sections 3.6.1.2 and 3.6.1.4 respectively. The mouse with the highest antibody titre was selected for a final boost of 100 μg of purified rGGT intravenously 2 days before the fusion. Hybridoma cells were generated by fusing immune spleen cells with mouse SP2-0/Ag14 myeloma cells following the manufacturer's instructions of the ClonaCell®-HY hybridoma kit (StemCell technologies). MAb in supernatants of hybridoma cultures

were screened with an ELISA test using purified rGGT as antigen. Positive hybridoma clones were subcloned twice by limiting dilution. Ascitic fluid was obtained by introducing 1 x 10^5 hybridoma cells via intraperitoneal inoculation into BALB/c mice pre-primed with Incomplete Freund's Adjuvant. All procedures on the use of laboratory animals were done in accordance with the regulations and guidelines of the National Advisory Committee for Laboratory Animal Research, Singapore.

3.6.2.2 Characterization of MAbs from different clones

All anti-GGT MAbs were purified from ascitic fluid using Protein G sepharose columns and stored at -20°C. The isotype of each MAb was determined using the IsoStrip Mouse Monoclonal Antibody Isotyping Kit (Roche). Specificity of MAb to *H. pylori* GGT was determined by western blot analysis as described in section 3.6.1.4.

3.6.2.3 Epitope mapping strategy

A library of 267 peptides, consisting of 15 amino acids overlapping by 12 (3-offset) corresponding to the sequence of GGT, was commercially synthesized (PepSets™; Chiron Mimotopes). The biotinylated peptides were resuspended at a concentration of 5 mg/ml in 40% acetonitrile and stored in aliquots at −20°C. The peptides were diluted with 0.1% PBS-T before use.

Indirect ELISA was performed as follows: 96-well flat-bottom plates (Nunc) were coated with 100 µl streptavidin (Sigma-Aldrich) at a concentration of 5 µg/ml and left to evaporate to dryness overnight at 37°C. Wells were blocked with 2% BSA-PBS-T for 1 hour at room temperature and coated with 100 µl of peptides (2.5 µg/ml) for another 1 hour. Respective MAbs (1:1000 dilution) were used as primary antibody

and goat anti-mouse IgG conjugated with horseradish peroxidase (1:2000 dilution, DakoCytomation) was used as secondary antibody. The substrate used was TMB (BD PharMingen) as described in section 3.6.1.2. Absorbance was determined at a wavelength of 450 nm with subtraction of absorbance at 570 nm in a microplate reader (Bio-Rad). Overlapping regions on positive adjacent peptides were used to map the minimum epitope sequence specific to each MAb.

3.7 Neutralization of GGT activity using MAbs

A total of 5×10^6 *H. pylori* were pre-incubated with various amounts (0.25-30 μg) of different MAbs for 1 hour at 37°C in a 96-well microtitre plate. Mouse IgG_1, IgG_{2a} and IgG_{2b} isotype controls were used in parallel at the same concentrations. Quantitative detection of GGT activity was then carried out as previously described in section 3.5.5.5. Percentage inhibition of GGT activity was calculated as follows:

$$\% \text{ inhibition} = \frac{\text{GGT activity without MAb} - \text{GGT activity with MAb}}{\text{GGT activity without MAb}} \times 100\%$$

Where indicated, ability of MAbs to neutralize bovine GGT (1 mU; Sigma-Aldrich) was also tested in the same manner.

3.8 Purification of native GGT (nGGT) from *H. pylori*

3.8.1 Culture of *H. pylori*

H. pylori 88-3887 was used as the source for purification of nGGT. The 3-day old bacteria cultures grown on 30 CBA plates were harvested, washed twice with 20 ml of PBS and resuspended in a final volume of 10 ml of PBS. Bacterial cells were disrupted by sonication (30 seconds × 10 with 30 seconds rest at each interval) and the cellular debris along with unbroken cells was removed by centrifugation at 8000 ×

g for 15 minutes at 4°C. The supernatant was centrifuged at 20,000 × g for 90 minutes at 4°C and the clear supernatant was collected, membrane filtered (0.2 µm, Sartorius) and used for nGGT purification.

3.8.2 Preparation of immunoaffinity resin

Purified MAb 1G1 (5 mg) was diluted in coupling buffer (Appendix 26A) at 5 mg/ml and immobilized on 2 ml of CNBr-activated Sepharose 4B (Amersham Biosciences) overnight at 4°C with gentle rotation. Excess ligand was washed away with at least 5 medium volumes of coupling buffer. Remaining active groups were blocked with 0.1 M Tris-HCl buffer (pH 8.0) (Appendix 26B) for 2 hours and the resin was packed into a column according to the manufacturer's instructions.

3.8.3 Immunoaffinity chromatography

The sample obtained as described in section 3.8.1 was loaded in the CNBr-activated Sepharose 4B column pre-equilibrated with PBS buffer. After 5 column volumes wash with PBS, bound nGGT was eluted with elution buffer (Appendix 26C) Fractions with GGT activity (measured using GGT activity assay as described in section 3.5.5.5) were neutralized by dropwise addition of neutralization buffer (50-100 µl/ml fraction) (Appendix 26D) and stored at -20°C until use. The purified nGGT was analyzed by SDS-PAGE (as described in section 3.4) and the protein concentration was measured by Bradford protein assay (as described in section 3.3).

3.9 Immunogold-labeling transmission electron microscopy (TEM)

3.9.1 Preparation of cells and ultrathin sectioning

Post-embedding immunogold-labeling TEM was performed as previously described (Kaur *et al.*, 2002) with slight modifications. *H. pylori* strain 88-3887 was harvested from a 3-day old plate culture and washed with PBS. It was then fixed in PBS containing 4% paraformaldehyde, 0.2% glutaraldehyde and 2% sucrose for 5 hours at 4°C. The fixed cells were washed in 2% sucrose-PBS thrice for 5 minutes each and resuspended in 2% sucrose-PBS overnight at 4°C. The next day, the cells were washed twice with water for 10 minutes and subsequently dehydrated in an ascending graded series of ethanol (ranging from 25% ethanol to absolute) at room temperature. Infiltration using LR white resin (Ted Pella) was carried out over 2 days. On the first day, the sample was passed through 4 changes of LR white (1 part ethanol: 1 part LR white for 30 minutes, 3 parts ethanol: 7 parts LR white for 30 minutes, 1 change of pure LR white for 30 minutes, followed by another change of pure LR white overnight). On the second day, the sample was infiltrated with 4 changes of pure LR white for 30 minutes each. After the fourth change, the sample was embedded in a gelatin capsule. Briefly, 1 mm of block sample was placed in the gelatin capsule and LR white was filled to the brim. The capsule was then incubated at 50°C for a minimum of 48 hours until polymerization of LR white had occurred. Ultrathin sections (70-100 nm) of the sample were cut using an ultramicrotome (Ultracut E, Leica) and subjected to immunogold-labeling on a nickel grid.

3.9.2 Localization of GGT in *H. pylori*

The ultrathin sections were washed twice with PBS for 5 minutes each and neutralized with 3 changes of 0.05 M glycine-PBS for 5 minutes each. Following

which, the sections were blocked with 5% BSA-PBS for 1 hour to reduce non-specific binding. The sections were then washed with 0.1% BSA-PBS and then incubated with MAb 1G1 (1:50 dilution) raised against rGGT (as described in section 3.6.2.1) for 2 hours at room temperature. This was followed by incubation with anti-mouse antibody conjugated with 10 nm gold (1:30 dilution, Ted Pella) as the secondary antibody for an additional 2 hours at room temperature. After washing, sections were then fixed with 2% glutaraldehyde-PBS for 5 minutes. Thereafter, the sections were stained with 1% osmium tetroxide, 8% uranyl acetate, followed by lead citrate for 5 minutes each before viewing under JEOL JEM-1010 transmission electron microscope. Pre-immune serum served as negative control.

3.10 Construction of deletion mutants in *H. pylori* by a PCR-based approach

3.10.1 Design of gene-targeting constructs

The *H. pylori* deletion mutants (Δ*ggt*, Δ*vacA*, Δ*vacA*/*ggt*, Δ*cagA*, Δ*cagA*/*ggt*, Δ*ureAB* and Δ*ureAB*/*ggt*) were constructed using a modified 3-step PCR approach as described by Tan and Berg (2004). Genomic DNA of *H. pylori* strain 88-3887 was extracted as described in section 3.2.1 and used as the template for PCR amplification. The *ggt* gene was replaced by a kanamycin resistance cassette while the *cagA*, *vacA* and *ureAB* genes were replaced by a chloramphenicol resistance cassette. Primers (Table 5) were designed according to the known *H. pylori* 26695 DNA sequence (Tomb *et al.*, 1997) for the amplification of two flanking DNA sequences of the gene of interest. Using the construction of Δ*ggt* as an example (Figure 6), the 5' flanking DNA fragment of 557 bp was amplified using primers ggt1 and ggt2. This fragment included part of HP1119 and a 3' overhang complementary to the kanamycin resistance cassette. The 3' flanking fragment was 522 bp and included part of HP1117

and a 5' overhang complementary to the kanamycin resistance cassette. The 3' flanking fragment was amplified using primers ggt3 and ggt4. Another two primers, kanF and kanR, were designed to amplify the kanamycin resistance cassette from plasmid pILL600 (kindly provided by Dr. Labigne A., Pasteur Institute, Paris, France). PCR amplification conditions were set as 30 cycles of denaturation at 94°C for 1 minute, annealing at 55°C for 45 seconds and elongation at 72°C for 2 minutes. The three PCR reactions were carried out separately in an amplification thermal cycler (Bio-Rad) and the PCR amplified gene products were purified using a gel extraction kit (Qiagen) as described in section 3.5.1.4.

A second round of PCR amplification was carried out to ligate the three DNA fragments. The three separate DNA fragments were used as templates (50 ng of each) and ligation was carried out in one PCR mixture. Primers ggt1 and ggt4 were used and PCR conditions were set as 30 cycles of denaturation at 94°C for 1 minute, annealing at 55°C for 45 seconds and elongation at 72°C for 3 minutes. Vent polymerase (New England Biolabs) was used to amplify the 2442 bp fragment. The PCR amplified DNA fragment was purified using a gel extraction kit (Qiagen) as described in section 3.5.1.4. The other isogenic mutants (Δ*vacA*, Δ*vacA*/*ggt*, Δ*cagA*, Δ*cagA*/*ggt*, Δ*ureAB* and Δ*ureAB*/*ggt*) were constructed using a similar approach. Δ*cag*PAI was constructed by transforming plasmid pJP46 (kindly provided by Prof. Haas R., Ludwig-Maximilians-University Munich, Germany) (Odenbreit *et al.*, 2001) into *H. pylori* 88-3887.

Table 5. Primers used for the construction of isogenic mutants.

Deletion mutant	Primer	Primer sequence (5' → 3')	Reference
	camF	TTATCAGTGCGACAAACTGGG	
	camR	GATATAGATTGAAAAGTGGAT	
	kanF	GATAAACCCAGCGAACCAT	
	kanR	GGTACTAAAACAATTCATCCAGTA	
Δggt	ggt1	CGAACATGATGCAGCAATTGCAA	
	ggt2	ATGGTTCGCTGGGTTTATCCGTCTCA TCTGTTTTCCTTTCAAT	
	ggt3	GGATGAATTGTTTTAGTACCCGATGT TAGATCTAAAATGGTGTGT	
	ggt4	CCACGGCTTTCTTTTCATCTTTA	
ΔcagA	cagA1	GCTCCATTTTAAGCAACTCCAT	
	cagA2	CCCAGTTTGTCGCACTGATAACCTAGT TTCATACTATCGGTAT	
	cagA3	ATCCACTTTTCAATCTATATCGGTCTTG CTGTTAAGCATCTT	
	cagA4	ATTAAGAACGCGATTGATTTGC	
ΔvacA	vacA1	CGTTGAGCGTTTTAGAAAGCAT	
	vacA2	CCCAGTTTGTCGCACTGATAAGCACAA AGGGTG CGACTTTA	
	vacA3	ATCCACTTTTCAATCTATATCGCATAC ACCACAAGC TTGTTA	
	vacA4	CCCAAGTGGAATATTATGCGTT	
ΔureAB	ure1	TCCCTAAAGGGATTTTCAAGATGT	
	ure2	CCCAGTTTGTCGCACTGATAACCATGT GTTCGT GGATGGCAA	(Tan and Berg, 2004)
	ure3	ATCCACTTTTCAATCTATATCATTCTCC TATTC TTAAAGTGTTTT	
	ure4	CATGGGGGCGTGGTGGATTA	

Overlaps between primers ggt2 and kanF, primers ggt3 and kanR are shown in red. Overlaps between primers cagA2 and camF, primers cagA3 and camR, primers vacA2 and camF, primers vacA3 and camR, primers ure2 and camF, primers ure3 and camR are shown in blue. (F: Forward primer; R: Reverse primer; kan: kanamycin; cam: chloramphenicol).

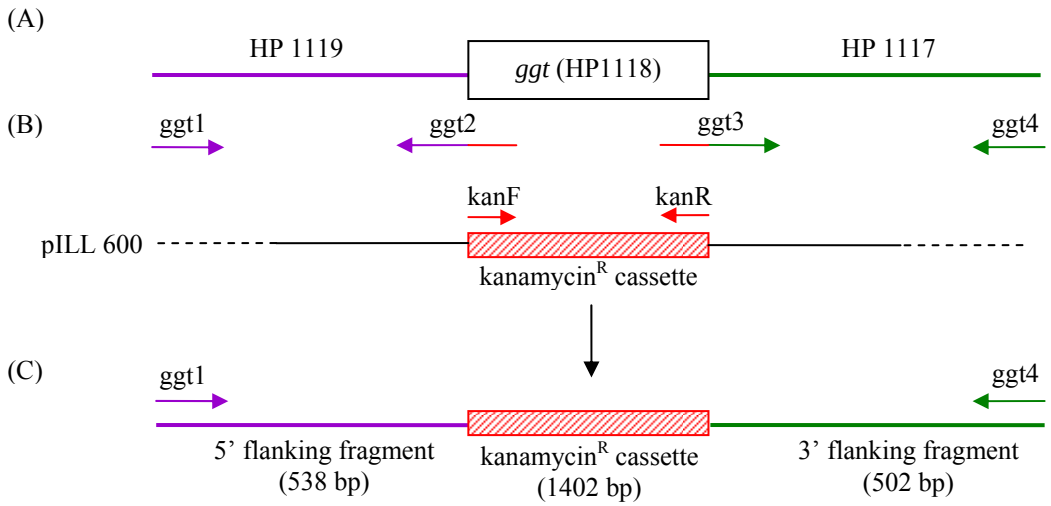

Figure 6. Diagrammatical representation of gene-targeting construct. (A) Location of *ggt* gene in genome of *H. pylori* 26695. (B) Design of 3 sets of primers based on the known sequences. (C) Final construct of 2442 bp used to transform *H. pylori*.

3.10.2 Transformation of *H. pylori* with gene-targeting DNA constructs

Half a plate of a 3-day-old culture of *H. pylori* 88-3887 cells with confluent growth was transferred onto a fresh CBA plate and incubated at 37°C in a CO_2 incubator with 5% CO_2 for 4 hours. Following which, approximately 300 ng of targeting DNA fragment was overlayed onto the surface of the bacterial culture on the CBA plate. After incubation at 37°C with 5% CO_2 for 48 hours, the lawn of bacterial cells was transferred onto 2 fresh CBA plates containing 20 µg/ml kanamycin (for Δ*ggt* and Δ*cag*PAI) or 15 µg/ml chloramphenicol (for Δ*cagA*, Δ*vacA* and Δ*ureAB*) using an inoculation loop and the plates were further incubated at 37°C with 5% CO_2 for 3-4 days. The colonies that grew on the selective CBA plates were selected and sub-cultured for three rounds to purify the deletion mutants. Subsequently, the isolated cultures were maintained on selective CBA plates supplemented with the respective antibiotics. The purified deletion mutants were also preserved in BHI broth medium supplemented with 10% horse serum, kanamycin (20 µg/ml) or chloramphenicol (15 µg/ml), 20% glycerol and stored at -80°C.

3.10.3 Identification of isogenic *H. pylori* mutant of interest

PCR amplification was used to identify the different *H. pylori* mutants using various primers. Due to homologous recombination of the antibiotic resistance gene in place of the gene of interest, the wild type and deletion mutant would give PCR products of different sizes as illustrated in Table 6. Confirmation of the *cag*PAI deletion in *H. pylori* 88-3887 was carried out by checking the presence of the *cag*PAI empty site.

In addition, GGT assay was used to analyze GGT activity in Δ*ggt* as described in section 3.5.5.5. Urease assay was used to analyze urease activity in Δ*ureAB*. In brief, equal volumes (0.5 ml/0.5 ml) of bacterial culture and urease reagent (pH 6.8) (Appendix 27) were mixed in a microfuge tube. A positive test for urease is indicated by a colour change of the reagent from orange to magenta within minutes.

Table 6. Primers used to check for positive isogenic mutants.

Deleted gene(s)	Primers (5'→3')	PCR product size	
		Wild type	Isogenic mutant
ggt	ggt1 and ggt4 (Table 5)	2869 bp	2442 bp
cagA	cagA1 and cagA4 (Table 5)	4730 bp	1799 bp
vacA	vacA1 and vacA4 (Table 5)	5006 bp	1778 bp
ureAB	ure1 and ure4 (Table 5)	3619 bp	2010 bp
*cag*PAI	Luni1: ACA TTT TGG CTA AAT AAA CGC TG R5280: GGT TGC ACG CAT TTT CCC TTA ATC	-	1908 bp (Mukhopadhyay *et al.*, 2000)

3.11 Cell culture

3.11.1 AGS gastric cancer epithelial cells

Human gastric adenocarcinoma cell line AGS (CRL-1739; American Type Culture Collection, Manassas, VA) was cultured in F-12K nutrient mixture, Kaighn's

modification (Sigma-Aldrich) supplemented with 10% fetal calf serum (Gibco) (Appendix 28). The culture flasks were incubated at 37°C in a CO_2 water-jacketed incubator (Forma Scientific) with 95% humidity and 5% CO_2.

3.11.2 HeLa cervical cancer cells

Human cervical adenocarcinoma cell line HeLa (CCL-2; American Type Culture Collection, Manassas, VA) was cultured in Roswell Park Memorial Institute (RPMI)-1640 medium (Sigma-Aldrich) supplemented with 10% fetal calf serum (Gibco) and 2 mM L-glutamine (Appendix 29). Cells were incubated at 37°C under 5% CO_2 in a CO_2 water-jacketed incubator.

3.11.3 Primary human gastric cells

Human gastric biopsies were kindly provided by A/Prof. Yeoh K.G. (National University of Singapore). Primary gastric epithelial cells were isolated from these gastric biopsies and cultured according to the method described by Smoot *et al.* (2000).

3.11.3.1 Tissue collection

Gastric biopsies were obtained from patients undergoing upper endoscopy at National University Hospital. Informed consent was obtained from all patients for gastroscopy and biopsies. All biopsies were obtained from the antrum of the stomach and were taken from areas of grossly normal gastric mucosa. The specimens were collected in Leibowitz's L-15 medium (Gibco) containing 1% penicillin/streptomycin (Gibco) (Appendix 30A) for transport to the research laboratory.

3.11.3.2 Coating of culture dishes

Type 1 rat tail collagen (Gibco) and fibronectin (Gibco) were diluted into Ham's F-12 medium at a concentration of 0.05% and 0.01% respectively (Appendix 30B) and culture dishes were incubated for 1-2 hours at 37°C before gastric cells were plated.

3.11.3.3 Isolation and culture of gastric cells

The biopsies were placed into a 100 mm culture dish containing 5 ml of collagenase/dispase solution (Appendix 30C). They were then minced with a sterile scalpel into pieces approximately 1 mm in size. The minced tissue in collagenase/dispase solution was transferred into a sterile bottle (with addition of 20 ml of collagenase/dispase solution) and incubated at 37°C for 1 hour. The bottle was gently shaken every 15 minutes. Afterwhich, the tissue was pelleted by centrifugation at 250 × g for 5 minutes at 4 °C. The collagenase/dispase was discarded and the tissue was washed once in 10 ml of PBS and pelleted again by centrifugation. Finally, the cell pellet was resuspended in Ham's F-12 cell culture medium supplemented with 10% fetal calf serum, 1% pencillin/streptomycin, 0.2% fungizone (Appendix 30D) and placed into a coated 12-well tissue culture plate (from section 3.11.3.2). Approximately 2-3 biopsies were placed into each well. The following day, the cell culture was rinsed twice with PBS containing 1% pencillin/streptomycin and 0.2% fungizone to remove non-adherent cells before the addition of fresh Ham's F-12 cell culture medium (supplemented with 1% pencillin/streptomycin and 0.2% fungizone). The medium was changed every 3–4 days thereafter. Prior to infection with *H. pylori*, the culture medium containing antibiotics was removed and cells were rinsed thrice with Ham's F-12 cell culture medium without antibiotics.

3.11.4 Primary human macrophages

Primary human macrophages were kindly provided by A/Prof. Lu J.H. (National University of Singapore) and cultured according to the method previously described (Cao *et al.*, 2005). Monocytes were isolated from healthy adult blood donors (National University Hospital Blood Donation Centre, Singapore). In brief, peripheral blood mononuclear cells were isolated from the buffy coats using Ficoll-Paque Plus (Amersham Biosciences). After washing, the cells were allowed to adhere to tissue culture plates for 2 hours at 37°C. Non-adherent cells were removed by washing, and the adherent monocytes were harvested. The isolated monocytes were cultured at 1×10^6/ml in complete RPMI medium (Appendix 29). Macrophages were cultured from isolated monocytes in the presence of macrophage colony-stimulating factor (20 ng/ml) for 6 days.

3.12 Host-pathogen interaction study

3.12.1 Enumeration of cells

AGS cells were first washed twice with 10 ml of PBS to remove dead floating cells before the addition of 2 ml of 1% trypsin-EDTA. The cells were then incubated at 37ºC in a CO_2 water-jacketed incubator (Forma Scientific) for 10 minutes to ensure that all the cells had been detached from the flask surface. Cells were then enumerated using a cell counting chamber (Weber Scientific International Ltd) viewed under the inverted microscope (Olympus CKX41) at 400× magnification.

3.12.2 Enumeration of bacteria

Two CBA plates containing confluent growth of 3-day old *H. pylori* were harvested using sterile cotton swabs (Copan) into 10 ml of sterile PBS. The

suspension was centrifuged at 6000 × g for 5 minutes at 4°C. The bacterial cell pellet was washed thrice with sterile PBS as above. The pellet obtained was then resuspended in 2 ml of sterile PBS. The bacterial suspension was then used for enumeration by spread plate method and spectrophotometric reading at OD_{600}.

Serial 10-fold dilutions were made from 1 ml of the bacterial suspension obtained. Aliquots of 100 µl of the respective dilutions were spread evenly onto CBA plates using a sterile glass spreader. Each dilution was carried out in duplicates. The plates were incubated at 37ºC in a humidified incubator with 5% CO_2 for 3 days. Following which, the number of colonies (within the range of 30-300 colonies) formed on the CBA plate were counted.

Concurrently, serial 2-fold dilutions up to 1:64 were made from 1 ml of the bacterial suspension obtained. The turbidity of the suspension was measured at an absorbance of 600 nm using a spectrophotometer (Beckman Coulter). The viable bacterial cell count (CFU/ml) was plotted against the OD_{600} reading to obtain a standard curve. This curve was subsequently used as a guide for estimation of *H. pylori* population based on OD_{600} of the bacterial cultures in subsequent experiments.

3.12.3 Infection study

The bacterial cultures were harvested using sterile cotton swabs (Copan) and washed thrice in sterile PBS. The bacteria were then centrifuged at 6000 × g for 10 minutes at 4°C. After washing, the bacterial cell pellet was resuspended in the appropriate volume of PBS and used for infecting the cell lines at a multiplicity of infection (MOI) of 100:1 (Li *et al.*, 2009) for all experiments. Where indicated, cell lines were treated with nGGT or rGGT at an approximately equivalent amount to that produced by the viable bacteria.

3.13 Role of GGT in ROS generation

3.13.1 Hydrogen peroxide (H_2O_2) assay

H_2O_2 production from AGS cells or primary human gastric cells was measured as previously described (Mohanty *et al.*, 1997) using the Amplex red hydrogen peroxide/peroxidase assay kit (Molecular Probes, USA) according to the manufacturer's instructions. Briefly, cells were seeded in 96-well plates and allowed to adhere for 24 hours prior to the experiments. After treating with *H. pylori* or purified nGGT protein (1.5 mU), the cells (1.8×10^4 cells/well) were washed 3 times with PBS. The cell medium was then replaced by Krebs-Ringer phosphate buffer, pH 7.4, containing 145 mM NaCl, 5.7 mM sodium phosphate, 4.9 mM KCl, 0.5 mM $CaCl_2$, 1.2 mM $MgSO_4$ and 1 g/L glucose. Cells incubated in the absence of *H. pylori* or GGT served as control. Stimulation of GGT activity was performed by adding the acceptor dipeptide glycyl-glycine (1 mM) and the substrate GSH (0.1 mM). To inhibit the GGT activity, the competitive GGT inhibitor SBC (10 mM) was added to cell samples just prior to the assay for H_2O_2 release. Where indicated, Fe^{3+} (20 μM) or iron chelator desferrioxamine (DFO; 50 μM) was added to stimulate and inhibit thiol-dependent iron reduction, respectively (Stark *et al.*, 1993). A combination of one or more of the compounds was also added to observe the effects on H_2O_2 generation. The fluorescence generated in each sample was measured in triplicates in a Tecan Infinite^{TM} M200 Spectrometer (excitation/emission wavelengths: 530/590 nm).

3.13.2 NF-κB activation

3.13.2.1 Extraction of cytosolic and nuclear fractions

AGS cells were grown to confluency in 75 cm^2 tissue culture flasks before the addition of *H. pylori* 88-3887 (wild type) or various isogenic mutants at an MOI of

100:1. Uninfected cells served as control. After 4 hours post-infection, the cells were harvested with a cell scraper, washed thrice with PBS and then pelleted by centrifugation at 250 × g for 5 minutes. Following which, cells were lysed in 2 pellet volumes of hypotonic buffer A (Appendix 31A) and incubated on ice for 10 - 15 minutes with occasional tapping. After centrifugation at 500 × g for 5 minutes, the supernatant (cytosolic fraction) was collected and stored. The nuclear pellet was washed twice with buffer A before 100 µl of nuclear extraction buffer C (Appendix 31B) was added to the pellet and incubated on ice for 45 minutes with periodic tapping. The sample was then centrifuged at 20,000 × g and the supernatant (nuclear extract) was collected. Cytosolic and nuclear protein concentrations were determined by Bradford protein assay (as described in section 3.3) before the proteins were quickly frozen at -20^{o}C until use.

3.13.2.2 Western blot analysis

Cytosolic and nuclear protein fractions were subjected to SDS-PAGE (20 µg/lane) and transferred onto PVDF membranes by electroblotting. Membranes were blocked with 5% skim milk overnight at 4°C. NF-κB subunit p65 and IκB were detected with respective MAbs at 1:1000 dilution for 2 hours at room temperature using anti-NF-κB subunit p65 (BD Biosciences) and anti-IκB (IMGENEX), respectively. Blots were then incubated with goat anti-mouse antibody conjugated with horseradish peroxidase (1:2000 dilution, DakoCytomation) for 1 hour at room temperature. Signals were detected using enhanced chemiluminescence detection kit (Pierce) according to the manufacturer's protocol. Purity of the different cell fractions was tested using antibody against nuclear lamin A/C (1:1000 dilution; Cell Signalling) and cytosolic β-tubulin (1:1000 dilution; Cell Signalling). Densitometric

quantification of western blot bands was performed using ImageJ version 1.44i analysis software.

3.13.3 Determination of IL-8 production

AGS cells, primary gastric cells or macrophages were seeded in 12-well plates for 24 hours. The culture medium was replaced by fresh medium prior to the experiments. Cells incubated in the absence of *H. pylori* or nGGT were used as control. The supernatant of the cells (3×10^5 cells/well) incubated with *H. pylori* wild type (MOI 100:1) or the various deletion mutants or 25 mU purified *H. pylori* nGGT protein was collected after 4 or 24 hours. The aliquot supernatant was stored at -20^{o}C until use.

The concentration of IL-8 in cell culture supernatants was determined by commercially available ELISA kit (BD OptEIA^{TM}; BD Biosciences) according to the manufacturer's instructions. Briefly, 96-well plates (Nunc) were coated overnight at 4°C with 100 µl per well of capture antibody diluted in coating buffer (Appendix 23). Thereafter, the wells were washed thrice with 0.05% PBS-T and blocked with PBS containing 10% fetal calf serum for 1 hour at room temperature. Cytokine standards and supernatant samples after various treatments were added to the wells and any IL-8 present will bind to the immobilized antibody. The wells were washed with 0.05% PBS-T and avidin-horseradish peroxidase conjugate mixed with biotinylated anti-human IL-8 specific antibody was then added. The wells were again washed with 0.05% PBS-T and TMB substrate solution (100 µl) was added for 30 minutes. A blue colour was generated in direct proportion to the amount of specific cytokine present in the initial sample. The reaction was stopped with 2N H_2SO_4 solution (0.05 ml) and the

colour changed from blue to yellow. The OD was measured within 30 minutes using a microplate reader (Bio-Rad) at 450 nm with subtraction of absorbance at 570 nm.

3.14 Role of intracellular GGT in AGS cells

3.14.1 Presence of *H. pylori* GGT in host cells

3.14.1.1 TEM

AGS cells were grown in 75 cm^2 flasks to 80% confluency and incubated with *H. pylori* wild type or Δ*ggt*. After 24 hours, cells were harvested and processed for immunogold-labeling TEM as previously described in section 3.9.

3.14.1.2 Confocal laser scanning microscopy (CLSM) analysis

AGS cells were seeded on sterile coverslips placed in 6-well plates. After 24 hours, the cells (3×10^5 cells/well) were treated with *H. pylori* wild type or Δ*ggt* at MOI 100:1 or rGGT (25 mU). After 24 hours, the culture medium was decanted and the AGS monolayer was washed with pre-chilled PBS. The cells were then fixed in 3.7% formaldehyde (Merck) in PBS for 20 minutes at room temperature before being permeabilized with 0.2% PBS-Triton-X for 10 minutes at room temperature. The cells were washed thrice for 5 minutes each with PBS and blocked with 2% BSA-PBS overnight at 4°C. The monolayer was then incubated with MAb 1G1 against the small subunit of GGT (1:200 dilution in 2% BSA-PBS) for 90 minutes at 4°C. After washing with PBS thrice for 5 minutes each, the monolayer was incubated with Cy3-labeled goat anti-mouse IgG (Invitrogen) at 1:300 dilution in 2% BSA-PBS for 90 minutes at 4°C in the dark. The cells were then washed thrice for 5 minutes each with PBS. Cell nuclei were stained with Hoechst 33342 (2 μg/ml; Molecular Probes) for 10 minutes. Coverslips were then mounted onto microscope slides, sealed with

FluorSave™ Reagent (Calbiochem) and viewed using a confocal laser microscope (Olympus Fluoview 1000).

3.14.1.3 Western blot analysis

AGS cells were grown in 75 cm^2 flasks to 80% confluency and incubated with *H. pylori* wild type, Δ*ggt* or rGGT (500 mU). At the respective time-points (0h, 0.5h, 1h, 2h, 4h and 24h), cells were harvested and the nuclear and cytosolic fractions were extracted as described in section 3.13.2.1. Cell fractions were then analyzed by western blot analysis for the presence of *H. pylori* GGT using polyclonal antibody raised against rGGTS (1:4000 dilution). β-tubulin and lamin A/C were used as loading controls for cytosolic and nuclear fractions respectively.

3.14.2 Endocytosis of GGT

3.14.2.1 Specificity of uptake

AGS cells were grown to confluency in a 6-well tissue culture plate. Cells were then co-incubated with either purified rGGT, heat-denatured rGGT (after boiling for 10 minutes), rGGTL or rGGTS for 4 hours. The cells were then lysed with lysis buffer (Appendix 32) and the whole cell lysates were probed for the presence of rGGT, rGGTL or rGGTS by western blot analysis. Antibodies used were MAb 2B5 (1:3000) and MAb 1G1 (1:4000) to detect for the large and small subunits of GGT respectively.

3.14.2.2 Inhibitor study

The effects of two pharmacological agents: chlorpromazine (CPZ; Sigma-Aldrich) and nystatin (NYS; Sigma-Aldrich) on rGGT uptake by AGS cells were

examined. The optimum concentration used for each drug was determined by incubating AGS cells with various concentrations of each drug (CPZ, 5-30 μg/ml; NYS, 5-50 μg/ml) for 5 hours and measuring the cell viability by 3-(4, 5-dimethylthiazolyl-2)-2, 5-diphenyltetrazolium bromide (MTT) assay. Briefly, the medium was changed and 0.5 ml of diluted MTT solution [100 μl MTT stock solution (Appendix 33A) per 1 ml medium] was added to each well. Following 2 hour incubation, the culture medium supernatant was removed from the wells without disrupting the formazan crystal precipitate. The crystals were then dissolved in 0.5 ml lysis solution (Appendix 33B) per well. Absorbance was measured at 570 nm using a microplate reader (Bio-Rad). Cell viability is expressed as a fraction of control cells absorbance (taken as 1).

After determining the optimal concentration for each drug, AGS cells were first pre-incubated with CPZ (15 μg/ml, 30 minutes) or NYS (25 μg/ml, 60 minutes) before the addition of rGGT to the cells. After 4 hours, uptake of rGGT by AGS cells was then analyzed by western blot analysis (as described in section 3.14.1.3) and CLSM (as described in section 3.14.1.2). Control cells were incubated without rGGT nor inhibitors while uninhibited cells were incubated with rGGT but without inhibitors for the same period of time. β-tubulin and hepatocyte growth factor receptor (c-Met; Santa Cruz) were used as loading controls for cytosolic and membrane fractions, respectively. Densitometric quantification of western blot bands was performed using ImageJ version 1.44i analysis software.

3.14.3 Co-immunoprecipitation (Co-IP)

Co-IP analysis was carried out according to the protocol as described with slight modifications (Yahiro *et al.*, 2003). In brief, 3-day-old *H. pylori* 88-3887 was

harvested and washed thrice with PBS. The bacterial cell pellet was suspended in lysis buffer (Appendix 32) and incubated on a rotary shaker in a slow head-to-tail motion at 4°C for 2 hours. Separately, AGS cells were cultured to confluency (as described in section 3.11.1). Harvested AGS cells were then subjected to the same procedures. Following which, *H. pylori* and AGS cells lysates were centrifuged at 10,000 × g and the resultant protein supernatants were mixed and pre-cleared with Protein A/G sepharose (50 µl slurry) without antibody for another 2 hours at 4°C on a rotary shaker. Cleared lysates were then incubated with either MAb 1G1 against rGGT (1 µg) or various anti-importin antibodies (1 µg; Santa Cruz) and the antibody complex was pulled down by Protein A/G sepharose (50 µl slurry) for 2 hours at 4°C on a rotary shaker. Protein A/G sepharose beads with antibody complex were centrifuged briefly and washed five times with lysis buffer to remove unbound proteins. Thereafter, the beads were re-suspended in 50 µl of 5 × SDS sample buffer (Appendix 10) and subjected to SDS-PAGE analysis as described in section 3.4. Western blot was employed to detect for the presence of either GGT or specific importins (β1, β2 and β3; Santa Cruz) in the pulled-down complexes.

3.14.4 Small interfering RNA (siRNA) knockdown of importin β1

siRNA transfection was employed to down-regulate the expression level of human importin β1. Karyopherin β1 siRNA (h) which consists of a pool of 3 target-specific 19-25 nucleotide siRNAs (sc-35736, Santa Cruz) was used according to the manufacturer's protocol. The lyophilized siRNA was re-suspended in RNase-free water before use. In brief, AGS cells were first seeded in a 6-well tissue culture plate. After 24 hours, cells (50-60% confluency) were transfected with siRNA (20-80 pmols) using siRNA transfection reagent (Santa Cruz) and further incubated for 6

hours, after which the transfection mixture was replaced with normal cell culture medium for another 24 hours. After 48 hours, cells were lysed to check for optimal siRNA concentration required to knockdown importin β1 expression using western blot analysis. Untreated cells were used as internal control and these cells were incubated with transfection reagent only without siRNA. In a separate experiment, AGS cells were transfected with the optimum amount of siRNA and subsequently treated with rGGT for 4 hours. Amount of rGGT in the cytosolic and nuclear fractions of the cells was determined by western blot analysis as previously described (section 3.14.1.3). Densitometric quantification of western blot bands was performed using ImageJ version 1.44i analysis software.

3.14.5 Intracellular glutathione (GSH) analysis

AGS cells were plated in 0.9 cm^2 Lab-Tek chambered cover glass (Nunc) 24 hours prior to infection with *H. pylori* or treatment with rGGT (0.5-10 mU). Triple staining was performed using 2 μg/ml propidium iodide (PI) (BD Biosciences) to identify dead cells, 2 μg/ml Hoechst 33342 (Molecular Probes) to localize nuclei and 5 μM CellTracker green 5-chloromethylfluorescein diacetate (CMFDA; Molecular Probes) which detects GSH with a specificity of 95% (Markovic *et al.*, 2007). After 24 hours of treatment, AGS cells were first stained with 5 μM CMFDA in serum-free F-12K medium for 30 minutes at 37°C and 5% CO_2. Following washing with pre-warmed F12-K medium, the cells were left to rest for another 30 minutes at 37°C and 5% CO_2 in fresh F-12K medium containing 10% fetal calf serum. In the last 5 minutes of incubation, 2 μg/ml PI and 2 μg/ml Hoechst 33342 were added to the medium. Thereafter, the cells were washed with PBS and fixed with 3.7% formaldehyde in PBS for 15 minutes at room temperature. After fixing, cells were washed thrice with

PBS, mounted with a cover slip and sealed with FluorSave™ Reagent (Calbiochem). The stained cells were then viewed under CLSM as described in section 3.14.1.2. Mean fluorescence intensity of CMFDA in 100 cell nuclei (as defined by Hoechst 33342 staining) from at least 5 different fields was analyzed by ImageJ software version 1.44i.

3.15 Assessment of role of GGT in vacuolation

AGS cells, HeLa cells or primary human gastric cells were seeded in 12-well culture plates at a density of 1.5×10^4 cells per cm^2 (Papini *et al.*, 1994). After 24 hours, the cells were treated with *H. pylori* wild type or the various deletion mutants for an additional 24 hours. Where indicated, rGGT (10 mU), ammonium chloride (3 mM) or glutamine (2 mM) was co-incubated with the cells.

3.15.1 Cell morphology

AGS cells were seeded in a 35 mm plastic bottom dish (Nunc) at a density of 1.5×10^4 cells per cm^2. After 24 hours, cells were infected with *H. pylori* wild type or Δ*ggt* as described in section 3.12.3. Infected cells were then placed into the Biostation IMQ microscope chamber (Nikon) for real-time observation under phase-contrast microscopy. Uninfected AGS cells served as control. The water and chamber temperature were stabilized at 37°C to prevent focus drift during recording. Time-lapse images were taken for a total period of 24 hours with 5 minutes interval between each image acquisition. Images were viewed using ImageJ software version 1.44i. Where indicated, cells were also inspected for vacuolation using a phase contrast microscope (Olympus CKX41).

3.15.2 Neutral red dye uptake assay

Extent of vacuolation was quantified using neutral red uptake assay as previously described with slight modifications (Cover *et al.*, 1991). Neutral red is a membrane permeable basic dye that accumulates in acidic vacuoles and provides a quantitative estimation of the total volume taken up by vacuolar compartments (Papini *et al.*, 1993a). Briefly, the media overlaying the cells was removed and replaced with 0.2 ml of freshly prepared 0.05% neutral red in PBS containing 0.3% BSA for 5 minutes (Appendix 34A-B). Cells were then washed three times with 0.5 ml of the same buffer. The neutral red dye taken up by the vacuoles was then extracted from the cells by the addition of 0.2 ml of 70% ethanol in water containing 0.37% HCl (Appendix 34C). The OD was measured using a microplate reader (Bio-Rad) at 534 nm with subtraction of absorbance at 405 nm. Neutral red dye uptake is expressed as absorbance per 10^5 cells. All experiments were done in triplicates.

3.15.3 Inhibitor studies

3.15.3.1 Serine-borate complex (SBC)

AGS cells were incubated for 24 hours at 37°C with *H. pylori* (as described in section 3.12.3) in the presence of SBC (10 mM; Sigma-Aldrich), a competitive inhibitor of GGT. Cytoplasmic vacuolation of AGS cells was quantitated using neutral red dye uptake assay as described in section 3.15.2.

3.15.3.2 MAbs against GGT

AGS cells were pre-incubated with MAbs (10 μg) for 24 hours at 37°C prior to incubation with *H. pylori*. Mouse IgG_{2a} and IgG_{2b} isotype controls were used in parallel at the same concentration. Cytoplasmic vacuolation of AGS cells was

quantitated using neutral red dye uptake assay as described in section 3.15.2. Results are expressed as a percentage of the maximal value of neutral red dye uptake as induced by wild type *H. pylori* in the absence of MAbs.

3.16 Detection of serum antibody against rGGT in *H. pylori*-infected patients

rGGT (0.1 μg) was used as antigen to detect the presence of antibody against GGT in sera obtained from *H. pylori*-positive patients by ELISA (as described in section 3.6.1.2). A total of 58 and 65 sera samples (1:100 dilution) from patients with and without *H. pylori* infection respectively were tested. Horseradish-peroxidase-conjugated rabbit anti-human IgG (1:2000) (DakoCytomation) was used as secondary antibody. Sera were collected with patients' consent. Status of *H. pylori* infection was confirmed earlier by culture, histological examinations, rapid urease test and/or presence of serum antibodies to *H. pylori* acid glycine extract antigens by ELISA. All samples were randomly selected.

3.17 Statistical analysis

Data was analyzed with the SPSS statistical software package (version 10.0; SPSS Inc., Chicago, IL, USA). Values are expressed as mean ± standard deviation (SD). Statistical difference between two defined groups was determined with the unpaired two-tailed Student's *t* test or Mann-Whitney U test. Values of $P<0.05$ were considered to be statistically significant.

RESULTS

4.1 Genotyping of *H. pylori*

Chromosomal DNA extracted from *H. pylori* strain 88-3887 amplified by PCR and analyzed by agarose gel electrophoresis shows that *H. pylori* strain 88-3887 harbours *vacA*, *cagA* and *iceA*1 genes but lacks *iceA*2 and *babA*2 genes (Figure 7).

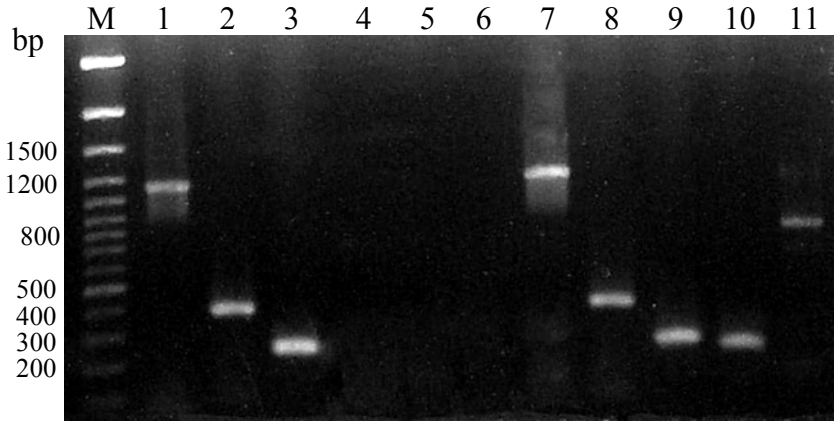

Figure 7. Genotyping of virulence genes in *H. pylori* strain 88-3887. M, 100 bp DNA ladder marker; PCR products showing: Lane 1, 1160 bp *vacA*; Lane 2, 400 bp *cagA*; Lane 3, 246 bp *iceA*1; Lane 4, *iceA*2 (negative); Lane 5, *babA*2 (negative). Lanes 7-11 are the positive controls for *cagA*, *vacA*, *iceA*1, *iceA*2 and *babA*2 respectively. Lane 6 is an empty lane.

4.2 Cloning and expression of rGGT, rGGTL and rGGTS

4.2.1 Construction of pRSET-*ggt*, pRSET-*ggtl* and pRSET-*ggts*

Genomic DNA of *H. pylori* strain 88-3887 was extracted and used as a template for PCR amplification of various constructs. Various inserts *ggt* (1626 bp), *ggtl* (1059 bp) and *ggts* (567 bp) were successfully amplified as shown in Figure 8A-C.

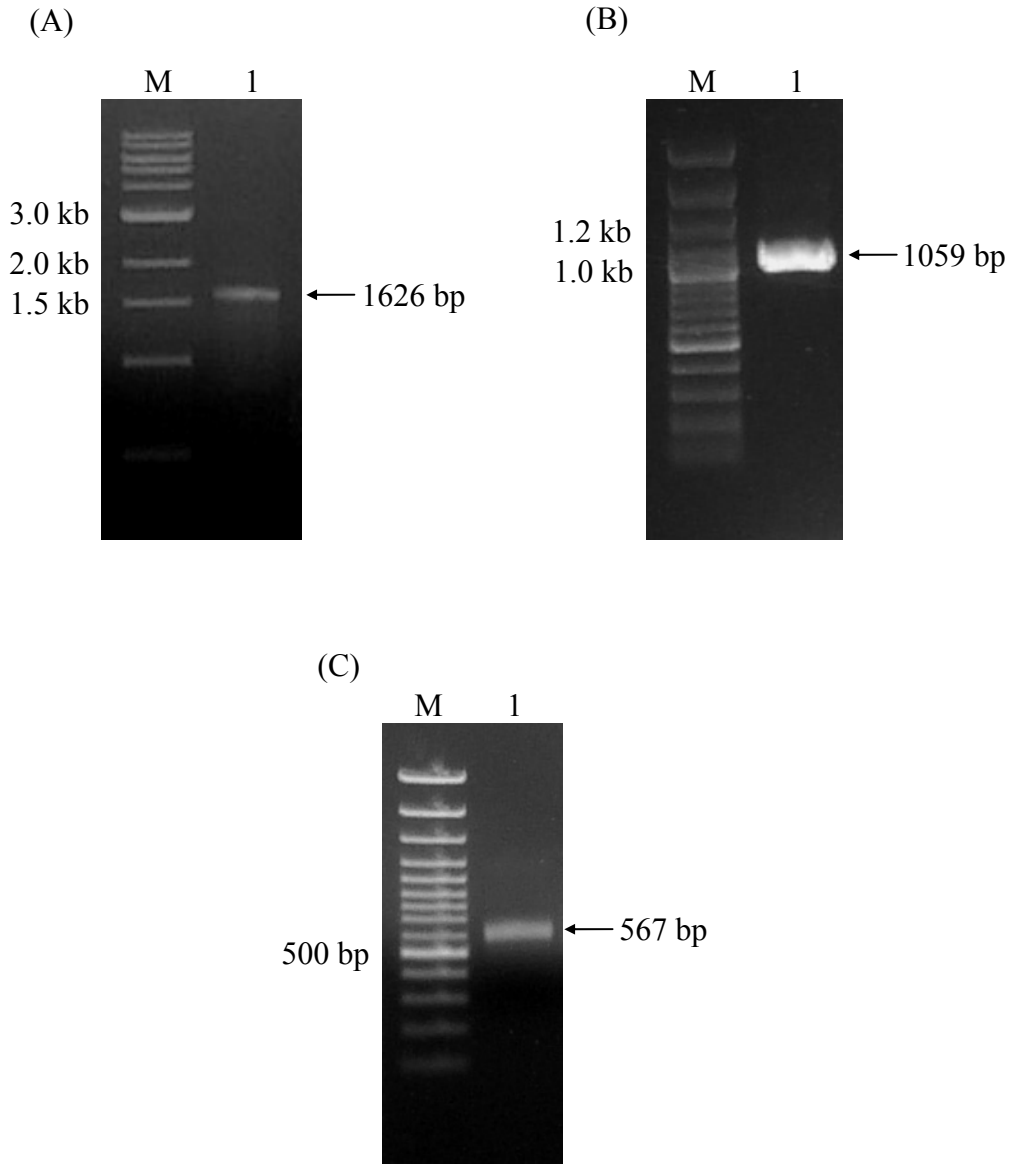

Figure 8. DNA gel electrophoresis of gene fragments encoding *ggt*, *ggtl* and *ggts*. (A) M, 1 kb DNA ladder marker; Lane 1, *ggt* gene fragment (1626 bp). (B) M, 100 bp DNA ladder marker; Lane 1, *ggtl* gene fragment (1059 bp). (C) M, 100 bp DNA ladder marker; Lane 1, *ggts* gene fragment (567 bp).

Restriction enzyme digest of expression vector pRSET-A with *Pst*I and *Hin*dIII yielded a linearized fragment of 2.9 kb (Figure 9). The restriction digest yielded cohesive ends that were compatible with those of *ggt*, *ggtl* and *ggts* gene fragments (digested with the same two restriction enzymes).

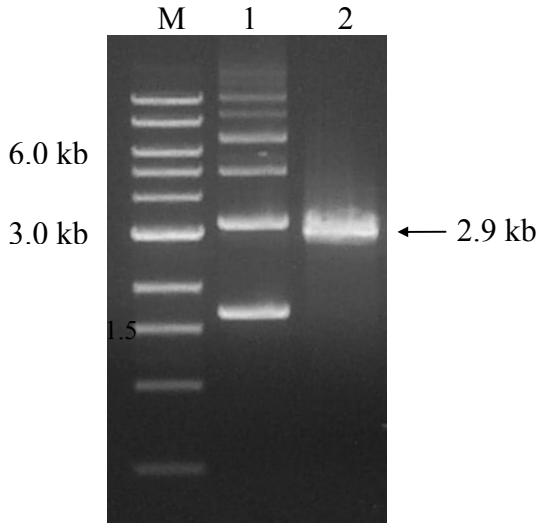

Figure 9. Restriction enzyme digest of expression vector pRSET-A. M, 1 kb DNA ladder marker; Lane 1, uncut plasmid pRSET-A; Lane 2, linearized vector after digestion with *Pst*I and *Hin*dIII (2.9 kb).

4.2.2 Identification of positive clones after transformation

After transformation into *E. coli* Top10 cells, the extracted recombinant plasmid from positive clones was digested with either *Pst*I or *Hin*dIII alone. Digestion of pRSET-*ggt* gave a single band of size 4506 bp (Figure 10A, lanes 2 and 3), pRSET-*ggtl* gave a single band of size 3939 bp (Figure 10B, lanes 2 and 3) and pRSET-*ggts* gave a single band of size 3447 bp (Figure 10C, lanes 2 and 3). Simultaneous digestion with *Pst*I and *Hin*dIII gave two DNA fragments corresponding to pRSET-A (~2.9 kb) and the inserts *ggt* (1626 bp; Figure 10A, lane 4), *ggtl* (1059 bp; Figure 10B, lane 4) or *ggts* (567 bp; Figure 10C, lane 4). Recombinant plasmids were also further confirmed by DNA sequencing (Figure 11).

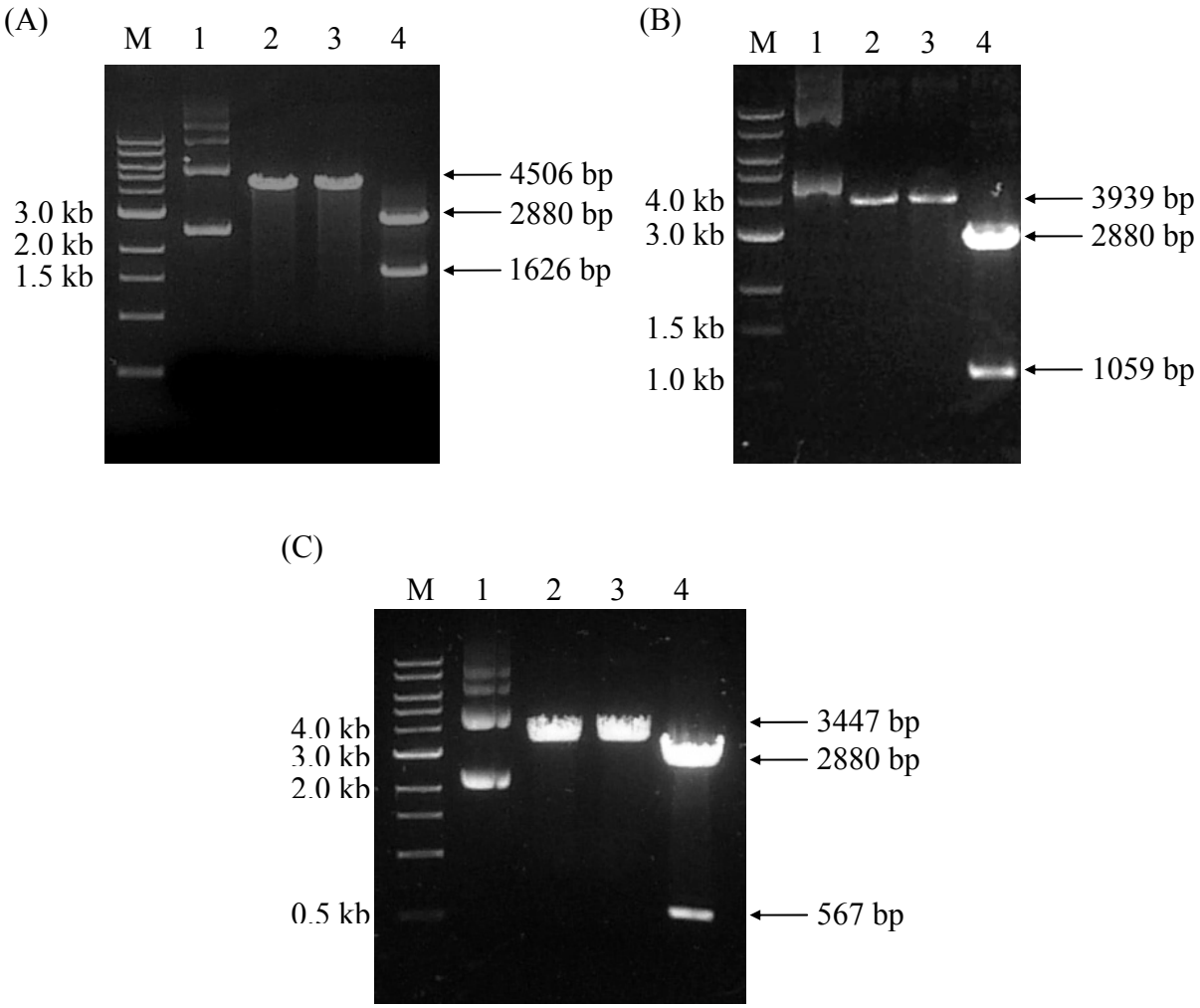

Figure 10. Screening of positive clones by restriction enzyme digest. (A) M, 1 kb DNA ladder marker; Lane 1, uncut recombinant pRSET-*ggt* plasmid; Lane 2, pRSET-*ggt* digested with *Pst*I; Lane 3, pRSET-*ggt* digested with *Hin*dIII; Lane 4, pRSET-*ggt* digested with *Pst*I and *Hin*dIII. (B) M, 1 kb DNA ladder marker; Lane 1, uncut recombinant pRSET-*ggtl* plasmid; Lane 2, pRSET-*ggtl* digested with *Pst*I; Lane 3, pRSET-*ggtl* digested with *Hin*dIII; Lane 4, pRSET-*ggtl* digested with *Pst*I and *Hin*dIII. (C) M, 1 kb DNA ladder marker; Lane 1, uncut recombinant pRSET-*ggts* plasmid; Lane 2, pRSET-*ggts* digested with *Pst*I; Lane 3, pRSET-*ggts* digested with *Hin*dIII; Lane 4, pRSET-*ggts* digested with *Pst*I and *Hin*dIII.

GCGAGTTACCCCCCCATTAAAAACACTAAAGTAGGCTTAGCCCTTTCTAGCCA
CCCGCTAGCTAGTGAGATCGGGCAAAAGGTTTTAGAAGAGGGAGGTAATGCGA
TTGATGCGGCTGTAGCGATAGGTTTTGCTCTTGCGGTTGTCCATCCGGCAGCA
GGCAATATTGGTGGAGGCGGTTTTGCGGTTATCCATTTGGCTAATGGTGAAAA
TGTTGCGTTAGATTTTAGAGAAAAAGCCCCCTTAAAAGCCACTAAAAACATGT
TTTTAGACAAGCAAGGCAATGTAGTCCCTAAACTCAGCGAAGATGGCTATTTG
GCGGCCGGGGTTCCTGGAACGGTGGCAGGCATGGAAGCGATGCTGAAAAAATA
CGGCACTAAAAAACTATCGCAACTCATTGATCCTGCCATTAAATTGGCTGAAA
ATGGTTATGCGATTTCACAAAGACAAGCAGAAACCCTAAAGGAAGCAAGGGAG
CGGTTTTTAAAATACAGTTCTAGCAAAAAGTATTTTTTTAAAAAAGGCCATCT
TGATTATCAAGAAGGGGATTTGTTTGTCCAAAAAGATTTAGCCAAGACTTTGA
ATCAAATCAAAACGCTAGGCGCTAAAGGCTTTTATCAAGGGCAAGTCGCTGAG
CTTATTGAGAAAGACATGAAAAAAAATGGAGGGATTATCACTAAAGAAGATTT
AGCCAGTTACAATGTGAAATGGCGCAAACCCGTGGTAGGGAGTTATCGTGGGT
ATAAGATCATTTCTATGTCGCCGCCAAGTTCGGGAGGCACGCATTTGATCCAG
ATTTTAAATGTCATGGAAAATGCGGATTTAAGCGCCCTTGGGTATGGGGCTTC
TAAGAATATCCATATCGCTGCCGAAGCGATGCGTCAGGCTTATGCGGATAGAT
CGGTTTATATGGGAGACGCTGATTTTGTTTCGGTGCCGGTGGATAAATTGATT
AATAAAGCGTATGCCAAAAAGATTTTTGACACTATCCAGCCAGATACGGTTAC
GCCAAGCTCTCAAATCAAACCAGGAATGGGGCAGTTGCATGAGGGGAGCAATA
CCACGCATTATTCTGTAGCGGACAGGTGGGGGAATGCAGTCAGCGTTACTTAC
ACCATTAACGCTTCTTATGGAAGCGCTGCCAGTATTGATGGGGCAGGATTTTT
ATTGAACAATGAAATGGATGATTTTTCCATCAAGCCAGGGAATCCCAATCTCT
ATGGTTTAGTAGGGGGCGATGCGAATGCGATTGAAGCCAATAAGCGCCCTTTA
AGCTCCATGTCGCCTACGATTGTGTTGAAAAACAATAAGGTTTTTTTGGTGGT
GGGAAGCCCTGGAGGGTCTAGGATTATCACTACGGTGCTGCAAGTGATTTCTA
ATGTCATTGATTATAATATGAATATTTCTGAAGCGGTTTCAGCCCCAAGATTT
CACATGCAATGGCTCCCTGATGAATTAAGGATTGAAAAGTTTGGCATGCCCGC
TGATGTGAAAGACAACCTCACTAAAATGGGCTATCAAATCGTTACTAAGCCGG
TCATGGGTGATGTGAATGCGATCCAAGTTTTGCCTAAAACTAAAGGGAGCGTT
TTCTATGGTTCAACGGATCCAAGGAAAGAATTTTAA

Figure 11. DNA sequences of *H. pylori* 88-3887 *ggt, ggtl and ggts* gene fragments cloned into pRSET-A. Sequence of *ggtl* is coloured blue and *ggts* is coloured red. Sequence of *ggt* is a combination of blue and red.

4.2.3 Expression of rGGT, rGGTL and rGGTS

The expression vector containing the correct *ggt*, *ggtl* or *ggts* insert was transformed into the expression host *E. coli* BL21 (DE3). The expression of rGGT was achieved at 3 hours after induction with 0.4 mM IPTG. There was no significant difference in the expression of rGGT with higher IPTG concentrations between 0.4 –

0.8 mM. rGGT was found to be approximately 62 kDa (Figure 12A) and accounted for about 10-15% of total proteins after induction as analyzed using ImageJ software version 1.44i. Expression of rGGTL and rGGTS was achieved 3 hours after induction with 0.2 mM IPTG. rGGTL and rGGTS were approximately 40 kDa (Figure 12B) and 25 kDa (Figure 12C), respectively. The expressed rGGTL and rGGTS accounted for about 30-40% of total proteins after induction.

(A)

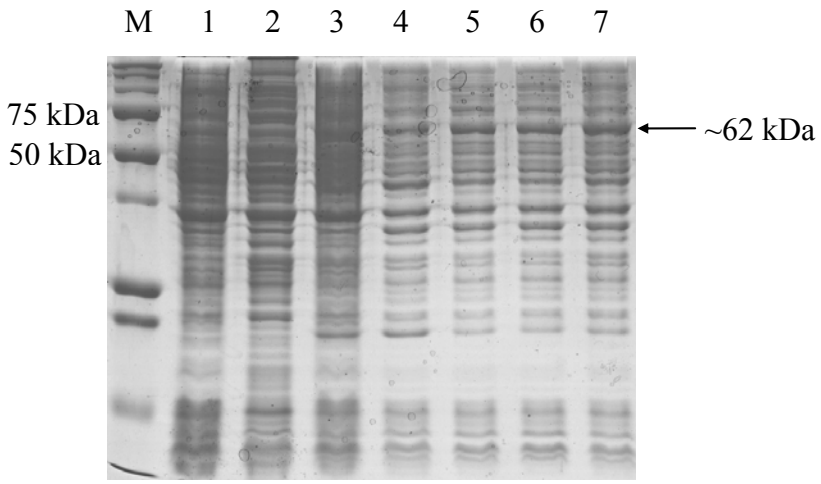

(B)

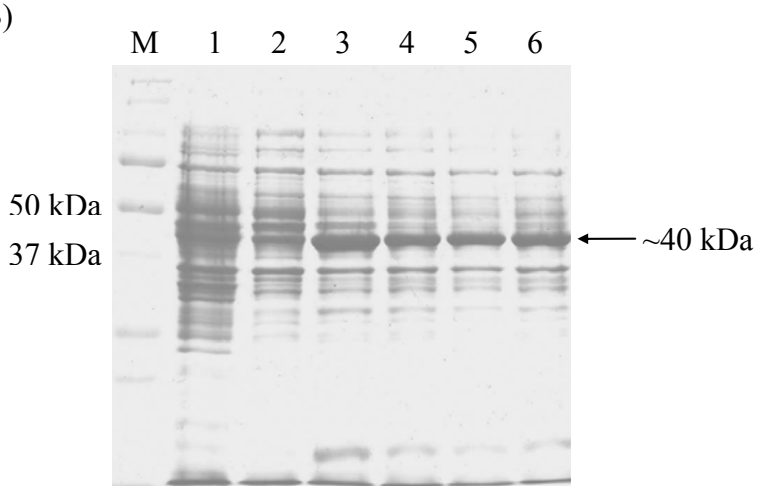

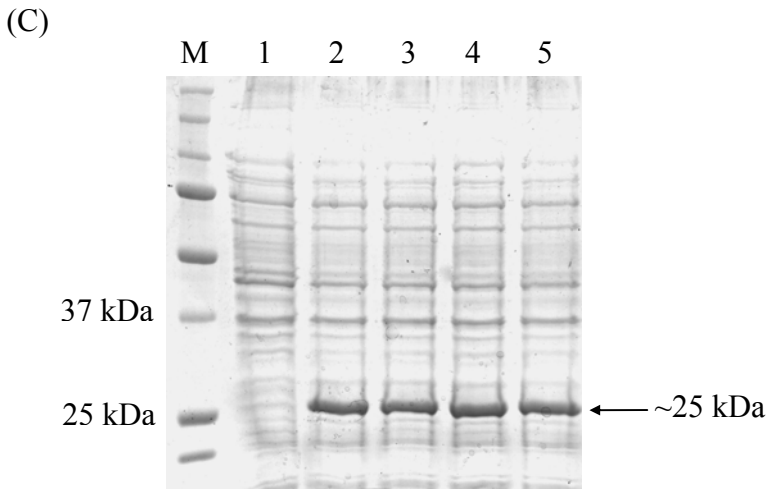

Figure 12. Expressed recombinant proteins after IPTG induction. (A) Expression of rGGT. Lane M, Prestained Precision Protein Standards (Bio-Rad); Lane 1, whole cell lysate of untransformed *E. coli* BL21; Lane 2, whole cell lysate of *E. coli* BL21 transformed with pRSET-A; Lane 3, whole cell lysate of uninduced *E. coli* BL21 transformed with pRSET-*ggt*; Lane 4, 0.2 mM IPTG induction; Lane 5, 0.4 mM IPTG induction; Lane 6, 0.6 mM IPTG induction; Lane 7, 0.8 mM IPTG induction. (B) Expression of rGGTL. Lane M, Prestained Precision Protein Standards (Bio-Rad); Lane 1, whole cell lysate of *E. coli* BL21 transformed with pRSET-A; Lane 2, whole cell lysate of uninduced *E. coli* BL21 transformed with pRSET-*ggtl*; Lane 3, 0.2 mM IPTG induction; Lane 4, 0.4 mM IPTG induction; Lane 5, 0.6 mM IPTG induction; Lane 6, 0.8 mM IPTG induction. (C) Expression of rGGTS. Lane M, Prestained Precision Protein Standards (Bio-Rad); Lane 1, whole cell lysate of uninduced *E. coli* BL21 transformed with pRSET-*ggts*; Lane 2, 0.2 mM IPTG induction; Lane 3, 0.4 mM IPTG induction; Lane 4, 0.6 mM IPTG induction; Lane 5, 0.8 mM IPTG induction.

4.2.4 Localization of rGGT, rGGTL and rGGTS in different cell fractions

After ultrasonication, the expressed rGGT protein was observed to exist in both the soluble (Figure 13A, lane 1) and insoluble fraction of the cell lysate (Figure 13A, lane 2). In contrast, rGGTL and rGGTS were found exclusively in the insoluble fraction of the cell sonicates (Figure 13B-C, lane 2).

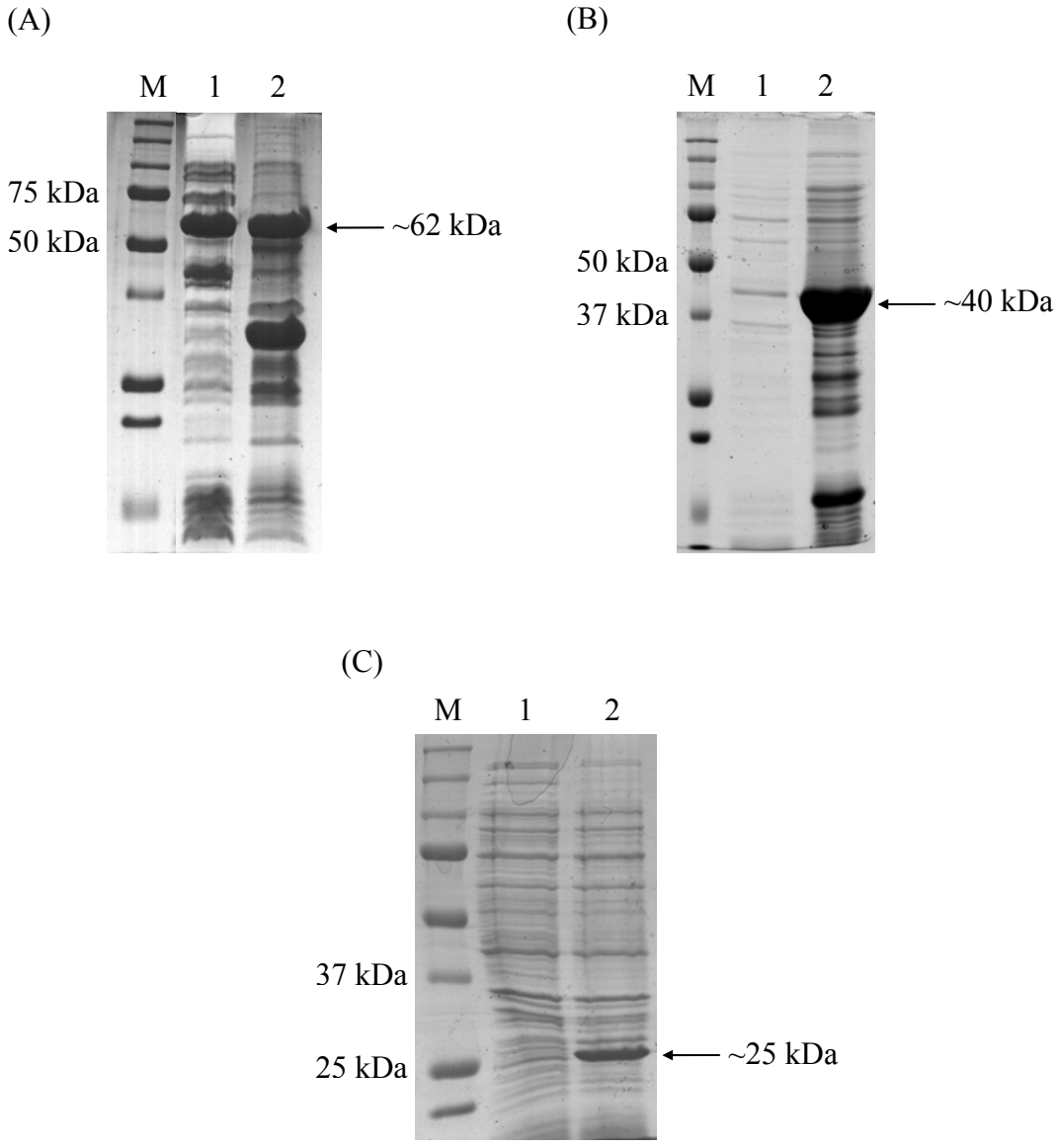

Figure 13. SDS-PAGE protein profile of soluble and insoluble protein fractions. (A) rGGT, (B) rGGTL, (C) rGGTS. Lane M, Prestained Precision Protein Standards (Bio-Rad); Lane 1, Soluble fraction; Lane 2, Insoluble fraction.

4.2.5 Purification of recombinant proteins by His-tag affinity chromatography

rGGT was eluted from a His-tag affinity chromatography column in 2 ml fractions with an imidazole concentration gradient ranging from 0.1 – 1 M (Figure 14A). Interestingly, 3 protein bands were obtained after purification (20 kDa, 40 kDa and 62 kDa respectively), indicating that rGGT is expressed as a 62 kDa precursor

that undergoes autocatalytic processing as has been previously reported (Boanca *et al.*, 2006). Purification of rGGTL and rGGTS was carried out under denaturing conditions and a single protein band of 40 kDa and 25 kDa was obtained respectively (Figure 14B-C). The yield of each recombinant protein (rGGT, rGGTL and rGGTS) was approximately 12-15 µg/ml of culture. Purity of recombinant proteins was >95% as assessed by silver staining after SDS-PAGE (data not shown).

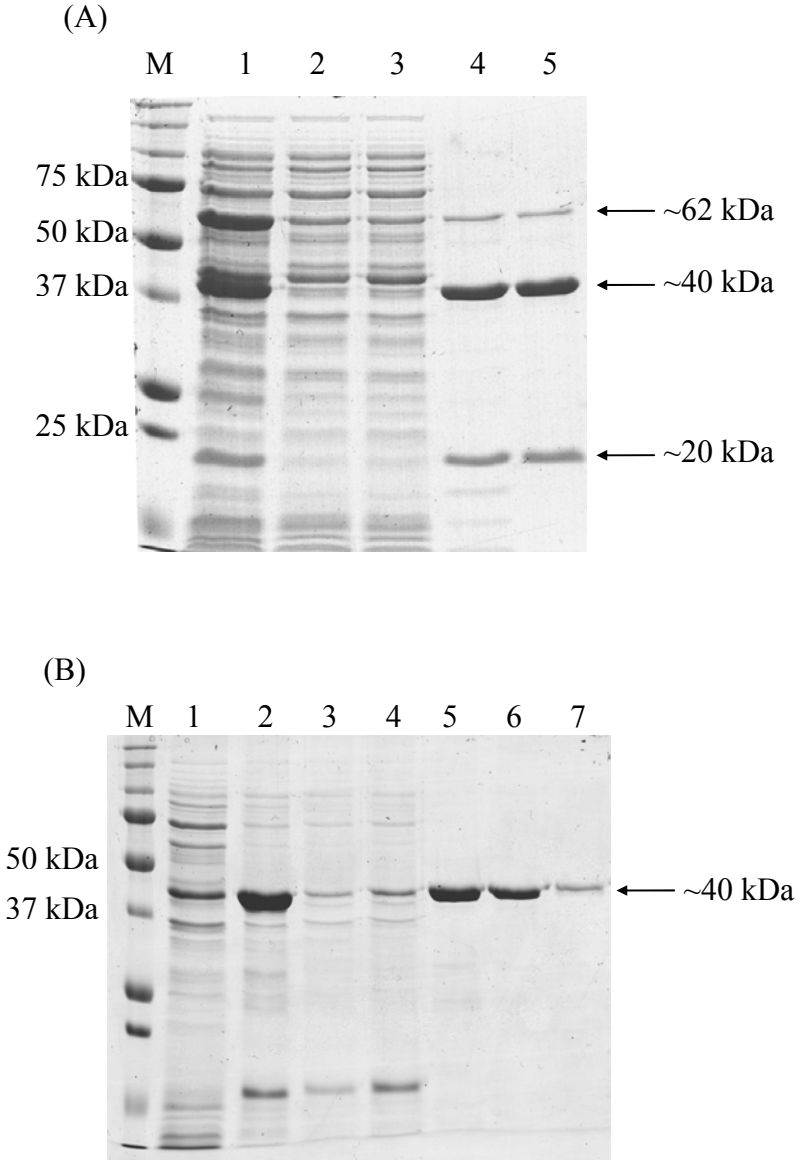

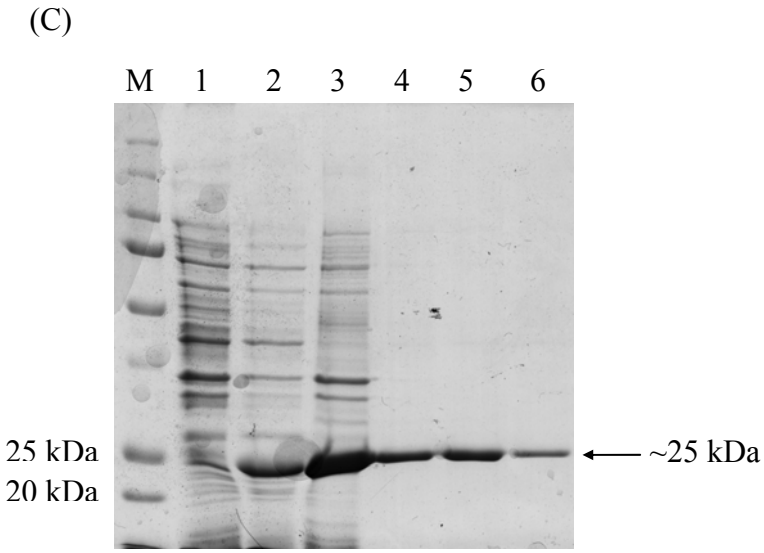

Figure 14. His-Tag affinity purification of recombinant proteins. (A) Purification of rGGT. Lane M, Prestained Precision Protein Standards (Bio-Rad); Lane 1, Soluble fraction of sonicated cells; Lanes 2-5, fractions eluted from His-tag column. (B) Purification of rGGTL. Lane M, Prestained Precision Protein Standards (Bio-Rad); Lane 1, Soluble fraction of sonicated cells; Lane 2, Insoluble fraction of sonicated cells; Lanes 3-7, fractions eluted from His-tag column. (C) Purification of rGGTS. Lane M, Prestained Precision Protein Standards (Bio-Rad); Lane 1, Soluble fraction of sonicated cells; Lane 2, Insoluble fraction of sonicated cells; Lane 3-6, fractions eluted from His-tag column.

4.2.6 Confirming identity of rGGT by mass spectrometry

MALDI-TOF mass spectrometry analysis confirmed the identity of the three protein bands obtained in Figure 14A as that of *H. pylori* GGT. The results indicate that the 40 kDa and 20 kDa protein bands are the large and small subunits of *H. pylori* GGT respectively while the 62 kDa protein band is that of the unprocessed rGGT (Figure 15). Purified rGGT also exhibited GGT activity of ~68 U/mg.

ASYPPIKNTKVGLALSSHPLASEIGQKVLEEGGNAIDAAVAIGFALAVVHPAA
GNIGGGGFAVIHLANGENVALDFREKAPLKATKNMFLDKQGNVVPKLSEDG
YLAAGVPGTVAGMEAMLKKYGTKKLSQLIDPAIKLAENGYAISQRQAETLKE
ARERFLKYSSSKKYFFKKGHLDYQEGDLFVQKDLAKTLNQIKTLGAKGFYQ
GQVAELIEKDMKKNGGIITKEDLASYNVKWRKPVVGSYRGYKIISMSPPSSG
GTHLIQILNVMENADLSALGYGASKNIHIAAEAMRQAYADRSVYMGDADFV
SVPVDKLINKAYAKKIFDTIQPDTVTPSSQIKPGMGQLHEGSNT↓THYSVADRW
GNAVSVTYTINASYGSAASIDGAGFLLNNEMDDFSIKPGNPNLYGLVGGDAN
AIEANKRPLSSMSPTIVLKNNKVFLVVGSPGGSRIITTVLQVISNVIDYNMNISE
AVSAPRFHMQWLPDELRIEKFGMPADVKDNLTKMGYQIVTKPVMGDVNAIQ
VLPKTKGSVFYGSTDPRKEF

Figure 15. Identification by MALDI-TOF mass spectrometry of the 3 protein bands of purified rGGT. Peptides coloured red were matched with the precursor (62 kDa) GGT protein; Peptides highlighted in yellow were matched with the large subunit (40 kDa) of GGT protein; Peptides highlighted in blue were matched with the small subunit (20 kDa) of GGT protein. Intramolecular autocatalytic cleavage site of the proenzyme which generates the large and small subunit is indicated by a vertical arrow.

4.3 Antibody production

4.3.1 Polyclonal antibody against rGGTS

4.3.1.1 Purification and characterization

Antibody against rGGTS raised in an immunized rabbit was detected by ELISA using 10 ng wild type *H. pylori* total cell lysate or Δ*ggt* lysate as antigen (Figure 16). As observed, antibody titre increased by >3-fold 28 days after the first immunization at day 0 and peaked on the 56th day.

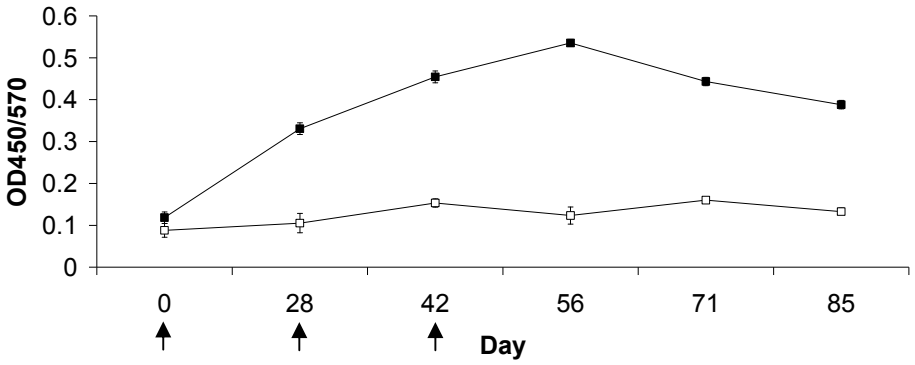

Figure 16. Antibody production profile. Antibody titre against rGGTS detected at different time points. The graph was plotted based on the values of 1:400 diluted sera against 10 ng wild type *H. pylori* lysate (■) or Δ*ggt* lysate (□). Vertical arrows indicate days on which rabbit was injected with 150 µg rGGTS.

Antibody against rGGTS was purified from rabbit sera using Protein A sepharose (Figure 17A) and was subsequently assayed for its binding specificity to the small subunit of GGT using western blot analysis. A single protein band of ~20 kDa corresponding to the small subunit of GGT was observed in the lane loaded with wild type *H. pylori* total cell lysate (Figure 17B, lane 1). No protein bands were observed in the lane loaded with Δ*ggt* cell lysate (Figure 17B, lane 2).

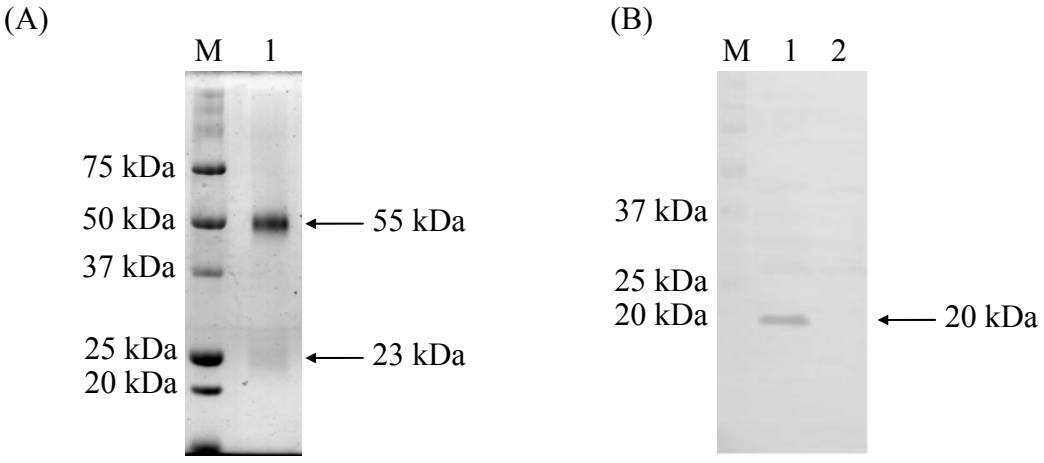

Figure 17. Western blot analysis using antiserum against rGGTS. (A) SDS-PAGE showing purified IgG from rabbit serum. Lane M, Prestained Precision Protein Standards (Bio-Rad); Lane 1, purified IgG. (B) Polyclonal antibodies raised against rGGTS were used as probe. Lane M, Prestained Precision Protein Standards (Bio-Rad); Lane 1, *H. pylori* wild type lysate; Lane 2, *H. pylori* Δ*ggt* lysate.

4.3.2 Monoclonal antibody against rGGT

4.3.2.1 Screening of immunized mice

A total of 5 BALB/c mice were immunized with rGGT. Sera were obtained 72 days (after 3 boosters) and 93 days (after 4 boosters) following initial immunization. The antibody titre against rGGT was shown to be over 1:6000 for all five mice as assayed by indirect ELISA method using 0.1 ng rGGT as antigen (Figure 18A). The specificity of the antibody was also tested using western blot analysis. Sera from all five mice were able to detect GGT from *H. pylori* wild type lysate (Figure 18B). No GGT bands were detected from Δ*ggt* lysate. Based on the ELISA and western blot results, mouse #2 was chosen for subsequent hybridoma production.

(A)

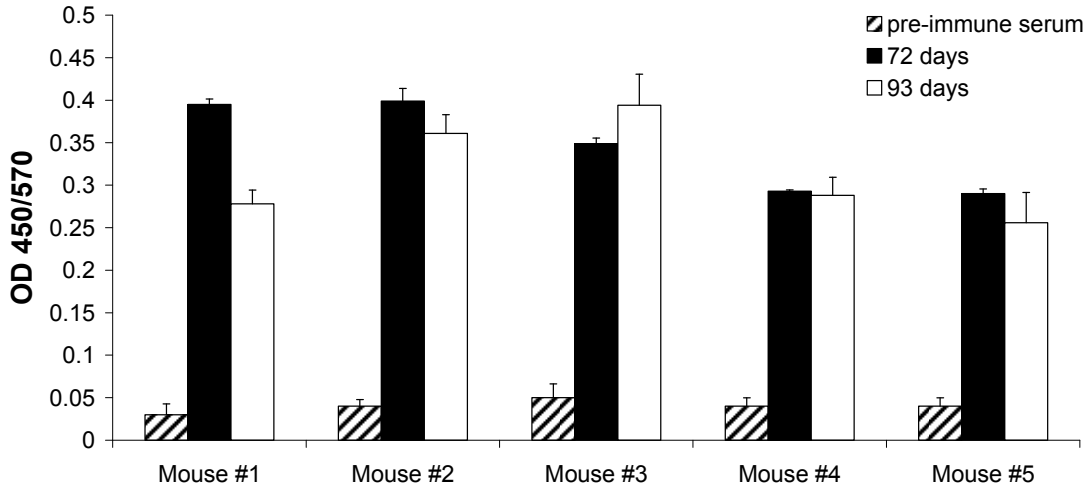

(B)

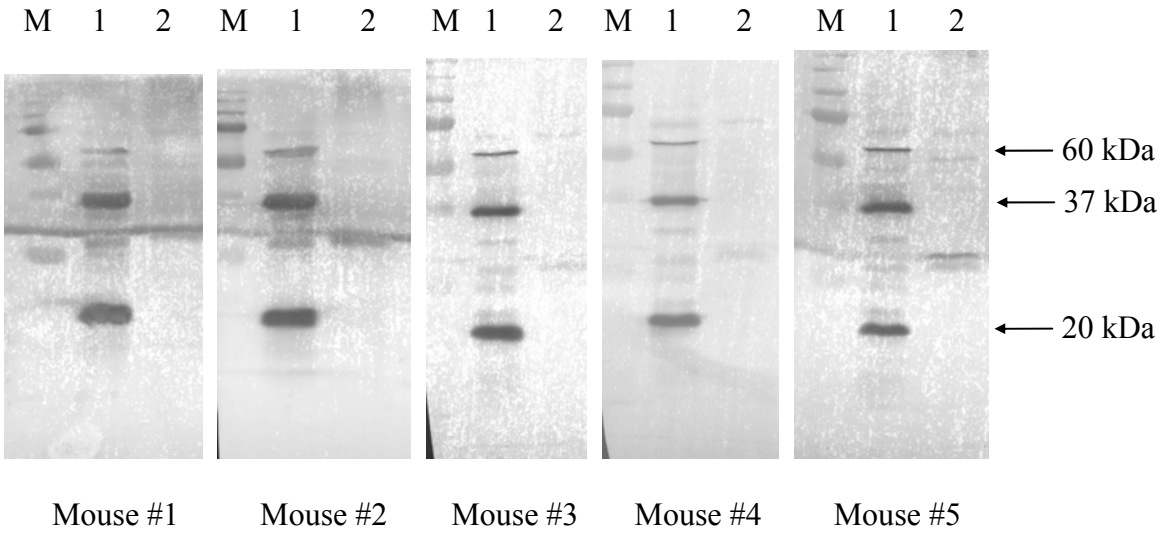

Figure 18. ELISA and western blot analysis using antiserum against rGGT. (A) Antibody titre against rGGT detected by ELISA 72 days and 93 days post-immunization based on values of 1:6000 diluted sera. (B) Western blot analysis using antibodies raised in mice against rGGT. Lane M, Prestained Precision Protein Standards (Bio-Rad); Lane 1, *H. pylori* wild type lysate; Lane 2, *H. pylori* Δ*ggt* lysate.

4.3.2.2 Characterization of MAbs

Ten hybridomas were obtained from different cultures of mouse myeloma cells fused with splenocytes from mouse #2. The hybridomas were subsequently used to produce ascitic fluid in mice. Figure 19 shows western blot analysis against *H. pylori* wild type lysate using the MAbs as probes. Six of the MAbs recognized only the large subunit (Clones 1G5, 1G10, 1H5, 2B5, 2G1 and 4A11) while the other four recognized only the small subunit (Clones 1G1, 3C10, 3F4 and 4F11). All of these MAbs were of the IgG class and could be classified into three isotypes, IgG_l, IgG_{2a} and IgG_{2b}. Interestingly, MAbs that recognized the large subunit of GGT were all IgG_1 and those against the small subunit were all IgG_2. Results are summarized in Table 7.

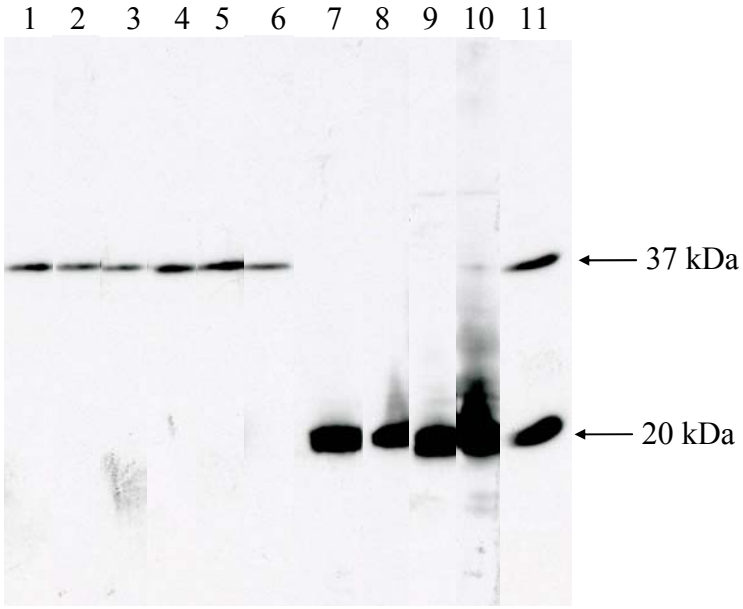

Figure 19. Specificity of MAbs raised against rGGT. Western blot analysis of *H. pylon* wild type lysate with ascitic fluids containing MAbs. Lanes: 1, 1G5; 2, 1G10; 3, 1H5; 4, 2B5; 5, 2G1; 6, 4A11; 7, 1G1; 8, 3C10; 9, 3F4; 10, 4F11; 11, polyclonal mouse anti-*H. pylori* GGT IgG (positive control).

Table 7. Summary of MAb isotypes and specificities.

Clone ID	Isotype	Specificity	
		Large subunit	Small subunit
1G5	IgG_1	+	-
1G10	IgG_1	+	-
1H5	IgG_1	+	-
2B5	IgG_1	+	-
2G1	IgG_1	+	-
4A11	IgG_1	+	-
1G1	IgG_{2b}	-	+
3C10	IgG_{2a}	-	+
3F4	IgG_{2a}	-	+
4F11	IgG_{2a}	-	+

4.3.2.3 Mapping of epitopes

Using a series of overlapping peptides (15 amino acids each) covering the sequence of *H. pylori* GGT, the epitopes which the MAbs recognized were identified by indirect ELISA method. Both the ELISA and western blot results confirmed that 6 of the clones recognized the large subunit of GGT and 4 of them recognized the small

subunit of GGT. Among the MAbs which were specific towards the large subunit, 3 different minimum epitopes were identified (amino acid position 42-50, 309-317 and 357-365 of GGT). All 4 MAbs towards the small subunit of GGT were found to recognize the same minimum epitope sequence (amino acid position 428-434 of GGT) as illustrated in Figure 20.

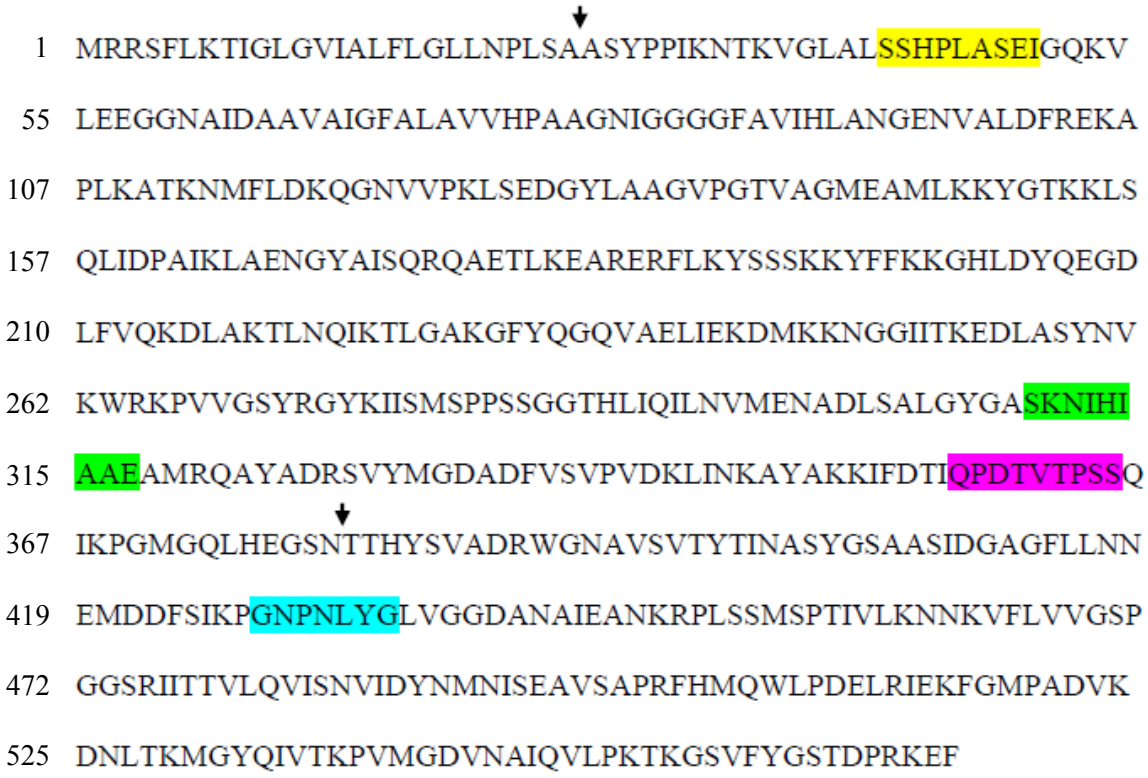

Figure 20. Identification of epitopes recognized by MAbs. Three different epitopes coloured yellow (MAbs 1G5, 4A11), green (MAb 2B5) and magenta (1G10, 1H5, 2G1) were identified on the large subunit of GGT. One epitope coloured blue (MAbs 1G1, 3C10, 3F4, 4F11) was identified on the small subunit of GGT. Cleavage sites of precursor GGT giving the large subunit and small subunit are indicated by arrows.

Epitopes that the 10 MAbs recognized were mapped on the 3-D crystal structure of recombinant *H. pylori* GGT (Boanca *et al.*, 2007) as observed in Figure 21. Individual epitopes are circled in red. Catalytic site of GGT present in the small subunit is boxed in yellow.

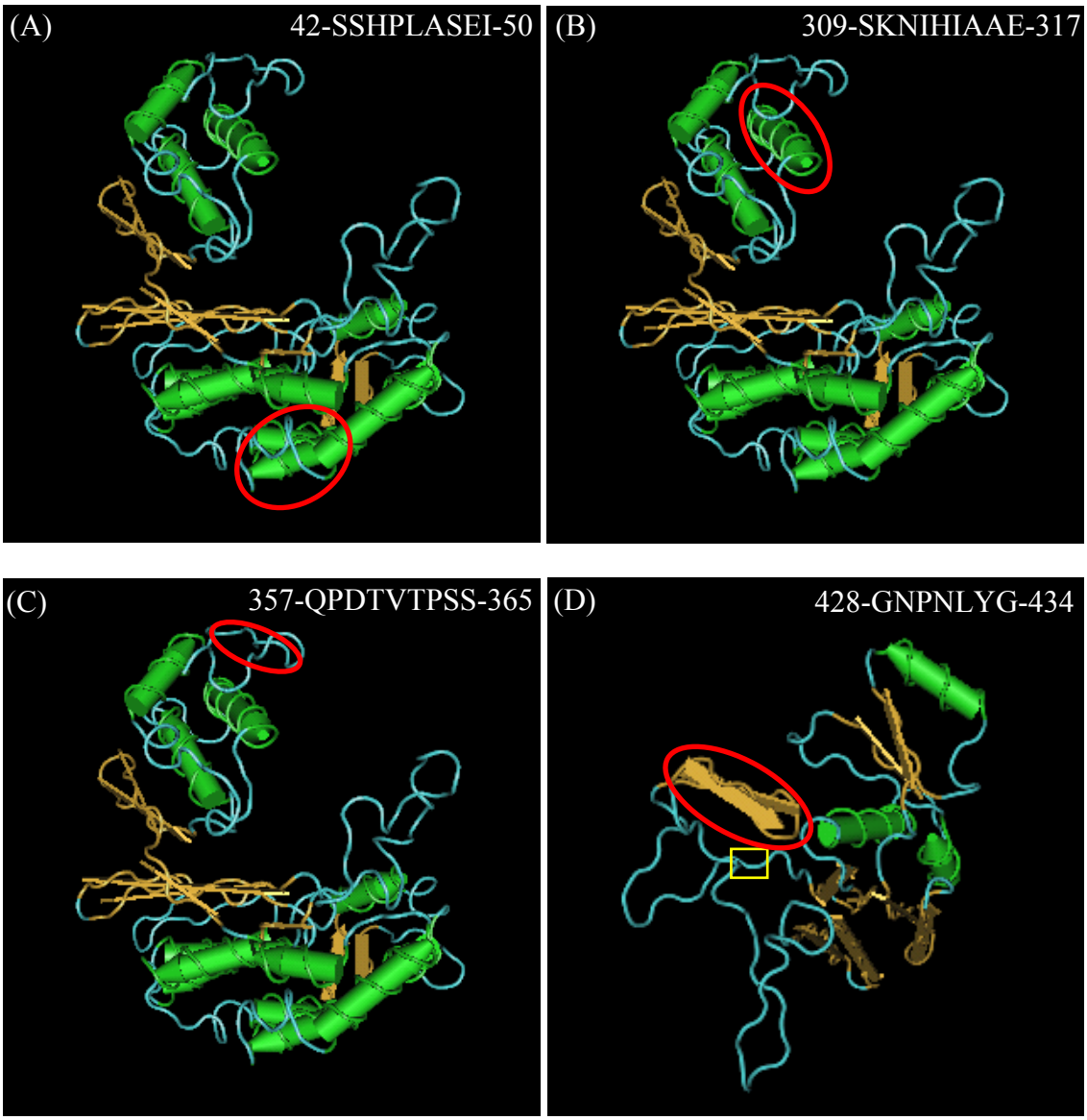

Figure 21. 3-D structures of individual large and small subunits of rGGT illustrating the epitopes which MAbs bind to. (A) Large subunit of rGGT. Epitope 42-SSHPLASEI-50 recognized by MAb 1G5 and 4A11 is circled in red. (B) Large subunit of rGGT. Epitope 309-SKNIHIAAE-317 recognized by MAb 2B5 is circled in red. (C) Large subunit of rGGT. Epitope 357-QPDTVTPSS-365 recognized by MAb 1G10, 1H5 and 2G1 is circled in red. (D) Small subunit of rGGT. Epitope 428-GNPNLYG-434 recognized by MAb 1G1, 3C10, 3F4 and 4F11 is circled in red. Catalytic site of rGGT is indicated by a yellow rectangle. 3-D crystal structure of rGGT was obtained from the Proten Data Bank (PDB ID: 2NQO) and viewed using Cn3D 4.1 software.

4.4 Inhibition of GGT catalytic activity by MAbs

4.4.1 Examination of neutralizing activity of MAbs from different clones

Among the 10 MAbs, 4 MAbs (1G1, 3C10, 3F4 and 4F11) inhibited *H. pylori* GGT activity with varying degrees of inhibition ranging from ~30 to ~93% (Figure 22). All 4 recognized the small subunit of GGT. The most potent inhibitor, MAb 1G1, inhibited 77.4% of GGT activity even at a low dose of 0.25 µg and achieved maximum inhibition of 93.0% at just 4 µg. MAbs 4F11, 3F4 and 3C10 inhibited 80.7%, 71.9% and 32.0% GGT activity respectively when the maximum dose (30 µg) was used. The other 6 MAbs specific against the large subunit failed to inhibit the GGT activity even at the highest dose (30 µg) tested. In addition, mouse IgG_{2a} and IgG_{2b} isotype negative controls did not inhibit GGT activity.

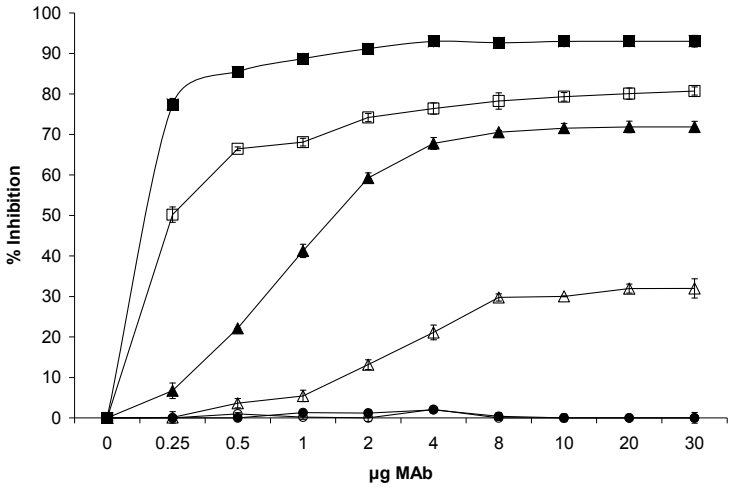

Figure 22. Neutralizing ability of MAbs on *H. pylori* 88-3887 GGT activity. A population of 5×10^6 *H. pylori* 88-3887 was pre-incubated with various amounts of MAb 1G1 (■), 4F11 (□), 3F4 (▲) or 3C10 (Δ) (0 to 30 µg of IgG protein) for 1 hour at 37°C on microtitre plates. Mouse IgG_{2a} (●) and IgG_{2b} (○) isotype controls were used in parallel at the same concentrations. Inhibition of GGT activity by MAbs was measured using GGT assay. Points are the averages for triplicate determinations.

4.4.2 Neutralizing activity of MAbs on different *H. pylori* strains

The ability of the MAbs to neutralize GGT activity was tested on various *H. pylori* strains including 26695, SS1 and NCTC11637 (Figure 23). MAb

1G1 showed the best neutralizing activity where it inhibited GGT activity of strains 26695, SS1 and NCTC 11637 by as high as 94.7%, 63.5% and 87.9%, respectively. In addition, mouse IgG_{2a} and IgG_{2b} isotype negative controls did not inhibit GGT activity. In this study, potency of the various MAbs in neutralizing GGT activity against the strains tested can be classified as follows: 1G1 > 4F11 > 3F4 > 3C10.

(A)

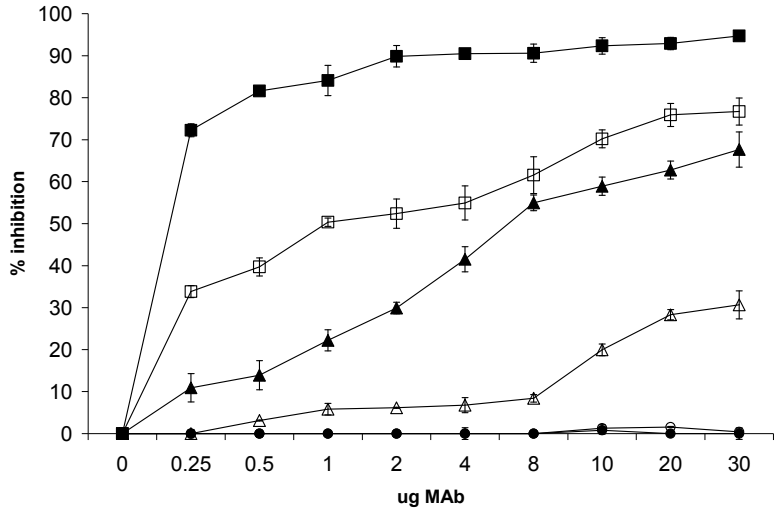

(B)

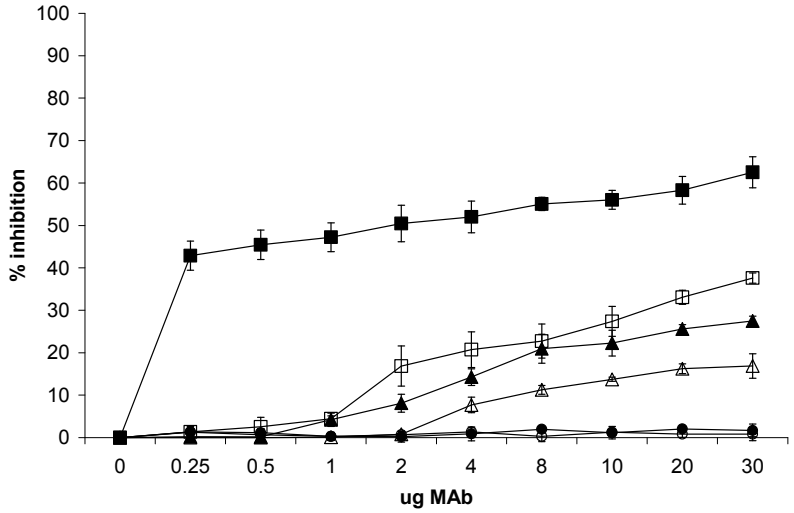

(C)

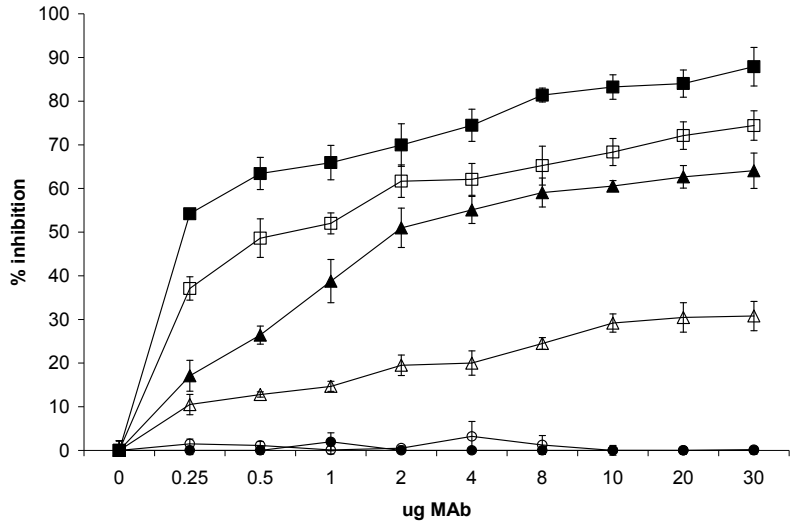

Figure 23. Neutralizing ability of MAbs on different *H. pylori* strains. (A) *H. pylori* strain 26695. (B) *H. pylori* strain SS1. (C) *H. pylori* strain NCTC 11637. A population of 5×10^6 *H. pylori* was pre-incubated with various amounts (0 to 30 μg of IgG protein) of MAb 1G1 (■), 4F11 (□), 3F4 (▲) or 3C10 (Δ) for 1 hour at 37°C on microtitre plates. Mouse IgG_{2a} (●) and IgG_{2b} (○) isotype controls were used in parallel at the same concentrations. Inhibition of GGT activity by MAbs was measured using GGT assay.

MAb 1G1, which was found to be the most potent inhibitor out of the 10 MAbs, was further tested for its ability to neutralize GGT activity of 7 clinical *H. pylori* strains. As observed in Figure 24, MAb 1G1 was effective in inhibiting their GGT activities with a range of 46.0-90.0% depending on the strains tested.

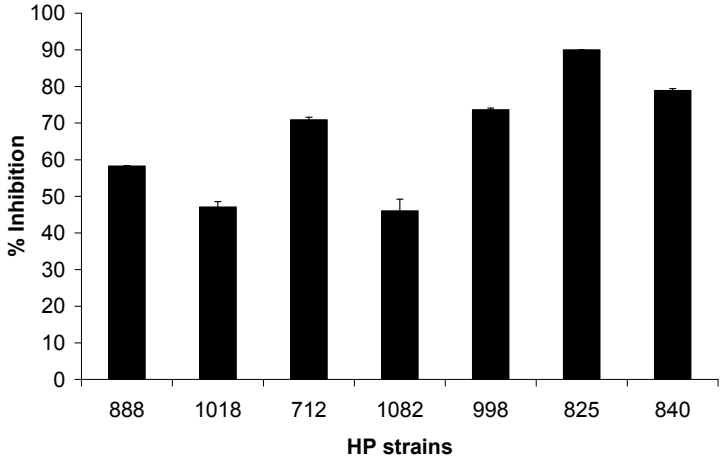

Figure 24. Neutralizing ability of MAb 1G1 on various clinical *H. pylori* strains. A population of 5×10^6 *H. pylori* was pre-incubated with 10 μg of MAb 1G1 for 1 hour at 37°C on microtitre plates. Inhibition of GGT activity by MAbs was measured using GGT assay.

4.4.3 Comparison of *H. pylori* 88-3887 GGT amino acid sequence with other GGTs

The nucleotide sequence of *H. pylori* 88-3887 *ggt* gene (as sequenced in section 4.2.2) was translated into amino acid sequence using ExPASy Translate tool (web.expasy.org/translate/). Figure 25 shows the amino acid sequence alignment of *H. pylori* GGT (residues 416-464) with other bacterial and mammalian homologues corresponding to these same amino acid positions using Clustal 2.0.12. The neutralizing epitope sequence recognized by MAbs 1G1, 3C10, 3F4 and 4F11 is indicated by a black bar and it is observed that this epitope sequence is highly conserved within *H. pylori* species. In contrast, this 7-amino acid epitope is not found in the GGTs of other bacterial (*Helicobacter suis*, *Helicobacter felis*, *Helicobacter mustelae*, *Helicobacter bilis*, *Helicobacter canis*, *Pseudomonas aeruginosa*, *Escherichia coli* and *Bacillus subtilis*) as well as mammalian (cow, human and rat) homologues.


```
H. pylori 88-3887   LNNEMDDFSIKPGNPNLYGLVGGDANAIEANKRPLSSMSPTIVLK-NNKV 464
H. pylori 26695     LNNEMDDFSIKPGNPNLYGLVGGDANAIEANKRPLSSMSPTIVLK-NNKV 464
H. pylori J99       LNNEMDDFSIKPGNPNLYGLVGGDANAIEANKRPLSSMSPTIVLK-NNKV 464
H. pylori G27       LNNEMDDFSIKPGNPNLYGLVGGDANAIEANKRPLSSMSPTIVLK-NNKV 464
H. pylori P12       LNNEMDDFSIKPGNPNLYGLVGGDANAIEANKRPLSSMSPTIVLK-NNKV 464
H. pylori NCTC11637 LNNEMDDFSIKPGNPNLYGLVGGDANAIEANKRPLSSMSPTIVLK-NNKV 464
H. pylori SS1       LNNEMDDFSIKPGNPNLYGLVGGDANAIEANKRPLSSMSPTIVLK-NNKV 464
H. suis             LNDEMDDFSIKAGTPNLYGVIGGDANAIEPNKRPLSSMSPTIVLK-NNKV 454
H. felis            LNNEMDDFSIKPGVPNLYGLVGGDANAIEPGKRPLSSMSPTIVLK-QNKV 459
H. mustelae         LNNEMDDFSIKPGVANLYGLVGGDANAIAPKKRPLSSMTPTIVLK-DNKP 458
H. bilis            LNNEMDDFSIKPGVANLYGLVGGEANAIVPRKRPLSSMSPTIILK-DGKL 461
H. canis            LNNEMDDFSIKPGVPNQYGLVGGDANAIAPGKRPLSSMSPTIVLD-KSKL 398
P. aeruginosa       LNDEMDDFTSKVGVPNMYGLIQGEANAIGPGRRPLSSMSPTIVTK-DGKT 460
E. coli             LNNQMDDFSAKPGVPNVYGLVGGDANAVGPNKRPLSSMSPTIVVK-DGKT 475
B. subtilis         LNNELTDFDAIPG----------GANEVQPNKRPLSSMTPTILFK-DDKP 477
Cow                 FNDEMDDFS-SPNIINQFGVPPSPANFIAPGKQPLSSMCPVIIVGDDGQV 464
Human               FNNEMDDFS-SPSITNEFGVPPSPANFIQPGKQPLSSMCPTIMVGQDGQV 465
Rat                 FNDEMDDFS-SPNFTNQFGVAPSPANFIKPGKQPLSSMCPSIIVDKDGKV 464
```

Figure 25. Comparison of amino acid sequence of *H. pylori* GGT (residues 416-464) and that of other bacterial and mammalian homologues. Multiple sequence alignment was performed using Clustal 2.0.12. Origin of the sequences are stated on the left. Numbers on the right indicate amino acid positions. The black bar corresponds to the position of the sequence recognized by the MAbs (1G1, 3C10, 3F4 and 4F11) on *H. pylori* 88-3887 GGT.

4.5 Purification of nGGT from *H. pylori*

H. pylori nGGT was purified in a one-step procedure by immunoaffinity chromatography using MAb 1G1. The purified *H. pylori* nGGT protein consisted of two protein bands with molecular masses of about 37 kDa and 20 kDa corresponding to the large and small subunit of GGT respectively (Figure 26). Purity of the protein was >95% as determined by silver staining after SDS-PAGE (data not shown).

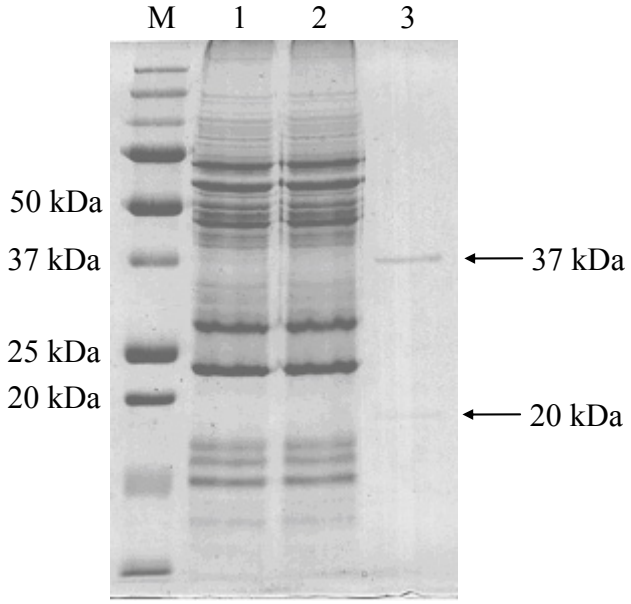

Figure 26. SDS-PAGE of purified native *H. pylori* GGT (nGGT). Lane M, Prestained Precision Protein Standards (Bio-Rad); Lane 1, *H. pylori* 88-3887 crude sample; Lane 2, unbound fraction; Lane 3, purified nGGT.

4.5.1 Total yield and recovery

Using this method, 0.067 mg of purified nGGT was obtained from an initial 8.12 mg of crude sample and specific GGT activity was shown to increase by 10-fold from 0.78 U/mg protein to 70.9 U/mg protein. The total GGT activity recovery was approximately 75%.

4.6 Localization of GGT in *H. pylori* by immunogold-labeling TEM

Ultrathin sections of *H. pylori* wild type and Δ*ggt* sections were probed with MAb 1G1 and secondary anti-mouse antibody conjugated with 10 nm gold. Gold particles were mainly observed on the outer cell membrane and periplasmic space of *H. pylori* wild type (Figure 27A-B) but were absent in the *ggt*-isogenic mutant (Figure 27C). Some gold particles were also observed in the cytoplasm of the bacteria. In contrast, no gold particles were observed in *H. pylori* wild type sections probed with pre-immune mouse sera (Figure 27D).

(A)

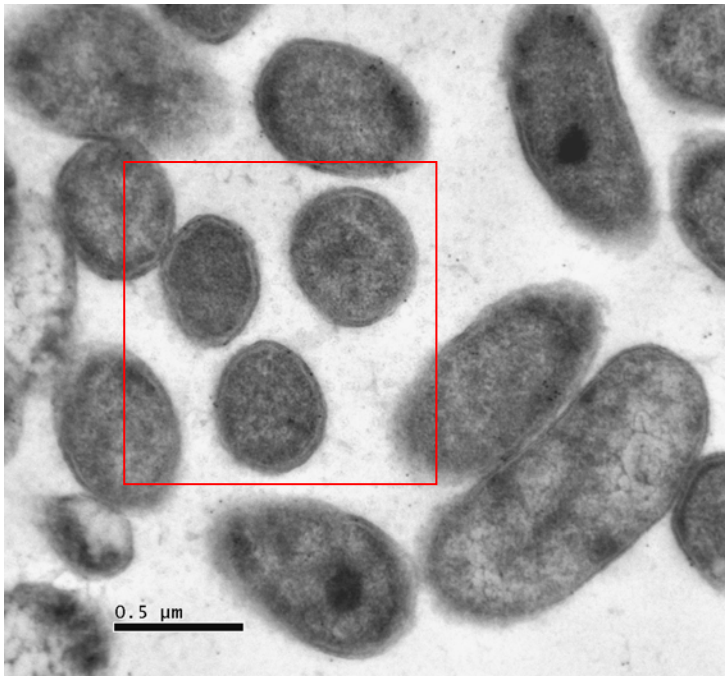

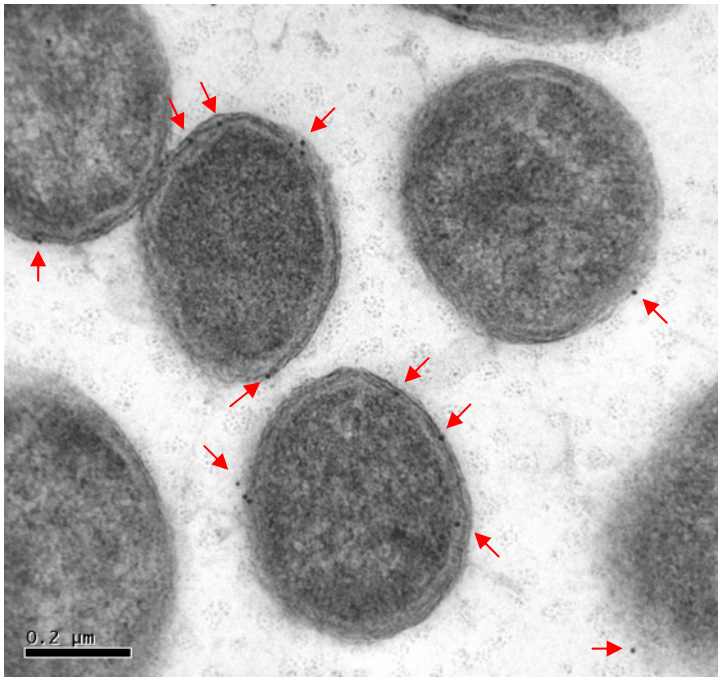

(B)

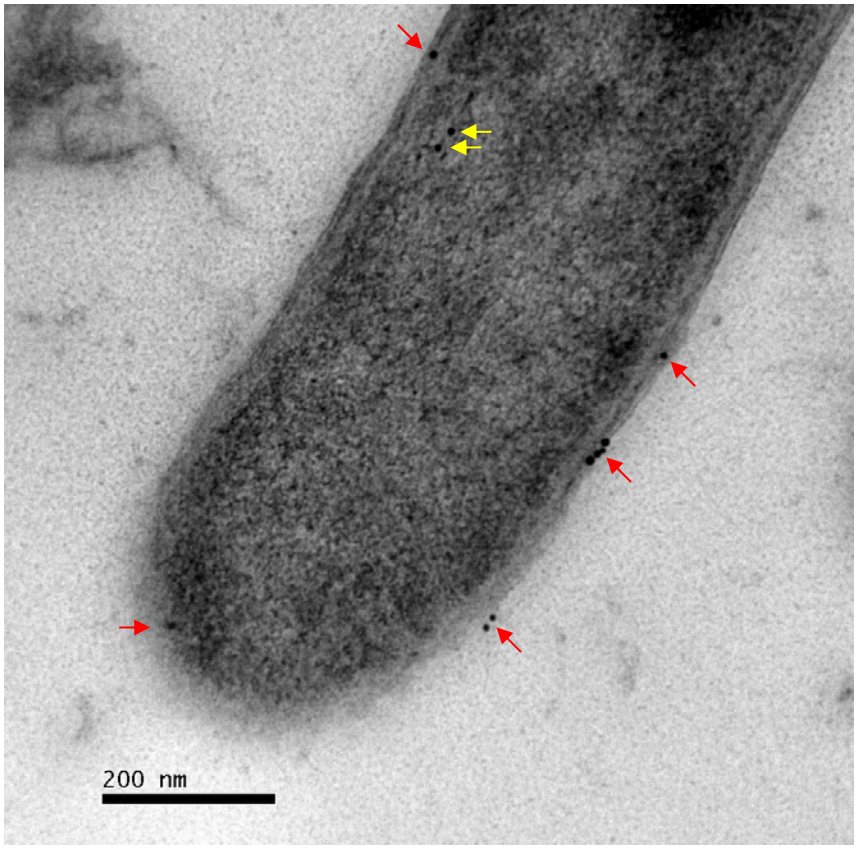

(C)

(D)

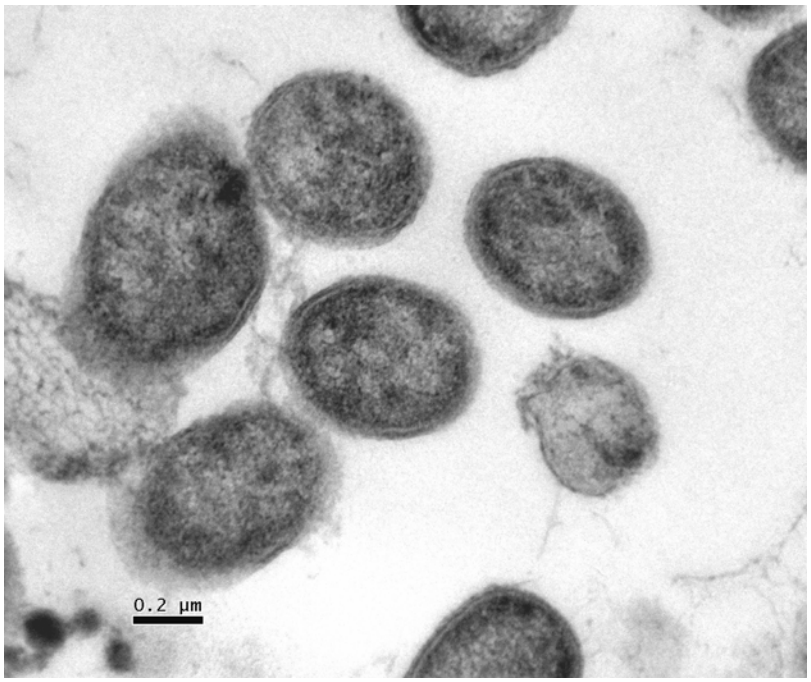

Figure 27. Localization of GGT in *H. pylori* by immunogold-labeling TEM. (A-B) *H. pylori* wild type and (C) Δ*ggt* labeled with MAb 1G1 and 10 nm gold particles. (D) *H. pylori* wild type labeled with pre-immune mouse sera. Red arrows indicate presence of GGT on the bacterial outer cell membrane or periplasmic space. Yellow arrows indicate presence of GGT in the bacterial cytoplasm. Micrographs are representative of 3 independent experiments.

4.7 Construction of various *H. pylori* isogenic mutants

Figure 28 shows the presence of the PCR amplified DNA fragments of various isogenic mutants that have been correctly constructed. Each fragment consists of the two flanking DNA fragments upstream and downstream (approximately 500 bp each) of the gene of interest on *H. pylori* strain 88-3887 genomic DNA. In place of the gene of interest is either the 1402 bp kanamycin resistance cassette or the 742 bp chloramphenicol resistance cassette. Thus, each of the isogenic construct comprises three DNA fragments (upstream region, specific antibiotic resistance cassette and downstream region) that were ligated and amplified, resulting in the construction of a gene-targeting construct used for the transformation of *H. pylori* strain 88-3887. Δ*cag*PAI was constructed by transforming plasmid pJP46 into *H. pylori* 88-3887.

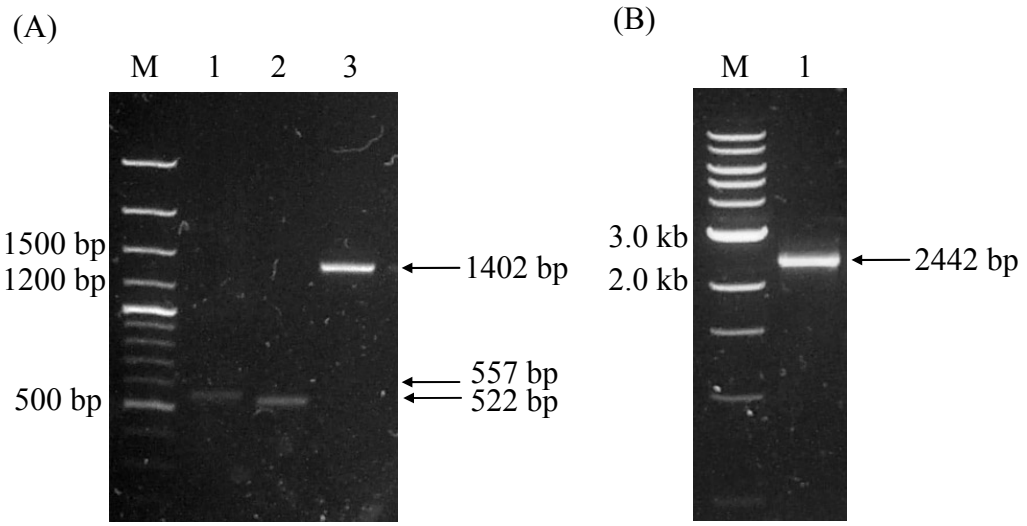

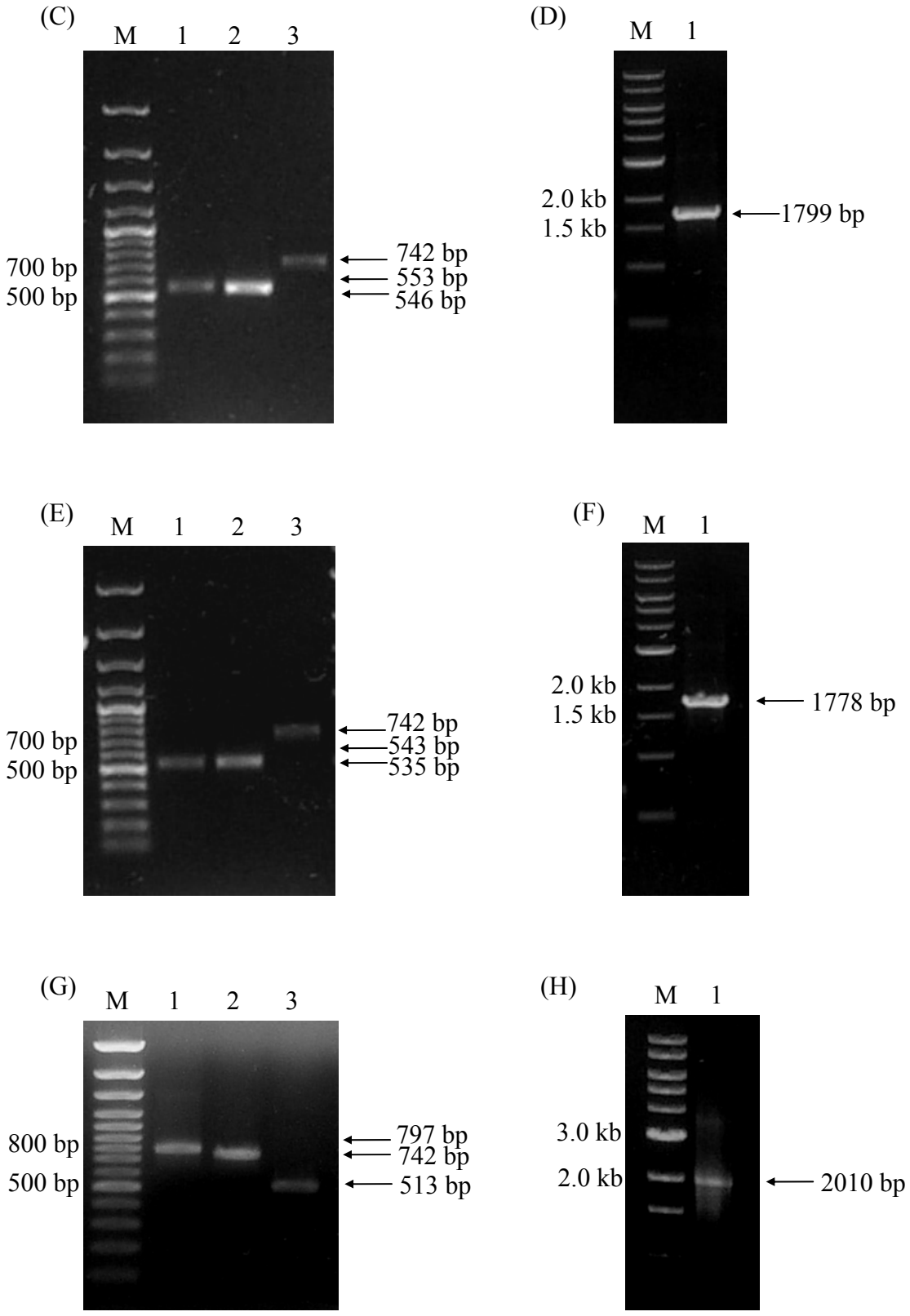

Figure 28. PCR amplified products for generation of various knockout constructs. (A) PCR products for generation of *ggt* knockout construct. Lane M, 100 bp DNA ladder; Lane 1, upstream region of *ggt* (557 bp, primers ggt1 and ggt2); Lane 2, downstream region of *ggt* (522 bp, primers ggt3 and ggt4); Lane 3, kanamycin resistance cassette (1402 bp, primers kanF and kanR). (B) Δ*ggt* construct. Lane M, 1 kb DNA ladder; Lane 1, *ggt* knockout construct (2442 bp, primers ggt1 and ggt4). (C) PCR products for generation of *cagA* knockout construct. Lane M, 100 bp DNA

ladder; Lane 1, upstream region of *cagA* (553 bp, primers cagA1 and cagA2); Lane 2, downstream region of *cagA* (546 bp, primers cagA3 and cagA4); Lane 3, chloramphenicol resistance cassette (742 bp, primers camF and camR). (D) Δ*cagA* construct. Lane M, 1 kb DNA ladder; Lane 1, *cagA* knockout construct (1799 bp, primers cagA1 and cagA4). (E) PCR products for generation of *vacA* knockout construct. Lane M, 100 bp DNA ladder; Lane 1, upstream region of *vacA* (543 bp, primers vacA1 and vacA2); Lane 2, downstream region of *vacA* (535 bp, primers vacA3 and vacA4); Lane 3, chloramphenicol resistance cassette (742 bp, primers camF and camR). (F) Δ*vacA* construct. Lane M, 1 kb DNA ladder; Lane 1, *vacA* knockout construct (1778 bp, primers vacA1 and vacA4). (G) PCR products for generation of *ureAB* knockout construct. Lane M, 100 bp DNA ladder; Lane 1, upstream region of *ureAB* (797 bp, primers ureAB1 and ureAB2); Lane 2, chloramphenicol resistance cassette (742 bp, primers camF and camR); Lane 3, downstream region of *ureAB* (513 bp, primers ureAB3 and ureAB4). (H) Δ*ureAB* construct. Lane M, 1 kb DNA ladder; Lane 1, *ureAB* knockout construct (2010 bp, primers ureAB1 and ureAB4).

After transformation of the various knockout constructs into *H. pylori* 88-3887, positive deletion mutants were confirmed by PCR. Chromosomal DNA extracted from the respective mutants gave a PCR product of a different size as compared to that from wild type (Figure 29) using the respective primers as previously listed in Table 6.

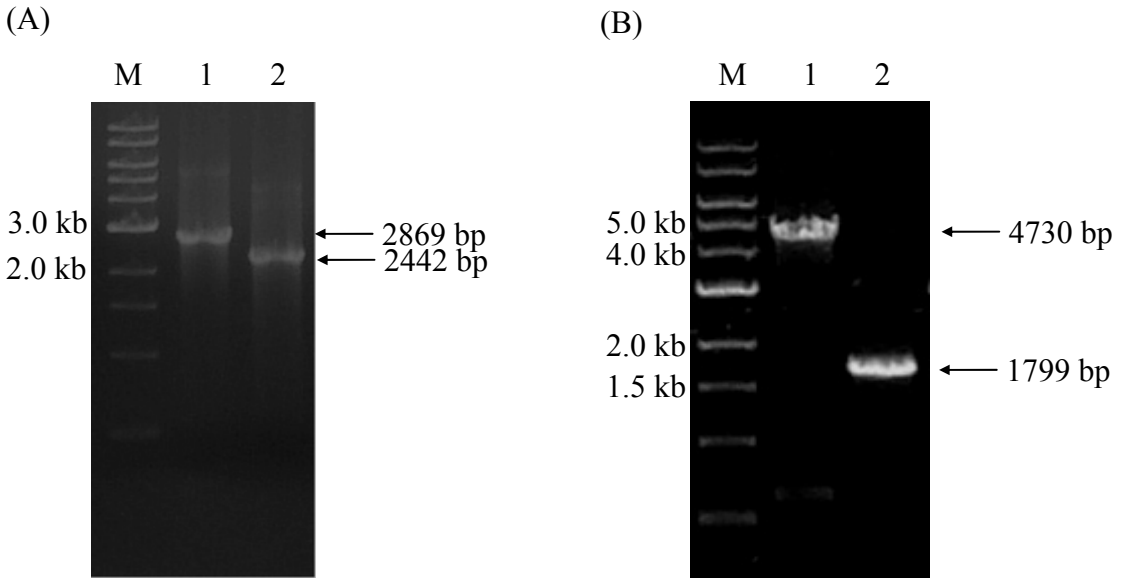

(C)

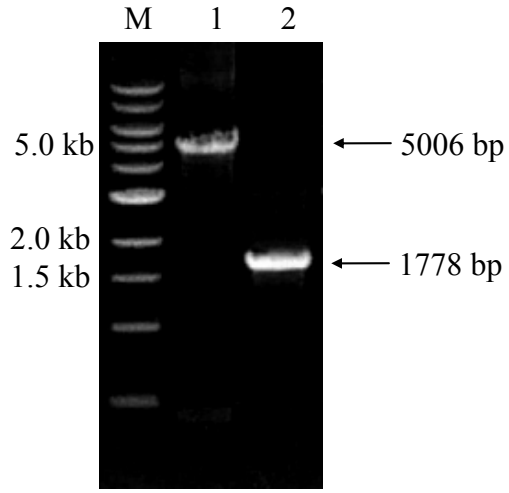
M
1
2
5.0 kb
2.0 kb
1.5 kb
5006 bp
1778 bp

(D)

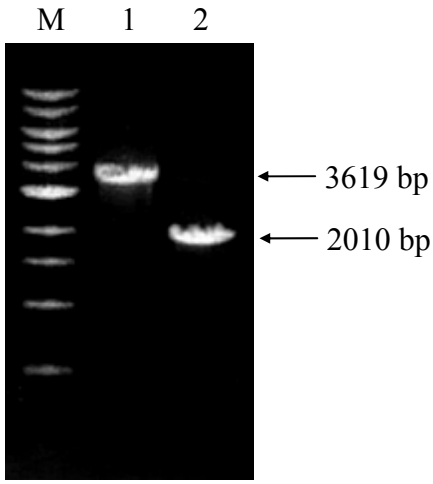
M
1
2
3619 bp
2010 bp

(E)

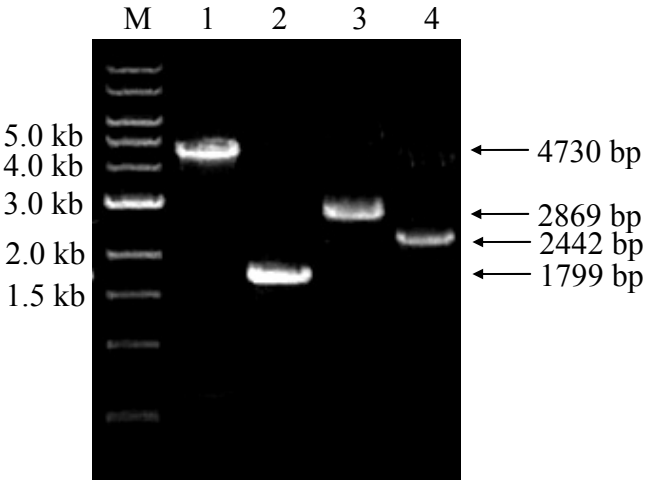
M
1
2
3
4
5.0 kb
4.0 kb
3.0 kb
2.0 kb
1.5 kb
4730 bp
2869 bp
2442 bp
1799 bp

(F)

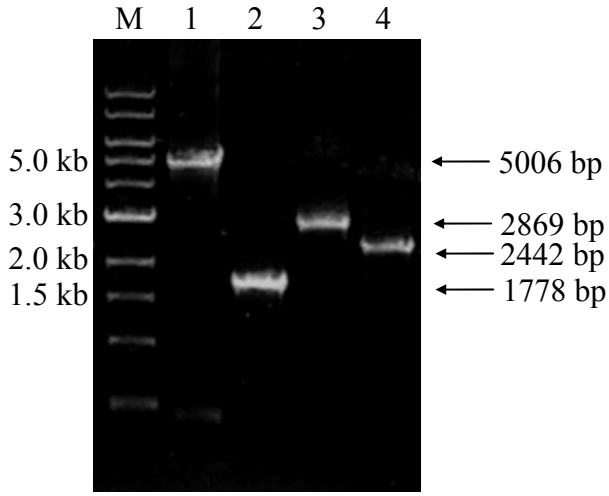
M
1
2
3
4
5.0 kb
3.0 kb
2.0 kb
1.5 kb
5006 bp
2869 bp
2442 bp
1778 bp

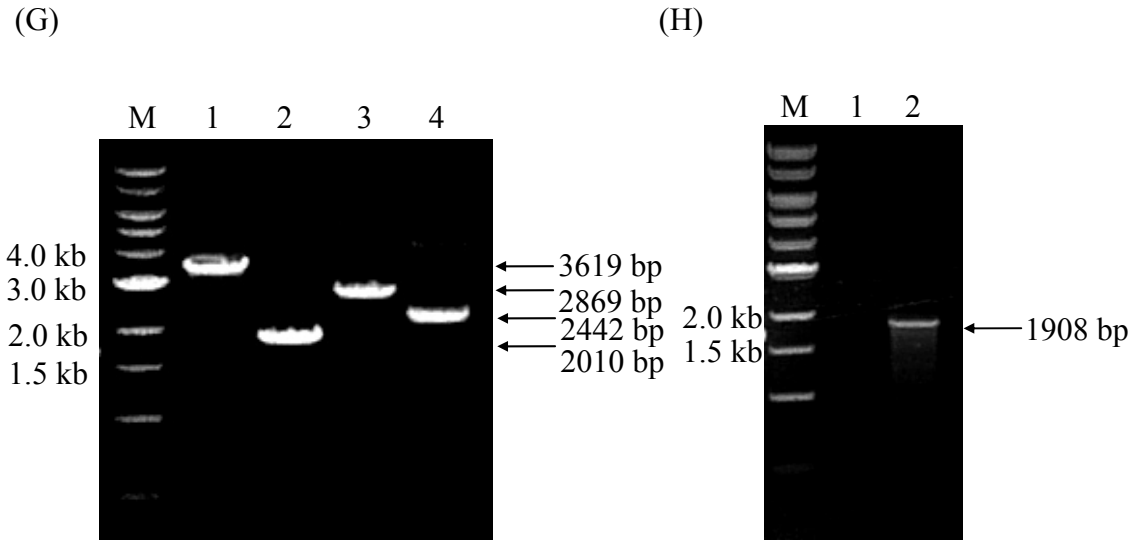

Figure 29. Identification of isogenic mutants by PCR amplification. Genomic DNA of wild type *H. pylori* 88-3887 and various knockout strains were extracted and subjected to PCR using different primer sets. (A) Confirmation of Δ*ggt*. Lane M, 1 kb DNA ladder; Lane 1, wild type (2869 bp, primers ggt1 and ggt4); Lane 2, Δ*ggt* (2442 bp, primers ggt1 and ggt4). (B) Confirmation of Δ*cagA*. Lane M, 1 kb DNA ladder; Lane 1, wild type (4730 bp, primers cagA1 and cagA4); Lane 2, Δ*cagA* (1799 bp, primers cagA1 and cagA4). (C) Confirmation of Δ*vacA*. Lane M, 1 kb DNA ladder; Lane 1, wild type (5006 bp, primers vacA1 and vacA4); Lane 2, Δ*vacA* (1778 bp, primers vacA1 and vacA4). (D) Confirmation of Δ*ureAB*. Lane M, 1 kb DNA ladder; Lane 1, wild type (3619 bp, primers ureAB1 and ureAB4); Lane 2, Δ*ureAB* (2010 bp, primers ureAB1 and ureAB4). (E) Confirmation of Δ*cagA/ggt*. Lane M, 1 kb DNA ladder; Lane 1, wild type (4730 bp, primers cagA1 and cagA4); Lane 2, Δ*cagA* (1799 bp, primers cagA1 and cagA4); Lane 3, wild type (2869 bp, primers ggt1 and ggt4); Lane 4, Δ*ggt* (2442 bp, primers ggt1 and ggt4). (F) Confirmation of Δ*vacA/ggt*. Lane M, 1 kb DNA ladder; Lane 1, wild type (5006 bp, primers vacA1 and vacA4); Lane 2, Δ*vacA* (1778 bp, primers vacA1 and vacA4); Lane 3, wild type (2869 bp, primers ggt1 and ggt4); Lane 4, Δ*ggt* (2442 bp, primers ggt1 and ggt4). (G) Confirmation of Δ*ureAB/ggt*. Lane M, 1 kb DNA ladder; Lane 1, wild type (3619 bp, primers ureAB1 and ureAB4); Lane 2, Δ*ureAB* (2010 bp, primers ureAB1 and ureAB4); Lane 3, wild type (2869 bp, primers ggt1 and ggt4); Lane 4, Δ*ggt* (2442 bp, primers ggt1 and ggt4). (H) Confirmation of Δ*cag*PAI. Lane M, 1 kb DNA ladder; Lane 1, wild type (absence of *cag*PAI empty site PCR fragment of 1908 bp, primers Luni1 and R5280); Lane 2, Δ*cag*PAI (1908 bp, primers Luni1 and R5280).

4.8 Enumeration of *H. pylori*

A plot of viable bacterial cell count (CFU/ml) against the OD_{600} reading based on different dilutions of a 3-day-old *H. pylori* strain 88-3887 culture was obtained (Figure 30). This standard curve was used in subsequent experiments to enumerate *H. pylori*.

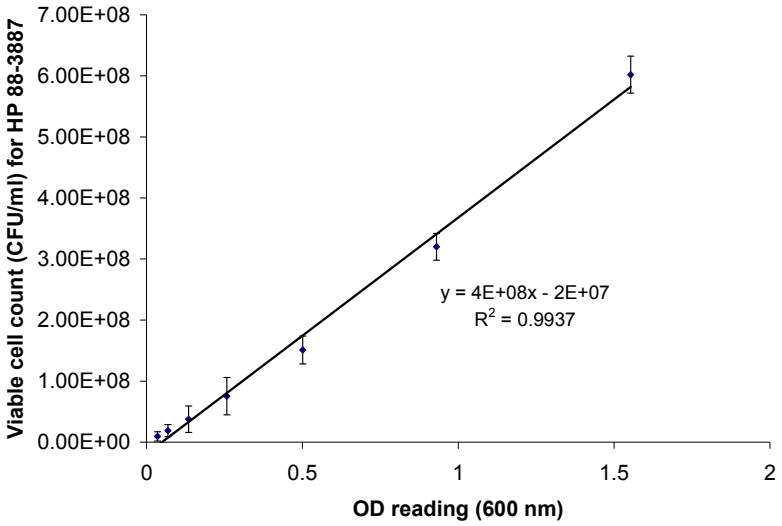

Figure 30. Standard curve for enumeration of *H. pylori*. Viable cell count (CFU/ml) was plotted against OD_{600} for *H. pylori* strain 88-3887. Data are representative of 3 independent experiments.

4.9 *H. pylori* GGT and H_2O_2 generation

4.9.1 GGT induces H_2O_2 production

AGS cells were co-cultured with *H. pylori* 88-3887, Δ*ggt* or purified nGGT and H_2O_2 generation was quantified by a fluorescence-based analysis. Figure 31A shows that H_2O_2 generation was significantly increased in the presence of *H. pylori* wild type as compared to control cells (5.79 ± 0.35 μM *vs* 1.05 ± 0.11 μM; $P<0.05$) but this effect was dramatically decreased in the presence of Δ*ggt* (5.79 ± 0.35 μM *vs* 2.67 ± 0.21 μM; $P<0.05$). In addition, H_2O_2 generation was also significantly increased in the presence of purified nGGT compared to control cells (2.82 ± 0.12 μM *vs* 1.05 ± 0.11 μM; $P<0.05$). The significance of GGT-mediated H_2O_2 generation was

further illustrated using primary human gastric epithelial cells which displayed a similar significant effect (Figure 31B).

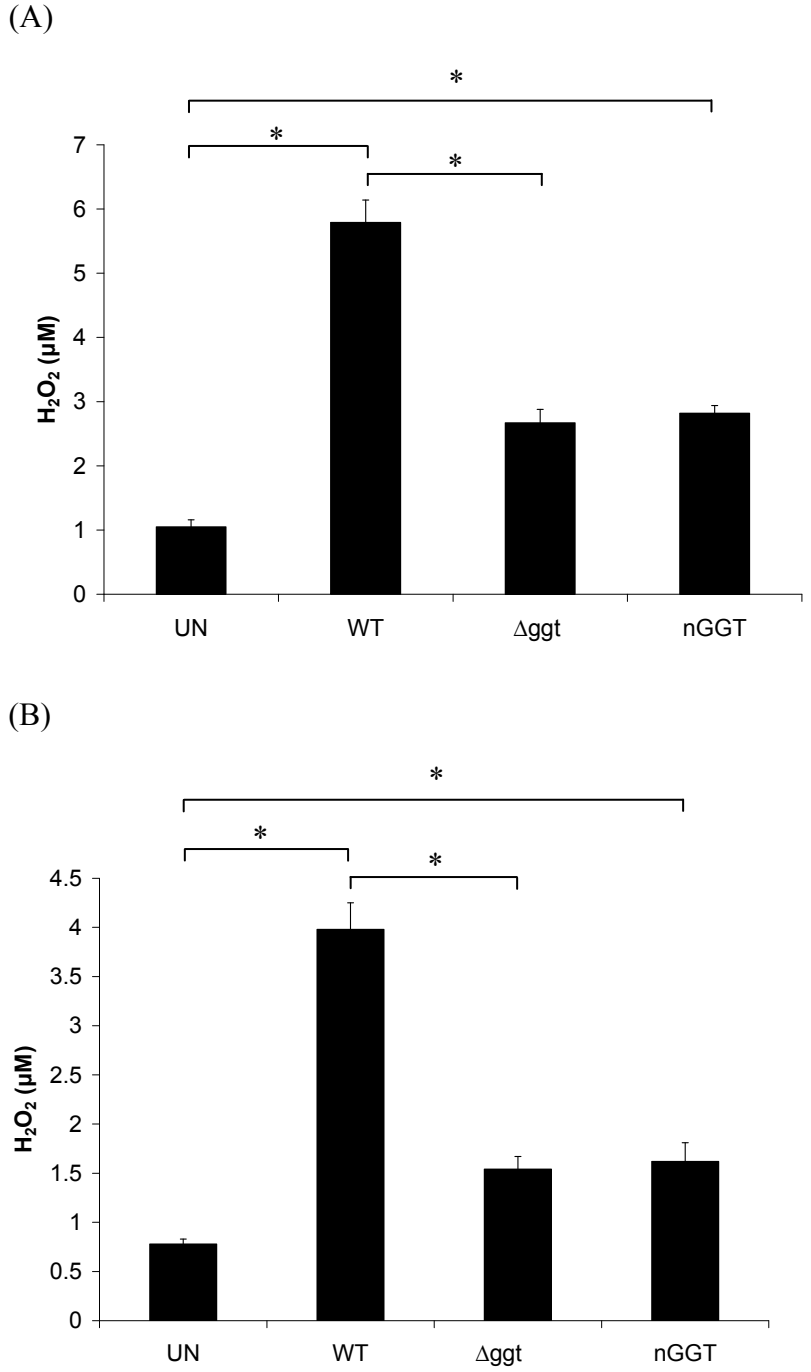

Figure 31. Effect of *H. pylori* GGT on H_2O_2 generation. (A) AGS cells. (B) primary human gastric epithelial cells. The respective cells were treated with *H. pylori* wild type, WT; *ggt*-isogenic mutant, Δ*ggt*; or purified native GGT, nGGT. H_2O_2 generation was examined by a fluorescence-based analysis. Uninfected cells, UN. Values represent mean ± SD of 3 independent experiments. **P*<0.05.

4.9.2 Effects of inhibitor and enhancer on GSH-dependent iron reduction

H_2O_2 production by AGS cells was assayed in the presence of purified nGGT under various conditions (Figure 32). Stimulation of GGT activity with its substrate GSH and the acceptor molecule glycyl-glycine significantly elevated the amount of H_2O_2 being generated compared to nGGT alone (8.31 ± 0.59 μM *vs* 2.82 ± 0.12 μM; $P<0.01$). Interestingly, H_2O_2 production was also increased with the addition of exogenous Fe^{3+} compared to cells treated with nGGT alone (4.86 ± 0.17 μM *vs* 2.82 ± 0.12 μM; $P<0.05$). Not surprisingly, H_2O_2 production was further increased in the presence of nGGT, GSH and Fe^{3+} compared to cells treated with nGGT alone (17.6 ± 0.76 μM *vs* 2.82 ± 0.12 μM; $P<0.01$). In contrast, addition of the GGT inhibitor SBC completely suppressed nGGT-mediated H_2O_2 production to a similar level as untreated cells, even in the presence of GSH. Similarly, H_2O_2 production was also significantly decreased ($P<0.05$) in the presence of the iron chelator, DFO.

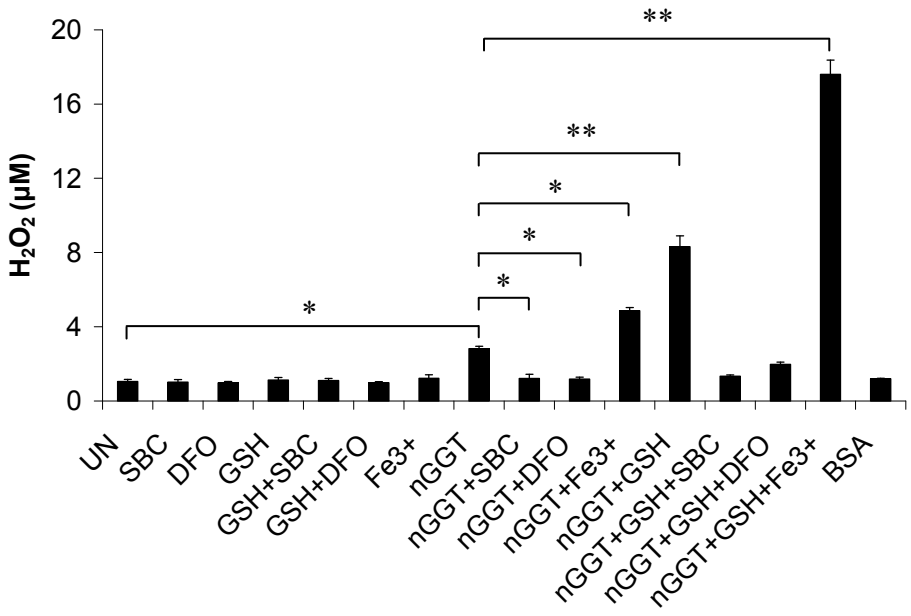

Figure 32. *H. pylori* purified native GGT induces H_2O_2 generation in AGS cells. Cells were treated with SBC, 10 mM serine-borate complex; DFO, 50 μM desferrioxamine; GSH, 0.1 mM glutathione and 1 mM glycyl-glycine; Fe^{3+}, 20 μM ferric iron; nGGT, 1.5 mU *H. pylori* purified native GGT; BSA, 10 ng bovine serum albumin and combination of one or more compounds. UN, untreated cells. Values represent mean ± SD of 3 independent experiments. **P*<0.05, ***P*<0.01.

4.9.3 *H. pylori* GGT induces NF-κB activation

As shown in Figure 33, a substantial increase in NF-κB translocation was observed in the nuclear extract of AGS cells infected with wild type *H. pylori*. In contrast, Δ*ggt*-treated cells showed significantly reduced levels of NF-κB translocation as compared to wild type-treated cells (relative density 0.68 *v* 1; $P<0.05$). In addition, degradation of IκB was also greater in wild type-treated cells compared to Δ*ggt*-treated cells (relative density 1 *v* 4.61; $P<0.01$), further confirming the results. As it has been previously reported that CagA (Kim *et al.*, 2006) and *cag*PAI (Glocker *et al.*, 1998) may also play a role in NF-κB activation, the ability of Δ*cagA*, Δ*cagA*/*ggt* and Δ*cag*PAI in inducing NF-κB translocation was also investigated. Interestingly, it was observed that NF-κB activation was dependent on the *cag*PAI but independent of CagA.

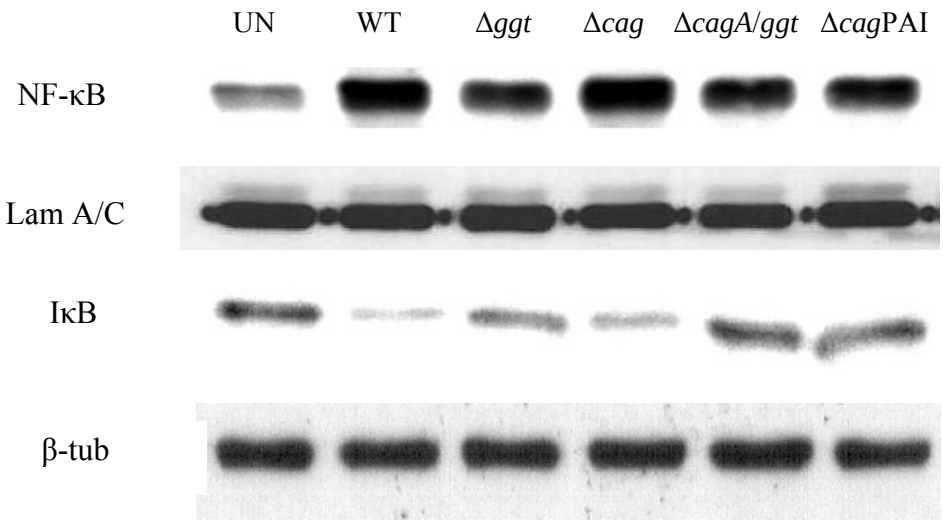

Figure 33. *H. pylori* GGT induces NF-κB activation. AGS cells were treated with *H. pylori* wild type (WT) or various mutants. NF-κB and IκB were detected in the nuclear and cytosolic fractions respectively. Lam A/C, antibody against lamin A/C; β-tub, antibody against β-tubulin. Immunblots are representative of 3 independent experiments.

4.9.4 *H. pylori* GGT and IL-8 production

4.9.4.1 IL-8 production induced by GGT

AGS cells were tested for enhanced IL-8 production following treatment with *H. pylori* or nGGT according to the method as described in section 3.13.3. As observed in Figure 34A-B, *H. pylori* wild type induced significantly higher levels of IL-8 production as compared to Δ*ggt* at both 4 and 24 hours post-infection ($P<0.05$). Interestingly, purified nGGT alone was also able to induce significantly greater IL-8 generation by AGS cells compared to the control cells ($P<0.05$). Additionally, purified rGGT was tested for its ability to induce IL-8 secretion in AGS cells and showed similar results as nGGT.

To further confirm the role of GGT in inducing IL-8 production, primary human gastric epithelial cells were also treated with *H. pylori*, nGGT or rGGT. The results showed a similar trend as compared to AGS cells (Figure 34C-D). As macrophages are also an important source of IL-8 generation in the stomach mucosa, the ability of *H. pylori*, nGGT and rGGT in inducing IL-8 production was tested on primary human macrophages. Interestingly, wild type *H. pylori* induced significantly higher IL-8 production as compared to Δ*ggt* at 4 hours post-infection ($P<0.05$) but the difference was no longer significant 24 hours post-infection (Figure 34E-F). Despite this, it was noted that nGGT or rGGT alone was able to induce a significant amount of IL-8 generation in macrophages compared to untreated cells at both 4 and 24 hours post-treatment ($P<0.05$).

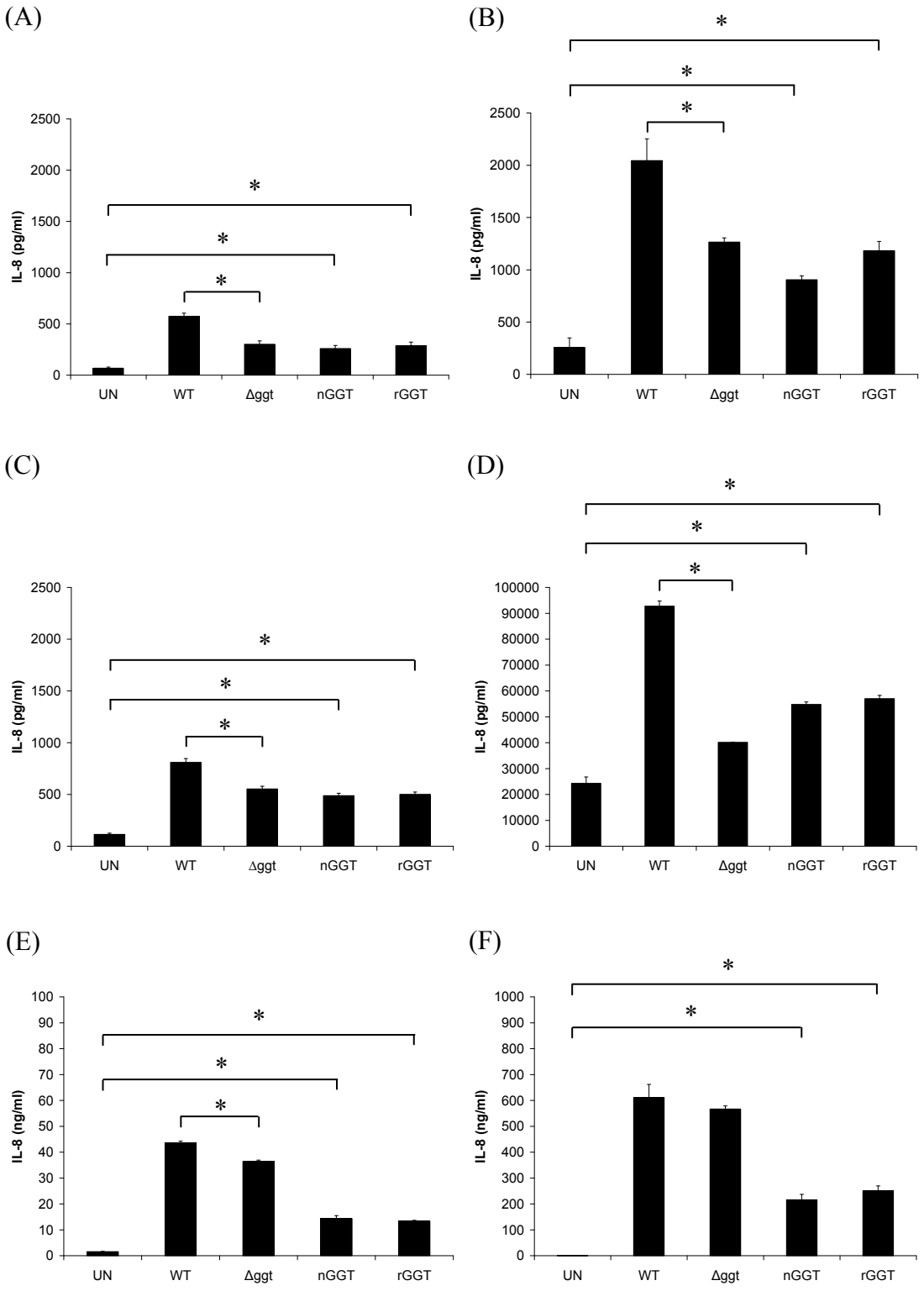

Figure 34. *H. pylori* GGT induces IL-8 production from various cell types. ELISA assay was employed to measure IL-8 generation from: AGS cells (A) 4 hours and (B) 24 post-infection; primary human gastric epithelial cells (C) 4 hours and (D) 24 hours post-infection; and primary human macrophages (E) 4 hours and (F) 24 hours post-infection. UN, uninfected cells; WT, wild type *H. pylori*; Δ*ggt*, *ggt*-isogenic mutant; nGGT, purified native GGT; rGGT, purified recombinant GGT. Values represent mean ± SD of 3 independent experiments. **P*<0.05.

4.9.4.2 Role of CagA and *cag*PAI in IL-8 induction

The role of CagA in inducing IL-8 generation has been controversial (Nozawa *et al.*, 2002; Lai *et al.*, 2011). To determine whether CagA works in concert with GGT to induce IL-8 production, AGS cells were infected with Δ*cagA* or Δ*cagA*/*ggt* (Figure 35). Interestingly, IL-8 production induced by Δ*cagA* was not significantly different from that induced by wild type *H. pylori* ($P>0.05$) but was significantly reduced when infected with Δ*cagA*/*ggt* ($P<0.05$). The role of other *cag*PAI proteins in IL-8 induction was also tested by infecting AGS cells with Δ*cag*PAI. From the results, it was observed that Δ*cag*PAI induced significantly less IL-8 generation compared to wild type *H. pylori* ($P<0.05$), suggesting that certain protein(s) encoded in the *cag*PAI (but not CagA) may also be involved in IL-8 induction.

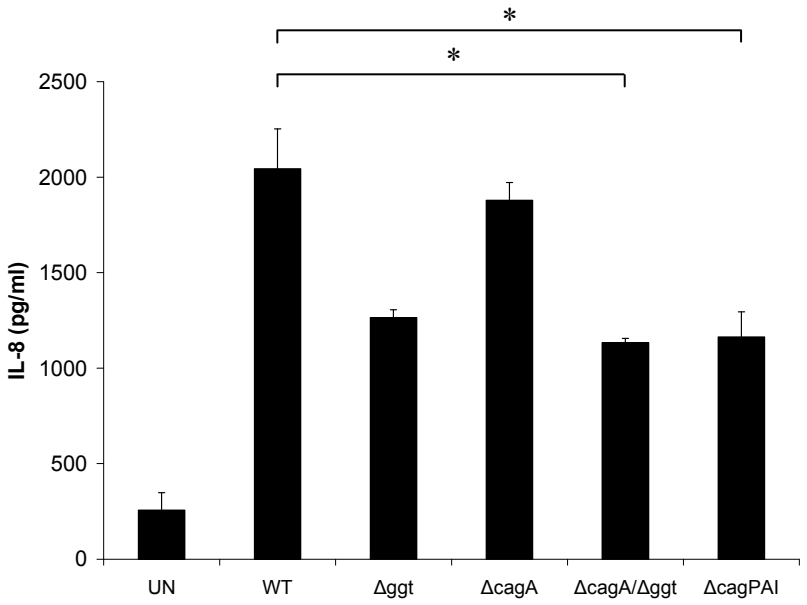

Figure 35. Involvement of *H. pylori cag*PAI in IL-8 induction in AGS cells. ELISA assay of IL-8 generation from AGS cells after treatments with *H. pylori* wild type (WT) or various mutants for 24 hours. UN, uninfected cells. Values represent mean ± SD of 3 independent experiments. **P*<0.05.

4.10 Internalization of *H. pylori* GGT in host cells

It was next investigated if GGT also translocates into host cells and if so, whether it exerts any effects intracellularly. To determine this, localization of *H. pylori* GGT in host AGS cells post-infection was performed using TEM, CLSM and western blot analysis.

4.10.1 TEM

Localization of GGT in AGS cells after infection with *H. pylori* was carried out using immunogold-labeling TEM. GGT was observed to be present mainly in the nuclei (indicated by 'Nu') of AGS cells as indicated by 20 nm gold particles, with a few gold particles present in the cytosol 24 hours post-infection (Figure 36B-C). No gold particles were observed in the uninfected control (Figure 36A) as well as AGS cells infected with *H. pylori* Δ*ggt* (Figure 36D), indicating that the antibody used is specific for *H. pylori* GGT. It was also noted that AGS cells infected with *H. pylori* wild type (Figure 36B-C) showed the presence of vacuoles (indicated by 'v') and condensation of chromatin into compact patches against the nuclear envelope (indicated by 'cc'), a hallmark of apoptosis (Kihlmark *et al.*, 2001). These characteristics were not observed in both the uninfected control and Δ*ggt*-infected AGS cells.

(A)

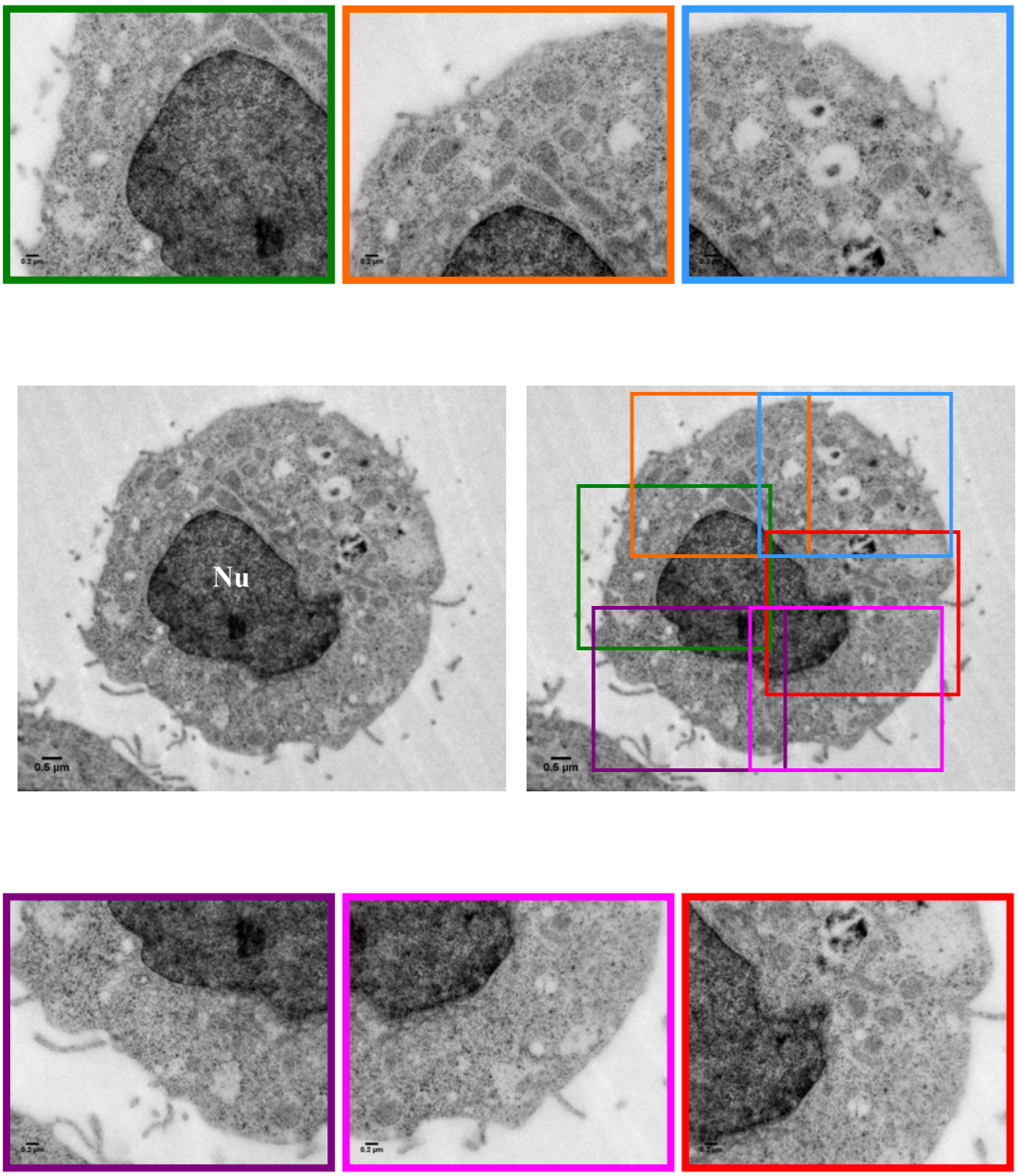

(B)

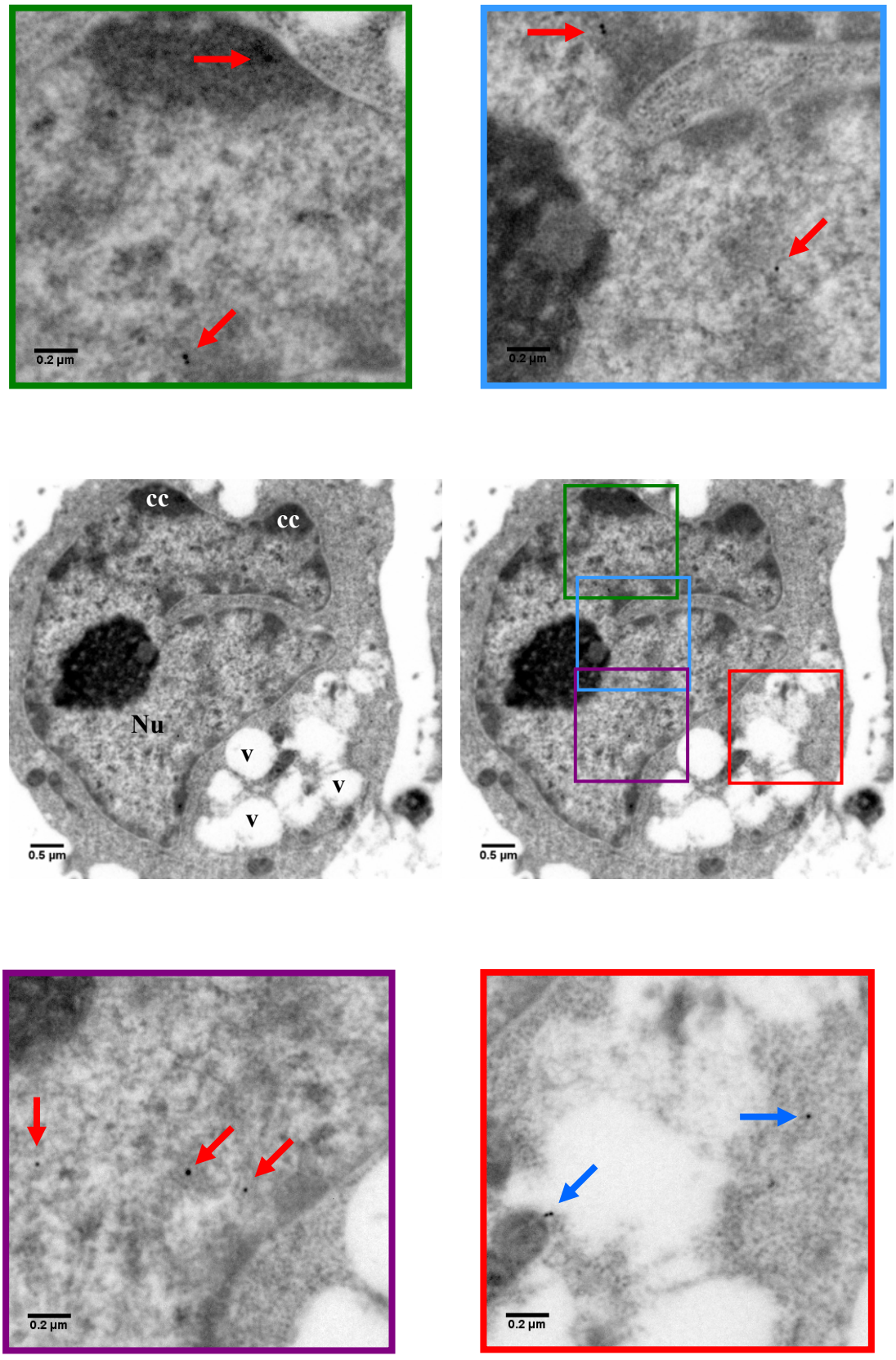

(C)

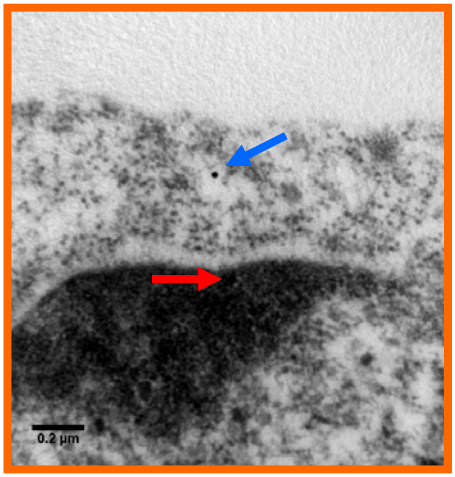

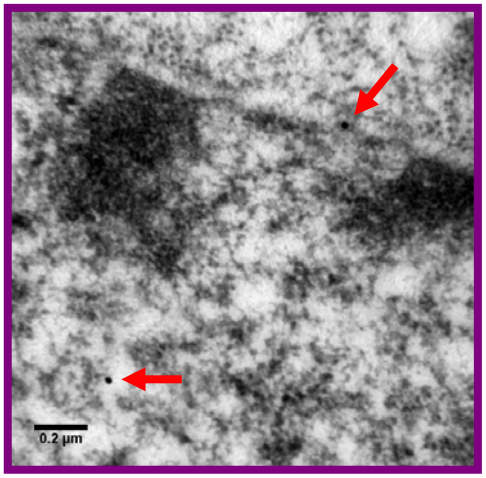

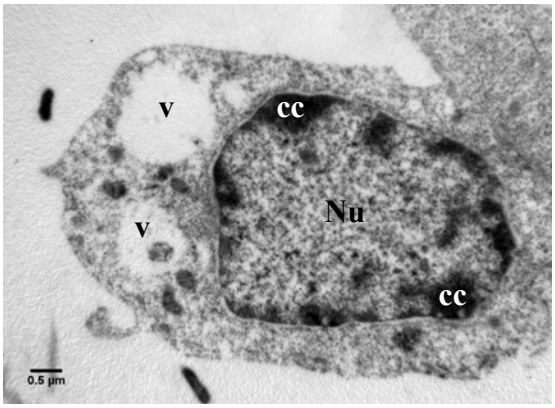

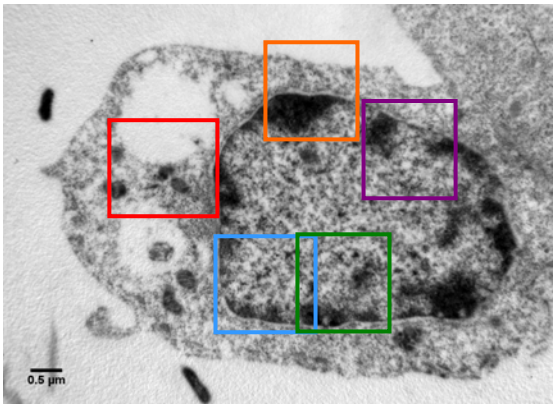

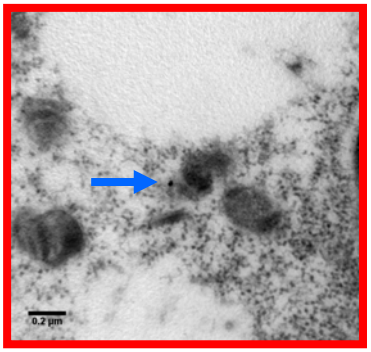

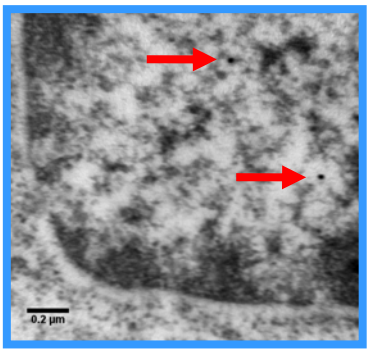

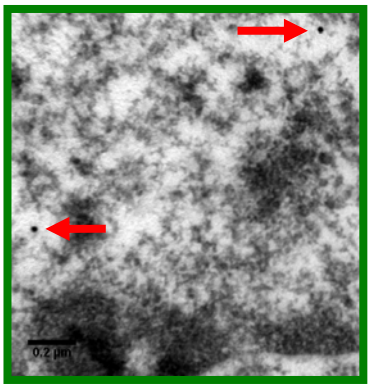

(D)

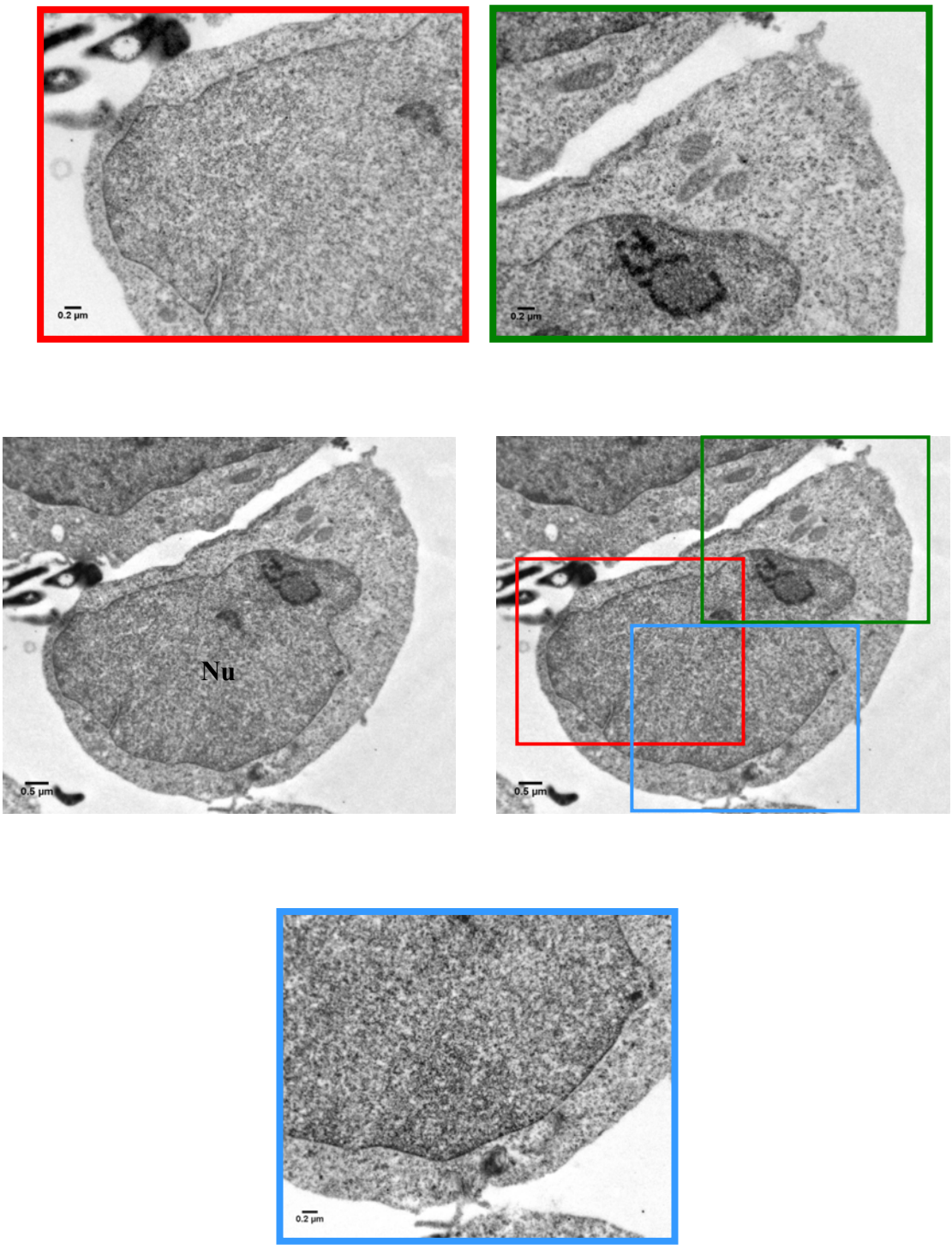

Figure 36. Localization of *H. pylori* GGT in AGS cells 24 hours post-infection. AGS cells were infected with *H. pylori* wild type or Δ*ggt* for 24 hours. Uninfected cells served as control. Cells were then processed for immunogold-labeling TEM as described in section 3.9. (A) Uninfected AGS cells. (B-C) AGS cells infected with *H. pylori* wild type. (D) AGS cells infected with *H. pylori* Δ*ggt*. GGT was labeled with MAb 1G1 and 20 nm immunogold secondary antibody. Red arrows indicate presence of GGT in the nucleus. Blue arrow indicates presence of GGT in the cell cytoplasm. Nu, nucleus; v, vacuole; cc, chromatin condensation.

4.10.2 CLSM

The presence of *H. pylori* GGT in AGS cells was also investigated using immunofluorescence. No GGT was observed in uninfected AGS cells (Figure 37A) as well as in *H. pylori* Δ*ggt*-infected AGS cells (Figure 37B). GGT was observed to be present mainly on extracellular *H. pylori* as well as in the nuclei of AGS cells infected with *H. pylori* wild type (Figure 37C). Interestingly, AGS co-incubated with purified rGGT alone also showed the presence of rGGT in the nuclei of the cells after 24 hours (Figure 37D).

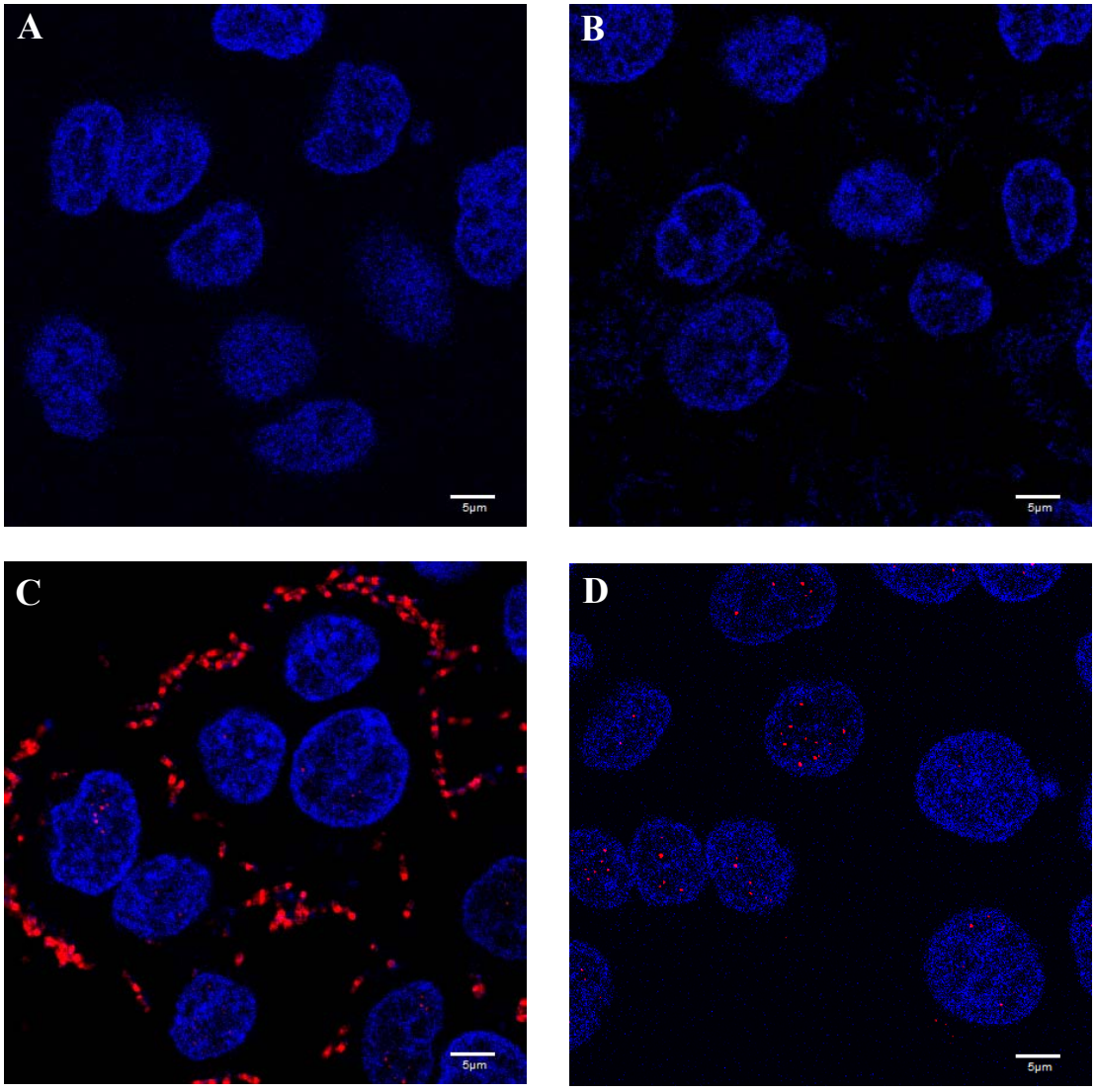

Figure 37. CLSM micrographs showing presence of *H. pylori* GGT in AGS cell nuclei. AGS cells were co-incubated with *H. pylori* wild type, Δ*ggt* or rGGT for 24 hours. Uninfected cells served as control. Cells were then processed for CLSM as

described in section 3.14.1.2. (A) Uninfected AGS cells. (B) AGS cells infected with *H. pylori* Δ*ggt*. (C) AGS cells infected with *H. pylori* wild type. (D) AGS cells treated with rGGT. Blue, nucleus stained with Hoechst 33342; Red, *H. pylori* GGT labeled with MAb 1G1 and Cy3. Scale bar represents 5 μm.

4.10.3 Western blot analysis of different cell fractions

Western blot analysis was employed to further confirm the presence of GGT in AGS cells after infection with *H. pylori*. Figure 38 shows that *H. pylori* GGT was detected in both the cytosolic and nuclear fractions of AGS cells as early as 1 hour post-infection. No β-tubulin nor lamin A/C was detected in the nuclear and cytosolic fractions respectively, indicating that the fractions were well separated and no cross-contamination was present.

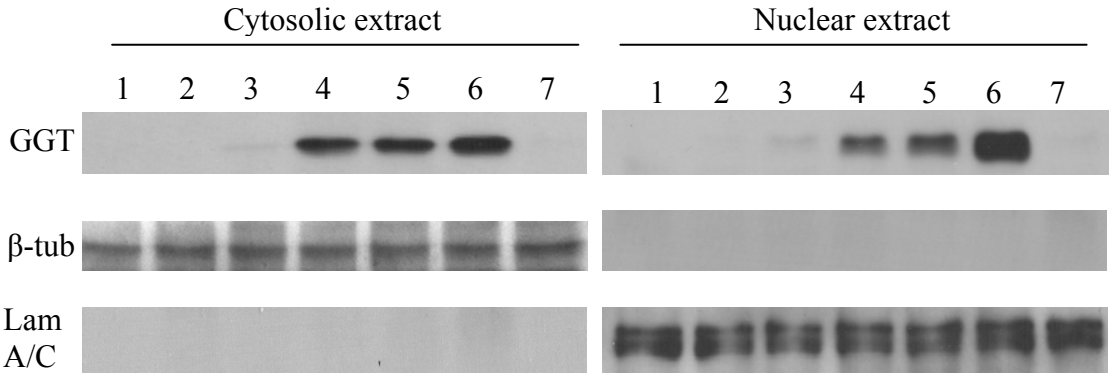

Figure 38. *H. pylori* GGT enters into host cells. AGS cells were infected with *H. pylori* wild type for 24 hours. The cytosolic and nuclear extracts were collected at various time-points and subjected to western blot analysis. Lane 1, 0 hour; Lane 2, 0.5 hour; Lane 3, 1 hour; Lane 4, 2 hours; Lane 5, 4 hours; Lane 6, 24 hours; Lane 7, AGS infected with Δ*ggt* (24 hours). GGT, polyclonal antibody raised against rGGTS; β-tub, antibody against β-tubulin; Lam A/C, antibody against lamin A/C.

To further confirm that rGGT was able to enter into host cell nuclei in the absence of *H. pylori* as observed by CLSM (section 4.10.2), western blot analysis was carried out on the cytosolic and nuclear fractions of rGGT-treated cells. Figure 39 shows that rGGT was also detected in AGS cells but at an earlier time-point of 30 minutes post-incubation.

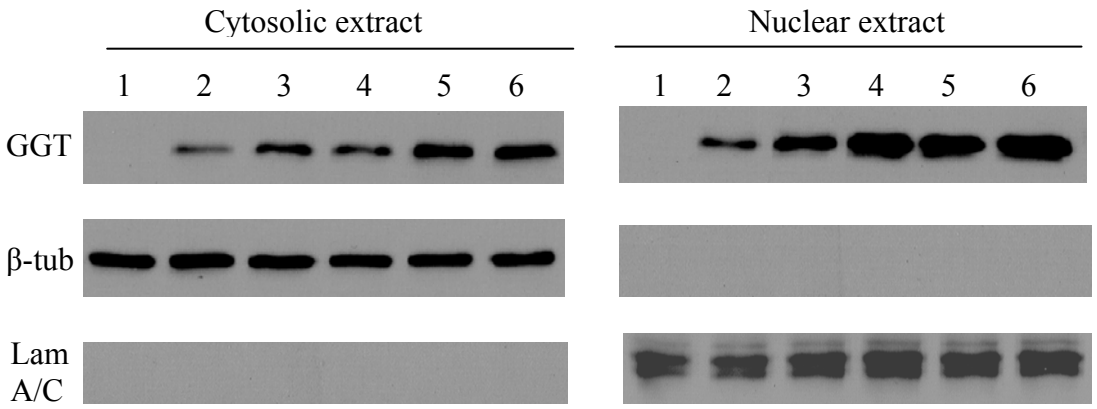

Figure 39. rGGT enters into host cells. AGS cells were co-incubated with rGGT for up to 24 hours. Cytosolic and nuclear extracts were obtained at various time-points. Lane 1, 0 hour; Lane 2, 0.5 hour; Lane 3, 1 hour; Lane 4, 2 hours; Lane 5, 4 hours; Lane 6, 24 hours. GGT, polyclonal antibody raised against rGGTS; β-tub, antibody against β-tubulin; Lam A/C, antibody against lamin A/C.

4.10.4 Internalization of GGT by cells is a specific process

AGS cells were incubated with either rGGT or heat-denatured rGGT (95°C, 10 minutes) and probed for the presence of intracellular rGGT after 2 and 4 hours. As observed in Figure 40, heat-denatured rGGT was not detected in AGS cells, implying that the uptake of rGGT requires it to be in its native conformation.

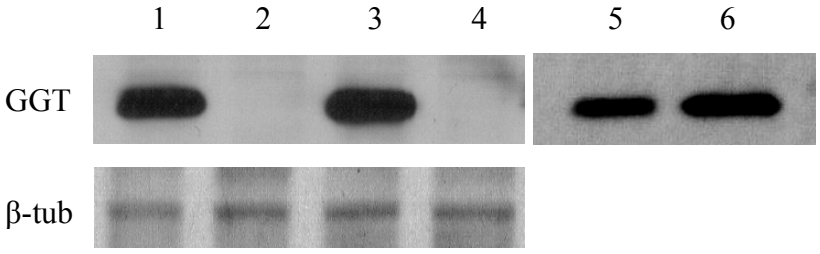

Figure 40. Heat-denatured rGGT is unable to enter into AGS cells. AGS cells were co-incubated with either rGGT or heat-denatured rGGT. Lane 1, AGS co-incubated with rGGT (2 hours); Lane 2, AGS co-incubated with heat-denatured rGGT (2 hours); Lane 3, AGS co-incubated with rGGT (4 hours); Lane 4, AGS co-incubated with heat-denatured rGGT (4 hours); Lane 5, rGGT positive control; Lane 6, rGGT (heat-denatured) positive control. GGT, polyclonal antibody raised against rGGTS; β-tub, antibody against β-tubulin.

AGS cells were also separately co-incubated with the individual recombinant subunits of GGT (rGGTL and rGGTS). Using western blot analysis, it was observed that neither rGGTL nor rGGTS could enter into AGS cells (Figure 41).

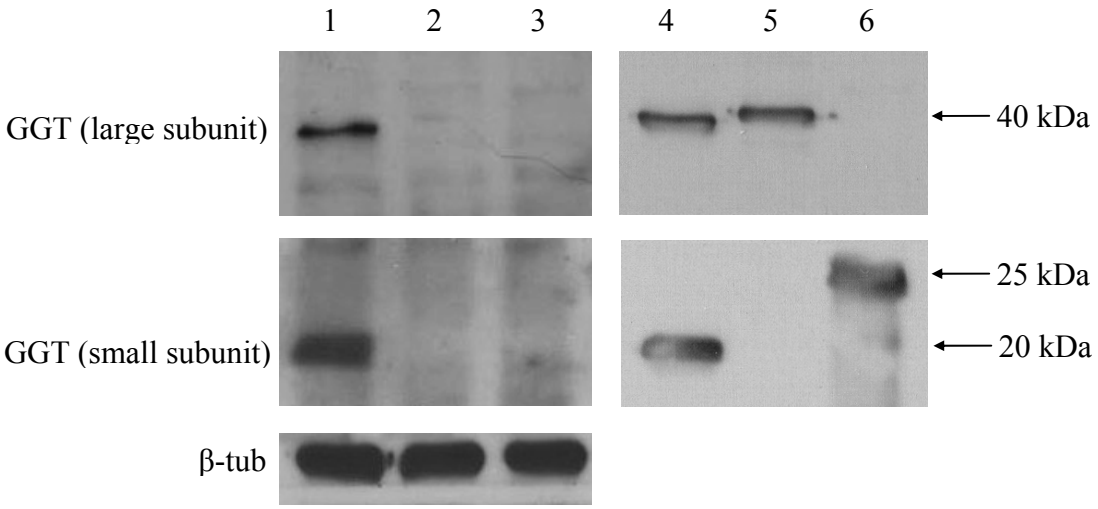

Figure 41. rGGTL and rGGTS are unable to enter into AGS cells separately. AGS cells were co-incubated with rGGT, rGGTL or rGGTS for 24 hours. AGS whole cell lysates were probed using MAb 2B5 or MAb 1G1. Lane 1, AGS co-incubated with rGGT; Lane 2, AGS co-incubated with rGGTL; Lane 3, AGS co-incubated with rGGTS; Lane 4, rGGT positive control; Lane 5, rGGTL positive control; Lane 6, rGGTS positive control.

4.10.4.1 GGT is endocytosed by a clathrin-dependent pathway

Since the uptake of GGT is specific and requires it to be in its native conformation, it was hypothesized that GGT enters into the cell via receptor-mediated endocytosis. To determine whether GGT was taken up by the cells by clathrin-mediated endocytosis or caveolin-dependent endocytosis (Conner and Schmid, 2003), pharmalogical agents CPZ and NYS were used to inhibit the respective endocytic pathways (Pho *et al.*, 2000). Drug cytotoxicity tests showed that CPZ at a concentration of 15 μg/ml and NYS at a concentration of 25 μg/ml maintained cell viability at 81% and 100% respectively (Figure 42). Hence, these concentrations,

which have also been reported to be used previously (Parker *et al.*, 2010), were chosen for the subsequent inhibitor studies.

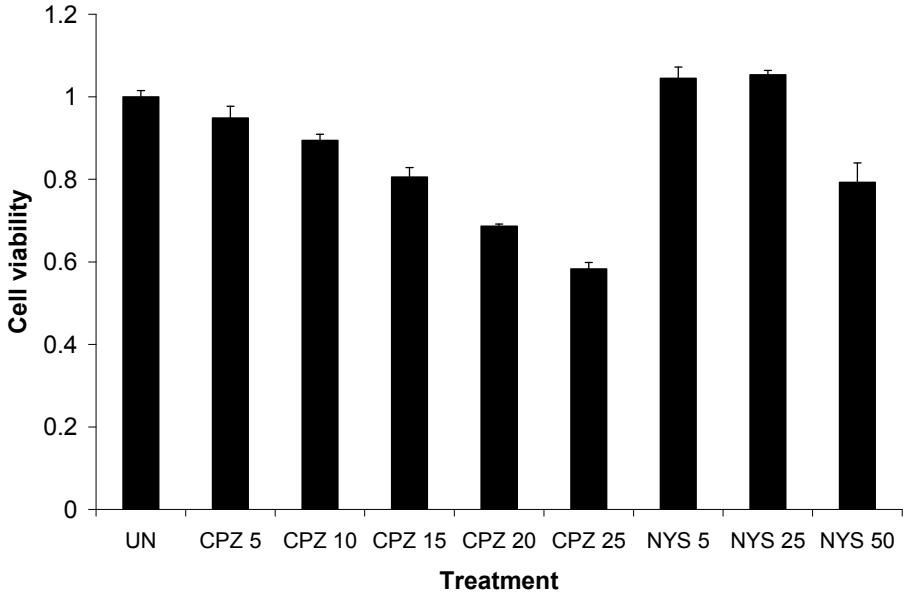

Figure 42. Assessment of drug cytotoxicity of CPZ and NYS to AGS cells. AGS cells were treated with CPZ (5-25 μg/ml) or NYS (5-50 μg/ml) for 5 hours and cell viability was measured by MTT assay. Untreated cells (UN) served as control. CPZ, chlorpromazine; NYS, nystatin.

After treating AGS cells with the respective inhibitors, presence of rGGT in whole cell lysates 4 hours post-incubation was probed by western blot analysis (Figure 43A). It was observed that in the presence of CPZ, the amount of rGGT detected in whole cell lysates decreased to approximately 67% as compared to the uninhibited cells (treated with rGGT only) as determined by ImageJ software. The cells were then further separated into membrane and cytosolic fractions. Interestingly, it was found that majority of rGGT was present in the membrane fraction of CPZ-treated cells while most were present in the cytosolic fraction in both NYS-treated and uninhibited cells (Figure 43B). These results indicate that GGT is likely to be taken up by AGS cells via the clathrin-mediated endocytosis pathway.

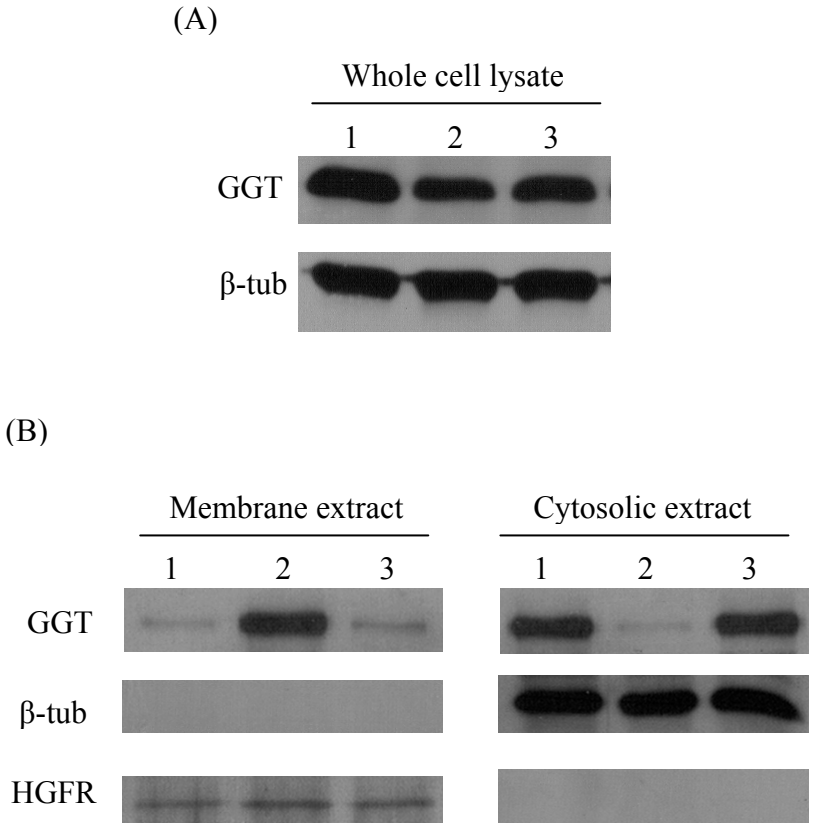

Figure 43. Effect of CPZ and NYS on rGGT internalization by AGS cells. AGS cells were either pre-treated with CPZ (15 μg/ml) or NYS (25 μg/ml) for 30 minutes and 60 minutes respectively and then incubated with rGGT for another 4 hours. (A) Presence of rGGT in whole cell lysates. (B) Presence of rGGT in membrane and cytosolic extracts of cells. Lane 1, uninhibited cells (treated with rGGT only); Lane 2, CPZ-treated cells; Lane 3, NYS-treated cells. GGT, polyclonal antibody raised against rGGTS; β-tub, antibody against β-tubulin; HGFR, antibody against hepatocyte growth factor receptor.

Cells treated with CPZ or NYS were also observed under CLSM. From Figure 44, it was noted that in CPZ-treated cells, the addition of rGGT led to its accumulation along the cell periphery and rGGT was also not observed in the nuclei of these cells. This was in contrast to uninhibited or NYS-treated cells where rGGT was found to be mainly intracellular.

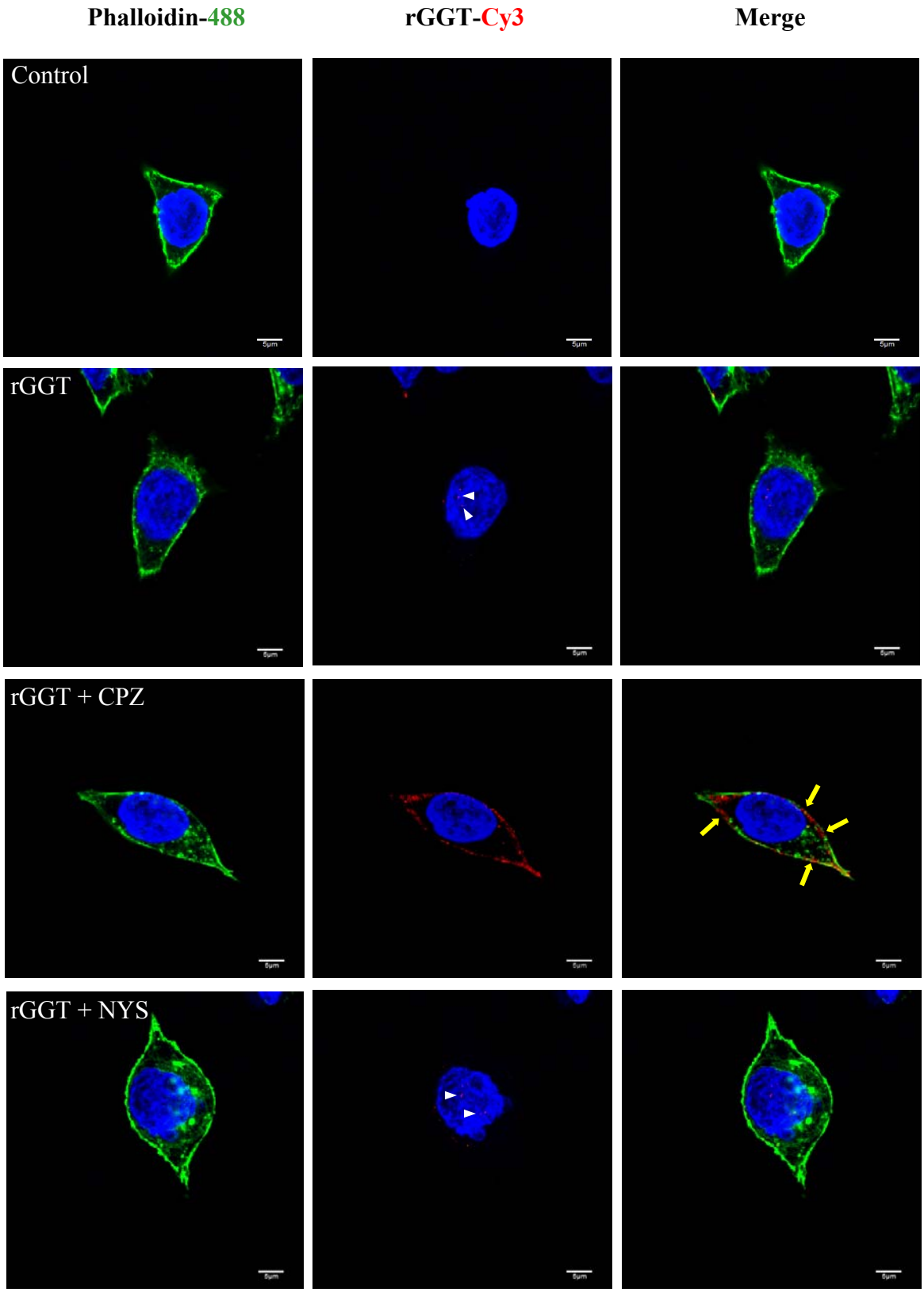

Figure 44. CLSM micrographs showing inhibition of rGGT internalization in the presence of CPZ. AGS cells were pre-treated with CPZ (15 µg/ml) or NYS (25 µg/ml) for 30 minutes and 60 minutes respectively before the addition of rGGT for 4 hours. Control cells were not incubated with rGGT nor treated with any of the inhibitors. Green, actin cytoskeleton stained with phalloidin-488; Red, rGGT labeled

with MAb 1G1 and Cy3; Blue, nucleus stained with Hoechst 33342. rGGT present in the nuclei of NYS-treated and uninhibited (incubated with rGGT only) cells are indicated by white arrowheads. A merged image shows accumulation of rGGT on the periphery of CPZ-treated cells as indicated by yellow arrows. Scale bar represents 5 μm.

4.10.5 Nuclear import of GGT is dependent on importin β1

4.10.5.1 GGT forms a complex with host protein importin β1

Co-IP of various importin β proteins and *H. pylori* GGT was carried out to determine if *H. pylori* GGT could be a possible cargo of these importins. Immunoblot analysis revealed that only importin β1 co-immunoprecipitated with GGT while importins β2 and β3 did not (Figure 45A, C and E). As a confirmation, reverse co-IP analysis showed that GGT only co-immunoprecipitated with importin β1 but not importins β2 and β3 (Figure 45B, D and F), suggesting that nuclear import of GGT may be dependent on importin β1.

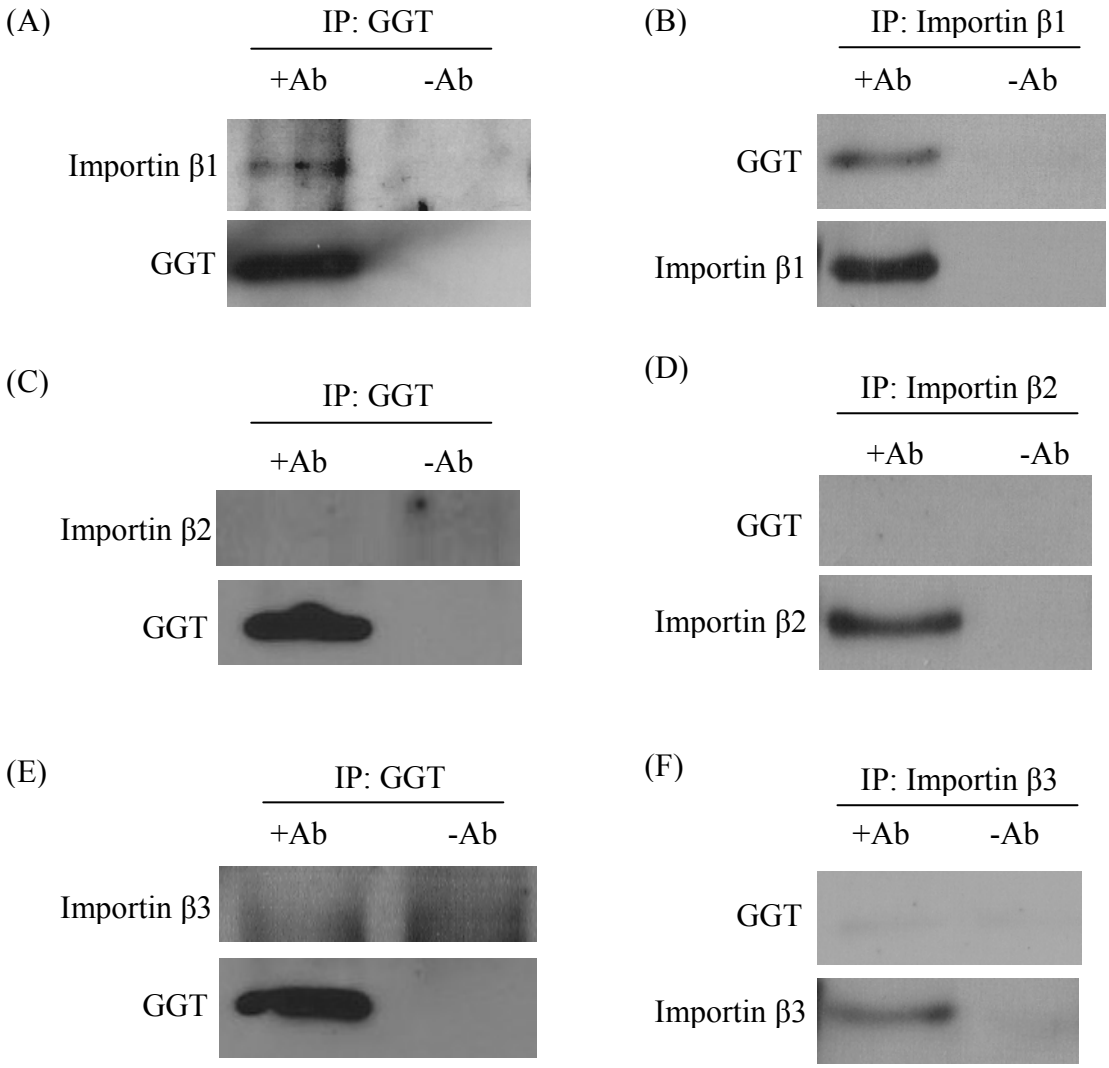

Figure 45. *H. pylori* GGT co-immunoprecipitates with importin β1. AGS cell lysate was co-incubated with *H. pylori* 88-3887 lysate and subject to co-IP using MAb 1G1 against GGT followed by immunoblotting with antibodies against (A) importin β1, (C) importin β2 and (E) importin β3. Reverse co-IP was carried out using polyclonal antibody against (B) importin β1, (D) importin β2 or (F) importin β3 followed by immunoblotting with polyclonal antibody raised against rGGTS. In all experiments, lysates incubated with Protein G or protein A beads without antibody served as negative control.

4.10.5.2 siRNA knockdown of importin β1

Since *H. pylori* GGT co-immunoprecipitates with importin β1, it was hypothesized that nuclear import of GGT depended on importin β1. To study its role in nuclear import, knockdown of importin β1 expression was performed using siRNA against importin β1. Optimal siRNA amount was determined to be 80 pmol where importin β1 expression was decreased by >80% as observed in Figure 46. Hence, this amount of siRNA was used in the subsequent experiments.

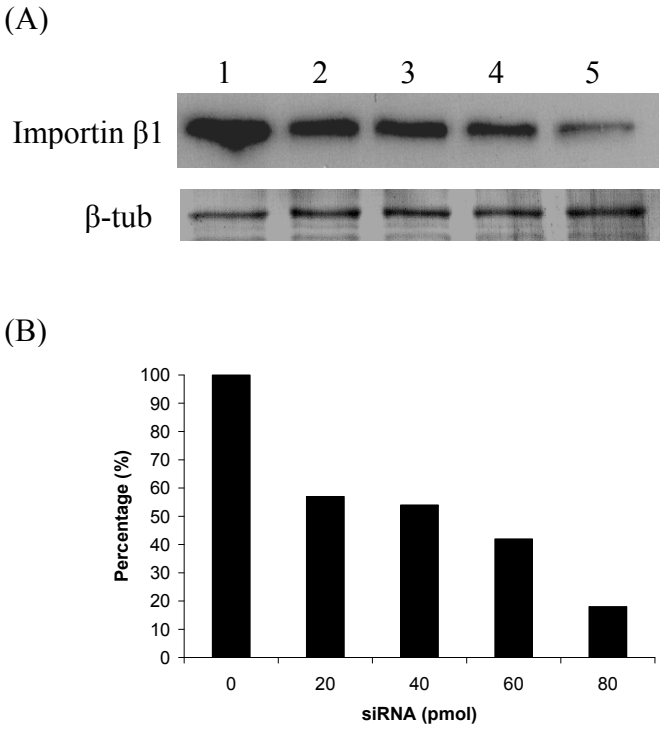

Figure 46. Dose-dependent knockdown of importin β1 using siRNA. AGS cells were transfected with various amounts of importin β1 siRNA (20-80 pmol). (A) Proteins from the total cell lysate 72 hours post-transfection were analyzed by western blotting. Lane 1, 0 pmol; Lane 2; 20 pmol; Lane 3, 40 pmol; Lane 4, 60 pmol; Lane 5, 80 pmol siRNA. β-tub, antibody against β-tubulin. (B) Densitometric quantification of the corresponding bands was performed using ImageJ version 1.44i analysis software. Values are expressed as the percentage of importin β1 expression compared to control cells (lane 1).

Effect of importin β1 knockdown on nuclear import of GGT was investigated. It was observed under CLSM that knockdown of importin β1 expression resulted in rGGT being mainly found in the cytoplasm of AGS cells 4 hours post-incubation as opposed to untreated cells (incubated with rGGT only) where rGGT was observed to be mainly in the cell nuclei (Figure 47A). Likewise, it was also noted that the amount of rGGT in the cytosolic fractions of AGS cells was significantly increased in siRNA-treated cells compared to untreated cells (relative density 1.65 *v* 1; $P<0.05$) although the total amount of rGGT in the whole cell lysates was similar in both cases as shown in western blot analysis (Figure 47B). In contrast, amount of rGGT in the nuclear fraction was significantly less in siRNA-treated cells compared to the control (relative density 0.55 *v* 1; $P<0.05$). Taken together, these results indicate that nuclear import of *H. pylori* GGT is dependent on importin β1.

(A)

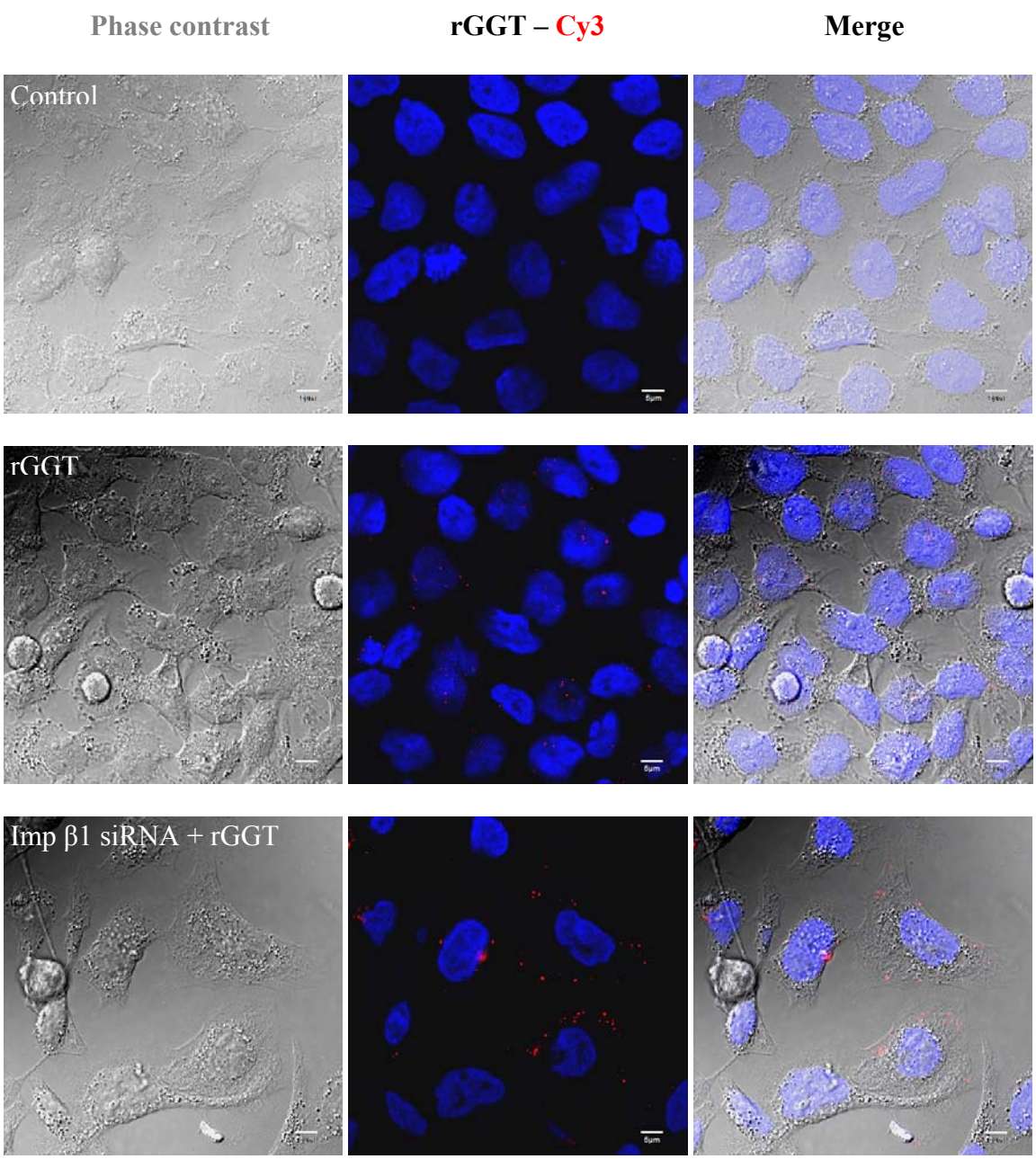
Phase contrast
rGGT – Cy3
Merge
Control
rGGT
Imp β1 siRNA + rGGT

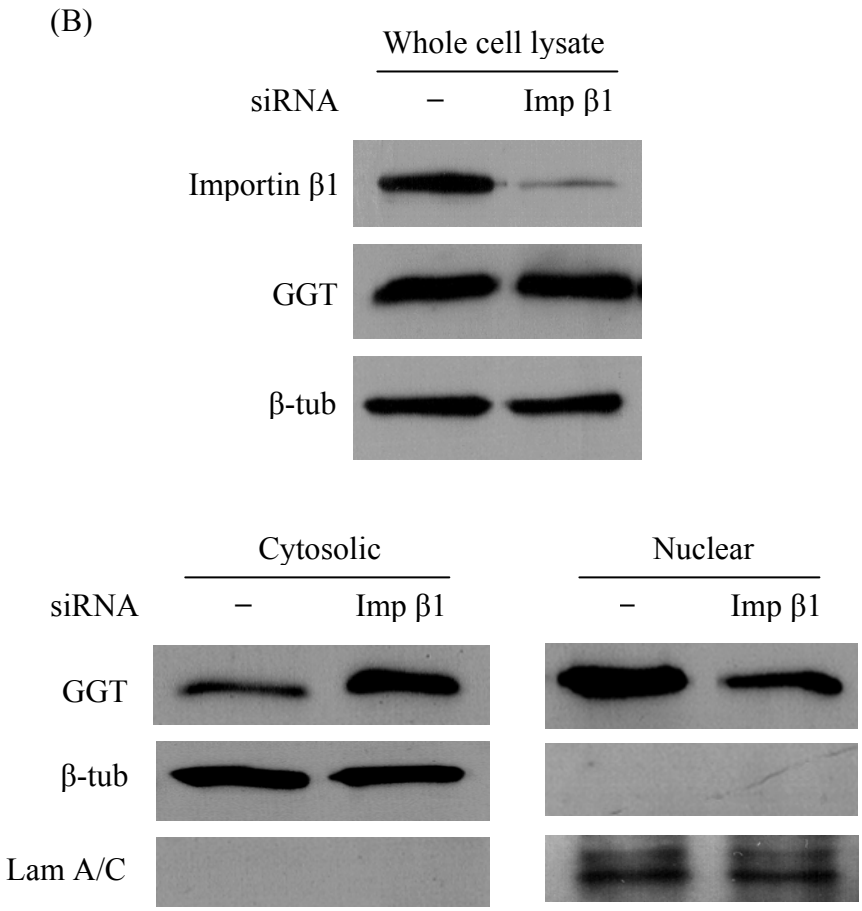

Figure 47. Nuclear import of GGT is dependent on importin β1. (A) AGS cells were transfected with importin β1 (Imp β1) siRNA before the addition of rGGT for 4 hours. Red, rGGT labeled with MAb 1G1 and Cy3; Blue, nucleus stained with Hoechst 33342. Control cells were not incubated with rGGT nor treated with Imp β1 siRNA. A merged image shows accumulation of rGGT in the cytoplasm of Imp β1 siRNA-treated cells. Scale bar represents 5 μm. (B) AGS cells were transfected with Imp β1 siRNA or transfection reagent only (−). Proteins from the total whole cell, cytosolic and nuclear lysates were then analyzed by western blotting with antibodies as indicated. Importin β1, antibody against importin β1; GGT, antibody raised against rGGTS; β-tub, antibody against β-tubulin, Lam A/C, antibody against lamin A/C. Immunblots are representative of 3 independent experiments.

4.10.6 Role of GGT in affecting nuclear GSH levels in AGS cells

Since GSH is one of the main substrates of GGT and levels of GSH in the cell nuclei are high (~15mM) (Bellomo *et al.*, 1997), it was speculated that GGT may deplete nuclear GSH after it was imported into the nucleus. Thus, the role of GGT in the cell nucleus was next investigated. Using the fluorochrome CMFDA to detect GSH, it was observed that GSH levels were drastically lower in AGS cells infected

with wild type *H. pylori* as compared to cells infected with Δ*ggt* (Figure 48A). Interestingly, rGGT alone also induced a depletion of intracellular GSH level, indicating that GGT is involved. Using Hoechst 33342 staining to delineate the nuclear area, GSH content (CMFDA green fluorescence) within the nuclear perimeter was then measured and plotted in arbitrary units. As observed in Figure 48B, cells infected with *H. pylori* wild type displayed a significant depletion of nuclear GSH compared to cells infected with Δ*ggt* ($P<0.01$). Control cells, on the other hand, exhibited high levels of nuclear GSH. In addition, rGGT also significantly depleted nuclear GSH in a dose-dependent manner, strongly suggesting that one of the actions of GGT on the host is to reduce its GSH stores.

(A)

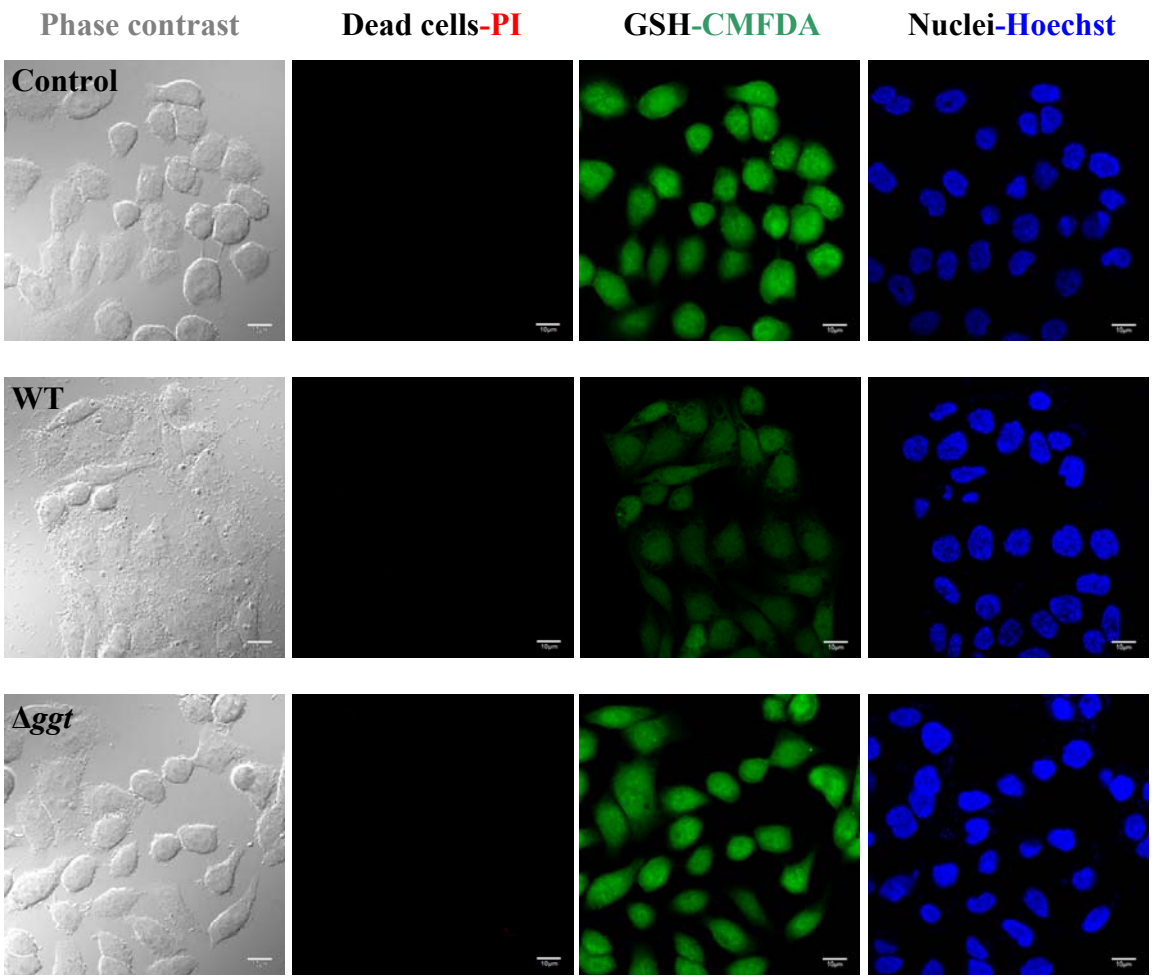

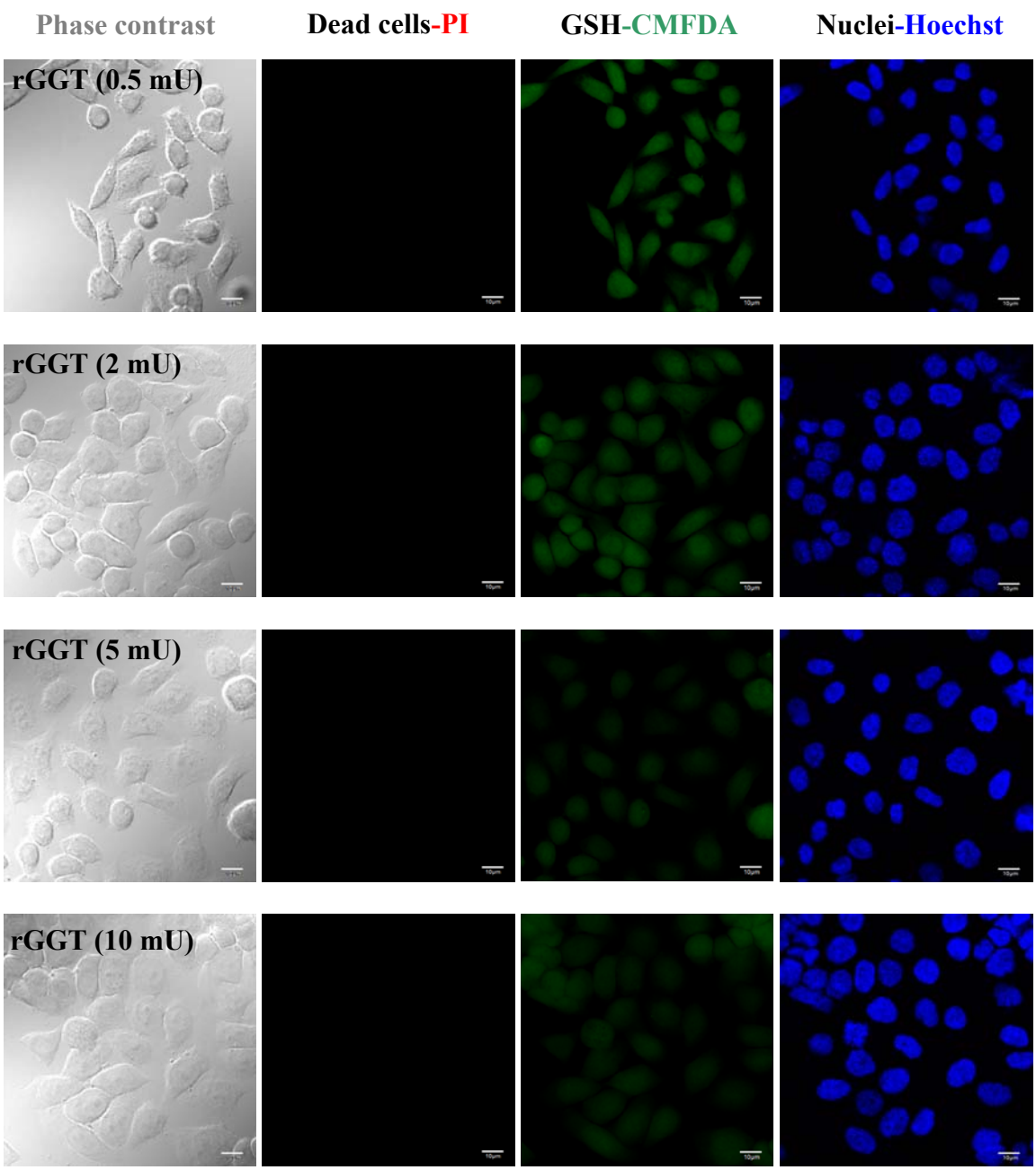
Phase contrast
Dead cells-PI
GSH-CMFDA
Nuclei-Hoechst
rGGT (0.5 mU)
rGGT (2 mU)
rGGT (5 mU)
rGGT (10 mU)

(B)

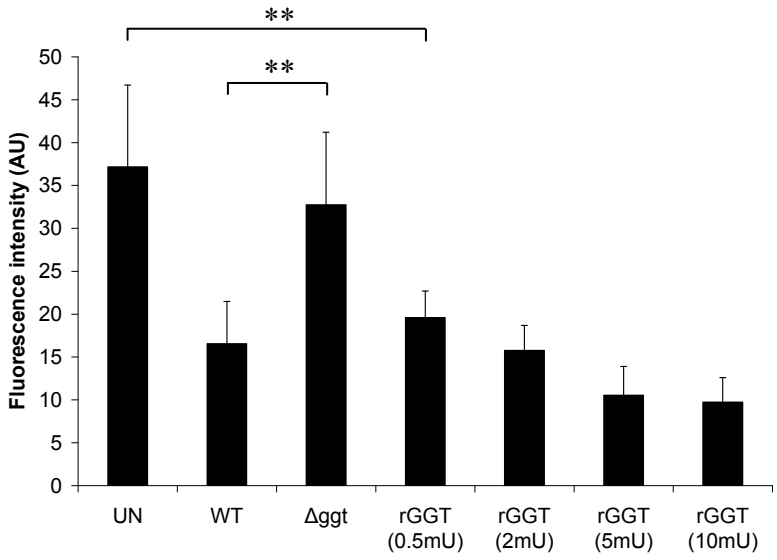

Figure 48. *H. pylori* GGT depletes nuclear GSH. (A) Representative CLSM micrographs of AGS cells co-incubated with *H. pylori* wild type (WT), Δ*ggt* or rGGT (0.5-10 mU) for 24 hours. Red, PI which stains dead cells; Green, CMFDA which marks GSH; Blue, Hoechst 33342 which stains nucleus. Control cells were not infected with *H. pylori* nor treated with rGGT. Scale bar represents 10 μm. (B) Mean CMFDA fluorescence intensity in nuclear area (defined by Hoechst 33342 staining) of 100 cells from at least 5 different fields was quantified using ImageJ software version 1.44i. Values represent mean ± SD of 3 independent experiments. ***P*<0.01.

4.10.6.1 Inhibition of endocytosis of GGT

To confirm that depletion of nuclear GSH was due to intracellular GGT, CPZ-treated cells were co-incubated with rGGT and subject to CMFDA staining. Figure 49 shows that rGGT (2 mU) induced significantly less GSH depletion when its uptake was inhibited by CPZ compared to NYS-treated and uninhibited (incubated with rGGT only) cells ($P<0.05$). As a control, CPZ itself did not induce any depletion of nuclear GSH. The results suggest that depletion of nuclear GSH is dependent on intracellular GGT.

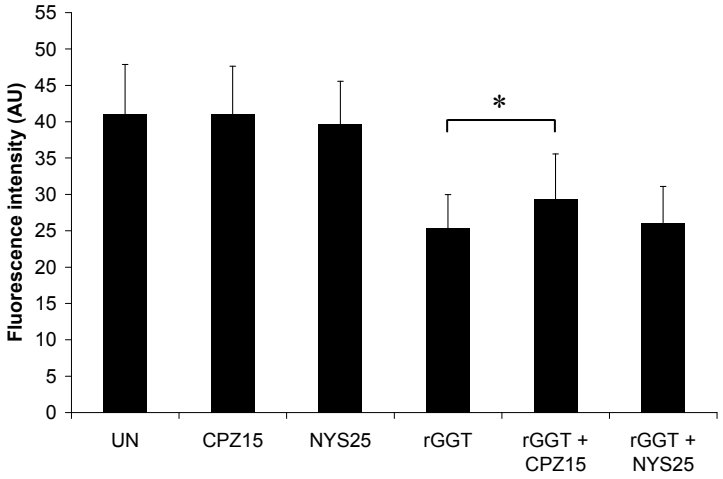

Figure 49. Intracellular rGGT depletes nuclear GSH. AGS cells were pre-treated with CPZ (15 μg/ml) or NYS (25 μg/ml) before the addition of rGGT (2 mU) for 4 hours. Control cells (UN) were not incubated with rGGT nor treated with any of the inhibitors. Mean CMFDA fluorescence intensity in nuclear area (defined by Hoechst 33342 staining) of 100 cells from at least 5 different fields was quantified using ImageJ software version 1.44i. *$P<0.05$.

4.10.6.2 Inhibition of nuclear import of GGT

To further prove that depletion of nuclear GSH was due to rGGT which had been imported into the nucleus, nuclear CMFDA fluorescence was measured in importin β1-knockdown cells treated with rGGT. Similarly, GSH depletion was significantly less in importin β1-knockdown cells co-incubated with rGGT as compared to normal cells treated with rGGT (P<0.05) (Figure 50). GSH levels in importin β1-knockdown cells remained similar to control cells. Taken together, the results indicate that nuclear-imported GGT affects GSH levels in the nucleus of cells.

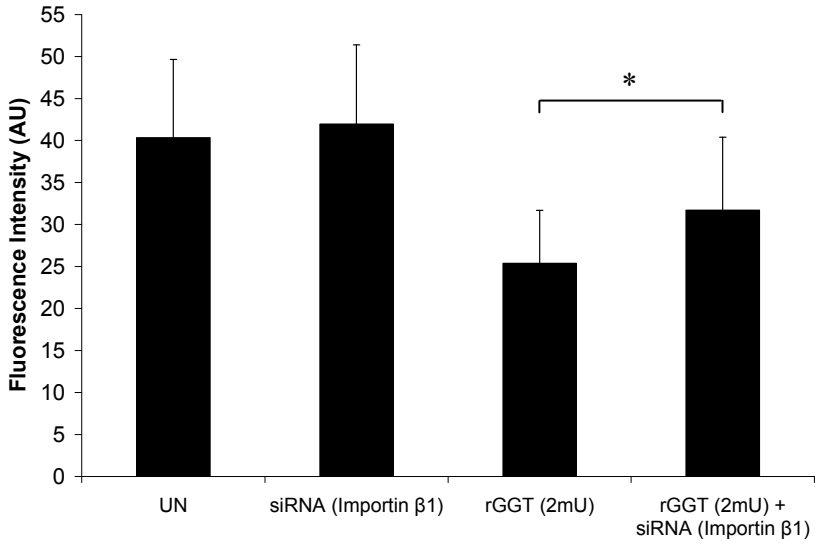

Figure 50. Nuclear-imported rGGT depletes nuclear GSH. AGS cells were transfected with importin β1 siRNA before addition of rGGT (2 mU) for 4 hours. Control cells (UN) were not incubated with rGGT nor treated with importin β1 siRNA. Mean CMFDA fluorescence intensity in nuclear area (defined by Hoechst 33342 staining) of 100 cells from at least 5 different fields was quantified using ImageJ software version 1.44i. *P<0.05.

4.11 Role of *H. pylori* GGT in potentiating vacuolation in host cells

4.11.1 Real-time phase contrast microscopy of vacuolation formation in *H. pylori*-infected AGS cells

Live cell imaging of infected AGS cells was carried out to compare if *H. pylori* wild type (Video 1) and Δ*ggt* (Video 2) induced different morphological changes in cells. Uninfected cells (Video 3) served as control (Videos 1-3 can be found in Appendix 35). As observed in Figure 51, micrographs of selected time points showing cell morphology of AGS cells were fairly similar when infected with either wild type or Δ*ggt* for the first 16 hours. The hummingbird phenotype, characterized by a beak-like extension of the cells (Moese *et al.*, 2004), was observed in both cases (Figure 51A-B) from 4 to 14 hours post-infection (red arrows). From 12 hours, both strains also induced the formation of small vacuoles at the perinuclear region of AGS cells (yellow arrows). The number of vacuoles that started to appear continued to increase until about 16 hours post-infection where differences then began to be more apparent. In particular, in wild type-infected AGS cells, vacuolation continued to increase up to 22 hours post-infection (Figure 51A). However, in the Δ*ggt*-infected cells, vacuolation was observed to have plateaued off and did not show any marked increase after 16 hours (Figure 51B). Neither the hummingbird phenotype nor vacuolation was observed in uninfected cells (Figure 51C).

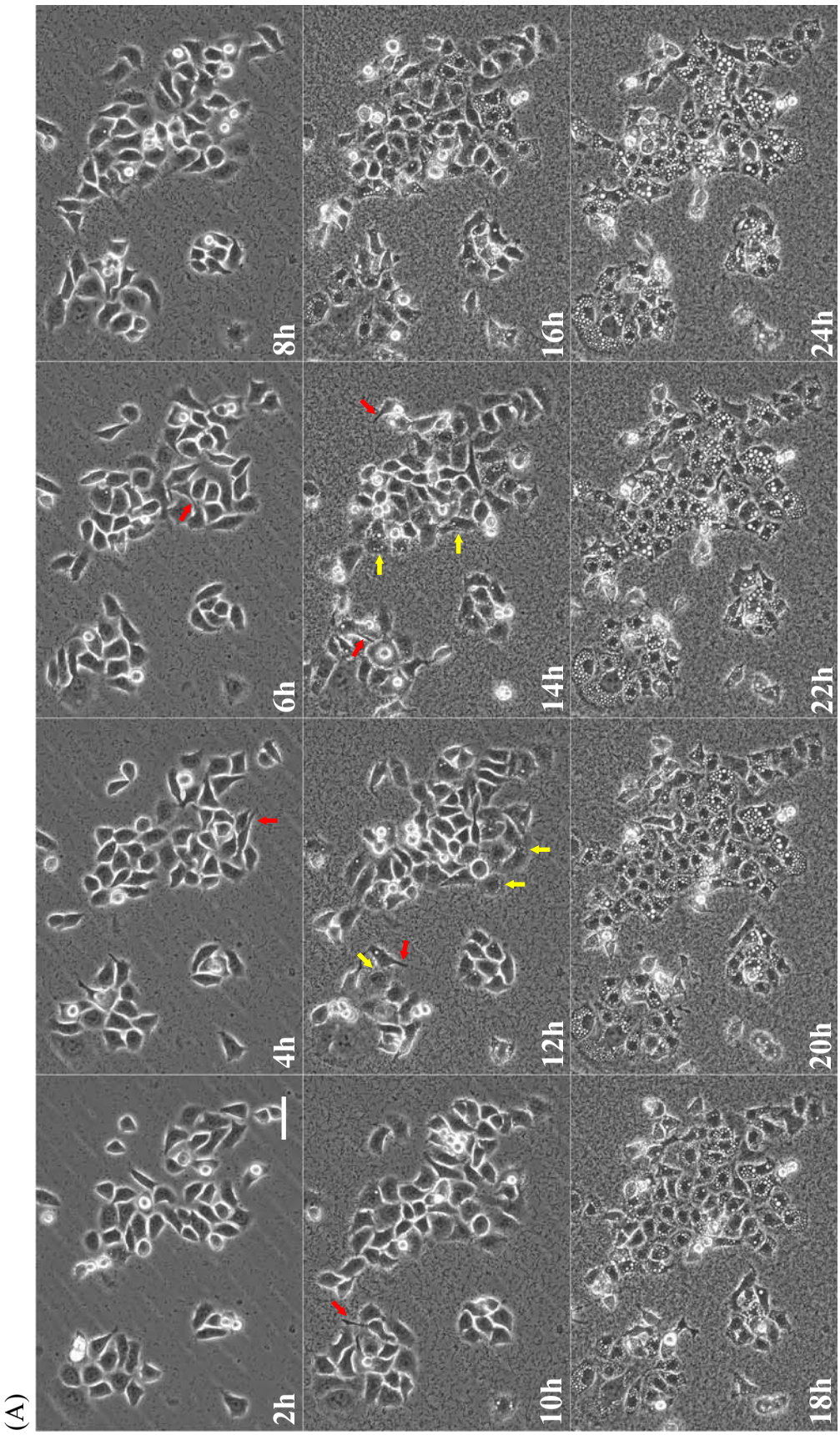
(A)
2h
4h
6h
8h
10h
12h
14h
16h
18h
20h
22h
24h

(B)

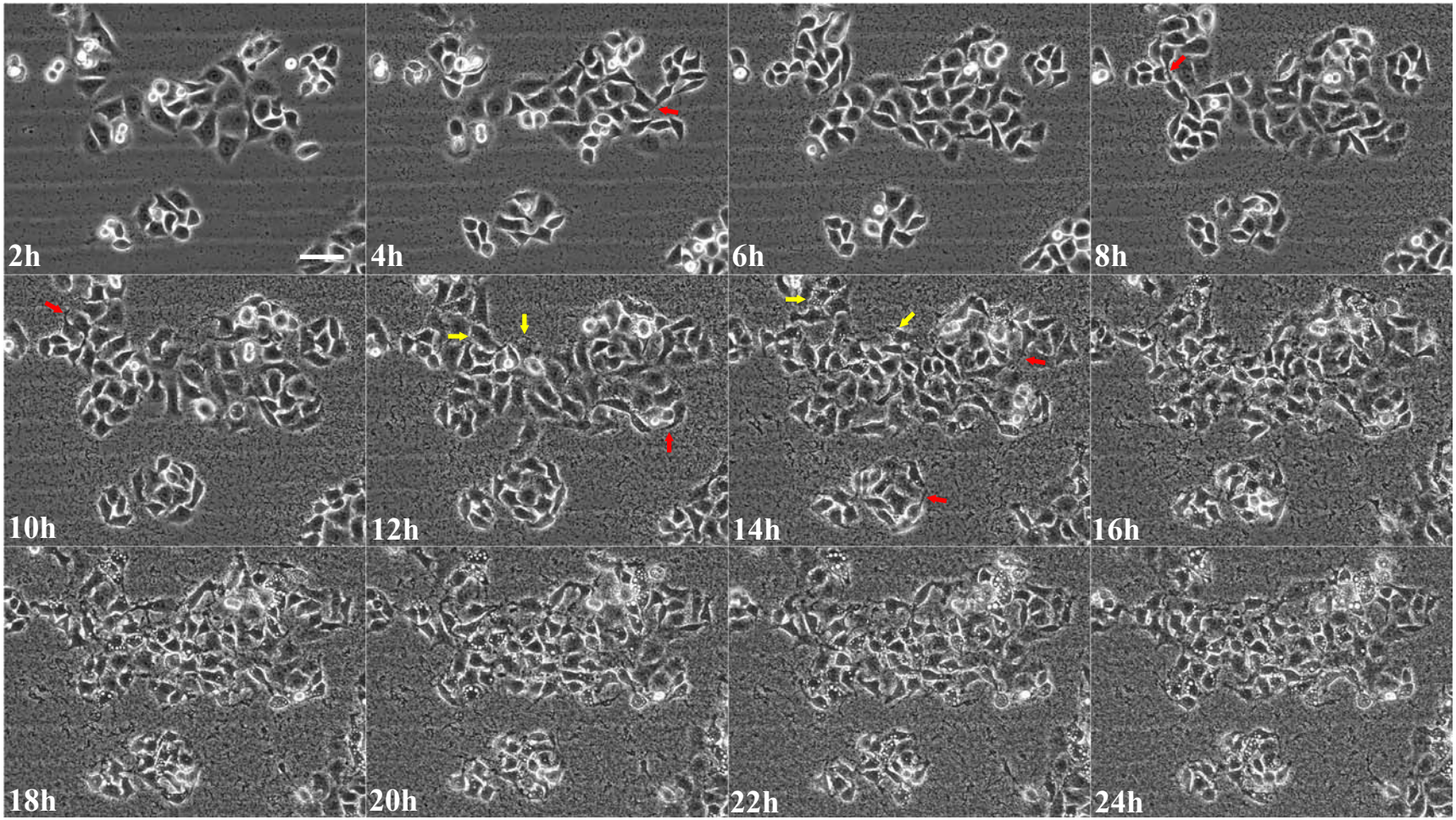

(C)

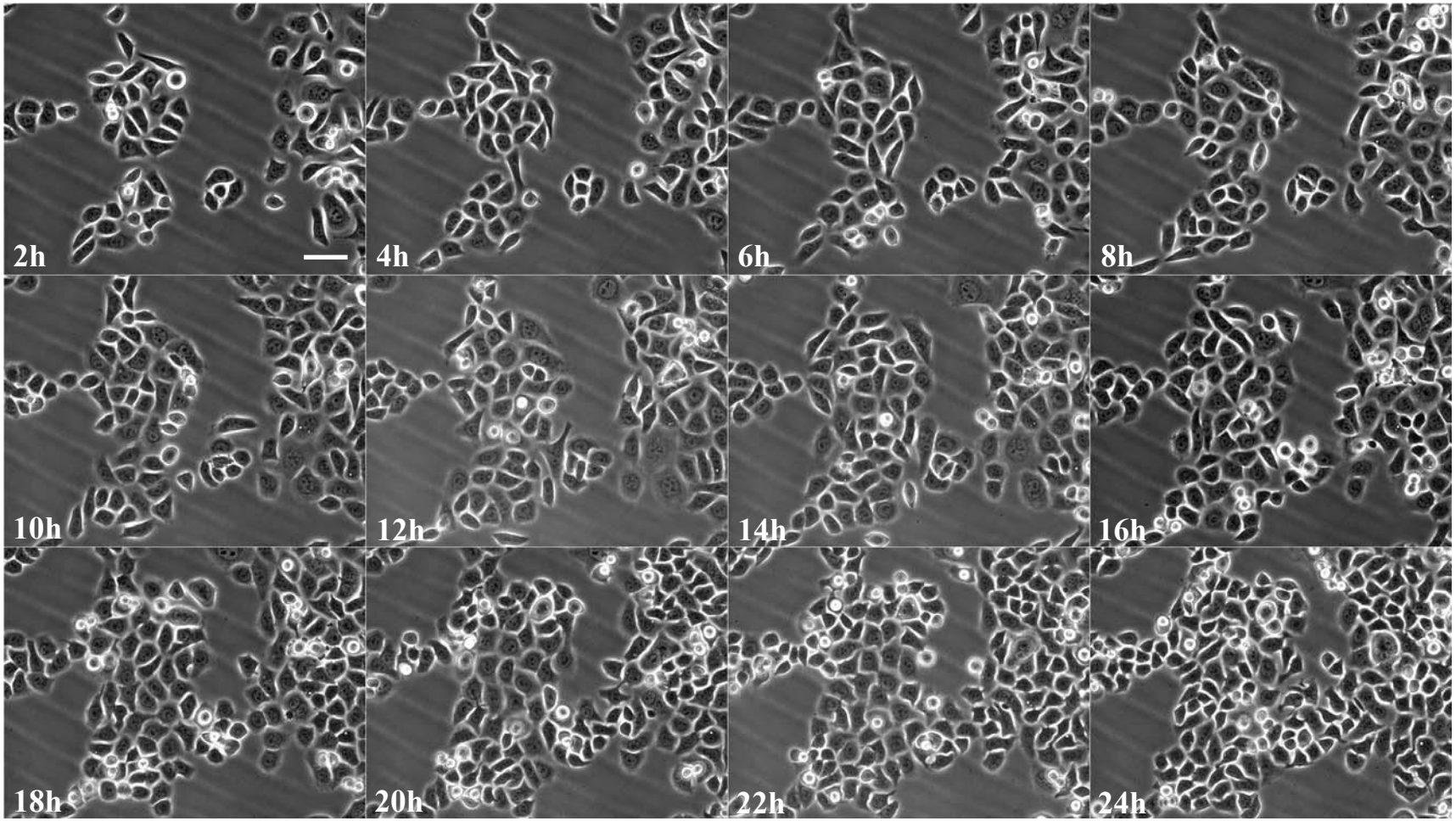

Figure 51. Live-cell imaging of *H. pylori*-infected AGS cells. AGS cells were infected with (A) *H. pylori* wild type or (B) Δ*ggt* over a 24 hour period. (C) Uninfected cells served as control. Time-lapse micrographs are shown at 2 hour intervals. Time from the start of infection is indicated in white. Hummingbird phenotype is indicated with a red arrow. Perinuclear vacuoles are indicated with a yellow arrow. Scale bar represents 50 μm. See Videos 1, 2 and 3 respectively for the full time course (Appendix 35).

4.11.2 Vacuolation induction in AGS cells treated with *H. pylori*

Neutral red dye was used to better visualize and semi-quantitate the vacuolation induced by *H. pylori*. As observed in Figure 52, no vacuoles were observed in uninfected AGS cells (Figure 52A-B). However, AGS cells co-cultured with *H. pylori* wild type took up more neutral red dye (Figure 52C-D) as compared with Δ*ggt*-infected cells 24 hours post-infection (Figure 52E-F).

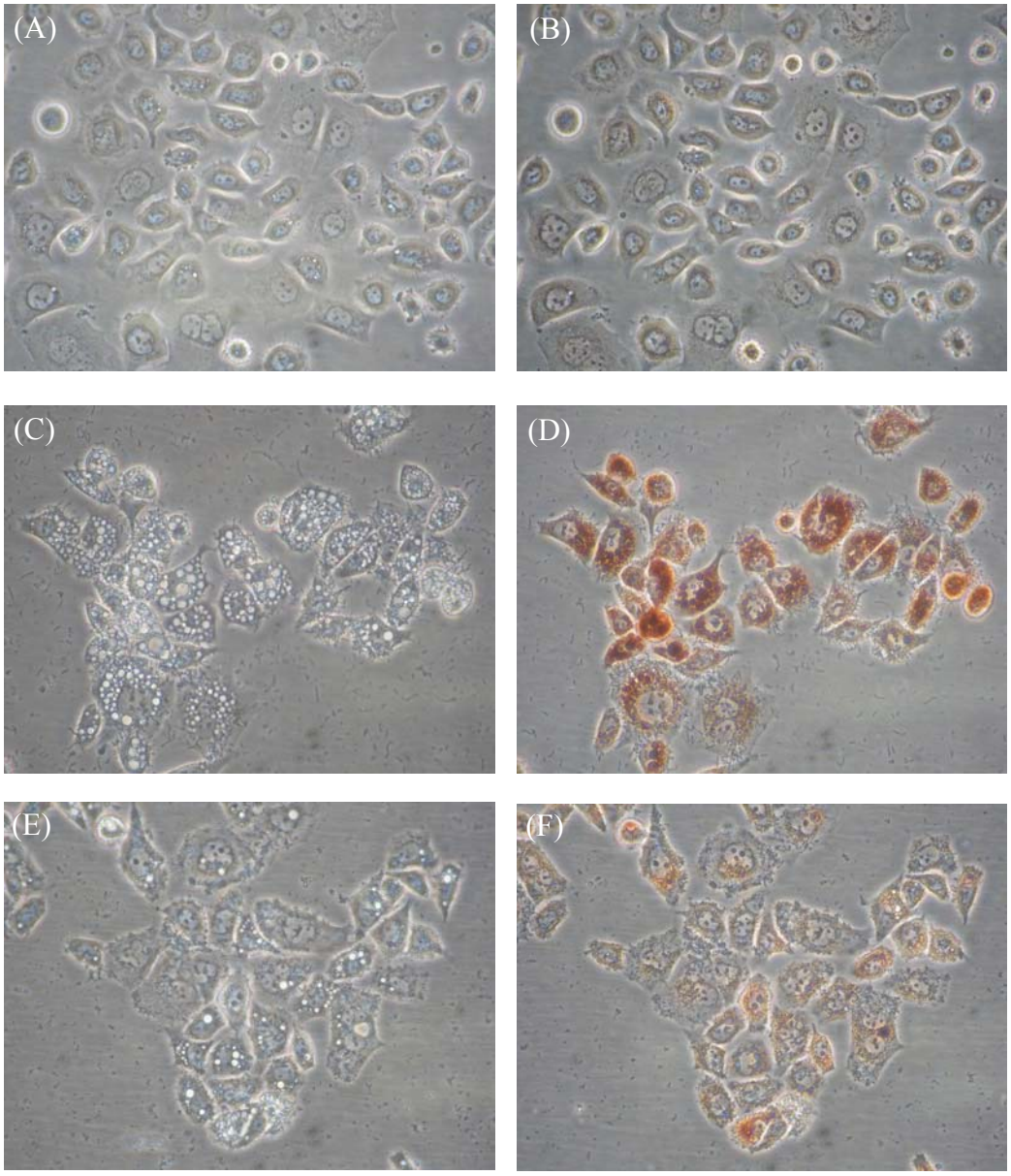

Figure 52. Cell morphology and neutral red uptake by AGS cells infected with *H. pylori*. (A) Uninfected AGS cells, (C) *H. pylori* wild type-treated AGS cells or (E) Δ*ggt*-treated AGS cells were observed using phase contrast microscopy. The cells were subjected to neutral red dye uptake assay (B, D and F respectively) and observed

under the microscope. Original magnification, ×400. Extent of vacuolation is indicated by the intensity of red colouration retained within the cells. Uninfected cells served as control.

This was further confirmed by a quantitative assay based on neutral red dye uptake assay where AGS cells co-cultured with Δ*ggt* accumulated significantly less neutral red dye than cells co-cultured with the wild type strain ($P<0.05$) starting from 12 hours post-infection (Figure 53). As the extent of vacuolation started to plateau between 20 to 24 hours post-infection, subsequent experiments were carried out using a 24 hour infection time period.

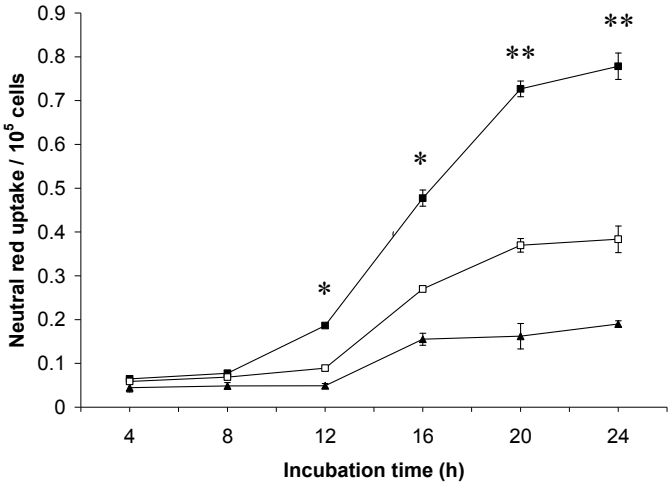

Figure 53. Time course of vacuolation in AGS cells co-cultured with *H. pylori.* AGS cells were co-cultured with *H. pylori* wild type (■) or Δ*ggt* (□) for various time-points up to 24 hours. (▲) indicates uninfected cells. The cells were then subjected to neutral red dye uptake assay. Values represent mean ± SD of 3 independent experiments. **P*<0.05, ***P*<0.01.

4.11.3 Cellular vacuolation in various cell types infected with *H. pylori*

Primary human gastric epithelial cells were infected with *H. pylori* wild type or Δ*ggt* for 24 hours. Using phase contrast microscopy, it was observed that primary gastric cells were also susceptible to vacuolation induced by *H. pylori*. Similar to that observed in AGS cells, uninfected cells displayed minimal vacuolation (Figure 54A-

B) while *H. pylori* wild type induced more vacuoles (Figure 54C-D) in the primary gastric epithelial cells as compared to that induced by Δ*ggt* (Figure 54E-F). Neutral red dye uptake assay was also carried out on the *H. pylori*-infected cells to quantitate vacuolation and the results showed a similar trend to that of AGS cells (Figure 55).

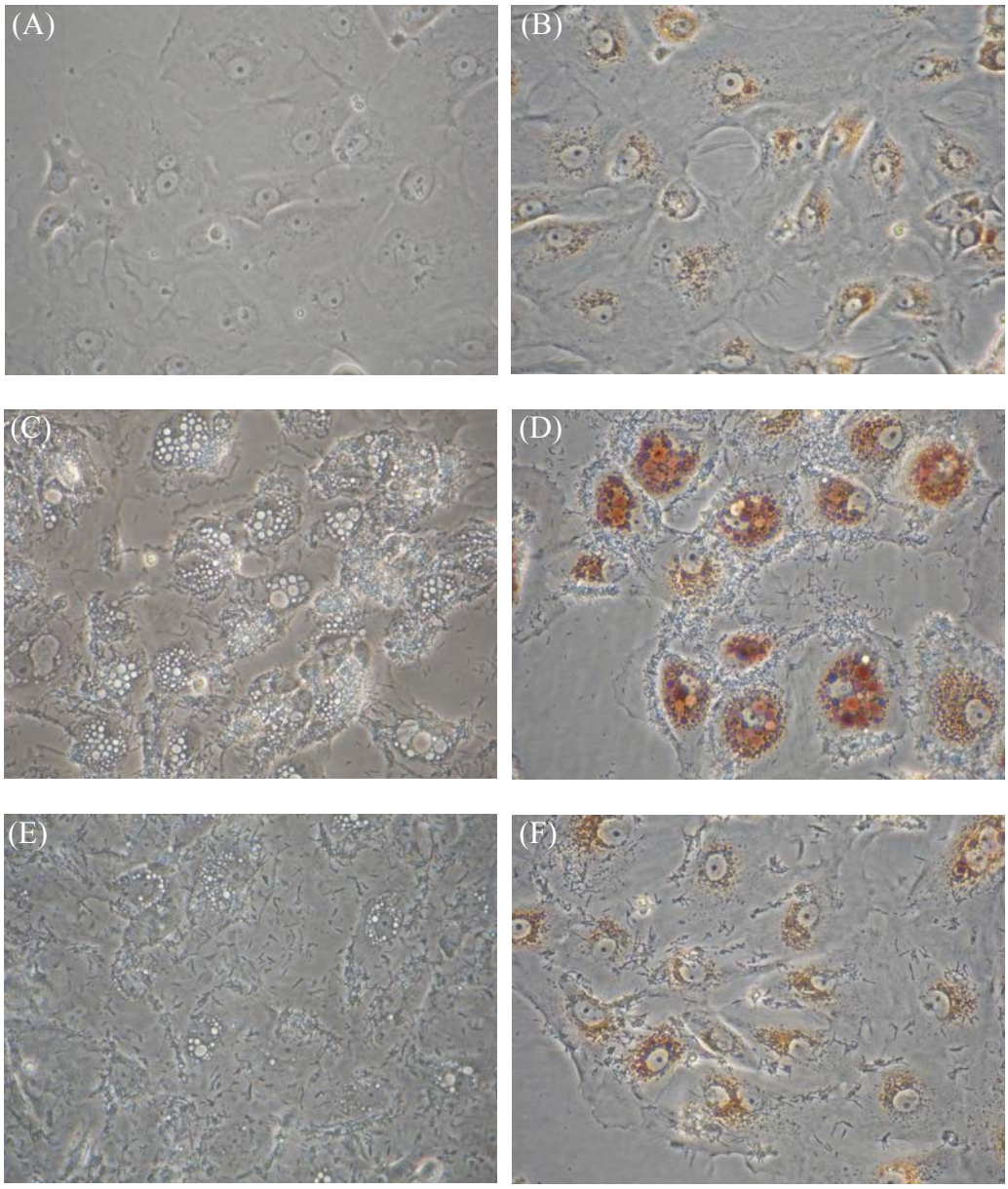

Figure 54. Cell morphology and neutral red uptake by primary gastric cells infected with *H. pylori*. (A) Uninfected cells, (C) *H. pylori* wild type-treated cells or (E) Δ*ggt*-treated cells were observed using phase contrast microscopy. The cells were subjected to neutral red dye uptake assay (B, D and F, respectively) and observed under the microscope. Original magnification, ×400.

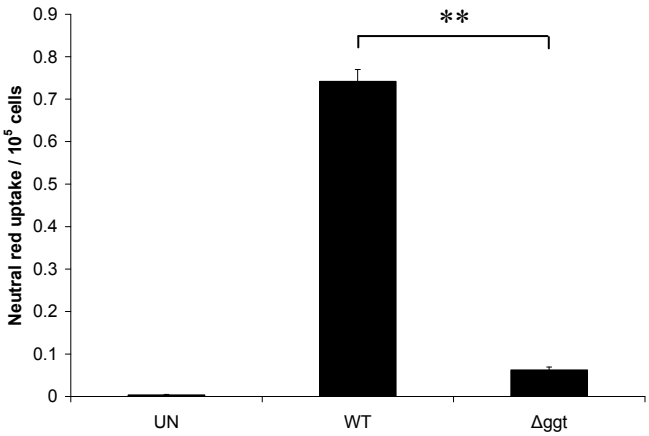

Figure 55. Neutral red dye uptake assay showing vacuolation in *H. pylori*-infected primary gastric cells. Primary human gastric epithelial cells were co-cultured with *H. pylori* wild type (WT) or Δ*ggt* for 24 hours. The cells were then subjected to neutral red dye uptake assay. Uninfected cells (UN) served as control. Values represent mean ± SD of 3 independent experiments. ***P*<0.01.

The role of GGT in vacuole formation was also investigated in HeLa cells, a human cervical adenocarcinoma cell line. Similar to AGS and primary gastric cells, Δ*ggt* induced significantly less neutral red dye uptake in HeLa cells compared to *H. pylori* wild type 24 hours post-infection (*P*<0.01) as shown in Figure 56.

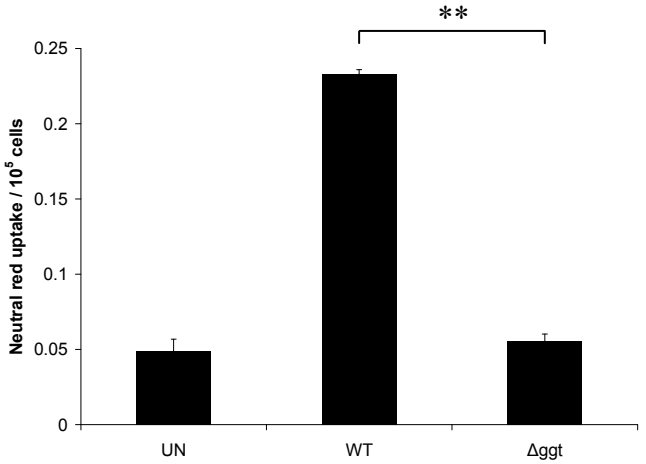

Figure 56. Vacuolation in HeLa cells infected with *H. pylori*. HeLa cells were co-cultured with *H. pylori* wild type (WT) or Δ*ggt* for 24 hours. The cells were then subjected to neutral red dye uptake assay. Uninfected cells (UN) served as control. Values represent mean ± SD of 3 independent experiments. ***P*<0.01.

4.11.4 Involvement of GGT, VacA and urease in cellular vacuolation

VacA has been reported as the inducer of vacuolation in host cells (Cover *et al.*, 1993). This study examines its involvement by co-culturing AGS cells with Δ*vacA*. The results show that Δ*vacA* induced minimal vacuolation in AGS cells even after 24 hours post-infection (Figure 57), indicating that the vacuolation observed was dependent on the presence of VacA. It was also observed that Δ*ureAB* induced significantly less vacuolation compared to the wild type strain ($P<0.05$), implying that urease does play a role in inducing vacuolation as previously reported (Cover *et al.*, 1991). Interestingly, Δ*ggt* induced significantly less vacuolation compared to Δ*ureAB* ($P<0.05$). In addition, vacuolation induced by Δ*ureAB/ggt* was abolished to a similar level as that induced by Δ*vacA*.

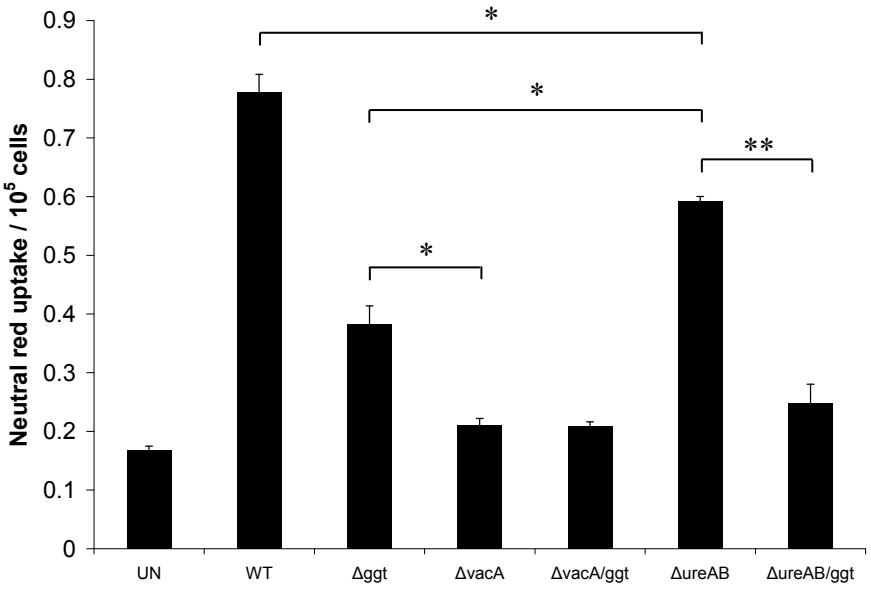

Figure 57. Effects of GGT, VacA and urease in induction of vacuolation in AGS cells. AGS cells were co-cultured with *H. pylori* wild type (WT), Δ*ggt*, Δ*vacA*, Δ*vacA/ggt*, Δ*ureAB* or Δ*ureAB/ggt* at MOI 100 for 24 hours. The cells were then subjected to neutral red dye uptake assay. Uninfected cells (UN) served as control. Values represent mean ± SD of 3 independent experiments. *$P<0.05$, **$P<0.01$.

Apart from potentiating the vacuolating activity of VacA, it was also investigated if GGT could induce vacuolation independently. AGS cells were co-incubated with rGGT alone and neutral red dye uptake assay was used to assess vacuolation. As observed in Figure 58, there was no significant difference (P>0.05) in neutral red dye uptake between rGGT-treated and untreated cells after 24 hours, implying that rGGT does not induce vacuolation on its own. Interestingly, when Δ*ggt* was supplemented with rGGT in AGS culture for 24 hours, vacuolation was almost restored to a similar level as that of *H. pylori* wild type (P<0.01), an effect not seen when Δ*vacA* or Δ*vacA/ggt* was co-incubated with rGGT. Co-incubation of *H. pylori* wild type and rGGT also significantly increased the extent of vacuolation compared to that induced by wild type alone (P<0.05).

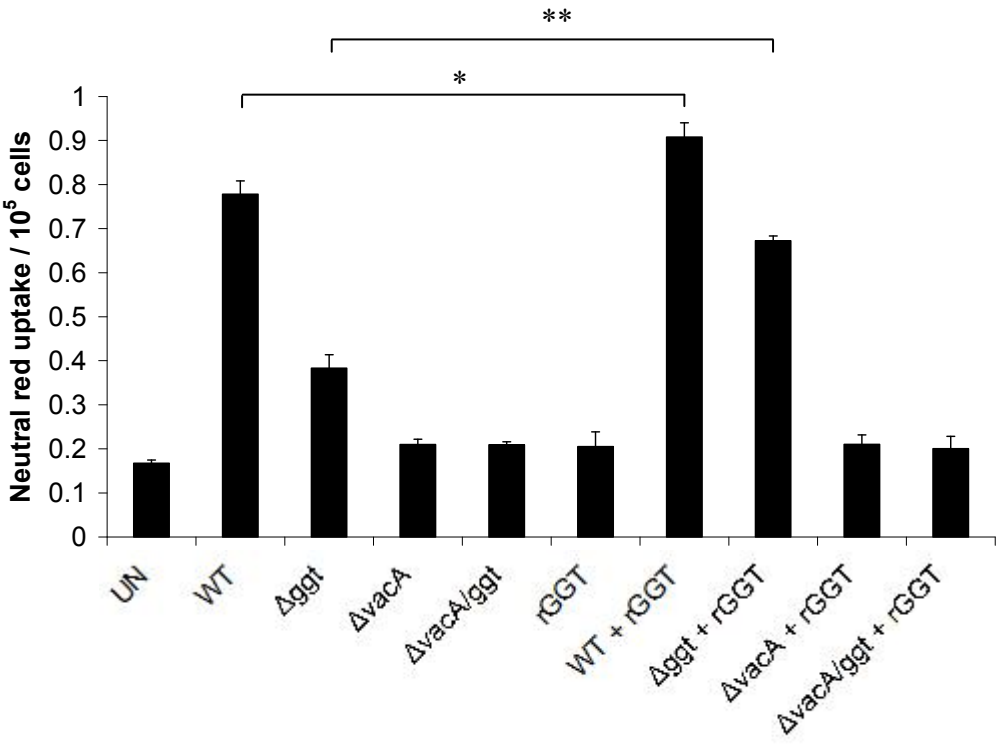

Figure 58. Effects of rGGT on vacuolation in AGS cells. AGS cells were co-cultured with *H. pylori* wild type (WT), Δ*ggt*, Δ*vacA*, Δ*vacA/ggt* and/or rGGT for 24 hours. Control cells (UN) were not infected with *H. pylori* nor treated with rGGT. Vacuolating activity was measured using neutral red dye uptake assay. Values represent mean ± SD of 3 independent experiments. *P<0.05, **P<0.01.

4.11.5 Role of ammonia produced by GGT

4.11.5.1 Vacuolation in glutamine-free media

Glutamine, being one of the substrates of GGT (Shibayama *et al.*, 2007), produces net ammonium ions upon hydrolysis by GGT. Since vacuolation by VacA requires the presence of weak bases such as ammonia (Cover *et al.*, 1992), investigation was performed to determine if the absence of glutamine in the medium would affect the extent of vacuolation in *H. pylori*-infected AGS cells. Indeed, it was observed that there was a significant decrease ($P<0.01$) in neutral red dye uptake in wild type-infected cells in the absence of glutamine (Figure 59). In comparison, neutral red dye uptake by AGS cells co-cultured with Δ*ggt* and Δ*vacA* were not affected in glutamine-free medium.

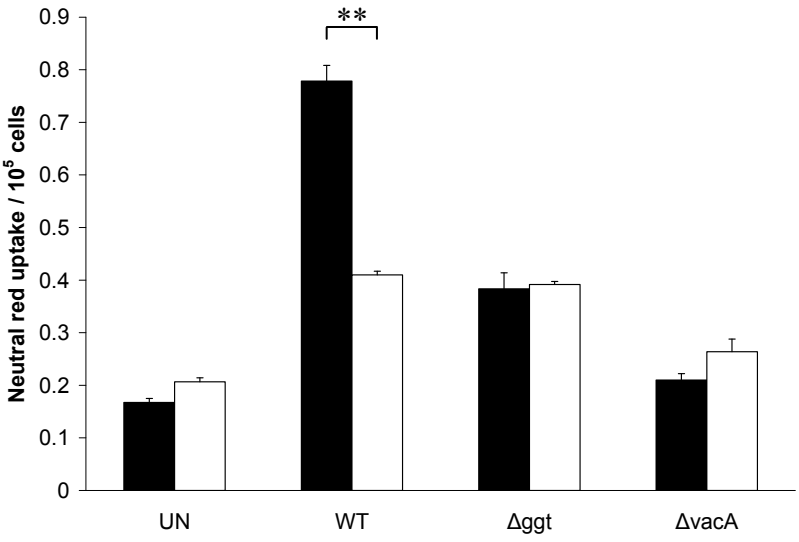

Figure 59. Hydrolysis of glutamine by GGT produces ammonia required for vacuolation. AGS cells were co-cultured with *H. pylori* wild type (WT), Δ*ggt* or Δ*vacA* for 24 hours in the presence (■) or absence (□) of 2 mM glutamine. Vacuolating activity was measured using neutral red dye uptake assay. Uninfected cells (UN) served as control. Values represent mean ± SD of 3 independent experiments. $^{**}P<0.01$.

4.11.5.2 Rescue of vacuolation induction using exogenous ammonium chloride

It was next investigated if the addition of an external source of ammonia could restore the vacuolating effect of Δ*ggt* on AGS cells according to the earlier hypothesis that GGT hydrolyzes glutamine to produce ammonia needed for vacuolation induction. In these experiments, *H. pylori* wild type or Δ*ggt* was co-cultured with AGS cells in the presence of 3 mM ammonium chloride. Interestingly, neutral red dye uptake induced by Δ*ggt* was restored to the level of that induced by the parental strain (Figure 60). In contrast, neutral red uptake in control cells or AGS co-cultured with Δ*vacA* in the presence of ammonium chloride did not show significant difference in neutral red dye uptake (P>0.05), indicating that 3 mM ammonium chloride does not induce vacuolation on its own.

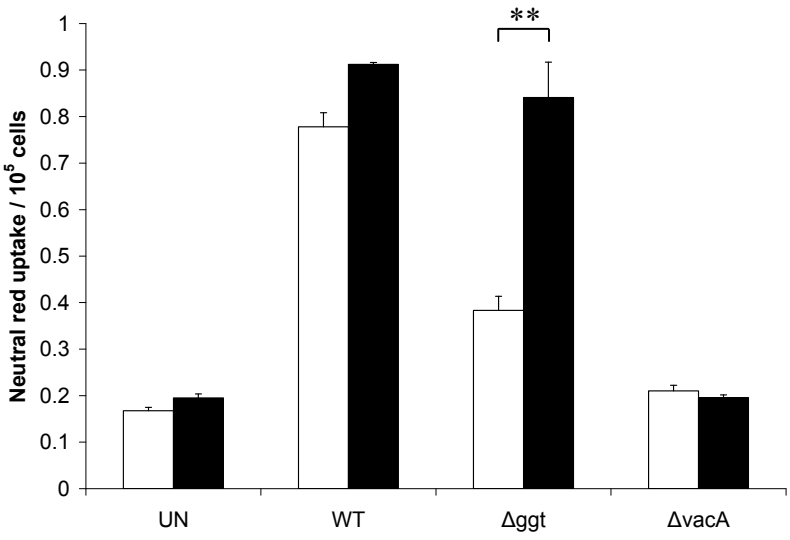

Figure 60. Exogenous ammonium chloride rescues ability of Δ*ggt* to induce vacuolation. AGS cells were co-cultured with *H. pylori* wild type (WT), Δ*ggt* or Δ*vacA* for 24 hours in the absence (□) or presence (■) of 3 mM ammonium chloride. Vacuolating activity was measured using neutral red dye uptake assay. Uninfected cells (UN) served as control. Values represent mean ± SD of 3 independent experiments. **P<0.01.

4.11.6 Inhibition of GGT activity and its effects on vacuolation

To further confirm that GGT activity potentiates vacuolation, its activity was inhibited by SBC, a competitive GGT inhibitor (Tate and Meister, 1978) as well as with MAbs possessing neutralizing activity as determined in section 4.4. Inhibition of GGT activity with SBC significantly decreased neutral red dye uptake induced by *H. pylori* wild type ($P<0.01$) but did not affect uninfected or Δ*ggt*-treated AGS cells (Figure 61). Similarly, neutralization of *H. pylori* GGT activity by using 4 MAbs (1G1, 3C10, 3F4 and 4F11) showed that three of them with neutralizing activity significantly decreased vacuolation ($P<0.05$) induced by *H. pylori* wild type by as high as 70.1% (Table 8). In addition, mouse IgG_{2a} and IgG_{2b} isotype negative controls failed to inhibit vacuolation.

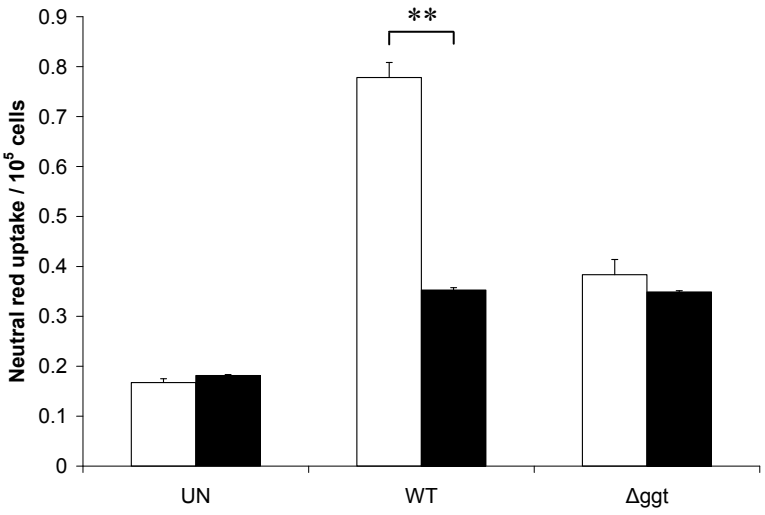

Figure 61. Inhibition of GGT activity affects vacuolation induced by *H. pylori*. AGS cells were co-cultured with *H. pylori* wild type or Δ*ggt* in the absence (□) or presence (■) of 10 mM SBC. Vacuolating activity was measured using neutral red dye uptake assay. Uninfected cells (UN) served as control. Values represent mean ± SD of 3 independent experiments. $^{**}P<0.01$.

Table 8. Inhibition of vacuolating activity of *H. pylori* by MAbs.

MAb	Neutral red dye uptake (% of WT)	Inhibition (%)
1G1	32.2 ± 1.5*	67.8
4F11	29.9 ± 1.9*	70.1
3F4	55.4 ± 1.6*	44.6
3C10	93.5 ± 1.7	6.5
IgG_{2a} isotype control	97.7 ± 2.0	2.3
IgG_{2b} isotype control	98.1 ± 2.1	1.9

AGS cells were pre-incubated with MAbs 24 hours prior to treatment with *H. pylori* wild type (WT) for a further 24 hours. Mouse IgG_{2a} and IgG_{2b} isotype controls were used in parallel at the same concentration. Neutral red dye uptake is represented as a percentage of that induced by WT ± SD from 3 independent experiments. **P*<0.05.

4.12 Antibody titre against rGGT in patients infected with *H. pylori*

Detection of anti-GGT antibodies in patient sera was carried out using rGGT as antigen. Figure 62 shows a box plot comparing anti-GGT titres from *H. pylori*-positive and *H. pylori*-negative subjects. Median antibody levels against GGT of *H. pylori*-positive subjects were found to be significantly higher than that of *H. pylori*-negative individuals (*P*<0.01).

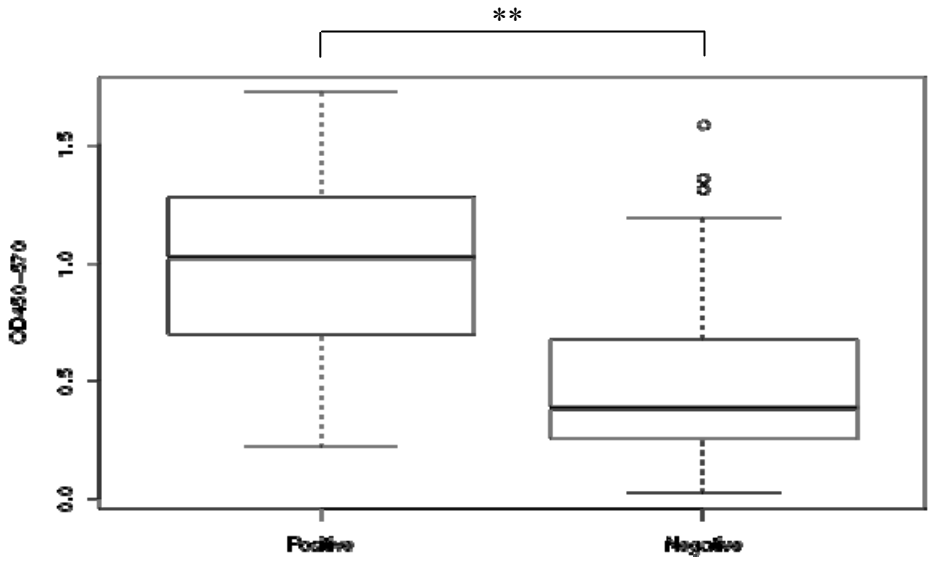

Figure 62. Seroprevalence to *H. pylori* GGT. Serum antibody titres to *H. pylori* in *H. pylori*-positive (n = 58) and –negative (n = 65) subjects. Serum antibodies to GGT were measured using ELISA with plates coated with rGGT. Boxes include 25^{th} – 75^{th} percentiles (interquartile range) and the median is shown as a bold line. Whiskers represent values within 1.5 × interquartile range of the lower and upper quartiles. Outliers are represented by empty circles. Data were analyzed statistically by Mann-Whitney U-test. ***P*<0.01.

DISCUSSION

5.1 Cloning, expression and purification of rGGT, rGGTL and rGGTS

E. coli has been extensively used as a host for the production of heterologous proteins. However, over-expression of these recombinant proteins may at times result in misfolding and aggregation of the protein in inclusion bodies (Baneyx and Mujacic, 2004). In this study, rGGT, rGGTL and rGGTS were successfully cloned and expressed in *E. coli*. rGGT was expressed in the precursor form as a ~62 kDa protein (inclusive of the N-terminal 6 × His-tag), indicating that it was not processed into the active form within the *E. coli* host and this was probably due to the absence of the signal peptide as reported previously (Chevalier *et al.*, 1999). rGGT was also present in both the soluble and insoluble fractions of *E. coli* sonicates in approximately equal proportions (Figure 13A). Since it was of interest to recover the biologically active form of the protein, rGGT was purified from the soluble instead of the insoluble fraction as insolubility generally indicates protein misfolding (Fahnert *et al.*, 2004). Interestingly, after purification, rGGT underwent autoprocessing to form the active enzyme consisting of the large and small subunits (40 and 20 kDa respectively) as observed under SDS-PAGE (Figure 14A). Purified rGGT was also enzymatically active with GGT activity of ~68 U/mg, indicating that it was efficiently purified in a functional form.

While rGGT was present in both the soluble and insoluble fractions, rGGTL and rGGTS were expressed exclusively in inclusion bodies (Figure 13B-C), an observation similar to a previous report (Boanca *et al.*, 2006). This indicates that both subunits of GGT must be present for proper folding of the proteins. As rGGTL and rGGTS were expressed in an insoluble form, they were purified under denaturing conditions in order to solubilize the proteins. Refolding of the recombinant proteins was then carried out against PBS buffer containing decreasing concentrations of urea.

Recovery of rGGTL and rGGTS after dialysis was relatively lower (~40%) compared to rGGT (~90%) as rGGTL and rGGTS tended to precipitate during the dialysis process. Hence, although rGGTL and rGGTS were expressed in greater amounts compared to rGGT in *E. coli*, final protein yields of rGGT, rGGTL and rGGTS were fairly similar and moderate (12 – 15 μg/ml).

5.2 MAbs against rGGT

5.2.1 Epitopes recognized by MAbs – possible mode of inhibition

A total of ten hybridoma clones were obtained after fusing splenocytes from mouse #2 with mouse myeloma cells. Of these, six recognized the large subunit and four recognized the small subunit of GGT as determined by western blot analysis. To map the antigenic epitopes, a series of synthetic overlapping peptides covering the entire sequence of GGT was screened. This method has been used previously to screen epitopes for MAbs against *H. pylori* urease (Hirota *et al.*, 2001) and allows for efficient identification of antigenic sequences. Among the MAbs targeting the large subunit of GGT, three different minimum epitopes were identified (residues 42-50: SSHPLASEI; 309-317: SKNIHIAAE and 357-365: QPDTVTPSS). Interestingly, for the MAbs targeting the small subunit of GGT, all four clones recognized the same minimum epitope (residues 428-434: GNPNLYG). Furthermore, MAbs against the small subunit of GGT were able to neutralize *H. pylori* 88-3887 GGT activity by as high as ~93% while those against the large subunit of GGT showed negligible inhibition, suggesting that the epitope found on the small subunit of GGT could be important for enzyme activity.

To investigate the underlying mode of inhibition by the MAbs, the catalytic site of GGT was examined. Biochemically, the active site of GGT has been

previously identified by Morrow *et al.* (2007). It comprises seven amino acids (Arg 103, Asn 400, Glu 419, Asp 422, Ser 451, Ser 452 and Gly 472) which form hydrogen bonds with the substrate to rigidly hold it in place, one critical amino acid (Tyr 433) which is part of a mobile active-site loop and Thr 380 which is positioned optimally for nucleophilic attack of the γ-glutamyl peptide bond. In addition, there are two amino acids (Gly 472 and Gly 473) that help stabilize the intermediate substrate during catalysis. As observed from the epitope mapping results, none of the MAbs against the large subunit of GGT recognized epitopes involving Arg 103, the only amino acid residue of the large subunit involved in enzyme catalysis. Hence, this may explain why the MAbs against the large subunit of GGT were unable to inhibit its enzymatic activity. Interestingly, the epitope that MAbs against the small subunit of GGT recognized spans a Tyr 433-containing loop which was identified in the same report to be important for GGT activity whereby conformational changes in the loop could possibly regulate substrate binding and subsequent catalytic activity. Hence, it is hypothesized that these neutralizing MAbs may affect access of substrate to the active site of GGT by inhibiting the necessary conformational changes required to allow substrate binding.

Another point of interest is that although all four MAb clones against the small subunit recognized the same epitope, neutralizing activity differed between them, ranging from ~30 to ~93% (Figure 22). One reason that could explain this phenomenon is that the various MAbs clones may have different binding affinities to the same epitope which in turn could affect their neutralizing activity. Interestingly, similar observations have been reported for anti-Fas IgG1 antibodies where it was found that different MAb clones recognizing the same epitope elicited different biological effects (induction *vs* inhibition of apoptosis) which correlated with their

relative binding affinities for Fas (Komada *et al.*, 1999). Affinity differences may arise due to amino acid sequence variations between the MAb clones which might affect the relative stability of the antibody-antigen complexes (Parhami-Seren and Margolies, 1996). Hence, to better visualize and map the actual amino acid residues involved in the binding between the MAbs and *H. pylori* GGT, more detailed analysis such as X-ray co-crystallography may be worth considering in future studies. In addition, surface plasmon resonance (Schuck, 1997) could also be carried out to determine the binding affinities between the respective MAbs and *H. pylori* GGT.

5.2.2 Inhibitory action of MAbs on GGT activity – comparison between *H. pylori* strains and with other organisms

The most potent neutralizing MAb 1G1 was generally effective in inhibiting the GGT activities of various *H. pylori* strains although some differences were observed in the extent of inhibition (46.0%-94.7%) between strains (Figures 23 and 24). To explain this phenomenon, it is postulated that GGT from different *H. pylori* strains may differ slightly in their 3-D conformation which might in turn affect antibody-antigen binding. Alternatively, varying levels of GGT expression between *H. pylori* strains may potentially contribute to the differences in inhibition observed. However, no such correlations were observed in this study which may be due to the small sample size tested. Hence, more *H. pylori* strains could be tested in future studies to test this hypothesis. Notably, it was also observed that the MAbs had low inhibitory activity against *H. pylori* SS1, a highly mouse-adapted strain (Lee *et a*l., 1997). As the MAbs were raised in mice, it is speculated that this strain may have adapted in a way such that it avoids detection by anti-GGT mouse antibodies generated by the host. Interestingly, it was also noted that the 7-residue neutralizing

epitope identified on *H. pylori* GGT is not conserved in GGTs of other bacterial and mammalian homologues (Figure 25), suggesting that the MAbs are specific for *H. pylori* GGT. This was further supported by the inability of these MAbs in neutralizing bovine GGT activity even at the highest MAb dose (30 μg) tested (data not shown).

5.2.3 Isotypes of MAbs generated against rGGT

It was observed that MAbs specific against the large subunit of GGT were all of IgG_1 isotype while those against the small subunit of GGT were majority of IgG_{2a} isotype. Production of IgG_1 isotype is indicative of a Th2 response in mice while that of IgG_{2a} signifies a Th1 response (Finkelman *et al*., 1988). This suggests that *H. pylori* GGT is capable of inducing a mixed Th1/Th2 adaptive immune response, a phenomenon also observed in individuals infected with *H. pylori* (Goll *et al*., 2007). Importantly, this mixed response has been implicated in the promotion of chronic infection by *H. pylori* and inhibition of pathogen clearance by the host (Goll *et al*., 2007).

5.3 Purification of nGGT using MAb

Purification of nGGT from *H. pylori* has been performed previously using a sequential combination of methods in the following order: cation exchange chromatography, hydrophobic interactive chromatography, size exclusion chromatography, followed by a second cation exchange chromatography (Shibayama *et al.*, 2003). This purification method, although shown to be successful, is extremely slow, tedious and inevitably results in substantial loss of protein after each purification step.

In this study, purification of nGGT from *H. pylori* was achieved using a one-step affinity chromatography method. In particular, MAb 1G1 was immobilized on CNBr-activated Sepharose 4B and used to purify nGGT from *H. pylori* crude lysates. Unlike the previous methods of using ion exchange and gel filtration chromatography which only isolates proteins with similar characteristics, affinity chromatography has the advantage of isolating a specific protein in a simple and rapid manner, allowing purification to be achieved in a much shorter time. Using this method, purification of nGGT was extremely efficient where it was purified to a high purity comparable to previous methods (>95%) with only two bands of 37 and 20 kDa corresponding to the large and small subunit of GGT respectively (Figure 26). Total GGT activity recovery was also notably high at 75%. In addition, although low pH treatment was used to elute nGGT in the final purification step, nGGT was still enzymatically active (with GGT activity of 70.9 U/mg) after neutralization. This indicates that the catalytic site of the enzyme was not destroyed by the low pH treatment. Taken together, this simple and rapid purification method has been shown to effectively purify nGGT without affecting its enzymatic function.

5.4 Subcellular localization of GGT in *H. pylori*

Although GGT is present in various bacterial species, its cellular localization differs among them. For example, GGT of *E. coli* has been found to localize exclusively in the periplasmic space as a soluble enzyme (Suzuki *et al.*, 1986) whereas GGT of *Proteus mirabilis* was found to be mainly in the cell wall (peptidoglycan layer) and periplasmic space (Nakayama *et al.*, 1984). On the other hand, GGT of *Neisseria meningitis* is mainly associated with the inner membrane facing the cytoplasmic side (Takahashi and Watanabe, 2004) while GGT of *B. subtilis*

was found to be mainly secreted into the extracellular medium (Xu and Strauch, 1996).

To localize GGT in *H. pylori*, immunogold-labeling TEM was performed. This method is a powerful tool used for the precise localization of proteins in cells and several *H. pylori* proteins have been localized using this technique, including urease (Hawtin *et al.*, 1990) and heat shock protein 20 (Du and Ho, 2003). In this study, post-embedding immunogold labeling was employed. This technique provides an advantage over pre-embedding labeling as the latter requires extensive detergent treatment necessary for the penetration of gold conjugates into cells which may lead to the loss of specimen ultrastructure.

From the immunogold-labeled transmission electron micrographs, gold particles of 10 nm in diameter were mainly observed in the periplasmic space and on the outer membrane of *H. pylori* (Figure 27A-B). As *H. pylori* GGT is synthesized as a pro-enzyme with a typical N-terminal signal peptide that targets the protein to the periplasmic space (Chevalier *et al.*, 1999), presence of GGT in the periplasm was not surprising. It has been postulated that after the pro-enzyme is secreted into the periplasmic space, the signal peptide is cleaved and the protein is then efficiently processed into a large and small subunit which then associate in a non-covalent manner to form the active enzyme (Shibayama *et al.*, 2003). Apart from the periplasm, many gold particles were also observed on the outer membrane of the bacterium. As *H. pylori* GGT has been previously reported to be secreted into the extracellular medium (Bumann *et al.*, 2002), it is hypothesized that those GGT observed on the outer membrane were in the process of being secreted out of the bacterium although the mechanism of secretion has not been clearly elucidated to date. It is also worth noting that relatively few gold particles were found in the

cytoplasm of *H. pylori*, suggesting that GGT is efficiently secreted into the periplasmic space after expression. In addition, there were no gold particles observed in the two negative controls (Figure 27C-D), indicating that the MAb generated against GGT is specific. It is therefore postulated that as a surface and secreted protein of *H. pylori*, GGT may have a functional important role in interacting with gastric host cells during an infection.

5.5 Pathogenic effects of GGT on host cells

5.5.1 *H. pylori* GGT and H_2O_2 production

H. pylori infection in humans has been reported to be associated with excessive ROS levels (Davies *et al.*, 1994; Ding *et al.*, 2007) and diminished GSH in the infected gastric mucosa (Shirin *et al.*, 2001). Unfortunately, how *H. pylori* exerts such effects has not been clearly defined. It had been observed earlier that *H. pylori* nGGT is capable of inducing H_2O_2 production (Gong, 2006), however the mechanism by which this occurs remains unclear. To expand on the earlier study, the role of GGT in inducing H_2O_2 production was further investigated using AGS cells (Figure 31A) and primary gastric cells (Figure 31B). Interestingly, in the presence of both cell types, *H. pylori* Δ*ggt* was found to induce significantly less H_2O_2 generation compared to the parental strain ($P<0.05$), thus complementing the earlier findings using nGGT.

Mammalian GGT-mediated catabolism of extracellular GSH has been documented to produce ROS by thiol-dependent iron reduction (Drozdz *et al.*, 1998). This occurs when GGT cleaves the γ-glutamyl moiety of GSH, generating cysteinyl-glycine which is a thiol with much higher reactivity compared to GSH (Dominici *et al.*, 1999). As the pKa of cysteinyl-glycine is lower than that of GSH (Stark, 1991),

majority of it exists in the thiolate form (gly-cys–S^-) at near-neutral pH. Thiolate anions are capable of starting redox reactions with ferric ions, leading to the production of ROS and thiyl radicals (Dominici *et al.*, 1999) through a series of reactions as illustrated below:

$$GSH \xrightarrow{GGT} \gamma\text{-glutamate} + \text{gly-cys-}S^- + H^+$$

$$\text{gly-cys-}S^- + Fe^{3+} \longrightarrow \text{gly-cys-}S^{\bullet} + Fe^{2+}$$

$$Fe^{2+} + O_2 \longrightarrow Fe^{3+} + O_2^{\bullet-}$$

$$O_2^{\bullet-} + H_2O \longrightarrow O_2 + H_2O_2$$

As *H. pylori* GGT and mammalian GGT possess comparable hydrolysis rates (Boanca *et al.*, 2006), it is postulated that *H. pylori* GGT can also induce H_2O_2 production through GSH hydrolysis. Furthermore, GSH efflux has been reported for almost all mammalian cells (Meister and Anderson, 1983), including gastric cells (Shibayama *et al.*, 2007). From Figure 32, AGS cells treated with nGGT showed a significant rise in H_2O_2 production compared with untreated cells ($P<0.05$) and exhibited an even higher level of H_2O_2 in the presence of GSH and glycyl-glycine ($P<0.01$). This effect was inhibited in the presence of SBC, an inhibitor of GGT. In addition, treatment with the iron chelator DFO which inhibits formation of H_2O_2 generated by cysteinylglycine in the presence of transition metals (Dominici *et al.*, 1999) significantly reduced nGGT–dependent H_2O_2 generation ($P<0.05$). In contrast, the addition of exogenous Fe^{3+} significantly increased nGGT–mediated H_2O_2 production ($P<0.05$), indicating that *H. pylori*–mediated H_2O_2 generation occurs, at least in part, through this postulated pathway. Moreover, iron chelation has been reported to protect gastric cells against oxidant stress induced by *H. pylori* infection (Yajima *et al.*, 1995), further supporting this hypothesis.

ROS induces injury to the gastric mucosa, potentially predisposing the tissue to ulceration (Davies *et al.*, 1992; Bandyopadhyay *et al.*, 2002) and has also been suggested to be the causative factor for gastric cancer (Balkwill and Mantovani, 2001). In addition, oxidative stress was found to be related to *H. pylori* density as well as the development of severe gastric diseases (Zhang *et al.*, 1997), suggesting that ROS is important in the pathogenesis of peptic ulcers. Interestingly, it has recently been reported that H_2O_2 not only affects the host but also induces the upregulation of several virulence genes in *H. pylori*, including CagA and VacA, thereby leading to even greater cell damage (Huang and Chiou, 2011). Taken together, the finding that GGT induces H_2O_2 generation through GSH hydrolysis suggests that GGT may participate in the development of peptic ulcers and could possibly be a contributing factor in the progression of gastric cancer in *H. pylori* infections.

5.5.1.1 *H. pylori* GGT induces NF-κB activation and IL-8 upregulation in various cells types

In unstimulated cells, the transcription factor NF-κB is sequestered by IκB proteins in the cytoplasm as an inactive complex (Jacobs and Harrison, 1998). In response to various stimuli (e.g. ROS, TLR activation, etc), IκB gets phosphorylated and degraded in the proteasome, leaving NF-κB free to enter into the nucleus where it induces the expression of several immunologically important target genes (Schmitz and Baeuerle, 1995). As H_2O_2 has been shown to activate NF-κB in gastric epithelial cells (Takada *et al.*, 2003), NF-κB activation and degradation of IκB protein were analyzed using western blot method in this study. In *H. pylori* wild type-infected AGS cells, nuclear level of NF-κB was significantly increased while marked degradation of

IκB was observed concurrently (Figure 33). Interestingly, activation of NF-κB in cells infected with Δ*ggt* was found to be markedly reduced, indicating that GGT is involved in *H. pylori*-induced NF-κB activation.

Activation of NF-κB has been reported to induce expression of the chemokine IL-8 (Keates *et al*., 1997), an important mediator of the inflammatory response (Shimada *et al.*, 1999). Furthermore, *H. pylori* infection has been associated with elevated levels of gastric IL-8 (Gionchetti *et al.*, 1994; Fan *et al.*, 1995). Importantly, *H. pylori* nGGT was earlier shown to induce generation of H_2O_2 which in turn activates NF-κB and induces IL-8 production in gastric cancer cells (Gong, 2006). Hence, the ability of *H. pylori* GGT in inducing IL-8 generation in various cells types was examined in this study. IL-8 production was found to be significantly reduced (P<0.05) in AGS cells infected with Δ*ggt* when compared with wild type-treated AGS cells (Figure 34A-B). Notably, it was also observed that IL-8 production in Δ*ggt*-infected cells was not fully ablated. It is speculated that this residual IL-8 may have been induced through TLR2 and Nod1 activation by neutrophil activating protein (Amedei *et al*., 2006) and peptidoglycan (Viala *et al*., 2004) respectively. Furthermore, other *H. pylori* virulence factors such as OipA (Yamaoka *et al*., 2002a) and urease (Beswick *et al*., 2006) have also been reported to induce IL-8 secretion in gastric epithelial cells. In addition, both nGGT and rGGT alone induced significant levels of IL-8 in these cells (P<0.05). Furthermore, GGT-mediated NF-κB activation and IL-8 induction were also confirmed using luciferase reporter gene assay and IL-8 mRNA analysis (by real-time PCR) respectively[1] and the results strongly correlate with the findings presented in this study.

Apart from AGS cells, nGGT and rGGT were also able to induce IL-8 generation in primary human gastric epithelial cells with a similar trend as that

[1] Data for luciferase assay and real-time PCR were obtained by our collaborator, Dr. Gong M., and the results were published in Gastroenterology (2010). *139*, 564-573.

observed in AGS cells (Figure 34C-D). The main difference observed was that the induced IL-8 levels were excessively (~50 times) higher in primary gastric cells as compared to AGS cells. Similar observations have been observed in previous studies where the level of IL-8 induced by *H. pylori* was found to be 10-50 times higher in primary gastric epithelial cells as compared to that induced in MKN28, a gastric carcinoma cell line (Ogura *et al.*, 1998).

GGT-mediated IL-8 production was also investigated in macrophages, another important source of IL-8 in the gastric mucosa (Yoshikawa and Naito, 2000). IL-8 levels were found to be significantly reduced ($P<0.05$) in macrophages co-cultured with Δ*ggt* compared with wild type-treated cells 4 hours post-infection (Figure 34E-F), indicating that GGT is able to induce IL-8 in this cell type. However the observed difference in IL-8 was no longer significant between wild type- and Δ*ggt*-infected cells after 24 hours, suggesting that immune cells may be more influenced by other bacterial factors at later time-points. For example, VacA has been shown to induce IL-8 generation in promonocytic U937 cells and the difference in IL-8 stimulation between Δ*vacA* and the parental strain was found to be significant ($P<0.01$) even up to 12 hours post-infection (Hisatsune *et al.*, 2008). Another point to note is that, in this study, the difference in IL-8 generation between wild type- and Δ*ggt*-infected cells at 4 hours, although significant ($P<0.05$), was not as pronounced in macrophages compared to primary gastric or AGS cells. A possible reason for this observation is that macrophages respond differently to *H. pylori* virulence factors compared with gastric epithelial cells as has been described for *cag*PAI (Maeda *et al.*, 2001). Nevertheless, it was observed that in the presence of nGGT or rGGT alone, IL-8 generation in macrophages was significantly increased ($P<0.05$), clearly indicating that GGT is capable of inducing IL-8 production in multiple cell types. Taken

.

together, the results from this study show that GGT is capable of inducing H_2O_2 generation, NF-κB activation and IL-8 production in host cells.

5.5.1.1.1 Contributory role of *cag*PAI but not CagA

CagA has been shown to induce IL-8 production in gastric epithelial cells (Kim *et al.*, 2006; Lim *et al.*, 2009). However, its role remains debatable as conflicting results have also been observed by others (Crabtree *et al.*, 1995b; Sharma *et al.*, 1995; Nozawa *et al.*, 2002). In addition, it has been reported that NF-κB activation (and IL-8 induction) in gastric epithelial cells requires other proteins encoded within the *cag*PAI rather than CagA (Glocker *et al.*, 1998; Li *et al.*, 1999). To this end, the role of CagA and proteins encoded within the *cag*PAI in IL-8 induction was investigated using Δ*cagA* and Δ*cag*PAI respectively. It was observed that NF-κB activation (Figure 33) and IL-8 production (Figure 35) was independent of CagA. However, Δ*cag*PAI induced less NF-κB activation as well as IL-8 production compared with the wild type strain ($P<0.05$), indicating that protein(s) encoded in the *cag*PAI (but not CagA) were indeed involved in the stimulation of IL-8 which is in agreement with a previous report (Fischer *et al.*, 2001). In addition, translocation of *H. pylori* peptidoglycan into gastric epithelial cells through the T4SS (which is encoded by the *cag*PAI) has also been shown to induce NF-κB activation and IL-8 production through Nod1 signalling (Viala *et al*., 2004). Thus, the role of *cag*PAI here may be to transport peptidoglycan into host cells. Notably, NF-κB activation and IL-8 production were significantly lower in AGS cells co-cultured with Δ*cagA*/*ggt* compared to cells infected with Δ*cagA*. This observation reinforces the importance of GGT in *H. pylori*-induced NF-κB activation and IL-8 generation.

.

5.5.1.2 *H. pylori* GGT and DNA damage

ROS is known to cause oxidative DNA damage and induce strand breaks in DNA (Kryston *et al.*, 2011). Hence, it was postulated that GGT-mediated H_2O_2 production may also play a role in inducing DNA damage. In collaboration with Dr. Gong M., extent of DNA damage was found to be significantly higher ($P<0.05$) in wild type-infected compared to Δ*ggt*-infected AGS cells as determined using flow cytometry analysis for 8-hydroxyguanosine and Comet assay.[1] Furthermore, nGGT also induced significantly more DNA damage compared to control cells ($P<0.05$). Interestingly, the presence of N-acetylcysteine (NAC), a H_2O_2 scavenger, inhibited DNA damage induction, thus indicating a role of GGT-mediated H_2O_2 in inducing DNA damage. Taken together, these results clearly show that GGT-mediated H_2O_2 is capable of inducing DNA damage in gastric epithelial cells. Considering the evidence that increased oxidative DNA damage is linked to the severity of *H. pylori*–mediated gastroduodenal diseases (Farinati *et al.*, 1998; Ladeira *et al.*, 2004), the results further reinforce the importance of GGT in the pathogenesis of *H. pylori*.

[1] Data for flow cytometry and Comet assay were obtained by our collaborator, Dr. Gong M., and the results were published in Gastroenterology (2010). *139*, 564-573.

5.5.2 Internalization of *H. pylori* GGT by gastric epithelial cells

Being a secreted enzyme of *H. pylori*, GGT has the potential to mediate important host-pathogen interactions. Hence, it was of great interest to investigate if GGT could translocate into host cells and whether there were any subsequent downstream effects. In this study, three different techniques (immunogold-labeling TEM, CLSM and western blot analysis) were used to show that GGT was indeed capable of entering into AGS cells upon *H. pylori* infection. All three methods showed consistent results in that GGT localized mainly to the host cell nucleus after translocation (Figures 36-38). Interestingly, it was also noted that in the absence of *H. pylori*, rGGT alone was able to enter into the cells, indicating that uptake of GGT is independent of other bacterial factors. From the time-course study, GGT was detected in the nuclei of AGS cells within 1 hour of infection with *H. pylori* while rGGT was detected within 30 minutes post-incubation (Figures 38-39). One possible reason to explain this apparent discrepancy could be due to the time taken for GGT to be secreted out of *H. pylori* before it can be taken up by the cells. Nevertheless, uptake of GGT has been shown to be a rapid process and the timing is comparable to that of other *H. pylori* factors that also enter into host cells (e.g. VacA) (Gauthier *et al.*, 2005). It was therefore of interest to investigate into how GGT was taken up by host cells.

5.5.2.1 Endocytosis pathway involved

Cellular uptake of extracellular proteins requires specific endocytic mechanisms as proteins are unable to pass through the cell membrane freely. *H. pylori* has generally been considered a non-invasive pathogen (Petersen and Krogfelt, 2003) although it has been previously observed to invade gastric epithelial cells albeit with a

low invasion frequency of 1-3% (Wyle *et al.*, 1990; Noach *et al.*, 1994b) through a zipper-like mechanism (Kwok *et al.*, 2002). However, it is unlikely that GGT detected in AGS cells came from internalized *H. pylori* for two main reasons. Firstly, TEM results from this study show that *H. pylori* GGT was detected within AGS cells even in the absence of intracellular bacteria (Figure 36B-C) and secondly, rGGT alone (without bacteria) was also capable of being endocytosed by AGS cells (Figures 37 and 39). These observations suggest that uptake of *H. pylori* GGT by gastric cells occurs via a pinocytic mechanism rather than ingestion of the whole bacterium.

Of the four main pinocytic mechanisms, the study went on to investigate if uptake of GGT was a non-selective process or one that required a specific recognition of the protein. Heat-denaturation of rGGT was found to completely abrogate its uptake by AGS cells (Figure 40), suggesting that recognition of GGT native structure prior to endocytosis is required. Furthermore, rGGTL or rGGTS on its own were also unable to be taken up by the cells (Figure 41). Hence, it was hypothesized that internalization of GGT occurred via receptor-mediated endocytosis rather than the non-selective macropinocytic pathway (Kerr and Teasdale, 2009).

Selective uptake of molecules can occur via three mechanistically different pathways, namely clathrin-mediated endocytosis, caveolin-mediated endocytosis and clathrin- and caveolin-independent endocytosis. Inhibitors of clathrin-mediated and caveolae-mediated endocytosis were used to investigate the pathway by which *H. pylori* GGT is internalized by AGS cells. Various ways of inhibiting clathrin-mediated endocytosis have been reported including the use of hypertonic sucrose (Daukas and Zigmond, 1985), potassium depletion (Larkin *et al.*, 1983) and cytosolic acidification (Sandvig *et al.*, 1988). These methods, however, have unwanted side effects on the cells such as inhibiting other internalization pathways (e.g. caveolae-

mediated endocytosis) (Page *et al.*, 1998) and/or affecting the actin cytoskeleton (Rajasekaran *et al.*, 2001; Suzuki and Namiki, 2007) which may confound the results obtained and obscure interpretations. Another widely used inhibitor of clathrin-mediated endocytosis is the pharmalogical agent CPZ. CPZ is a cationic amphipathic drug that inhibits clathrin-mediated endocytosis by translocating clathrin from the plasma membrane to intracellular vesicles (Wang *et al.*, 1993) and is relatively specific in action. However, one disadvantage of CPZ is that it is cytotoxic to cells at high concentrations (Vercauteren *et al.*, 2010). Cell viability of AGS in the presence of CPZ was thus determined and it was found that >80% of cells remained viable at a CPZ concentration of 15 μg/ml (Figure 42). Hence, this concentration was used to inhibit clathrin-mediated endocytosis in subsequent experiments. It is noted, however, that these cells may have some dysfunctional activities even though they remained viable. Inhibition of caveolin-dependent endocytosis has been achieved using the antibiotic NYS whose mechanism of action is to sequester cholesterol (Chen *et al.*, 2011), hence disrupting formation of caveolae on the cell membrane. NYS is specific in action and does not affect the clathrin-mediated endocytotic pathway (Smart and Anderson, 2002), making it a suitable candidate for probing caveolae-mediated endocytosis. Similarly, cytotoxicity of NYS was investigated on AGS cells and it was found that at a concentration of 25 μg/ml, cells remained 100% viable (Figure 42).

Using CPZ and NYS to inhibit clathrin-mediated and caveolae-mediated endocytosis respectively, addition of rGGT resulted in its accumulation mainly in the membrane fraction of CPZ-treated AGS cells (Figure 43B). In contrast, rGGT was observed to be mostly present in the cytosolic fractions of NYS-treated and uninhibited cells (incubated with rGGT only), suggesting that rGGT is endocytosed via the clathrin-mediated pathway. CLSM micrographs of similarly-treated cells

showed analogous results (Figure 44), further confirming the findings. A point to note, however, is that a small amount of rGGT was still detected in the cytosol of AGS cells at the concentration of CPZ used (Figure 43B). There are two possible explanations that may account for this observation. Firstly, the concentration of CPZ (15 μg/ml) used in this study, though less cytotoxic to cells, may not be sufficient in completely blocking clathrin-mediated endocytosis (Parker *et al.*, 2010). A second possible reason for this observation is that *H. pylori* GGT may be taken up by cells through more than one pathway (e.g. clathrin- and caveolin-independent endocytosis). Interestingly, internalization of VacA by cells has also been suggested to occur via more than one endocytic pathway (Ricci *et al.*, 2000). Nevertheless, the results clearly show that uptake of *H. pylori* GGT is mainly dependent on clathrin-mediated endocytosis although other less dominant pathways of internalization may also be involved.

5.5.2.2 Nuclear import mechanism

After investigating the route of entry into the cells, it was next of interest to determine how GGT enters into the cell nuclei. Cytoplasmic-nuclear transport is a highly selective process that requires imported proteins to be "recognized" by their NLSs and docked to the NPC so as to pass through the otherwise impermeable nuclear membrane (Chook and Suel, 2011). As proteins in the importin β family have been reported to be the main mediators of nuclear import (Chook and Blobel, 2001), it was first investigated if *H. pylori* GGT complexes with them. Using co-IP, *H. pylori* GGT was found to complex with importin β1 but not with importins β2 and β3 (Figure 45). This led to the postulation that importin β1 may be the mediator of GGT import into the cell nucleus. Subsequently, using siRNA knockdown of importin β1

expression, nuclear import of GGT was found to be indeed dependent on importin β1 (Figure 47).

Nuclear-targeted proteins contain NLSs which are first recognized by importins before they are being imported into the nucleus by the latter (Marfori *et al.*, 2011). Importin β1 can bind the NLS of their cargoes either directly or through an adaptor protein known as importin α which generally binds to classical NLSs (Chook and Suel, 2011). From this study, it is not clear how GGT is transported into the cell nuclei as it was not predicted to contain a classical NLS using PredictNLS software (https://rostlab.org/owiki/index.php/PredictNLS) and NucPred (Brameier *et al.*, 2007). Hence, it is unlikely that GGT is imported into the cell nuclei via the classical importin α/β pathway. However, since nuclear import of GGT is dependent on importin β1, it is also possible that GGT may either be "piggy-backing" on a host protein that contains a classical NLS or itself contain an atypical NLS (Marfori *et al.*, 2011) that can be recognized by importin α. Alternatively, GGT could also be transported into the cell nucleus by a non-classical pathway whereby it interacts directly with importin β1 (without the need for importin α) as has been reported for many proteins including HIV-1 Tat and Rev proteins (Truant and Cullen, 1999). Unfortunately, apart from the classical NLSs, these atypical NLSs are less well-defined and lack consistent consensus motifs, hence making it extremely difficult to predict their presence in GGT.

5.5.2.3 GGT depletes nuclear GSH

GSH has been considered essential for survival in eukaryotic but not in prokaryotic cells (Grant *et al.*, 1996). It is a major antioxidant in cells and functions to neutralize free radicals and reactive oxygen compounds (Valko *et al.*, 2006). In the

nucleus, GSH protects the genome against oxidative stress or ionizing radiation (Biaglow *et al.*, 1983) and has also been documented to play an important role in the synthesis of DNA (Thelander and Reichard, 1979). In addition, GSH has been suggested to help maintain nuclear homeostasis (Dijkwel and Wenink, 1986) as well as regulate cell proliferation (Atzori *et al.*, 1990).

Several studies have demonstrated that the cell nucleus is more reduced compared to the cytosol (15mM GSH vs 11mM respectively) (Bellomo *et al.*, 1997; Schafer and Buettner, 2001). Since GGT was earlier found to localize mainly to the cell nucleus after internalization, it was hypothesized that GGT would deplete nuclear GSH levels, leading to a redox imbalance. As it is not possible to specifically measure nuclear GSH concentrations using standard cell fractionation and cytochemical methods (Soderdahl *et al.*, 2003), confocal microscopy using the fluorochrome CMFDA followed by image analysis was used in this study. This method has been used in many studies (Voehringer *et al.*, 1998; Markovic *et al.*, 2007) as CMFDA binds reduced GSH with a high specificity of 95% (Hedley and Chow, 1994) and the intensity of fluorescence can be correlated with the amount of GSH present in different cell compartments. In this study, it was found that AGS cells infected with *H. pylori* wild type had significantly lower levels of nuclear GSH as compared to cells infected with Δ*ggt* (Figure 48). In addition, rGGT alone (in the absence of bacteria) was also able to deplete nuclear GSH levels in a dose-dependent manner, providing direct evidence that GGT plays a vital role in reducing nuclear GSH. Furthermore, inhibition of endocytosis or nuclear import of rGGT (using CPZ and importin β1 siRNA respectively) both led to significantly less nuclear GSH depletion compared to uninhibited cells treated with rGGT (Figures 49 and 50). Taken together, the results

indicate that import of GGT into the nucleus contributes significantly to the depletion of nuclear GSH levels.

GSH in the nucleus plays an important role in cellular physiology. A depletion of nuclear GSH has been reported to interfere with cell cycle progression, leading to a decrease in cell proliferation (Markovic *et al.*, 2010). This is because cells require a reduced nuclear environment to maintain normal cell cycle progression (Markovic *et al.*, 2009). In addition, reduction in nuclear GSH levels has been found to be associated with DNA fragmentation and apoptosis in cells exposed to ionizing radiation, indicating that GSH plays a critical role in protecting nuclear DNA integrity (Morales *et al.*, 1998). Coincidentally, *H. pylori* GGT has also been previously reported to cause apoptosis in gastric epithelial cells (Shibayama *et al.*, 2003), inhibit T cell proliferation (Schmees *et al.*, 2007) and induce cell cycle arrest (Kim *et al.*, 2010). However, the exact underlying mechanisms as to how GGT elicits such cellular effects have not been clearly elucidated. It is therefore hypothesized that GGT induces such cellular perturbations by depleting GSH stores in the nucleus.

5.5.3 *H. pylori* GGT potentiates cell vacuolation

5.5.3.1 Morphological changes induced by GGT

Real-time microscopy was carried out to investigate the morphological changes in AGS cells induced by *H. pylori* wild type and Δ*ggt*. It has been previously reported that infection by *H. pylori* induces the hummingbird phenotype in AGS cells which is characterized by thin, needle-like elongations with lengths ranging from 20 to 70 μm (Moese *et al.*, 2004). This phenomenon occurs due to *H. pylori* CagA being translocated and phosphorylated in AGS cells, leading to the activation of various signalling pathways which induce cytoskeletal arrangements (Backert *et al.*, 2001). In this study, it was observed that both *H. pylori* wild type (Figure 51A) and Δ*ggt* (Figure 51B) induced the hummingbird phenotype in AGS cells from 4 hours post-infection, suggesting that GGT probably does not affect translocation of CagA nor the subsequent signalling pathways involved in cytoskeletal rearrangements.

Apart from the hummingbird phenotype, *H. pylori* infection has also been reported to induce the formation of large vacuoles in AGS cells (Konishi *et al.*, 1992). This morphology is induced by the cytotoxin VacA which forms anion-selective channels in endosomal compartments and through a series of events, eventually lead to subsequent influx of water into the endosomes (Papini *et al.*, 2001). In addition, vacuoles induced by VacA have been reported to originate from the perinuclear region which then rapidly fill up the cell cytoplasm (Papini *et al.*, 1996). From the time-lapse images, it was observed that both *H. pylori* wild type and Δ*ggt* induced the formation of small perinuclear vesicles that started to be visible 12 hours post-infection. In wild type-infected AGS cells, these vacuoles started to increase until almost the entire cell cytoplasm was filled at 24 hours post-infection. However, it was noted that the vacuoles in Δ*ggt*-infected cells did not increase much after 16 hours

post-infection. Neutral red dye uptake results (Figure 53) strongly correlated with the morphological observations, further confirming the results. Through these initial findings, it was postulated that GGT played an important role in the vacuolation process.

5.5.3.2 Observations among different cell lines used

VacA-induced vacuolation has been reported to affect several cell lines albeit with varying sensitivities (de Bernard *et al.*, 1998). Hence, it was also of interest to investigate whether GGT affected vacuolation in other cell lines. In particular, two types of cells were chosen in this study: primary human gastric epithelial cells and the HeLa cell line. Primary human gastric epithelial cells were chosen as they are not transformed and would better mimic the characteristics of cells *in vivo*. In addition, they have also been previously reported to be susceptible to VacA-induced vacuolation (Harris *et al.*, 1996). The HeLa cell line was also employed as it is highly susceptible to VacA-induced vacuolation (de Bernard *et al.*, 1998) and has been extensively used in many studies involving VacA (Cover *et al.*, 1993; Papini *et al.*, 1993a; Gauthier *et al.*, 2007).

From the results, it was observed that both primary human gastric epithelial cells and HeLa cells were indeed highly susceptible to vacuolation induced by *H. pylori* wild type as measured by neutral red dye assay (Figures 55 and 56 respectively). Interestingly, vacuolation induced by Δ*ggt* was also significantly less ($P<0.01$) than that induced by the wild type strain in both cell types, indicating that the mechanism by which GGT affects vacuolation is not exclusive to gastric cells and is possibly common to all susceptible cell types. Furthermore as vacuolation in primary human gastric epithelial cells were also affected by GGT, coupled with the

observation that *H. pylor*i-induced cytoplasmic vacuolation has been reported *in vivo* (Telford *et al.*, 1994), it is postulated that GGT would play an important role in potentiating vacuolation in the natural infection setting.

5.5.3.3 Interplay between *H. pylori* GGT, urease and VacA in vacuolation

In this study, it was observed that AGS cells co-cultured with Δ*ggt* displayed significantly less neutral red dye uptake ($P<0.05$) as compared to the wild type strain (Figure 53). This difference was prominent after 12 hours and showed a similar trend up to 24 hours post-infection. Interestingly, although Δ*ggt* induced significantly more vacuolation as compared to Δ*vacA* ($P<0.05$) 24 hours post-infection (Figure 57), this was approximately 2.8-fold lesser than that induced by wild type after taking into account the background neutral red dye uptake by the control cells. Furthermore, the ability of Δ*ggt* to induce vacuolation was restored when rGGT was exogenously supplemented to the cell culture medium although rGGT was not found to possess intrinsic vacuolating activity (Figure 58). Taken together, the results show that although vacuolation requires the presence of VacA, the extent of vacuolation induced is also dependent on the potentiating effect of GGT.

Previous studies have shown that VacA induces the formation of vacuoles in cells but not unless ammonia or other permeant weak bases are present in the extracellular medium (Cover *et al.*, 1992; Ricci *et al.*, 1997). In view of this, it was noted that one of the principal physiological roles of *H. pylori* GGT is to metabolize extracellular glutamine as a source of glutamate for its own metabolism, a reaction which would inevitably result in the generation of ammonia (Shibayama *et al.*, 2007). Results from this study show that the extent of vacuolation in AGS cells infected with *H. pylori* wild type in glutamine-free medium was significantly decreased ($P<0.01$) to

the level of that induced by Δ*ggt* (Figure 59), suggesting that glutamine could be a potential source of ammonia (through hydrolysis by GGT) which is vital in vacuolation induction by VacA (Cover *et al.*, 1992). To further confirm our theory, an exogenous supply of ammonia in the form of ammonium chloride successfully rescued the ability of Δ*ggt* to induce vacuolation to the level of that induced by the wild type strain (Figure 60). These results indicate that the absence of GGT does not affect the upstream events leading to vacuolation since ammonium chloride alone was sufficient to restore vacuolating activity of Δ*ggt.* Hence, Δ*ggt*, devoid of expressed GGT to provide the function of generating ammonia from glutamine, could be one of the reasons why significantly less vacuolation was observed when AGS cells were co-cultured with Δ*ggt* as compared to wild type. Furthermore, inhibition of GGT activity either by SBC or MAbs with neutralizing activity (as determined in section 4.4) markedly inhibited *H. pylori*-induced vacuolation (Figure 61 and Table 8), indicating that vacuolation induction is indeed dependent on GGT activity.

Urease has been previously reported to be the main potentiator of VacA-dependent vacuolation by converting urea to carbon dioxide and ammonia (Cover *et al.*, 1991). However, results from this study indicate that it is not the only factor contributing to the generation of ammonia required for vacuolation as Δ*ureAB* was still able to induce a significant amount ($P<0.05$) of vacuolation in AGS cells (Figure 57). This is in agreement with a previous report whereby vacuolation induced in Sfl Ep cells by broth-culture filtrates from a urease-isogenic mutant did not differ significantly to that induced by the parental strain in the absence of urea (Konishi *et al.*, 1992). In the same report, it was also found that a large portion of ammonia in the broth filtrates was a urease-independent metabolic product of the bacteria, indicating that there are other bacterial factors responsible for the production of ammonia

essential for vacuolation induction. Interestingly, neutral red uptake induced by Δ*ggt* was significantly lesser than that induced by Δ*ureAB* ($P<0.05$), suggesting that GGT could be the other important ammonia-generating factor. In addition, vacuolation induced by Δ*ureAB/ggt* was abolished to a similar level as that induced by Δ*vacA*. Collectively, the results suggest that GGT and urease are the two main potentiators of VacA-mediated vacuolation and it is proposed that GGT may play a more major role here as compared to the latter.

Induction of cell vacuolation is strongly associated with pathogenic strains of *H. pylori* and is believed to induce cell suffering and eventually cell death (Papini *et al.*, 1993b; de Bernard *et al.*, 1998), resulting in a chronic inflammatory response in the gastric mucosa of the host (Papini *et al.*, 1994). This study shows that although GGT does not have intrinsic vacuolating activity, it plays an important role alongside VacA in inducing vacuolation in gastric epithelial cells by hydrolyzing glutamine, yielding ammonia that strongly potentiates vacuole formation. Hence, this could be another reason as to why *H. pylori* with higher GGT activity is associated with more severe gastroduodenal diseases (Gong, 2006).

5.5.4 Proposed mechanism of GGT-mediated *H. pylori* pathogenesis

In summary, it is proposed that *H. pylori* GGT influences cellular processes via several pathways as illustrated in Figure 63: (1) GGT generates ROS from GSH hydrolysis via thiol-dependent iron reduction. This in turn activates the NF-κB pathway, upregulates expression of the inflammatory chemokine IL-8 and induces DNA damage in host cells. (2) GGT is internalized by gastric epithelial cells via clathrin-mediated endocytosis where it then localizes to the cell nucleus in an importin β1-dependent manner. Subsequently, nuclear GSH is depleted by GGT,

making the cell more vulnerable to ROS insults which GGT itself produces via extracellular GSH hydrolysis. This redox imbalance may then lead to downstream effects such as DNA damage and apoptosis. (3) *H. pylori* secretes VacA which induces vacuolation in host cells. Through the generation of ammonia from glutamine hydrolysis, GGT (and to a lesser extent, urease) potentiates VacA-dependent vacuolation, resulting in additional stress on the cell. Taken together, GGT is a potent virulence factor that elicits multiple routes of damage in host cells.

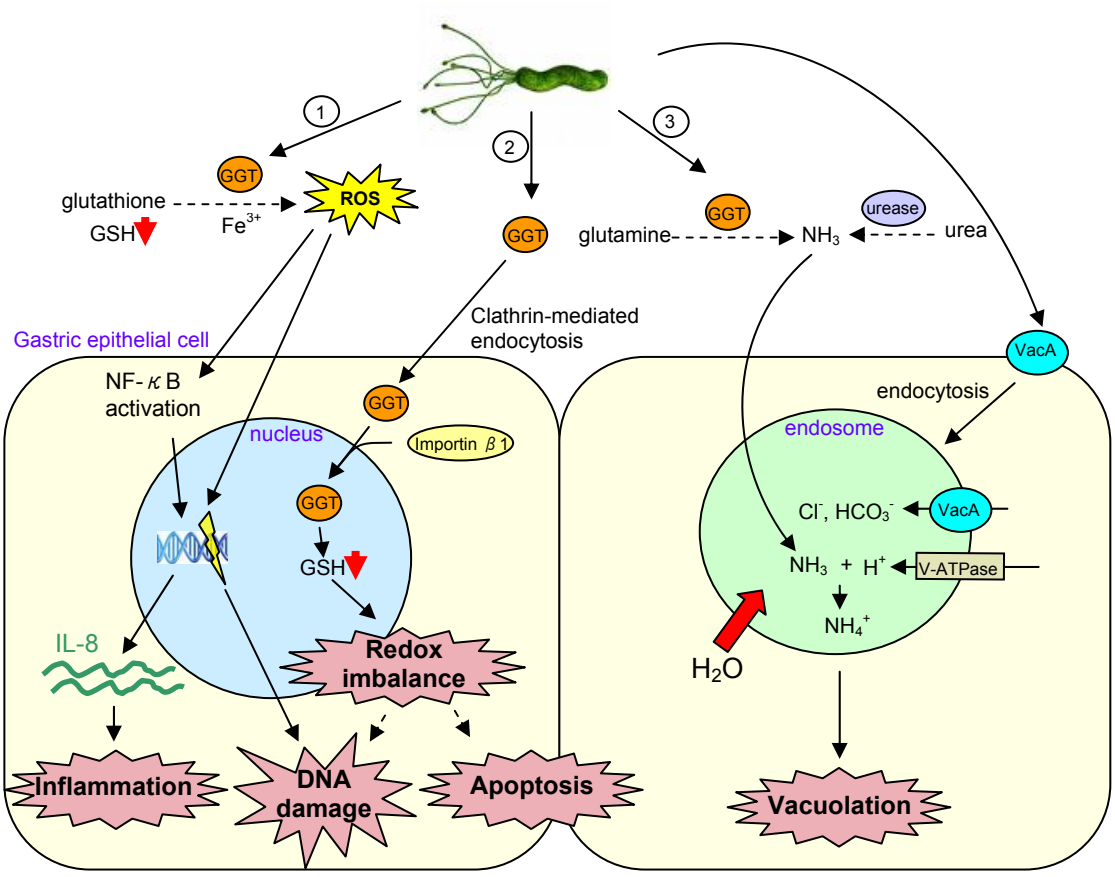

Figure 63. Proposed model outlining the roles of GGT in *H. pylori* pathogenesis.

Apart from directly damaging gastric epithelial cells as evident from this study, production of the chemokine IL-8 by gastric epithelial cells (in response to GGT and other *H. pylori* factors) subsequently attracts immune cells such as neutrophils and macrophages into the sites of infection (Kusugami *et al.*, 1997).

However, these innate immune defenses are not sufficient to clear the infection as *H. pylori* is able to evade phagocytosis and killing by these cells, leading to chronic inflammation and an increase in local tissue damage (Grebowska *et al*., 2008). In addition, GGT has also been reported to inhibit the proliferation of T cells (Schmees *et al*., 2007), hence playing an immunosuppressive role. Furthermore, GGT has been shown to induce expression of FoxP3 transcription factor (Fassi Fehri *et al*., 2010), a master regulator and marker of regulatory T cells. Regulatory T cells regulate the adaptive immune response by suppressing the immune responses of other immune cells and have been implicated to play an important role in *H. pylori*-related gastric carcinogenesis (Kandulski *et al*., 2010). Hence, GGT also plays a substantial role in modulating the immune response such that persistent infection by the bacterium and chronic inflammation can occur, both of which are important aspects in the development of gastroduodenal diseases and cancer (Coussens and Werb, 2002).

5.6 GGT as a potential diagnostic marker for *H. pylori* infections

Various tests have been developed for detecting *H. pylori* infection and these can be broadly divided into invasive and non-invasive methods. Invasive tests include endoscopic examination and biopsy-based histology and culture of the organism. These tests are extremely reliable in detecting for *H. pylori* (Gold *et al.*, 2000) but are expensive and require expertise to carry out, hence they may not be the most appropriate method-of-choice under some clinical settings. Non-invasive methods, on the other hand, include urea breath test, stool antigen test and serology. These tests do not require the need for endoscopy and are hence more suitable for certain groups of patients (especially young children). In addition, tests such as serology are cheaper in cost and more convenient.

As GGT is both surface localized and secreted by *H. pylori*, it was investigated if *H. pylori* GGT could be a suitable candidate antigen for use in serodiagnosis. Using rGGT as antigen, the level of anti-GGT antibody was found to be significantly higher ($P<0.01$) in serum from *H. pylori*-positive patients compared to *H. pylori*-negative controls although relatively wide variations were observed among both groups of subjects (Figure 62). In addition, ELISA readings were comparatively high in serum from *H. pylori*-positive patients (0.98 ± 0.39), indicating that *H. pylori* GGT is capable of inducing a relatively strong immune response during bacterial infection.

Compared to whole cell antigens or ultrasonicates currently used in some *H. pylori* diagnostic tests (Hoang *et al*., 2004; Leal *et al*., 2008), purified rGGT antigen has the advantage of reducing the risks of non-specific binding and cross-reactivity to antigens of other species. This would result in increased specificity although sensitivity of the test may be slightly decreased (Hirschl *et al.*, 1990). Other advantages of using rGGT as an antigen is that GGT is found in all *H. pylori* strains, is highly conserved within *H. pylori* species and shares only 22% protein sequence homology to human GGT (Chevalier *et al.*, 1999), thus making it an ideal candidate for use in detecting *H. pylori* infections. In all, this study has uncovered the potential of using anti-GGT in patients' sera to detect for *H. pylori* infections. Additionally, the strong association between *H. pylori* GGT activity and peptic ulcer disease (Gong, 2006) leads us to speculate that the use of purified rGGT as an antigen may have a prognostic potential in identifying individuals at risk of developing severe gastric diseases. This is an interesting area which is currently being explored.

5.7 Conclusion

This study has demonstrated *H. pylori* GGT to be an important virulence factor of the bacterium. To this end, using purified nGGT and rGGT as well as various *H. pylori* isogenic constucts, three distinct findings were established as illustrated in Figure 63. Firstly, GGT was found to induce the generation of ROS, activate NF-κB, upregulate the production of IL-8 and induce oxidative DNA damage in gastric epithelial cells. This suggests that GGT contributes to the pro-inflammatory response of the host during *H. pylori* infection. Secondly, GGT was shown to be internalized through clathrin-mediated endocytosis and subsequently imported into the nuclei of gastric epithelial cells in an importin β1-dependent manner. This novel property of GGT results in the depletion of nuclear GSH, an important antioxidant present in host cells. Hence, it is evident that GGT not only generates ROS extracellularly, but also infiltrates into the host cell nucleus to decrease its antioxidant defence, potentially increasing the susceptibility of the cells to oxidant-mediated injury. Thirdly, GGT was also observed to strongly potentiate VacA-dependent vacuolation through the generation of ammonia from glutamine, thus provoking further stress on the host. As chronic inflammation, DNA damage and depletion of nuclear GSH are important cornerstones in carcinogenesis (Rakoff-Nahoum, 2006; Markovic *et al*., 2010; Kryston *et al.*, 2011), it is hypothesized that GGT could play an imperative role in *H. pylori*-mediated gastric cancer.

MAbs raised against rGGT were found to be potent inhibitors of *H. pylori* GGT enzymatic activity. Importantly, the neutralizing epitope was identified as GNPNLYG (residues 428-434) which is highly conserved in *H. pylori* GGT and spans a Tyr 433-containing loop critical for catalytic activity (Morrow *et al.*, 2007). Neutralizing MAbs against GGT may help attenuate the virulence of the bacterium.

Thus, these MAbs could be humanized and further investigated as a possible future therapeutic approach against *H. pylori*. Being a surface-localized (this study) and secreted protein of *H. pylori* (Bumann *et al*., 2002), GGT was also found to induce a host immune response where a significantly higher anti-GGT antibody level was observed in *H. pylori*-positive subjects compared to *H. pylori*-negative controls ($P<0.05$). Thus the potential of rGGT in being a diagnostic marker for *H. pylori* infections could be further explored with a larger sample size so as to validate its practical use.

Taken together, the results from this work have conclusively shown that GGT is a critical virulence factor of *H. pylori* with pleiotropic effects. The enzyme is not only important for the pathogen's own metabolism but also damages host cells through which more nutrients may be released for its benefit and survival in the hostile gastric environment. Intriguingly, the findings in this study provide new insights into the mechanisms underlying *H. pylori* pathogenesis where the pathogenic role of GGT should not be underrated. Given that all *H. pylori* strains express GGT (Chevalier *et al.,* 1999) and are therefore all potentially able to cause disease, GGT should be considered as a promising target for the development of new therapeutic approaches in the management of *H. pylori* infection.

5.8 Future work

As *H. pylori* GGT was found to be specifically recognized and subsequently internalized by gastric epithelial cells via clathrin-mediated endocytosis, it would be of great interest to identify the specific receptor(s) involved in this recognition in future studies. In addition, the exact molecular events underlying the route of GGT from the cell membrane to host cell nuclei have not been elucidated. For example, it is

currently not known how GGT, which is present in the endosome after endocytosis, is able to bind cytoplasmic importin β1 before being imported into the nucleus. One possibility could be that GGT-bearing endosomes may first fuse with Golgi, undergo retrograde transport to the endoplasmic reticulum (ER) and subsequently get extracted into the cytosol by the ER-associated degradation system as has been hypothesized for EGFR nuclear entry (Lo *et al.*, 2006). Whether GGT indeed uses this pathway to escape from endosomes requires future extensive research.

It is also intriguing that despite a highly conserved GGT sequence (Chevalier *et al.*, 1999), there exists substantial differences in GGT activity between different *H. pylori* strains (Gong and Ho, 2004). Hence, the underlying mechanism(s) governing regulation of GGT expression in *H. pylori* is another area of considerable interest. Few studies have examined this in detail although there is some evidence that expression of GGT may be regulated both at the transcriptional and post-transcriptional levels (Tsao *et al.*, 2009; Wachino *et al.*, 2010). Understanding the mechanisms underlying its regulation would certainly shed more light into GGT-mediated pathogenesis and could possibly lead to novel therapeutic approaches against *H. pylori* infections.

REFERENCES

Aberkane, H., Frank, P., Galteau, M.M., and Wellman, M. (2001). Acivicin induces apoptosis independently of gamma-glutamyltranspeptidase activity. Biochem Biophys Res Commun *285*, 1162-1167.

Akanuma, M., Maeda, S., Ogura, K., Mitsuno, Y., Hirata, Y., Ikenoue, T., Otsuka, M., Watanabe, T., Yamaji, Y., Yoshida, H., Kawabe, T., Shiratori, Y., and Omata, M. (2002). The evaluation of putative virulence factors of *Helicobacter pylori* for gastroduodenal disease by use of a short-term Mongolian gerbil infection model. J Infect Dis *185*, 341-347.

Akopyants, N.S., Clifton, S.W., Kersulyte, D., Crabtree, J.E., Youree, B.E., Reece, C.A., Bukanov, N.O., Drazek, E.S., Roe, B.A., and Berg, D.E. (1998). Analyses of the *cag* pathogenicity island of *Helicobacter pylori*. Mol Microbiol *28*, 37-53.

Al-Sulami, A.A., Al-Taee, A.M., and Juma'a, M.G. (2010). Isolation and identification of *Helicobacter pylori* from drinking water in Basra governorate, Iraq. East Mediterr Health J *16*, 920-925.

Amedei, A., Cappon, A., Codolo, G., Cabrelle, A., Polenghi, A., Benagiano, M., Tasca, E., Azzurri, A., D'Elios, M.M., Del Prete, G., and de Bernard, M. (2006). The neutrophil-activating protein of *Helicobacter pylori* promotes Th1 immune responses. J Clin Invest *116*, 1092-1091.

Amieva, M.R., Vogelmann, R., Covacci, A., Tompkins, L.S., Nelson, W.J., and Falkow, S. (2003). Disruption of the epithelial apical-junctional complex by *Helicobacter pylori* CagA. Science *300*, 1430-1434.

Andersen, L.P., and Wadström, T. (2001). Basic Bacteriology and Culture. In: *Helicobacter pylori*: Physiology and Genetics. (Mobley, H.L.T., Mendz, G.L., and Hazell, S.L., Eds.), pp. 27-38. ASM Press, Washington DC.

Ando, T., Kusugami, K., Ohsuga, M., Shinoda, M., Sakakibara, M., Saito, H., Fukatsu, A., Ichiyama, S., and Ohta, M. (1996). Interleukin-8 activity correlates with histological severity in *Helicobacter pylori*-associated antral gastritis. Am J Gastroenterol *91*, 1150-1156.

Appelmelk, B.J., Simoons-Smit, I., Negrini, R., Moran, A.P., Aspinall, G.O., Forte, J.G., De Vries, T., Quan, H., Verboom, T., Maaskant, J.J., Ghiara, P., Kuipers, E.J., Bloemena, E., Tadema, T.M., Townsend, R.R., Tyagarajan, K., Crothers, J.M., Jr., Monteiro, M.A., Savio, A., and De Graaff, J. (1996). Potential role of molecular mimicry between *Helicobacter pylori* lipopolysaccharide and host Lewis blood group antigens in autoimmunity. Infect Immun *64*, 2031-2040.

Armstrong, D. (1996). *Helicobacter pylori* infection and dyspepsia. Scand J Gastroenterol Suppl *215*, 38-47.

Atherton, J.C. (2006). The pathogenesis of *Helicobacter pylori*-induced gastro-duodenal diseases. Annu Rev Pathol *1*, 63-96.

Atherton, J.C., Cao, P., Peek, R.M., Jr., Tummuru, M.K., Blaser, M.J., and Cover, T.L. (1995). Mosaicism in vacuolating cytotoxin alleles of *Helicobacter pylori*. Association of specific *vacA* types with cytotoxin production and peptic ulceration. J Biol Chem *270*, 17771-17777.

Atherton, J.C., Peek, R.M., Jr., Tham, K.T., Cover, T.L., and Blaser, M.J. (1997). Clinical and pathological importance of heterogeneity in *vacA*, the vacuolating cytotoxin gene of *Helicobacter pylori*. Gastroenterology *112*, 92-99.

Atzori, L., Dypbukt, J.M., Sundqvist, K., Cotgreave, I., Edman, C.C., Moldeus, P., and Grafstrom, R.C. (1990). Growth-associated modifications of low-molecular-weight thiols and protein sulfhydryls in human bronchial fibroblasts. J Cell Physiol *143*, 165-171.

Backert, S., Moese, S., Selbach, M., Brinkmann, V., and Meyer, T.F. (2001). Phosphorylation of tyrosine 972 of the *Helicobacter pylori* CagA protein is essential for induction of a scattering phenotype in gastric epithelial cells. Mol Microbiol *42*, 631-644.

Backert, S., and Selbach, M. (2008). Role of type IV secretion in *Helicobacter pylori* pathogenesis. Cell Microbiol *10*, 1573-1581.

Backert, S., Ziska, E., Brinkmann, V., Zimny-Arndt, U., Fauconnier, A., Jungblut, P.R., Naumann, M., and Meyer, T.F. (2000). Translocation of the *Helicobacter pylori* CagA protein in gastric epithelial cells by a type IV secretion apparatus. Cell Microbiol *2*, 155-164.

Balkwill, F., and Mantovani, A. (2001). Inflammation and cancer: back to Virchow? Lancet *357*, 539-545.

Bandyopadhyay, D., Biswas, K., Bhattacharyya, M., Reiter, R.J., and Banerjee, R.K. (2002). Involvement of reactive oxygen species in gastric ulceration: protection by melatonin. Indian J Exp Biol *40*, 693-705.

Baneyx, F., and Mujacic, M. (2004). Recombinant protein folding and misfolding in *Escherichia coli*. Nat Biotechnol *22*, 1399-1408.

Basu, M., Czinn, S.J., and Blanchard, T.G. (2004). Absence of catalase reduces long-term survival of *Helicobacter pylori* in macrophage phagosomes. Helicobacter *9*, 211-216.

Bauer, S., Krumbiegel, P., Richter, M., Richter, T., Roder, S., Rolle-Kampczyk, U., and Herbarth, O. (2011). Influence of sociodemographic factors on *Helicobacter pylori* prevalence variability among schoolchildren in Leipzig, Germany. A long-term follow-up study. Cent Eur J Public Health *19*, 42-45.

Beg, A.A., Ruben, S.M., Scheinman, R.I., Haskill, S., Rosen, C.A., and Baldwin, A.S., Jr. (1992). I kappa B interacts with the nuclear localization sequences of the subunits of NF-kappa B: a mechanism for cytoplasmic retention. Genes Dev *6*, 1899-1913.

Beil, W., Obst, B., Sewing, K.F., and Wagner, S. (2000). *Helicobacter pylori* reduces intracellular glutathione in gastric epithelial cells. Dig Dis Sci *45*, 1769-1773.

Bellomo, G., Palladini, G., and Vairetti, M. (1997). Intranuclear distribution, function and fate of glutathione and glutathione-S-conjugate in living rat hepatocytes studied by fluorescence microscopy. Microsc Res Tech *36*, 243-252.

Berry, V., Jennings, K., and Woodnutt, G. (1995). Bactericidal and morphological effects of amoxicillin on *Helicobacter pylori*. Antimicrob Agents Chemother *39*, 1859-1861.

Beswick, E.J., Pinchuk, I.V., Minch, K., Suarez, G., Sierra, J.C., Yamaoka, Y., and Reyes, V.E. (2006). The *Helicobacter pylori* urease B subunit binds to CD74 on gastric epithelial cells and induces NF-kappaB activation and interleukin-8 production. Infect Immun *74*, 1148-1155.

Bhattacharyya, S., Warfield, K.L., Ruthel, G., Bavari, S., Aman, M.J., and Hope, T.J. (2010). Ebola virus uses clathrin-mediated endocytosis as an entry pathway. Virology *401*, 18-28.

Biaglow, J.E., Varnes, M.E., Clark, E.P., and Epp, E.R. (1983). The role of thiols in cellular response to radiation and drugs. Radiat Res *95*, 437-455.

Bizzozero, G. (1893). Ueber die schlauchformigen drusen des magendarmkanals und die bezienhungen ihres epithels zu dem oberflachenepithel der schleimhaut. Arch Mikr Anat *42*, 82.

Blaser, M.J., Perez-Perez, G.I., Kleanthous, H., Cover, T.L., Peek, R.M., Chyou, P.H., Stemmermann, G.N., and Nomura, A. (1995). Infection with *Helicobacter pylori* strains possessing *cagA* is associated with an increased risk of developing adenocarcinoma of the stomach. Cancer Res *55*, 2111-2115.

Boanca, G., Sand, A., and Barycki, J.J. (2006). Uncoupling the enzymatic and autoprocessing activities of *Helicobacter pylori* gamma-glutamyltranspeptidase. J Biol Chem *281*, 19029-19037.

Boanca, G., Sand, A., Okada, T., Suzuki, H., Kumagai, H., Fukuyama, K., and Barycki, J.J. (2007). Autoprocessing of *Helicobacter pylori* gamma-glutamyltranspeptidase leads to the formation of a threonine-threonine catalytic dyad. J Biol Chem *282*, 534-541.

Bounous, G., and Molson, J.H. (2003). The antioxidant system. Anticancer Res *23*, 1411-1415.

Brameier, M., Krings, A., and MacCallum, R.M. (2007). NucPred--predicting nuclear localization of proteins. Bioinformatics *23*, 1159-1160.

Bumann, D., Aksu, S., Wendland, M., Janek, K., Zimny-Arndt, U., Sabarth, N., Meyer, T.F., and Jungblut, P.R. (2002). Proteome analysis of secreted proteins of the gastric pathogen *Helicobacter pylori*. Infect Immun *70*, 3396-3403.

Busiello, I., Acquaviva, R., Di Popolo, A., Blanchard, T.G., Ricci, V., Romano, M., and Zarrilli, R. (2004). *Helicobacter pylori* gamma-glutamyltranspeptidase upregulates COX-2 and EGF-related peptide expression in human gastric cells. Cell Microbiol *6*, 255-267.

Busler, V.J., Torres, V.J., McClain, M.S., Tirado, O., Friedman, D.B., and Cover, T.L. (2006). Protein-protein interactions among *Helicobacter pylori* Cag proteins. J Bacteriol *188*, 4787-4800.

Calam, J., Gibbons, A., Healey, Z.V., Bliss, P., and Arebi, N. (1997). How does *Helicobacter pylori* cause mucosal damage? Its effect on acid and gastrin physiology. Gastroenterology *113 (Suppl 6)*, S43-49.

Cao, W., Lee, S.H., and Lu, J. (2005). CD83 is preformed inside monocytes, macrophages and dendritic cells, but it is only stably expressed on activated dendritic cells. Biochem J *385*, 85-93.

Catrenich, C.E., and Makin, K.M. (1991). Characterization of the morphologic conversion of *Helicobacter pylori* from bacillary to coccoid forms. Scand J Gastroenterol Suppl *181*, 58-64.

Censini, S., Lange, C., Xiang, Z., Crabtree, J.E., Ghiara, P., Borodovsky, M., Rappuoli, R., and Covacci, A. (1996). *cag*, a pathogenicity island of *Helicobacter pylori*, encodes type I-specific and disease-associated virulence factors. Proc Natl Acad Sci U S A *93*, 14648-14653.

Chen, X.G., Correa, P., Offerhaus, J., Rodriguez, E., Janney, F., Hoffmann, E., Fox, J., Hunter, F., and Diavolitsis, S. (1986). Ultrastructure of the gastric mucosa harboring *Campylobacter*-like organisms. Am J Clin Pathol *86*, 575-582.

Chen, Y., Wang, S., Lu, X., Zhang, H., Fu, Y., and Luo, Y. (2011). Cholesterol sequestration by nystatin enhances the uptake and activity of endostatin in endothelium via regulating distinct endocytic pathways. Blood *117*, 6392-6403.

Chevalier, C., Thiberge, J.M., Ferrero, R.L., and Labigne, A. (1999). Essential role of *Helicobacter pylori* gamma-glutamyltranspeptidase for the colonization of the gastric mucosa of mice. Mol Microbiol *31*, 1359-1372.

Chiba, T., Marusawa, H., Seno, H., and Watanabe, N. (2008). Mechanism for gastric cancer development by *Helicobacter pylori* infection. J Gastroenterol Hepatol *23*, 1175-1181.

Chikhi, N., Holic, N., Guellaen, G., and Laperche, Y. (1999). Gamma-glutamyl transpeptidase gene organization and expression: a comparative analysis in rat, mouse, pig and human species. Comp Biochem Physiol B Biochem Mol Biol *122*, 367-380.

Chook, Y.M., and Blobel, G. (2001). Karyopherins and nuclear import. Curr Opin Struct Biol *11*, 703-715.

Chook, Y.M., and Suel, K.E. (2011). Nuclear import by karyopherin-betas: recognition and inhibition. Biochim Biophys Acta *1813*, 1593-1606.

Christophe, D., Christophe-Hobertus, C., and Pichon, B. (2000). Nuclear targeting of proteins: how many different signals? Cell Signal *12*, 337-341.

Chu, S.H., Kim, H., Seo, J.Y., Lim, J.W., Mukaida, N., and Kim, K.H. (2003). Role of NF-kappaB and AP-1 on *Helicobater pylori*-induced IL-8 expression in AGS cells. Dig Dis Sci *48*, 257-265.

Cole, S.P., Cirillo, D., Kagnoff, M.F., Guiney, D.G., and Eckmann, L. (1997). Coccoid and spiral *Helicobacter pylori* differ in their abilities to adhere to gastric epithelial cells and induce interleukin-8 secretion. Infect Immun *65*, 843-846.

Coligan, J.E., and Current Protocols Online. (1992). Current protocols in immunology. Greene Pub. Associates and Wiley-Interscience, New York.

Conner, S.D., and Schmid, S.L. (2003). Regulated portals of entry into the cell. Nature *422*, 37-44.

Correa, P. (1988). A human model of gastric carcinogenesis. Cancer Res *48*, 3554-3560.

Coussens, L.M., and Werb, Z. (2002). Inflammation and cancer. Nature *420*, 860-867.

Covacci, A., Censini, S., Bugnoli, M., Petracca, R., Burroni, D., Macchia, G., Massone, A., Papini, E., Xiang, Z., Figura, N., and Rappuoli, R. (1993). Molecular characterization of the 128-kDa immunodominant antigen of *Helicobacter pylori* associated with cytotoxicity and duodenal ulcer. Proc Natl Acad Sci U S A *90*, 5791-5795.

Covacci, A., Telford, J.L., Del Giudice, G., Parsonnet, J., and Rappuoli, R. (1999). *Helicobacter pylori* virulence and genetic geography. Science *284*, 1328-1333.

Cover, T.L., and Blanke, S.R. (2005). *Helicobacter pylori* VacA, a paradigm for toxin multifunctionality. Nat Rev Microbiol *3*, 320-332.

Cover, T.L., and Blaser, M.J. (1992a). *Helicobacter pylori* and gastroduodenal disease. Annu Rev Med *43*, 135-145.

Cover, T.L., and Blaser, M.J. (1992b). Purification and characterization of the vacuolating toxin from *Helicobacter pylori*. J Biol Chem *267*, 10570-10575.

Cover, T.L., Puryear, W., Perez-Perez, G.I., and Blaser, M.J. (1991). Effect of urease on HeLa cell vacuolation induced by *Helicobacter pylori* cytotoxin. Infect Immun *59*, 1264-1270.

Cover, T.L., Reddy, L.Y., and Blaser, M.J. (1993). Effects of ATPase inhibitors on the response of HeLa cells to *Helicobacter pylori* vacuolating toxin. Infect Immun *61*, 1427-1431.

Cover, T.L., Vaughn, S.G., Cao, P., and Blaser, M.J. (1992). Potentiation of *Helicobacter pylori* vacuolating toxin activity by nicotine and other weak bases. J Infect Dis *166*, 1073-1078.

Crabtree, J.E., Covacci, A., Farmery, S.M., Xiang, Z., Tompkins, D.S., Perry, S., Lindley, I.J., and Rappuoli, R. (1995a). *Helicobacter pylori* induced interleukin-8 expression in gastric epithelial cells is associated with CagA positive phenotype. J Clin Pathol *48*, 41-45.

Crabtree, J.E., and Lindley, I.J. (1994). Mucosal interleukin-8 and *Helicobacter pylori*-associated gastroduodenal disease. Eur J Gastroenterol Hepatol *6 (Suppl 1)*, S33-38.

Crabtree, J.E., Shallcross, T.M., Heatley, R.V., and Wyatt, J.I. (1991). Mucosal tumour necrosis factor alpha and interleukin-6 in patients with *Helicobacter pylori* associated gastritis. Gut *32*, 1473-1477.

Crabtree, J.E., Wyatt, J.I., Trejdosiewicz, L.K., Peichl, P., Nichols, P.H., Ramsay, N., Primrose, J.N., and Lindley, I.J. (1994). Interleukin-8 expression in *Helicobacter pylori* infected, normal, and neoplastic gastroduodenal mucosa. J Clin Pathol *47*, 61-66.

Crabtree, J.E., Xiang, Z., Lindley, I.J., Tompkins, D.S., Rappuoli, R., and Covacci, A. (1995b). Induction of interleukin-8 secretion from gastric epithelial cells by a *cagA* negative isogenic mutant of *Helicobacter pylori*. J Clin Pathol *48*, 967-969.

Dattoli, V.C., Veiga, R.V., da Cunha, S.S., Pontes-de-Carvalho, L.C., Barreto, M.L., and Alcantara-Neves, N.M. (2010). Seroprevalence and potential risk factors for *Helicobacter pylori* infection in Brazilian children. Helicobacter *15*, 273-278.

Daukas, G., and Zigmond, S.H. (1985). Inhibition of receptor-mediated but not fluid-phase endocytosis in polymorphonuclear leukocytes. J Cell Biol *101*, 1673-1679.

Davies, G.R., Simmonds, N.J., Stevens, T.R., Grandison, A., Blake, D.R., and Rampton, D.S. (1992). Mucosal reactive oxygen metabolite production in duodenal ulcer disease. Gut *33*, 1467-1472.

Davies, G.R., Simmonds, N.J., Stevens, T.R., Sheaff, M.T., Banatvala, N., Laurenson, I.F., Blake, D.R., and Rampton, D.S. (1994). *Helicobacter pylori* stimulates antral mucosal reactive oxygen metabolite production *in vivo*. Gut *35*, 179-185.

de Bernard, M., Moschioni, M., Papini, E., Telford, J., Rappuoli, R., and Montecucco, C. (1998). Cell vacuolization induced by *Helicobacter pylori* VacA toxin: cell line sensitivity and quantitative estimation. Toxicol Lett *99*, 109-115.

De Koster, E., Buset, M., Fernandes, E., and Deltenre, M. (1994). *Helicobacter pylori*: the link with gastric cancer. Eur J Cancer Prev *3*, 247-257.

Delves, P.J. (1995). Antibody applications: essential techniques. Wiley, New York.

Dijkwel, P.A., and Wenink, P.W. (1986). Structural integrity of the nuclear matrix: differential effects of thiol agents and metal chelators. J Cell Sci *84*, 53-67.

Ding, S.Z., Minohara, Y., Fan, X.J., Wang, J., Reyes, V.E., Patel, J., Dirden-Kramer, B., Boldogh, I., Ernst, P.B., and Crowe, S.E. (2007). *Helicobacter pylori* infection induces oxidative stress and programmed cell death in human gastric epithelial cells. Infect Immun *75*, 4030-4039.

Doenges, J.L. (1938). Spirochetes in the gastric glands of macacus rhesus and humans without definite history of related disease. Proc Soc Exp Med Biol *38*, 536-538.

Dominici, S., Valentini, M., Maellaro, E., Del Bello, B., Paolicchi, A., Lorenzini, E., Tongiani, R., Comporti, M., and Pompella, A. (1999). Redox modulation of cell surface protein thiols in U937 lymphoma cells: the role of gamma-glutamyl transpeptidase-dependent H_2O_2 production and S-thiolation. Free Radic Biol Med *27*, 623-635.

Dorrell, N., Martino, M.C., Stabler, R.A., Ward, S.J., Zhang, Z.W., McColm, A.A., Farthing, M.J., and Wren, B.W. (1999). Characterization of *Helicobacter pylori* PldA, a phospholipase with a role in colonization of the gastric mucosa. Gastroenterology *117*, 1098-1104.

Dossumbekova, A., Prinz, C., Mages, J., Lang, R., Kusters, J.G., Van Vliet, A.H., Reindl, W., Backert, S., Saur, D., Schmid, R.M., and Rad, R. (2006). *Helicobacter pylori* HopH (OipA) and bacterial pathogenicity: genetic and functional genomic analysis of *hopH* gene polymorphisms. J Infect Dis *194*, 1346-1355.

Drozdz, R., Parmentier, C., Hachad, H., Leroy, P., Siest, G., and Wellman, M. (1998). gamma-Glutamyltransferase dependent generation of reactive oxygen species from a glutathione/transferrin system. Free Radic Biol Med *25*, 786-792.

Du, R.J., and Ho, B. (2003). Surface localized Heat Shock Protein 20 (HslV) of *Helicobacter pylori*. Helicobacter *8*, 257-267.

Dube, C., Nkosi, T.C., Clarke, A.M., Mkwetshana, N., Green, E., and Ndip, R.N. (2009). *Helicobacter pylori* antigenemia in an asymptomatic population of Eastern Cape Province, South Africa: public health implications. Rev Environ Health *24*, 249-255.

Dubois, A. (1995). Spiral bacteria in the human stomach: the gastric helicobacters. Emerg Infect Dis *1*, 79-85.

Dubois, A., Fiala, N., Weichbrod, R.H., Ward, G.S., Nix, M., Mehlman, P.T., Taub, D.M., Perez-Perez, G.I., and Blaser, M.J. (1995). Seroepizootiology of *Helicobacter pylori* gastric infection in nonhuman primates housed in social environments. J Clin Microbiol *33*, 1492-1495.

Dundon, W.G., Nishioka, H., Polenghi, A., Papinutto, E., Zanotti, G., Montemurro, P., Del, G.G., Rappuoli, R., and Montecucco, C. (2002). The neutrophil-activating protein of *Helicobacter pylori*. Int J Med Microbiol *291*, 545-550.

Dunn, B.E., Campbell, G.P., Perez-Perez, G.I., and Blaser, M.J. (1990). Purification and characterization of urease from *Helicobacter pylori*. J Biol Chem *265*, 9464-9469.

Eaton, K.A., Brooks, C.L., Morgan, D.R., and Krakowka, S. (1991). Essential role of urease in pathogenesis of gastritis induced by *Helicobacter pylori* in gnotobiotic piglets. Infect Immun *59*, 2470-2475.

Eaton, K.A., Catrenich, C.E., Makin, K.M., and Krakowka, S. (1995). Virulence of coccoid and bacillary forms of *Helicobacter pylori* in gnotobiotic piglets. J Infect Dis *171*, 459-462.

Eaton, K.A., Morgan, D.R., and Krakowka, S. (1992). Motility as a factor in the colonisation of gnotobiotic piglets by *Helicobacter pylori*. J Med Microbiol *37*, 123-127.

Eftang, L.L., Esbensen, Y., Tannaes, T.M., Bukholm, I.R., and Bukholm, G. (2012). Interleukin-8 is the single most up-regulated gene in whole genome profiling of *H. pylori* exposed gastric epithelial cells. BMC Microbiol *12*, 9.

Epidemiological News Bulletin. (1996). Seroprevalence of *Helicobacter pylori* infection in Singapore. *22*, 31-32.

Ernst, P.B., and Gold, B.D. (2000). The disease spectrum of *Helicobacter pylori*: the immunopathogenesis of gastroduodenal ulcer and gastric cancer. Annu Rev Microbiol *54*, 615-640.

Fahnert, B., Lilie, H., and Neubauer, P. (2004). Inclusion bodies: formation and utilisation. Adv Biochem Eng Biotechnol *89*, 93-142.

Fan, X.G., Chua, A., Fan, X.J., and Keeling, P.W. (1995). Increased gastric production of interleukin-8 and tumour necrosis factor in patients with *Helicobacter pylori* infection. J Clin Pathol *48*, 133-136.

Farinati, F., Cardin, R., Degan, P., Rugge, M., Mario, F.D., Bonvicini, P., and Naccarato, R. (1998). Oxidative DNA damage accumulation in gastric carcinogenesis. Gut *42*, 351-356.

Fassi Fehri, L., Koch, M., Belogolova, E., Khalil, H., Bolz, C., Kalali, B., Mollenkopf, H.J., Beigier-Bompadre, M., Karlas, A., Schneider, T., Churin, Y., Gerhard, M., and Meyer, T.F. (2010). *Helicobacter pylori* induces miR-155 in T Cells in a cAMP-Foxp3-Dependent Manner. PLoS One *5*, e9500.

Ferguson, D.A., Jr., Li, C., Patel, N.R., Mayberry, W.R., Chi, D.S., and Thomas, E. (1993). Isolation of *Helicobacter pylori* from saliva. J Clin Microbiol *31*, 2802-2804.

Ferrero, R.L., Ave, P., Ndiaye, D., Bambou, J.C., Huerre, M.R., Philpott, D.J., and Memet, S. (2008). NF-kappaB activation during acute *Helicobacter pylori* infection in mice. Infect Immun *76*, 551-561.

Figura, N. (1997). *Helicobacter pylori* factors involved in the development of gastroduodenal mucosal damage and ulceration. J Clin Gastroenterol *25 (Suppl 1)*, S149-163.

Finkelman, F.D., Katona, I.M., Mosmann, T.R., and Coffman, R.L. (1988). IFN-gamma regulates the isotypes of Ig secreted *in vivo* humoral immune responses. J Immunol *140*, 1022–1027.

Fiocca, R., Villani, L., De Giacomo, C., Perego, M., Trespi, E., and Solcia, E. (1989). Morphological evidence of *Campylobacter pylori* pathogenicity in chronic gastritis and peptic ulcer. Acta Gastroenterol Belg *52*, 324-335.

Fischer, W. (2011). Assembly and molecular mode of action of the *Helicobacter pylori* Cag type IV secretion apparatus. FEBS J *278*, 1203-1212.

Fischer, W., Puls, J., Buhrdorf, R., Gebert, B., Odenbreit, S., and Haas, R. (2001). Systematic mutagenesis of the *Helicobacter pylori cag* pathogenicity island: essential genes for CagA translocation in host cells and induction of interleukin-8. Mol Microbiol *42*, 1337-1348.

Fitzgerald, D.C., Meade, K.G., McEvoy, A.N., Lillis, L., Murphy, E.P., MacHugh, D.E., and Baird, A.W. (2007). Tumour necrosis factor-alpha (TNF-alpha) increases nuclear factor kappaB (NFkappaB) activity in and interleukin-8 (IL-8) release from bovine mammary epithelial cells. Vet Immunol Immunopathol *116*, 59-68.

Forwood, J.K., Lam, M.H., and Jans, D.A. (2001). Nuclear import of Creb and AP-1 transcription factors requires importin-beta 1 and Ran but is independent of importin-alpha. Biochemistry *40*, 5208-5217.

Franco, R., Schoneveld, O., Georgakilas, A.G., and Panayiotidis, M.I. (2008). Oxidative stress, DNA methylation and carcinogenesis. Cancer Lett *266*, 6-11.

Freedberg, A.S., and Baron, L.E. (1940). The presence of spirochetes in human gastric mucosa. Am J Dig Dis *7*, 443-445.

Gauthier, N.C., Monzo, P., Gonzalez, T., Doye, A., Oldani, A., Gounon, P., Ricci, V., Cormont, M., and Boquet, P. (2007). Early endosomes associated with dynamic F-actin structures are required for late trafficking of *H. pylori* VacA toxin. J Cell Biol *177*, 343-354.

Gauthier, N.C., Monzo, P., Kaddai, V., Doye, A., Ricci, V., and Boquet, P. (2005). *Helicobacter pylori* VacA cytotoxin: a probe for a clathrin-independent and Cdc42-dependent pinocytic pathway routed to late endosomes. Mol Biol Cell *16*, 4852-4866.

Geis, G., Leying, H., Suerbaum, S., Mai, U., and Opferkuch, W. (1989). Ultrastructure and chemical analysis of *Campylobacter pylori* flagella. J Clin Microbiol *27*, 436-441.

Gerhard, M., Lehn, N., Neumayer, N., Boren, T., Rad, R., Schepp, W., Miehlke, S., Classen, M., and Prinz, C. (1999). Clinical relevance of the *Helicobacter pylori* gene for blood-group antigen-binding adhesin. Proc Natl Acad Sci U S A *96*, 12778-12783.

Gionchetti, P., Vaira, D., Campieri, M., Holton, J., Menegatti, M., Belluzzi, A., Bertinelli, E., Ferretti, M., Brignola, C., Miglioli, M., and Barbara, L. (1994). Enhanced mucosal interleukin-6 and -8 in *Helicobacter pylori*-positive dyspeptic patients. Am J Gastroenterol *89*, 883-887.

Glocker, E., Lange, C., Covacci, A., Bereswill, S., Kist, M., and Pahl, H.L. (1998). Proteins encoded by the *cag* pathogenicity island of *Helicobacter pylori* are required for NF-kappaB activation. Infect Immun *66*, 2346-2348.

Goh, K.L., and Parasakthi, N. (2001). The racial cohort phenomenon: seroepidemiology of *Helicobacter pylori* infection in a multiracial South-East Asian country. Eur J Gastroenterol Hepatol *13*, 177-183.

Gold, B.D., Colletti, R.B., Abbott, M., Czinn, S.J., Elitsur, Y., Hassall, E., Macarthur, C., Snyder, J., Sherman, P.M., and North American Society for Pediatric Gastroenterology and Nutrition. (2000). *Helicobacter pylori* infection in children: recommendations for diagnosis and treatment. J Pediatr Gastroenterol Nutr *31*, 490-497.

Goll, R., Gruber, F., Olsen, T., Cui, G., Raschpichler, G., Buset, M., Asfeldt, A.M., Husebekk, A., and Florholmen, J. (2007). *Helicobacter pylori* stimulates a mixed adaptive immune response with a strong T-regulatory component in human gastric mucosa. Helicobacter *12*, 185-192.

Gong, M. (2006). Characterization of *Helicobacter pylori* γ-glutamyl transpeptidase and its role in pathogenesis. Ph.D. thesis, National University of Singapore.

Gong, M., and Ho, B. (2004). Prominent role of gamma-glutamyl-transpeptidase on the growth of *Helicobacter pylori*. World J Gastroenterol *10*, 2994-2996.

Goodwin, C.S., Armstrong, J.A., Chilvers, T., Peters, M., Collins, M.D., Sly, L., McConnell, W., and Harper, W.E.S. (1989). Transfer of *Campylobacter pylori* and *Campylobacter mustelae* to *Helicobacter* gen. nov. as *Helicobacter pylori* comb. nov. and *Helicobacter mustelae* comb. nov., respectively. Int J Syst Bacteriol *39*, 397-405.

Goodwin, C.S., McCulloch, R.K., Armstrong, J.A., and Wee, S.H. (1985). Unusual cellular fatty acids and distinctive ultrastructure in a new spiral bacterium (*Campylobacter pyloridis*) from the human gastric mucosa. J Med Microbiol *19*, 257-267.

Graham, D.Y., Malaty, H.M., Evans, D.G., Evans, D.J., Jr., Klein, P.D., and Adam, E. (1991). Epidemiology of *Helicobacter pylori* in an asymptomatic population in the United States. Effect of age, race, and socioeconomic status. Gastroenterology *100*, 1495-1501.

Grant, C.M., MacIver, F.H., and Dawes, I.W. (1996). Glutathione is an essential metabolite required for resistance to oxidative stress in the yeast *Saccharomyces cerevisiae*. Curr Genet *29*, 511-515.

Grebowska, A., Moran, A.P., Matusiak, A., Bak-Romaniszyn, L., Czkwianianc, E., Rechciński, T., Walencka, M., Płaneta-Małecka, I., Rudnicka, W., and Chmiela, M. (2008). Anti-phagocytic activity of *Helicobacter pylori* lipopolysaccharide (LPS) - possible modulation of the innate immune response to these bacteria. Pol J Microbiol *57*, 185-192.

Gupta, V.R., Patel, H.K., Kostolansky, S.S., Ballivian, R.A., Eichberg, J., and Blanke, S.R. (2008). Sphingomyelin functions as a novel receptor for *Helicobacter pylori* VacA. PLoS Pathog *4*, e1000073.

Haigler, H.T., McKanna, J.A., and Cohen, S. (1979). Rapid stimulation of pinocytosis in human carcinoma cells A-431 by epidermal growth factor. J Cell Biol *83*, 82-90.

Hailstones, D., Sleer, L.S., Parton, R.G., and Stanley, K.K. (1998). Regulation of caveolin and caveolae by cholesterol in MDCK cells. J Lipid Res *39*, 369-379.

Handa, O., Naito, Y., and Yoshikawa, T. (2010). *Helicobacter pylori*: a ROS-inducing bacterial species in the stomach. Inflamm Res *59*, 997-1003.

Handt, L.K., Fox, J.G., Dewhirst, F.E., Fraser, G.J., Paster, B.J., Yan, L.L., Rozmiarek, H., Rufo, R., and Stalis, I.H. (1994). *Helicobacter pylori* isolated from the domestic cat: public health implications. Infect Immun *62*, 2367-2374.

Hanigan, M.H. (1998). gamma-Glutamyl transpeptidase, a glutathionase: its expression and function in carcinogenesis. Chem Biol Interact *111-112*, 333-342.

Hanigan, M.H., and Frierson, H.F., Jr. (1996). Immunohistochemical detection of gamma-glutamyl transpeptidase in normal human tissue. J Histochem Cytochem *44*, 1101-1108.

Hanigan, M.H., and Ricketts, W.A. (1993). Extracellular glutathione is a source of cysteine for cells that express gamma-glutamyl transpeptidase. Biochemistry *32*, 6302-6306.

Harris, A.G., Wilson, J.E., Danon, S.J., Dixon, M.F., Donegan, K., and Hazell, S.L. (2003). Catalase (KatA) and KatA-associated protein (KapA) are essential to persistent colonization in the *Helicobacter pylori* SS1 mouse model. Microbiology *149*, 665-672.

Harris, P.R., Cover, T.L., Crowe, D.R., Orenstein, J.M., Graham, M.F., Blaser, M.J., and Smith, P.D. (1996). *Helicobacter pylori* cytotoxin induces vacuolation of primary human mucosal epithelial cells. Infect Immun *64*, 4867-4871.

Hatakeyama, M. (2008). SagA of CagA in *Helicobacter pylori* pathogenesis. Curr Opin Microbiol *11*, 30-37.

Hawtin, P.R., Stacey, A.R., and Newell, D.G. (1990). Investigation of the structure and localization of the urease of *Helicobacter pylori* using monoclonal antibodies. J Gen Microbiol *136*, 1995-2000.

Hazell, S.L., Evans, D.J., Jr., and Graham, D.Y. (1991). *Helicobacter pylori* catalase. J Gen Microbiol *137*, 57-61.

Hazell, S.L., Lee, A., Brady, L., and Hennessy, W. (1986). *Campylobacter pyloridis* and gastritis: association with intercellular spaces and adaptation to an environment of mucus as important factors in colonization of the gastric epithelium. J Infect Dis *153*, 658-663.

Hedley, D.W., and Chow, S. (1994). Evaluation of methods for measuring cellular glutathione content using flow cytometry. Cytometry *15*, 349-358.

Henley, J.R., Krueger, E.W., Oswald, B.J., and McNiven, M.A. (1998). Dynamin-mediated internalization of caveolae. J Cell Biol *141*, 85-99.

Hessey, S.J., Spencer, J., Wyatt, J.I., Sobala, G., Rathbone, B.J., Axon, A.T., and Dixon, M.F. (1990). Bacterial adhesion and disease activity in *Helicobacter* associated chronic gastritis. Gut *31*, 134-138.

Higashi, H., Tsutsumi, R., Muto, S., Sugiyama, T., Azuma, T., Asaka, M., and Hatakeyama, M. (2002). SHP-2 tyrosine phosphatase as an intracellular target of *Helicobacter pylori* CagA protein. Science *295*, 683-686.

Hirota, K., Nagata, K., Norose, Y., Futagami, S., Nakagawa, Y., Senpuku, H., Kobayashi, M., and Takahashi, H. (2001). Identification of an antigenic epitope in *Helicobacter pylori* urease that induces neutralizing antibody production. Infect Immun *69*, 6597-6603.

Hirschl, A.M., Rathbone, B.J., Wyatt, J.I., Berger, J., and Rotter, M.L. (1990). Comparison of ELISA antigen preparations alone or in combination for serodiagnosing *Helicobacter pylori* infections. J Clin Pathol *43*, 511-513.

Hisatsune, J., Nakayama, M., Isomoto, H., Kurazono, H., Mukaida, N., Mukhopadhyay, A.K., Azuma, T., Yamaoka, Y., Sap, J., Yamasaki, E., Yahiro, K., Moss, J., and Hirayama, T. (2008). Molecular characterization of *Helicobacter pylori* VacA induction of IL-8 in U937 cells reveals a prominent role for p38MAPK in activating transcription factor-2, cAMP response element binding protein, and NF-kappaB activation. J Immunol *180*, 5017-5027.

Ho, B., and Vijayakumari, S. (1993). A simple and efficient continuous culture system for *Helicobacter pylori*. Microbios *76*, 59-66.

Hoang, T.T., Wheeldon, T.U., Bengtsson, C., Phung, D.C., Sörberg, M., and Granström, M. (2004). Enzyme-linked immunosorbent assay for *Helicobacter pylori* needs adjustment for the population investigated. J Clin Microbiol *42*, 627-630.

Hoffman, P.S., Vats, N., Hutchison, D., Butler, J., Chisholm, K., Sisson, G., Raudonikiene, A., Marshall, J.S., and Veldhuyzen van Zanten, S.J. (2003). Development of an interleukin-12-deficient mouse model that is permissive for colonization by a motile KE26695 strain of *Helicobacter pylori*. Infect Immun *71*, 2534-2541.

Hotchin, N.A., Cover, T.L., and Akhtar, N. (2000). Cell vacuolation induced by the VacA cytotoxin of *Helicobacter pylori* is regulated by the Rac1 GTPase. J Biol Chem *275*, 14009-14012.

Hua, J., and Ho, B. (1996). Is the coccoid form of *Helicobacter pylori* viable? Microbios *87*, 103-112.

Hua, J.S., Ho, B., Zheng, P.Y., and Yeoh, K.G. (2000). Prevalence of primary *Helicobacter pylori* resistance to metronidazole and clarithromycin in Singapore. World J Gastroenterol *6*, 119-121.

Huang, C.H., and Chiou, S.H. (2011). Proteomic analysis of upregulated proteins in *Helicobacter pylori* under oxidative stress induced by hydrogen peroxide. Kaohsiung J Med Sci *27*, 544-553.

Ilver, D., Arnqvist, A., Ogren, J., Frick, I.M., Kersulyte, D., Incecik, E.T., Berg, D.E., Covacci, A., Engstrand, L., and Boren, T. (1998). *Helicobacter pylori* adhesin binding fucosylated histo-blood group antigens revealed by retagging. Science *279*, 373-377.

Inoue, Y., Tanaka, N., Tanaka, Y., Inoue, S., Morita, K., Zhuang, M., Hattori, T., and Sugamura, K. (2007). Clathrin-dependent entry of severe acute respiratory syndrome coronavirus into target cells expressing ACE2 with the cytoplasmic tail deleted. J Virol *81*, 8722-8729.

International Agency for Research on Cancer. (1994). Schistosomes, liver flukes and *Helicobacter pylori*. IARC Monogr Eval Carcinog Risks Hum *61*, 1-241.

Isomoto, H., Moss, J., and Hirayama, T. (2010). Pleiotropic actions of *Helicobacter pylori* vacuolating cytotoxin, VacA. Tohoku J Exp Med *220*, 3-14.

Jackson, L., Britton, J., Lewis, S.A., McKeever, T.M., Atherton, J., Fullerton, D., and Fogarty, A.W. (2009). A population-based epidemiologic study of *Helicobacter pylori* infection and its association with systemic inflammation. Helicobacter *14*, 108-113.

Jacobs, M.D., and Harrison, S.C. (1998). Structure of an IkappaBalpha/NF-kappaB complex. Cell *95*, 749-758.

Jung, H.K., Lee, K.E., Chu, S.H., and Yi, S.Y. (2001). Reactive oxygen species activity, mucosal lipoperoxidation and glutathione in *Helicobacter pylori*-infected gastric mucosa. J Gastroenterol Hepatol *16*, 1336-1340.

Kai, H., Kitadai, Y., Kodama, M., Cho, S., Kuroda, T., Ito, M., Tanaka, S., Ohmoto, Y., and Chayama, K. (2005). Involvement of proinflammatory cytokines IL-1beta and IL-6 in progression of human gastric carcinoma. Anticancer Res *25*, 709-713.

Kandulski, A., Malfertheiner, P., and Wex, T. (2010). Role of regulatory T-cells in *H. pylori*-induced gastritis and gastric cancer. Anticancer Res *30*, 1093-1103.

Kang, J.Y., Yeoh, K.G., Ho, K.Y., Guan, R., Lim, T.P., Quak, S.H., Wee, A., Teo, D., and Ong, Y.W. (1997). Racial differences in *Helicobacter pylori* seroprevalence in Singapore: correlation with differences in peptic ulcer frequency. J Gastroenterol Hepatol *12*, 655-659.

Kaur, R., Dikshit, K.L., and Raje, M. (2002). Optimization of immunogold labeling TEM: an ELISA-based method for evaluation of blocking agents for quantitative detection of antigen. J Histochem Cytochem *50*, 863-873.

Keates, S., Hitti, Y.S., Upton, M., and Kelly, C.P. (1997). *Helicobacter pylori* infection activates NF-kappa B in gastric epithelial cells. Gastroenterology *113*, 1099-1109.

Keillor, J.W., Castonguay, R., and Lherbet, C. (2005). Gamma-glutamyl transpeptidase substrate specificity and catalytic mechanism. Methods Enzymol *401*, 449-467.

Kerr, M.C., and Teasdale, R.D. (2009). Defining macropinocytosis. Traffic *10*, 364-371.

Kihlmark, M., Imreh, G., and Hallberg, E. (2001). Sequential degradation of proteins from the nuclear envelope during apoptosis. J Cell Sci *114*, 3643-3653.

Kim, K.M., Lee, S.G., Kim, J.M., Kim, D.S., Song, J.Y., Kang, H.L., Lee, W.K., Cho, M.J., Rhee, K.H., Youn, H.S., and Baik, S.C. (2010). *Helicobacter pylori* gamma-glutamyltranspeptidase induces cell cycle arrest at the G1-S phase transition. J Microbiol *48*, 372-377.

Kim, K.M., Lee, S.G., Park, M.G., Song, J.Y., Kang, H.L., Lee, W.K., Cho, M.J., Rhee, K.H., Youn, H.S., and Baik, S.C. (2007). Gamma-glutamyltranspeptidase of *Helicobacter pylori* induces mitochondria-mediated apoptosis in AGS cells. Biochem Biophys Res Commun *355*, 562-567.

Kim, S.Y., Lee, Y.C., Kim, H.K., and Blaser, M.J. (2006). *Helicobacter pylori* CagA transfection of gastric epithelial cells induces interleukin-8. Cell Microbiol *8*, 97-106.

Klein, P.D., Graham, D.Y., Gaillour, A., Opekun, A.R., and Smith, E.O. (1991). Water source as risk factor for *Helicobacter pylori* infection in Peruvian children. Gastrointestinal Physiology Working Group. Lancet *337*, 1503-1506.

Kohler, M., Haller, H., and Hartmann, E. (1999). Nuclear protein transport pathways. Exp Nephrol *7*, 290-294.

Komada, Y., Inaba, H., Li, Q.S., Azuma, E., Zhou, Y.W., Yamamoto, H., and Sakurai, M. (1999). Epitopes and functional responses defined by a panel of anti-Fas (CD95) monoclonal antibodies. Hybridoma *18*, 391-398.

Konishi, H., Ishibashi, M., Morshed, M.G., and Nakazawa, T. (1992). Cytopathic effects of *Helicobacter pylori* on cultured mammalian cells. J Med Microbiol *37*, 118-122.

Kosugi, S., Hasebe, M., Matsumura, N., Takashima, H., Miyamoto-Sato, E., Tomita, M., and Yanagawa, H. (2009). Six classes of nuclear localization signals specific to different binding grooves of importin alpha. J Biol Chem *284*, 478-485.

Krysko, D.V., Denecker, G., Festjens, N., Gabriels, S., Parthoens, E., D'Herde, K., and Vandenabeele, P. (2006). Macrophages use different internalization mechanisms to clear apoptotic and necrotic cells. Cell Death Differ *13*, 2011-2022.

Kryston, T.B., Georgiev, A.B., Pissis, P., and Georgakilas, A.G. (2011). Role of oxidative stress and DNA damage in human carcinogenesis. Mutat Res *711*, 193-201.

Kuipers, E.J., Thijs, J.C., and Festen, H.P. (1995). The prevalence of *Helicobacter pylori* in peptic ulcer disease. Aliment Pharmacol Ther *9 (Suppl 2)*, 59-69.

Kumari, S., Mg, S., and Mayor, S. (2010). Endocytosis unplugged: multiple ways to enter the cell. Cell Res *20*, 256-275.

Kusters, J.G., Gerrits, M.M., Van Strijp, J.A., and Vandenbroucke-Grauls, C.M. (1997). Coccoid forms of *Helicobacter pylori* are the morphologic manifestation of cell death. Infect Immun *65*, 3672-3679.

Kusugami, K., Ando, T., Ohsuga, M., Imada, A., Shinoda, M., Konagaya, T., Ina, K., Kasuga, N., Fukatsu, A., Ichiyama, S., Nada, T., and Ohta, M. (1997). Mucosal chemokine activity in *Helicobacter pylori* infection. J Clin Gastroenterol *25 (Suppl 1)*, S203-210.

Kwok, T., Backert, S., Schwarz, H., Berger, J., and Meyer, T.F. (2002). Specific entry of *Helicobacter pylori* into cultured gastric epithelial cells via a zipper-like mechanism. Infect Immun *70*, 2108-2120.

Ladeira, M.S., Rodrigues, M.A., Salvadori, D.M., Queiroz, D.M., and Freire-Maia, D.V. (2004). DNA damage in patients infected by *Helicobacter pylori*. Cancer Epidemiol Biomarkers Prev *13*, 631-637.

Lai, C.H., Wang, H.J., Chang, Y.C., Hsieh, W.C., Lin, H.J., Tang, C.H., Sheu, J.J., Lin, C.J., Yang, M.S., Tseng, S.F., and Wang, W.C. (2011). *Helicobacter pylori* CagA-mediated IL-8 induction in gastric epithelial cells is cholesterol-dependent and requires the C-terminal tyrosine phosphorylation-containing domain. FEMS Microbiol Lett *323*, 155-163.

Laine, L., Schoenfeld, P., and Fennerty, M.B. (2001). Therapy for *Helicobacter pylori* in patients with nonulcer dyspepsia. A meta-analysis of randomized, controlled trials. Ann Intern Med *134*, 361-369.

Lam, M.H., Hu, W., Xiao, C.Y., Gillespie, M.T., and Jans, D.A. (2001). Molecular dissection of the importin beta1-recognized nuclear targeting signal of parathyroid hormone-related protein. Biochem Biophys Res Commun *282*, 629-634.

Lamaze, C., Dujeancourt, A., Baba, T., Lo, C.G., Benmerah, A., and Dautry-Varsat, A. (2001). Interleukin 2 receptors and detergent-resistant membrane domains define a clathrin-independent endocytic pathway. Mol Cell *7*, 661-671.

Lange, A., Mills, R.E., Lange, C.J., Stewart, M., Devine, S.E., and Corbett, A.H. (2007). Classical nuclear localization signals: definition, function, and interaction with importin alpha. J Biol Chem *282*, 5101-5105.

Langton, S.R., and Cesareo, S.D. (1992). *Helicobacter pylori* associated phospholipase A2 activity: a factor in peptic ulcer production? J Clin Pathol *45*, 221-224.

Larkin, J.M., Brown, M.S., Goldstein, J.L., and Anderson, R.G. (1983). Depletion of intracellular potassium arrests coated pit formation and receptor-mediated endocytosis in fibroblasts. Cell *33*, 273-285.

Leal, Y.A., Flores, L.L., García-Cortés, L.B., Cedillo-Rivera, R., and Torres, J. (2008). Antibody-based detection tests for the diagnosis of *Helicobacter pylori* infection in children: a meta-analysis. PLoS One *3*, e3751.

Lee, A., O'Rourke, J., De Ungria, M.C., Robertson, B., Daskalopoulos, G., and Dixon, M.F. (1997). A standardized mouse model of *Helicobacter pylori* infection: introducing the Sydney strain. Gastroenterology *112*, 1386-1397.

Lee, B.J., Cansizoglu, A.E., Suel, K.E., Louis, T.H., Zhang, Z., and Chook, Y.M. (2006). Rules for nuclear localization sequence recognition by karyopherin beta 2. Cell *126*, 543-558.

Lenton, K.J., Therriault, H., Fulop, T., Payette, H., and Wagner, J.R. (1999). Glutathione and ascorbate are negatively correlated with oxidative DNA damage in human lymphocytes. Carcinogenesis *20*, 607-613.

Letley, D.P., Lastovica, A., Louw, J.A., Hawkey, C.J., and Atherton, J.C. (1999). Allelic diversity of the *Helicobacter pylori* vacuolating cytotoxin gene in South Africa: rarity of the *vacA* s1a genotype and natural occurrence of an s2/m1 allele. J Clin Microbiol *37*, 1203-1205.

Leung, W.K., Siu, K.L., Kwok, C.K., Chan, S.Y., Sung, R., and Sung, J.J. (1999). Isolation of *Helicobacter pylori* from vomitus in children and its implication in gastro-oral transmission. Am J Gastroenterol *94*, 2881-2884.

Leunk, R.D., Johnson, P.T., David, B.C., Kraft, W.G., and Morgan, D.R. (1988). Cytotoxic activity in broth-culture filtrates of *Campylobacter pylori*. J Med Microbiol *26*, 93-99.

Li, Q., Liu, N., Shen, B., Zhou, L., Wang, Y., Sun, J., Fan, Z., and Liu, R.H. (2009). *Helicobacter pylori* enhances cyclooxygenase 2 expression via p38MAPK/ATF-2 signaling pathway in MKN45 cells. Cancer Lett *278*, 97-103.

Li, S.D., Kersulyte, D., Lindley, I.J., Neelam, B., Berg, D.E., and Crabtree, J.E. (1999). Multiple genes in the left half of the *cag* pathogenicity island of *Helicobacter pylori* are required for tyrosine kinase-dependent transcription of interleukin-8 in gastric epithelial cells. Infect Immun *67*, 3893-3899.

Lieberman, M.W., Barrios, R., Carter, B.Z., Habib, G.M., Lebovitz, R.M., Rajagopalan, S., Sepulveda, A.R., Shi, Z.Z., and Wan, D.F. (1995). gamma-Glutamyl transpeptidase. What does the organization and expression of a multipromoter gene tell us about its functions? Am J Pathol *147*, 1175-1185.

Lim, J.P., and Gleeson, P.A. (2011). Macropinocytosis: an endocytic pathway for internalising large gulps. Immunol Cell Biol *89*, 836-843.

Lim, J.W., Kim, K.H., and Kim, H. (2009). alphaPix interacts with *Helicobacter pylori* CagA to induce IL-8 expression in gastric epithelial cells. Scand J Gastroenterol *44*, 1166-1172.

Linz, B., Balloux, F., Moodley, Y., Manica, A., Liu, H., Roumagnac, P., Falush, D., Stamer, C., Prugnolle, F., van der Merwe, S.W., Yamaoka, Y., Graham, D.Y., Perez-Trallero, E., Wadstrom, T., Suerbaum, S., and Achtman, M. (2007). An African origin for the intimate association between humans and *Helicobacter pylori*. Nature *445*, 915-918.

Lo, H.W., Ali-Seyed, M., Wu, Y., Bartholomeusz, G., Hsu, S.C., and Hung, M.C. (2006). Nuclear-cytoplasmic transport of EGFR involves receptor endocytosis, importin beta1 and CRM1. J Cell Biochem *98*, 1570-1583.

Lu, Y., Redlinger, T.E., Avitia, R., Galindo, A., and Goodman, K. (2002). Isolation and genotyping of *Helicobacter pylori* from untreated municipal wastewater. Appl Environ Microbiol *68*, 1436-1439.

Lui, S.Y., Yeoh, K.G., and Ho, B. (2003). Metronidazole-resistant *Helicobacter pylori* is more prevalent in patients with nonulcer dyspepsia than in peptic ulcer patients in a multiethnic Asian population. J Clin Microbiol *41*, 5011-5014.

Lyons, S.D., Sant, M.E., and Christopherson, R.I. (1990). Cytotoxic mechanisms of glutamine antagonists in mouse L1210 leukemia. J Biol Chem *265*, 11377-11381.

Maeda, S., Akanuma, M., Mitsuno, Y., Hirata, Y., Ogura, K., Yoshida, H., Shiratori, Y., and Omata, M. (2001). Distinct mechanism of *Helicobacter pylori*-mediated NF-kappa B activation between gastric cancer cells and monocytic cells. J Biol Chem *276*, 44856-44864.

Maeda, S., Ogura, K., Yoshida, H., Kanai, F., Ikenoue, T., Kato, N., Shiratori, Y., and Omata, M. (1998). Major virulence factors, VacA and CagA, are commonly positive in *Helicobacter pylori* isolates in Japan. Gut *42*, 338-343.

Magalhaes, A., and Reis, C.A. (2010). *Helicobacter pylori* adhesion to gastric epithelial cells is mediated by glycan receptors. Braz J Med Biol Res *43*, 611-618.

Magnan, S.D., Shirota, F.N., and Nagasawa, H.T. (1982). Drug latentiation by gamma-glutamyl transpeptidase. J Med Chem *25*, 1018-1021.

Mahdavi, J., Sonden, B., Hurtig, M., Olfat, F.O., Forsberg, L., Roche, N., Angstrom, J., Larsson, T., Teneberg, S., Karlsson, K.A., Altraja, S., Wadstrom, T., Kersulyte, D., Berg, D.E., Dubois, A., Petersson, C., Magnusson, K.E., Norberg, T., Lindh, F., Lundskog, B.B., Arnqvist, A., Hammarstrom, L., and Boren, T. (2002). *Helicobacter pylori* SabA adhesin in persistent infection and chronic inflammation. Science *297*, 573-578.

Marcus, E.A., and Scott, D.R. (2001). Cell lysis is responsible for the appearance of extracellular urease in *Helicobacter pylori*. Helicobacter *6*, 93-99.

Marfori, M., Mynott, A., Ellis, J.J., Mehdi, A.M., Saunders, N.F., Curmi, P.M., Forwood, J.K., Boden, M., and Kobe, B. (2011). Molecular basis for specificity of nuclear import and prediction of nuclear localization. Biochim Biophys Acta *1813*, 1562-1577.

Markovic, J., Borras, C., Ortega, A., Sastre, J., Vina, J., and Pallardo, F.V. (2007). Glutathione is recruited into the nucleus in early phases of cell proliferation. J Biol Chem *282*, 20416-20424.

Markovic, J., Garcia-Gimenez, J.L., Gimeno, A., Vina, J., and Pallardo, F.V. (2010). Role of glutathione in cell nucleus. Free Radic Res *44*, 721-733.

Markovic, J., Mora, N.J., Broseta, A.M., Gimeno, A., de-la-Concepcion, N., Vina, J., and Pallardo, F.V. (2009). The depletion of nuclear glutathione impairs cell proliferation in 3t3 fibroblasts. PLoS One *4*, e6413.

Marshall, B.J., Armstrong, J.A., McGechie, D.B., and Glancy, R.J. (1985). Attempt to fulfil Koch's postulates for pyloric Campylobacter. Med J Aust *142*, 436-439.

Marshall, B.J., and Goodwin, C.S. (1987). Revised nomenclature of *Campylobacter pyloridis*. Int J Syst Bacteriol *37*, 68.

Marshall, B.J., Royce, H., Annear, D.I., Goodwin, C.S., Pearman, J.W., Warren, J.R., and Armstrong, J.A. (1984). Original isolation of *Campylobacter pyloridis* from human gastric mucosa. Microbios Lett *25*, 83-88.

Marshall, B.J., and Warren, J.R. (1984). Unidentified curved bacilli in the stomach of patients with gastritis and peptic ulceration. Lancet *1*, 1311-1315.

Martin, M.N., Saladores, P.H., Lambert, E., Hudson, A.O., and Leustek, T. (2007). Localization of members of the gamma-glutamyl transpeptidase family identifies sites of glutathione and glutathione S-conjugate hydrolysis. Plant Physiol *144*, 1715-1732.

Martin, M.N., and Slovin, J.P. (2000). Purified gamma-glutamyl transpeptidases from tomato exhibit high affinity for glutathione and glutathione S-conjugates. Plant Physiol *122*, 1417-1426.

Mates, J.M., Perez-Gomez, C., and Nunez de Castro, I. (1999). Antioxidant enzymes and human diseases. Clin Biochem *32*, 595-603.

Mazari-Hiriart, M., Lopez-Vidal, Y., and Calva, J.J. (2001). *Helicobacter pylori* in water systems for human use in Mexico City. Water Sci Technol *43*, 93-98.

McClain, M.S., Iwamoto, H., Cao, P., Vinion-Dubiel, A.D., Li, Y., Szabo, G., Shao, Z., and Cover, T.L. (2003). Essential role of a GXXXG motif for membrane channel formation by *Helicobacter pylori* vacuolating toxin. J Biol Chem *278*, 12101-12108.

McGovern, K.J., Blanchard, T.G., Gutierrez, J.A., Czinn, S.J., Krakowka, S., and Youngman, P. (2001). gamma-Glutamyltransferase is a *Helicobacter pylori* virulence factor but is not essential for colonization. Infect Immun *69*, 4168-4173.

McIntyre, T., and Curthoys, N.P. (1982). Renal catabolism of glutathione. Characterization of a particulate rat renal dipeptidase that catalyzes the hydrolysis of cysteinylglycine. J Biol Chem *257*, 11915-11921.

Megraud, F., and Broutet, N. (2000). Review article: have we found the source of *Helicobacter pylori*? Aliment Pharmacol Ther *14 (Suppl 3)*, 7-12.

Meister, A., and Anderson, M.E. (1983). Glutathione. Annu Rev Biochem *52*, 711-760.

Mercurio, F., Zhu, H., Murray, B.W., Shevchenko, A., Bennett, B.L., Li, J., Young, D.B., Barbosa, M., Mann, M., Manning, A., and Rao, A. (1997). IKK-1 and IKK-2: cytokine-activated IkappaB kinases essential for NF-kappaB activation. Science *278*, 860-866.

Meyer-ter-Vehn, T., Covacci, A., Kist, M., and Pahl, H.L. (2000). *Helicobacter pylori* activates mitogen-activated protein kinase cascades and induces expression of the proto-oncogenes c-*fos* and c-*jun*. J Biol Chem *275*, 16064-16072.

Miehlke, S., Kirsch, C., Agha-Amiri, K., Gunther, T., Lehn, N., Malfertheiner, P., Stolte, M., Ehninger, G., and Bayerdorffer, E. (2000). The *Helicobacter pylori vacA* s1, m1 genotype and *cagA* is associated with gastric carcinoma in Germany. Int J Cancer *87*, 322-327.

Mimuro, H., Suzuki, T., Tanaka, J., Asahi, M., Haas, R., and Sasakawa, C. (2002). Grb2 is a key mediator of helicobacter pylori CagA protein activities. Mol Cell *10*, 745-755.

Moayyedi, P., Soo, S., Deeks, J., Delaney, B., Harris, A., Innes, M., Oakes, R., Wilson, S., Roalfe, A., Bennett, C., and Forman, D. (2006). Eradication of *Helicobacter pylori* for non-ulcer dyspepsia. Cochrane Database Syst Rev *2*, CD002096.

Mobley, H.L. (1996). The role of *Helicobacter pylori* urease in the pathogenesis of gastritis and peptic ulceration. Aliment Pharmacol Ther *10 (Suppl 1)*, 57-64.

Mobley, H.L.T. (2001). Urease. In: *Helicobacter pylori*: Physiology and Genetics. (Mobley, H.L.T., Mendz, G.L., and Hazell, S.L., Eds.), pp. 179-191. ASM Press, Washington DC.

Moese, S., Selbach, M., Kwok, T., Brinkmann, V., Konig, W., Meyer, T.F., and Backert, S. (2004). *Helicobacter pylori* induces AGS cell motility and elongation via independent signaling pathways. Infect Immun *72*, 3646-3649.

Mohanty, J.G., Jaffe, J.S., Schulman, E.S., and Raible, D.G. (1997). A highly sensitive fluorescent micro-assay of H_2O_2 release from activated human leukocytes using a dihydroxyphenoxazine derivative. J Immunol Methods *202*, 133-141.

Molinari, M., Galli, C., Norais, N., Telford, J.L., Rappuoli, R., Luzio, J.P., and Montecucco, C. (1997). Vacuoles induced by *Helicobacter pylori* toxin contain both late endosomal and lysosomal markers. J Biol Chem *272*, 25339-25344.

Montecucco, C., and de Bernard, M. (2003). Molecular and cellular mechanisms of action of the vacuolating cytotoxin (VacA) and neutrophil-activating protein (HP-NAP) virulence factors of *Helicobacter pylori*. Microbes Infect *5*, 715-721.

Moodley, Y., and Linz, B. (2009). *Helicobacter pylori* sequences reflect past human migrations. Genome Dyn *6*, 62-74.

Moodley, Y., Linz, B., Yamaoka, Y., Windsor, H.M., Breurec, S., Wu, J.Y., Maady, A., Bernhoft, S., Thiberge, J.M., Phuanukoonnon, S., Jobb, G., Siba, P., Graham, D.Y., Marshall, B.J., and Achtman, M. (2009). The peopling of the Pacific from a bacterial perspective. Science *323*, 527-530.

Morales, A., Miranda, M., Sanchez-Reyes, A., Biete, A., and Fernandez-Checa, J.C. (1998). Oxidative damage of mitochondrial and nuclear DNA induced by ionizing radiation in human hepatoblastoma cells. Int J Radiat Oncol Biol Phys *42*, 191-203.

Morris, A., and Nicholson, G. (1987). Ingestion of *Campylobacter pyloridis* causes gastritis and raised fasting gastric pH. Am J Gastroenterol *82*, 192-199.

Morrow, A.L., Williams, K., Sand, A., Boanca, G., and Barycki, J.J. (2007). Characterization of *Helicobacter pylori* gamma-glutamyltranspeptidase reveals the molecular basis for substrate specificity and a critical role for the tyrosine 433-containing loop in catalysis. Biochemistry *46*, 13407-13414.

Mosammaparast, N., and Pemberton, L.F. (2004). Karyopherins: from nuclear-transport mediators to nuclear-function regulators. Trends Cell Biol *14*, 547-556.

Mukhopadhyay, A.K., Kersulyte, D., Jeong, J.Y., Datta, S., Ito, Y., Chowdhury, A., Chowdhury, S., Santra, A., Bhattacharya, S.K., Azuma, T., Nair, G.B., and Berg, D.E. (2000). Distinctiveness of genotypes of *Helicobacter pylori* in Calcutta, India. J Bacteriol *182*, 3219-3227.

Muotiala, A., Helander, I.M., Pyhala, L., Kosunen, T.U., and Moran, A.P. (1992). Low biological activity of *Helicobacter pylori* lipopolysaccharide. Infect Immun *60*, 1714-1716.

Nagata, K., Yu, H., Nishikawa, M., Kashiba, M., Nakamura, A., Sato, E.F., Tamura, T., and Inoue, M. (1998). *Helicobacter pylori* generates superoxide radicals and modulates nitric oxide metabolism. J Biol Chem *273*, 14071-14073.

Naito, Y., and Yoshikawa, T. (2002). Molecular and cellular mechanisms involved in *Helicobacter pylori*-induced inflammation and oxidative stress. Free Radic Biol Med *33*, 323-336.

Nakayama, R., Kumagai, H., and Tochikura, T. (1984). gamma-Glutamyltranspeptidase from *Proteus mirabilis*: localization and activation by phospholipids. J Bacteriol *160*, 1031-1036.

Ng, B.L., Ng, H.C., Goh, K.T., and Ho, B. (2001). *Helicobacter pylori* in familial clusters based on antibody profile. FEMS Immunol Med Microbiol *30*, 139-142.

Ng, B.L., Quak, S.H., Aw, M., Goh, K.T., and Ho, B. (2003). Immune responses to differentiated forms of *Helicobacter pylori* in children with epigastric pain. Clin Diagn Lab Immunol *10*, 866-869.

Nilsson, C., Sillen, A., Eriksson, L., Strand, M.L., Enroth, H., Normark, S., Falk, P., and Engstrand, L. (2003). Correlation between *cag* pathogenicity island composition and *Helicobacter pylori*-associated gastroduodenal disease. Infect Immun *71*, 6573-6581.

Nilsson, C., Skoglund, A., Moran, A.P., Annuk, H., Engstrand, L., and Normark, S. (2006). An enzymatic ruler modulates Lewis antigen glycosylation of *Helicobacter pylori* LPS during persistent infection. Proc Natl Acad Sci U S A *103*, 2863-2868.

Nishiya, D., Shimoyama, T., Fukuda, S., Yoshimura, T., Tanaka, M., and Munakata, A. (2000). Evaluation of the clinical relevance of the *iceA1* gene in patients with *Helicobacter pylori* infection in Japan. Scand J Gastroenterol *35*, 36-39.

Noach, L.A., Bosma, N.B., Jansen, J., Hoek, F.J., van Deventer, S.J., and Tytgat, G.N. (1994a). Mucosal tumor necrosis factor-alpha, interleukin-1 beta, and interleukin-8 production in patients with *Helicobacter pylori* infection. Scand J Gastroenterol *29*, 425-429.

Noach, L.A., Rolf, T.M., and Tytgat, G.N. (1994b). Electron microscopic study of association between *Helicobacter pylori* and gastric and duodenal mucosa. J Clin Pathol *47*, 699-704.

Nomura, A., Stemmermann, G.N., Chyou, P.H., Perez-Perez, G.I., and Blaser, M.J. (1994). *Helicobacter pylori* infection and the risk for duodenal and gastric ulceration. Ann Intern Med *120*, 977-981.

Nomura, A.M., Perez-Perez, G.I., Lee, J., Stemmermann, G., and Blaser, M.J. (2002). Relation between *Helicobacter pylori cagA* status and risk of peptic ulcer disease. Am J Epidemiol *155*, 1054-1059.

Norbury, C.C., Chambers, B.J., Prescott, A.R., Ljunggren, H.G., and Watts, C. (1997). Constitutive macropinocytosis allows TAP-dependent major histocompatibility complex class I presentation of exogenous soluble antigen by bone marrow-derived dendritic cells. Eur J Immunol *27*, 280-288.

Norkin, L.C., Anderson, H.A., Wolfrom, S.A., and Oppenheim, A. (2002). Caveolar endocytosis of simian virus 40 is followed by brefeldin A-sensitive transport to the endoplasmic reticulum, where the virus disassembles. J Virol *76*, 5156-5166.

Nozawa, Y., Nishihara, K., Peek, R.M., Nakano, M., Uji, T., Ajioka, H., Matsuura, N., and Miyake, H. (2002). Identification of a signaling cascade for interleukin-8 production by *Helicobacter pylori* in human gastric epithelial cells. Biochem Pharmacol *64*, 21-30.

O'Hara, A.M., Bhattacharyya, A., Mifflin, R.C., Smith, M.F., Ryan, K.A., Scott, K.G., Naganuma, M., Casola, A., Izumi, T., Mitra, S., Ernst, P.B., and Crowe, S.E. (2006). Interleukin-8 induction by *Helicobacter pylori* in gastric epithelial cells is dependent on apurinic/apyrimidinic endonuclease-1/redox factor-1. J Immunol *177*, 7990-7999.

Obst, B., Wagner, S., Sewing, K.F., and Beil, W. (2000). *Helicobacter pylori* causes DNA damage in gastric epithelial cells. Carcinogenesis *21*, 1111-1115.

Odenbreit, S., Gebert, B., Puls, J., Fischer, W., and Haas, R. (2001). Interaction of *Helicobacter pylori* with professional phagocytes: role of the *cag* pathogenicity island and translocation, phosphorylation and processing of CagA. Cell Microbiol *3*, 21-31.

Odenbreit, S., Puls, J., Sedlmaier, B., Gerland, E., Fischer, W., and Haas, R. (2000). Translocation of *Helicobacter pylori* CagA into gastric epithelial cells by type IV secretion. Science *287*, 1497-1500.

Odenbreit, S., Wieland, B., and Haas, R. (1996). Cloning and genetic characterization of *Helicobacter pylori* catalase and construction of a catalase-deficient mutant strain. J Bacteriol *178*, 6960-6967.

Ogura, K., Takahashi, M., Maeda, S., Ikenoue, T., Kanai, F., Yoshida, H., Shiratori, Y., Mori, K., Mafune, K.I., and Omata, M. (1998). Interleukin-8 production in primary cultures of human gastric epithelial cells induced by *Helicobacter pylori*. Dig Dis Sci *43*, 2738-2743.

Olofsson, A., Vallström, A., Petzold, K., Tegtmeyer, N., Schleucher, J., Carlsson, S., Haas, R., Backert, S., Wai, S.N., Gröbner, G., and Arnqvist, A. (2010). Biochemical

and functional characterization of *Helicobacter pylori* vesicles. Mol Microbiol *77*, 1539-1555.

Ota, H., Nakayama, J., Momose, M., Hayama, M., Akamatsu, T., Katsuyama, T., Graham, D.Y., and Genta, R.M. (1998). *Helicobacter pylori* infection produces reversible glycosylation changes to gastric mucins. Virchows Arch *433*, 419-426.

Ottemann, K.M., and Lowenthal, A.C. (2002). *Helicobacter pylori* uses motility for initial colonization and to attain robust infection. Infect Immun *70*, 1984-1990.

Owen, R.J. (1995). Bacteriology of *Helicobacter pylori*. Bailliere's Clin Gastroenterol *9*, 415-446.

Page, E., Winterfield, J., Goings, G., Bastawrous, A., and Upshaw-Earley, J. (1998). Water channel proteins in rat cardiac myocyte caveolae: osmolarity-dependent reversible internalization. Am J Physiol *274*, H1988-2000.

Palmeri, D., and Malim, M.H. (1999). Importin beta can mediate the nuclear import of an arginine-rich nuclear localization signal in the absence of importin alpha. Mol Cell Biol *19*, 1218-1225.

Papini, E., Bugnoli, M., de Bernard, M., Figura, N., Rappuoli, R., and Montecucco, C. (1993a). Bafilomycin A1 inhibits *Helicobacter pylori*-induced vacuolization of HeLa cells. Mol Microbiol *7*, 323-327.

Papini, E., de Bernard, M., Bugnoli, M., Milia, E., Rappuoli, R., and Montecucco, C. (1993b). Cell vacuolization induced by *Helicobacter pylori*: inhibition by bafilomycins A1, B1, C1 and D. FEMS Microbiol Lett *113*, 155-159.

Papini, E., de Bernard, M., Milia, E., Bugnoli, M., Zerial, M., Rappuoli, R., and Montecucco, C. (1994). Cellular vacuoles induced by *Helicobacter pylori* originate from late endosomal compartments. Proc Natl Acad Sci U S A *91*, 9720-9724.

Papini, E., Gottardi, E., Satin, B., de Bernard, M., Massari, P., Telford, J., Rappuoli, R., Sato, S.B., and Montecucco, C. (1996). The vacuolar ATPase proton pump is present on intracellular vacuoles induced by *Helicobacter pylori*. J Med Microbiol *45*, 84-89.

Papini, E., Satin, B., Bucci, C., de Bernard, M., Telford, J.L., Manetti, R., Rappuoli, R., Zerial, M., and Montecucco, C. (1997). The small GTP binding protein rab7 is essential for cellular vacuolation induced by *Helicobacter pylori* cytotoxin. EMBO J *16*, 15-24.

Papini, E., Zoratti, M., and Cover, T.L. (2001). In search of the *Helicobacter pylori* VacA mechanism of action. Toxicon *39*, 1757-1767.

Parhami-Seren, B., and Margolies, M.N. (1996). Contribution of heavy chain junctional amino acid diversity to antibody affinity among p-azophenylarsonate-specific antibodies. J Immunol *157*, 2066-2072.

Parker, H., Chitcholtan, K., Hampton, M.B., and Keenan, J.I. (2010). Uptake of *Helicobacter pylori* outer membrane vesicles by gastric epithelial cells. Infect Immun *78*, 5054-5061.

Parsonnet, J., Hansen, S., Rodriguez, L., Gelb, A.B., Warnke, R.A., Jellum, E., Orentreich, N., Vogelman, J.H., and Friedman, G.D. (1994). *Helicobacter pylori* infection and gastric lymphoma. N Engl J Med *330*, 1267-1271.

Parton, R.G., Joggerst, B., and Simons, K. (1994). Regulated internalization of caveolae. J Cell Biol *127*, 1199-1215.

Peek, R.M., Jr., and Blaser, M.J. (2002). *Helicobacter pylori* and gastrointestinal tract adenocarcinomas. Nat Rev Cancer *2*, 28-37.

Peek, R.M., Jr., Thompson, S.A., Donahue, J.P., Tham, K.T., Atherton, J.C., Blaser, M.J., and Miller, G.G. (1998). Adherence to gastric epithelial cells induces expression of a *Helicobacter pylori* gene, *iceA*, that is associated with clinical outcome. Proc Assoc Am Physicians *110*, 531-544.

Perez-Perez, G.I., Rothenbacher, D., and Brenner, H. (2004). Epidemiology of *Helicobacter pylori* infection. Helicobacter *9 (Suppl 1)*, 1-6.

Petersen, A.M., and Krogfelt, K.A. (2003). *Helicobacter pylori*: an invading microorganism? A review. FEMS Immunol Med Microbiol *36*, 117-126.

Peterson, W.L. (1991). *Helicobacter pylori* and peptic ulcer disease. N Engl J Med *324*, 1043-1048.

Pho, M.T., Ashok, A., and Atwood, W.J. (2000). JC virus enters human glial cells by clathrin-dependent receptor-mediated endocytosis. J Virol *74*, 2288-2292.

Rajasekaran, S.A., Palmer, L.G., Moon, S.Y., Peralta Soler, A., Apodaca, G.L., Harper, J.F., Zheng, Y., and Rajasekaran, A.K. (2001). Na,K-ATPase activity is required for formation of tight junctions, desmosomes, and induction of polarity in epithelial cells. Mol Biol Cell *12*, 3717-3732.

Rakoff-Nahoum, S. (2006). Why cancer and inflammation? Yale J Biol Med *79*, 123-130.

Ramarao, N., Gray-Owen, S.D., and Meyer, T.F. (2000). *Helicobacter pylori* induces but survives the extracellular release of oxygen radicals from professional phagocytes using its catalase activity. Mol Microbiol *38*, 103-113.

Reyrat, J.M., Lanzavecchia, S., Lupetti, P., de Bernard, M., Pagliaccia, C., Pelicic, V., Charrel, M., Ulivieri, C., Norais, N., Ji, X., Cabiaux, V., Papini, E., Rappuoli, R., and Telford, J.L. (1999). 3D imaging of the 58 kDa cell binding subunit of the *Helicobacter pylori* cytotoxin. J Mol Biol *290*, 459-470.

Rhead, J.L., Letley, D.P., Mohammadi, M., Hussein, N., Mohagheghi, M.A., Eshagh Hosseini, M., and Atherton, J.C. (2007). A new *Helicobacter pylori* vacuolating

cytotoxin determinant, the intermediate region, is associated with gastric cancer. Gastroenterology *133*, 926-936.

Ricci, V., Galmiche, A., Doye, A., Necchi, V., Solcia, E., and Boquet, P. (2000). High cell sensitivity to *Helicobacter pylori* VacA toxin depends on a GPI-anchored protein and is not blocked by inhibition of the clathrin-mediated pathway of endocytosis. Mol Biol Cell *11*, 3897-3909.

Ricci, V., Sommi, P., Fiocca, R., Romano, M., Solcia, E., and Ventura, U. (1997). *Helicobacter pylori* vacuolating toxin accumulates within the endosomal-vacuolar compartment of cultured gastric cells and potentiates the vacuolating activity of ammonia. J Pathol *183*, 453-459.

Riddick, G., and Macara, I.G. (2007). The adapter importin-alpha provides flexible control of nuclear import at the expense of efficiency. Mol Syst Biol *3*, 118.

Robinson, K., Argent, R.H., and Atherton, J.C. (2007). The inflammatory and immune response to *Helicobacter pylori* infection. Best Pract Res Clin Gastroenterol *21*, 237-259.

Roebuck, K.A. (1999a). Oxidant stress regulation of IL-8 and ICAM-1 gene expression: differential activation and binding of the transcription factors AP-1 and NF-kappaB (Review). Int J Mol Med *4*, 223-230.

Roebuck, K.A. (1999b). Regulation of interleukin-8 gene expression. J Interferon Cytokine Res *19*, 429-438.

Romaniuk, P.J., Zoltowska, B., Trust, T.J., Lane, D.J., Olsen, G.J., Pace, N.R., and Stahl, D.A. (1987). *Campylobacter pylori*, the spiral bacterium associated with human gastritis, is not a true *Campylobacter* sp. J Bacteriol *169*, 2137-2141.

Sabharanjak, S., Sharma, P., Parton, R.G., and Mayor, S. (2002). GPI-anchored proteins are delivered to recycling endosomes via a distinct cdc42-regulated, clathrin-independent pinocytic pathway. Dev Cell *2*, 411-423.

Sakamoto, S., Watanabe, T., Tokumaru, T., Takagi, H., Nakazato, H., and Lloyd, K.O. (1989). Expression of Lewis^{a}, Lewis^{b}, Lewis^{x}, Lewis^{y}, siayl-Lewis^{a}, and sialyl-Lewis^{x} blood group antigens in human gastric carcinoma and in normal gastric tissue. Cancer Res *49*, 745-752.

Sambrook, J., Fritsch, E.F., and Maniatis, T. (1989). Molecular cloning: a laboratory manual. Cold Spring Harbor Laboratory, New York.

Sandvig, K., Olsnes, S., Petersen, O.W., and van Deurs, B. (1988). Inhibition of endocytosis from coated pits by acidification of the cytosol. J Cell Biochem *36*, 73-81.

Schafer, F.Q., and Buettner, G.R. (2001). Redox environment of the cell as viewed through the redox state of the glutathione disulfide/glutathione couple. Free Radic Biol Med *30*, 1191-1212.

Schmees, C., Prinz, C., Treptau, T., Rad, R., Hengst, L., Voland, P., Bauer, S., Brenner, L., Schmid, R.M., and Gerhard, M. (2007). Inhibition of T-cell proliferation by *Helicobacter pylori* gamma-glutamyl transpeptidase. Gastroenterology *132*, 1820-1833.

Schmitz, M.L., and Baeuerle, P.A. (1995). Multi-step activation of NF-kappa B/Rel transcription factors. Immunobiology *193*, 116-127.

Schreck, R., Albermann, K., and Baeuerle, P.A. (1992). Nuclear factor kappa B: an oxidative stress-responsive transcription factor of eukaryotic cells (a review). Free Radic Res Commun *17*, 221-237.

Schreck, R., Rieber, P., and Baeuerle, P.A. (1991). Reactive oxygen intermediates as apparently widely used messengers in the activation of the NF-kappa B transcription factor and HIV-1. EMBO J *10*, 2247-2258.

Schuck, P. (1997). Use of surface plasmon resonance to probe the equilibrium and dynamic aspects of interactions between biological macromolecules. Annu Rev Biophys Struct *26*, 541–566.

Scott, D.R., Marcus, E.A., Weeks, D.L., and Sachs, G. (2002). Mechanisms of acid resistance due to the urease system of *Helicobacter pylori*. Gastroenterology *123*, 187-195.

Segal, E.D., Cha, J., Lo, J., Falkow, S., and Tompkins, L.S. (1999). Altered states: involvement of phosphorylated CagA in the induction of host cellular growth changes by *Helicobacter pylori*. Proc Natl Acad Sci U S A *96*, 14559-14564.

Selbach, M., Moese, S., Hauck, C.R., Meyer, T.F., and Backert, S. (2002). Src is the kinase of the *Helicobacter pylori* CagA protein *in vitro* and *in vivo*. J Biol Chem *277*, 6775-6778.

Seo, J.H., Lim, J.W., Kim, H., and Kim, K.H. (2004). *Helicobacter pylori* in a Korean isolate activates mitogen-activated protein kinases, AP-1, and NF-kappaB and induces chemokine expression in gastric epithelial AGS cells. Lab Invest *84*, 49-62.

Seto, K., Hayashi-Kuwabara, Y., Yoneta, T., Suda, H., and Tamaki, H. (1998). Vacuolation induced by cytotoxin from *Helicobacter pylori* is mediated by the EGF receptor in HeLa cells. FEBS Lett *431*, 347-350.

Shahamat, M., Mai, U., Paszko-Kolva, C., Kessel, M., and Colwell, R.R. (1993). Use of autoradiography to assess viability of *Helicobacter pylori* in water. Appl Environ Microbiol *59*, 1231-1235.

Shahamat, M., Mai, U.E., Paszko-Kolva, C., Yamamoto, H., and Colwell, R.R. (1991). Evaluation of liquid media for growth of *Helicobacter pylori*. J Clin Microbiol *29*, 2835-2837.

Shanks, A.M., and El-Omar, E.M. (2009). *Helicobacter pylori* infection, host genetics and gastric cancer. J Dig Dis *10*, 157-164.

Sharma, S.A., Tummuru, M.K., Miller, G.G., and Blaser, M.J. (1995). Interleukin-8 response of gastric epithelial cell lines to *Helicobacter pylori* stimulation *in vitro*. Infect Immun *63*, 1681-1687.

Sheu, S.M., Sheu, B.S., Yang, H.B., Li, C., Chu, T.C., and Wu, J.J. (2002). Presence of *iceA1* but not *cagA*, *cagC*, *cagE*, *cagF*, *cagN*, *cagT*, or *orf13* genes of *Helicobacter pylori* is associated with more severe gastric inflammation in Taiwanese. J Formos Med Assoc *101*, 18-23.

Shevchenko, A., Wilm, M., Vorm, O., and Mann, M. (1996). Mass spectrometric sequencing of proteins silver-stained polyacrylamide gels. Anal Chem *68*, 850-858.

Shibayama, K., Kamachi, K., Nagata, N., Yagi, T., Nada, T., Doi, Y., Shibata, N., Yokoyama, K., Yamane, K., Kato, H., Iinuma, Y., and Arakawa, Y. (2003). A novel apoptosis-inducing protein from *Helicobacter pylori*. Mol Microbiol *47*, 443-451.

Shibayama, K., Wachino, J., Arakawa, Y., Saidijam, M., Rutherford, N.G., and Henderson, P.J. (2007). Metabolism of glutamine and glutathione via gamma-glutamyltranspeptidase and glutamate transport in *Helicobacter pylori*: possible significance in the pathophysiology of the organism. Mol Microbiol *64*, 396-406.

Shimada, T., Watanabe, N., Hiraishi, H., and Terano, A. (1999). Redox regulation of interleukin-8 expression in MKN28 cells. Dig Dis Sci *44*, 266-273.

Shimizu, T., Kusugami, K., Ina, K., Imada, A., Nishio, Y., Hosokawa, T., Ohsuga, M., Shimada, M., Noshiro, M., Kaneko, H., and Ando, T. (2000). *Helicobacter pylori*-associated gastric ulcer exhibits enhanced mucosal chemokine activity at the ulcer site. Digestion *62*, 87-94.

Shirin, H., Pinto, J.T., Liu, L.U., Merzianu, M., Sordillo, E.M., and Moss, S.F. (2001). *Helicobacter pylori* decreases gastric mucosal glutathione. Cancer Lett *164*, 127-133.

Smart, E.J., and Anderson, R.G. (2002). Alterations in membrane cholesterol that affect structure and function of caveolae. Methods Enzymol *353*, 131-139.

Smith, M.F. Jr., Mitchell, A., Li, G., Ding, S., Fitzmaurice, A.M., Ryan, K., Crowe, S., and Goldberg, J.B. (2003). Toll-like receptor (TLR) 2 and TLR5, but not TLR4, are required for *Helicobacter pylori*-induced NF-kappa B activation and chemokine expression by epithelial cells. J Biol Chem *278*, 32552-32560.

Smith, T.K., Ikeda, Y., Fujii, J., Taniguchi, N., and Meister, A. (1995). Different sites of acivicin binding and inactivation of gamma-glutamyl transpeptidases. Proc Natl Acad Sci U S A *92*, 2360-2364.

Smoot, D.T., Resau, J.H., Earlington, M.H., Simpson, M., and Cover, T.L. (1996). Effects of *Helicobacter pylori* vacuolating cytotoxin on primary cultures of human gastric epithelial cells. Gut *39*, 795-799.

Smoot, D.T., Sewchand, J., Young, K., Desbordes, B.C., Allen, C.R., and Naab, T. (2000). A method for establishing primary cultures of human gastric epithelial cells. Methods Cell Sci *22*, 133-136.

Soderdahl, T., Enoksson, M., Lundberg, M., Holmgren, A., Ottersen, O.P., Orrenius, S., Bolcsfoldi, G., and Cotgreave, I.A. (2003). Visualization of the compartmentalization of glutathione and protein-glutathione mixed disulfides in cultured cells. FASEB J *17*, 124-126.

Soldati, T., and Schliwa, M. (2006). Powering membrane traffic in endocytosis and recycling. Nat Rev Mol Cell Biol *7*, 897-908.

Solnick, J.V., Chang, K., Canfield, D.R., and Parsonnet, J. (2003). Natural acquisition of *Helicobacter pylori* infection in newborn rhesus macaques. J Clin Microbiol *41*, 5511-5516.

Spoden, G., Freitag, K., Husmann, M., Boller, K., Sapp, M., Lambert, C., and Florin, L. (2008). Clathrin- and caveolin-independent entry of human papillomavirus type 16--involvement of tetraspanin-enriched microdomains (TEMs). PLoS One *3*, e3313.

Staal, F.J., Anderson, M.T., Staal, G.E., Herzenberg, L.A., and Gitler, C. (1994). Redox regulation of signal transduction: tyrosine phosphorylation and calcium influx. Proc Natl Acad Sci U S A *91*, 3619-3622.

Stark, A.A. (1991). Oxidative metabolism of glutathione by gamma-glutamyl transpeptidase and peroxisome proliferation: the relevance to hepatocarcinogenesis. A hypothesis. Mutagenesis *6*, 241-245.

Stark, A.A., Zeiger, E., and Pagano, D.A. (1993). Glutathione metabolism by gamma-glutamyltranspeptidase leads to lipid peroxidation: characterization of the system and relevance to hepatocarcinogenesis. Carcinogenesis *14*, 183-189.

Steer, H.W. (1975). Ultrastructure of cell migration through the gastric epithelium and its relationship to bacteria. J Clin Pathol *28*, 639-646.

Stuart, L.M., and Ezekowitz, R.A. (2008). Phagocytosis and comparative innate immunity: learning on the fly. Nat Rev Immunol *8*, 131-141.

Suganuma, M., Kuzuhara, T., Yamaguchi, K., and Fujiki, H. (2006). Carcinogenic role of tumor necrosis factor-alpha inducing protein of *Helicobacter pylori* in human stomach. J Biochem Mol Biol *39*, 1-8.

Sugimoto, M., and Yamaoka, Y. (2009). The association of *vacA* genotype and *Helicobacter pylori*-related disease in Latin American and African populations. Clin Microbiol Infect *15*, 835-842.

Sugimoto, M., Zali, M.R., and Yamaoka, Y. (2009). The association of *vacA* genotypes and *Helicobacter pylori*-related gastroduodenal diseases in the Middle East. Eur J Clin Microbiol Infect Dis *28*, 1227-1236.

Suzuki, H., Kumagai, H., and Tochikura, T. (1986). gamma-Glutamyltranspeptidase from *Escherichia coli* K-12: formation and localization. J Bacteriol *168*, 1332-1335.

Suzuki, H., Miura, S., Imaeda, H., Suzuki, M., Han, J.Y., Mori, M., Fukumura, D., Tsuchiya, M., and Ishii, H. (1996). Enhanced levels of chemiluminescence and platelet activating factor in urease-positive gastric ulcers. Free Radic Biol Med *20*, 449-454.

Suzuki, K., and Namiki, H. (2007). Cytoplasmic pH-dependent spreading of polymorphonuclear leukocytes: regulation by pH of PKC subcellular distribution and F-actin assembly. Cell Biol Int *31*, 279-288.

Swanson, J.A. (2008). Shaping cups into phagosomes and macropinosomes. Nat Rev Mol Cell Biol *9*, 639-649.

Swanson, J.A., and Watts, C. (1995). Macropinocytosis. Trends Cell Biol *5*, 424-428.

Takada, Y., Mukhopadhyay, A., Kundu, G.C., Mahabeleshwar, G.H., Singh, S., and Aggarwal, B.B. (2003). Hydrogen peroxide activates NF-kappa B through tyrosine phosphorylation of I kappa B alpha and serine phosphorylation of p65: evidence for the involvement of I kappa B alpha kinase and Syk protein-tyrosine kinase. J Biol Chem *278*, 24233-24241.

Takahashi, H., and Watanabe, H. (2004). Post-translational processing of *Neisseria meningitidis* gamma-glutamyl aminopeptidase and its association with inner membrane facing to the cytoplasmic space. FEMS Microbiol Lett *234*, 27-35.

Takizawa, C.G., Weis, K., and Morgan, D.O. (1999). Ran-independent nuclear import of cyclin B1-Cdc2 by importin beta. Proc Natl Acad Sci U S A *96*, 7938-7943.

Talley, N.J., and Quan, C. (2002). Review article: *Helicobacter pylori* and nonulcer dyspepsia. Aliment Pharmacol Ther *16 (Suppl 1)*, 58-65.

Talley, N.J., and Xia, H.H. (1998). *Helicobacter pylori* infection and non-ulcer dyspepsia. Br Med Bull *54*, 63-69.

Tammer, I., Brandt, S., Hartig, R., Konig, W., and Backert, S. (2007). Activation of Abl by *Helicobacter pylori*: a novel kinase for CagA and crucial mediator of host cell scattering. Gastroenterology *132*, 1309-1319.

Tan, S., and Berg, D.E. (2004). Motility of urease-deficient derivatives of *Helicobacter pylori*. J Bacteriol *186*, 885-888.

Taniguchi, N., and Ikeda, Y. (1998). gamma-Glutamyl transpeptidase: catalytic mechanism and gene expression. Adv Enzymol Relat Areas Mol Biol *72*, 239-278.

Tate, S.S., and Meister, A. (1974). Interaction of gamma-glutamyl transpeptidase with amino acids, dipeptides, and derivatives and analogs of glutathione. J Biol Chem *249*, 7593-7602.

Tate, S.S., and Meister, A. (1977). Affinity labeling of gamma-glutamyl transpeptidase and location of the gamma-glutamyl binding site on the light subunit. Proc Natl Acad Sci U S A *74*, 931-935.

Tate, S.S., and Meister, A. (1978). Serine-borate complex as a transition-state inhibitor of gamma-glutamyl transpeptidase. Proc Natl Acad Sci U S A *75*, 4806-4809.

Tate, S.S., and Meister, A. (1981). gamma-Glutamyl transpeptidase: catalytic, structural and functional aspects. Mol Cell Biochem *39*, 357-368.

Telford, J.L., Ghiara, P., Dell'Orco, M., Comanducci, M., Burroni, D., Bugnoli, M., Tecce, M.F., Censini, S., Covacci, A., Xiang, Z., Papini, E., Montecucco, C., Parente, L., and Rappuoli, R. (1994). Gene structure of the *Helicobacter pylori* cytotoxin and evidence of its key role in gastric disease. J Exp Med *179*, 1653-1658.

Thelander, L., and Reichard, P. (1979). Reduction of ribonucleotides. Annu Rev Biochem *48*, 133-158.

Thomas, J.E., Gibson, G.R., Darboe, M.K., Dale, A., and Weaver, L.T. (1992). Isolation of *Helicobacter pylori* from human faeces. Lancet *340*, 1194-1195.

Thompson, G.A., and Meister, A. (1976). Hydrolysis and transfer reactions catalyzed by gamma-glutamyl transpeptidase; evidence for separate substrate sites and for high affinity of L-cystine. Biochem Biophys Res Commun *71*, 32-36.

Thompson, G.A., and Meister, A. (1977). Interrelationships between the binding sites for amino acids, dipeptides, and gamma-glutamyl donors in gamma-glutamyl transpeptidase. J Biol Chem *252*, 6792-6798.

Tili, E., Michaille, J.J., Wernicke, D., Alder, H., Costinean, S., Volinia, S., and Croce, C.M. (2011). Mutator activity induced by microRNA-155 (miR-155) links inflammation and cancer. Proc Natl Acad Sci U S A *108*, 4908-4913.

Tomb, J.F., White, O., Kerlavage, A.R., Clayton, R.A., Sutton, G.G., Fleischmann, R.D., Ketchum, K.A., Klenk, H.P., Gill, S., Dougherty, B.A., Nelson, K., Quackenbush, J., Zhou, L., Kirkness, E.F., Peterson, S., Loftus, B., Richardson, D., Dodson, R., Khalak, H.G., Glodek, A., McKenney, K., Fitzegerald, L.M., Lee, N., Adams, M.D., Hickey, E.K., Berg, D.E., Gocayne, J.D., Utterback, T.R., Peterson, J.D., Kelley, J.M., Cotton, M.D., Weidman, J.M., Fujii, C., Bowman, C., Watthey, L., Wallin, E., Hayes, W.S., Borodovsky, M., Karp, P.D., Smith, H.O., Fraser, C.M., and Venter, J.C. (1997). The complete genome sequence of the gastric pathogen *Helicobacter pylori*. Nature *388*, 539-547.

Torok, A.M., Bouton, A.H., and Goldberg, J.B. (2005). *Helicobacter pylori* induces interleukin-8 secretion by Toll-like receptor 2- and Toll-like receptor 5-dependent and -independent pathways. Infect Immun *73*, 1523-1531.

Torres, V.J., VanCompernolle, S.E., Sundrud, M.S., Unutmaz, D., and Cover, T.L. (2007). *Helicobacter pylori* vacuolating cytotoxin inhibits activation-induced proliferation of human T and B lymphocyte subsets. J Immunol *179*, 5433-5440.

Townsend, D.M., Tew, K.D., and Tapiero, H. (2003). The importance of glutathione in human disease. Biomed Pharmacother *57*, 145-155.

Traub, L.M. (2011). Regarding the amazing choreography of clathrin coats. PLoS Biol *9*, e1001037.

Tricottet, V., Bruneval, P., Vire, O., Camilleri, J.P., Bloch, F., Bonte, N., and Roge, J. (1986). *Campylobacter*-like organisms and surface epithelium abnormalities in active, chronic gastritis in humans: an ultrastructural study. Ultrastruct Pathol *10*, 113-122.

Truant, R., and Cullen, B.R. (1999). The arginine-rich domains present in human immunodeficiency virus type 1 Tat and Rev function as direct importin beta-dependent nuclear localization signals. Mol Cell Biol *19*, 1210-1217.

Tsao, M.Y., Lin, T.L., Hsieh, P.F., and Wang, J.T. (2009). The 3'-to-5' exoribonuclease (encoded by HP1248) of *Helicobacter pylori* regulates motility and apoptosis-inducing genes. J Bacteriol *191*, 2691-2702.

Uemura, N., Okamoto, S., Yamamoto, S., Matsumura, N., Yamaguchi, S., Yamakido, M., Taniyama, K., Sasaki, N., and Schlemper, R.J. (2001). *Helicobacter pylori* infection and the development of gastric cancer. N Engl J Med *345*, 784-789.

Valko, M., Leibfritz, D., Moncol, J., Cronin, M.T., Mazur, M., and Telser, J. (2007). Free radicals and antioxidants in normal physiological functions and human disease. Int J Biochem Cell Biol *39*, 44-84.

Valko, M., Rhodes, C.J., Moncol, J., Izakovic, M., and Mazur, M. (2006). Free radicals, metals and antioxidants in oxidative stress-induced cancer. Chem Biol Interact *160*, 1-40.

van der Bliek, A.M., Redelmeier, T.E., Damke, H., Tisdale, E.J., Meyerowitz, E.M., and Schmid, S.L. (1993). Mutations in human dynamin block an intermediate stage in coated vesicle formation. J Cell Biol *122*, 553-563.

van Doorn, L.J., Figueiredo, C., Sanna, R., Plaisier, A., Schneeberger, P., de Boer, W., and Quint, W. (1998). Clinical relevance of the *cagA*, *vacA*, and *iceA* status of *Helicobacter pylori*. Gastroenterology *115*, 58-66.

Vandenbroucke-Grauls, C.M., and Appelmelk, B.J. (1998). *Helicobacter pylori* LPS: molecular mimicry with the host and role in autoimmunity. Ital J Gastroenterol Hepatol *30 (Suppl 3)*, S259-260.

Veldhuyzen van Zanten, S.J., and Sherman, P.M. (1994). Indications for treatment of *Helicobacter pylori* infection: a systematic overview. CMAJ *150*, 189-198.

Vercauteren, D., Vandenbroucke, R.E., Jones, A.T., Rejman, J., Demeester, J., De Smedt, S.C., Sanders, N.N., and Braeckmans, K. (2010). The use of inhibitors to study endocytic pathways of gene carriers: optimization and pitfalls. Mol Ther *18*, 561-569.

Viala, J., Chaput, C., Boneca, I.G., Cardona, A., Girardin, S.E., Moran, A.P., Athman, R., Memet, S., Huerre, M.R., Coyle, A.J., DiStefano, P.S., Sansonetti, P.J., Labigne, A., Bertin, J., Philpott, D.J., and Ferrero, R.L. (2004). Nod1 responds to peptidoglycan delivered by the *Helicobacter pylori cag* pathogenicity island. Nat Immunol *5*, 1166-1174.

Vijayakumari, S., Khin, M.M., Jiang, B., and Ho, B. (1995). The pathogenic role of the coccoid form of *Helicobacter pylori*. Cytobios *82*, 251-260.

Voehringer, D.W., McConkey, D.J., McDonnell, T.J., Brisbay, S., and Meyn, R.E. (1998). Bcl-2 expression causes redistribution of glutathione to the nucleus. Proc Natl Acad Sci U S A *95*, 2956-2960.

Wachino, J., Shibayama, K., Suzuki, S., Yamane, K., Mori, S., and Arakawa, Y. (2010). Profile of Expression of *Helicobacter pylori* gamma-glutamyltranspeptidase. Helicobacter *15*, 184-192.

Wada, K., Hiratake, J., Irie, M., Okada, T., Yamada, C., Kumagai, H., Suzuki, H., and Fukuyama, K. (2008). Crystal structures of *Escherichia coli* gamma-glutamyltranspeptidase in complex with azaserine and acivicin: novel mechanistic implication for inhibition by glutamine antagonists. J Mol Biol *380*, 361-372.

Wang, L.H., Rothberg, K.G., and Anderson, R.G. (1993). Mis-assembly of clathrin lattices on endosomes reveals a regulatory switch for coated pit formation. J Cell Biol *123*, 1107-1117.

Warren, J.R., and Marshall, B.J. (1983). Unidentified curved bacilli on gastric epithelium in active chronic gastritis. Lancet *1*, 1273-1275.

Watanabe, T., Tsuge, H., Imagawa, T., Kise, D., Hirano, K., Beppu, M., Takahashi, A., Yamaguchi, K., Fujiki, H., and Suganuma, M. (2010). Nucleolin as cell surface receptor for tumor necrosis factor-alpha inducing protein: a carcinogenic factor of *Helicobacter pylori*. J Cancer Res Clin Oncol *136*, 911-921.

Weeks, D.L., Eskandari, S., Scott, D.R., and Sachs, G. (2000). A H+-gated urea channel: the link between *Helicobacter pylori* urease and gastric colonization. Science *287*, 482-485.

West, M.B., Wickham, S., Quinalty, L.M., Pavlovicz, R.E., Li, C., and Hanigan, M.H. (2011). Autocatalytic cleavage of human gamma-glutamyl transpeptidase is highly dependent on N-glycosylation at asparagine 95. J Biol Chem *286*, 28876-28888.

Whitfield, J.B. (2001). Gamma glutamyl transferase. Crit Rev Clin Lab Sci *38*, 263-355.

Wickham, S., Regan, N., West, M.B., Kumar, V.P., Thai, J., Li, P.K., Cook, P.F., and Hanigan, M.H. (2011). Divergent effects of compounds on the hydrolysis and transpeptidation reactions of gamma-glutamyl transpeptidase. J Enzyme Inhib Med Chem (In press). doi:10.3109/14756366.2011.597748.

Wiedemann, T., Loell, E., Mueller, S., Stoeckelhuber, M., Stolte, M., Haas, R., and Rieder, G. (2009). *Helicobacter pylori cag*-Pathogenicity island-dependent early immunological response triggers later precancerous gastric changes in Mongolian gerbils. PLoS One *4*, e4754.

Willen, R., Carlen, B., Wang, X., Papadogiannakis, N., Odselius, R., and Wadstrom, T. (2000). Morphologic conversion of *Helicobacter pylori* from spiral to coccoid form. Scanning (SEM) and transmission electron microscopy (TEM) suggest viability. Ups J Med Sci *105*, 31-40.

Wroblewski, L.E., Peek, R.M., Jr., and Wilson, K.T. (2010). *Helicobacter pylori* and gastric cancer: factors that modulate disease risk. Clin Microbiol Rev *23*, 713-739.

Wroblewski, L.E., Shen, L., Ogden, S., Romero-Gallo, J., Lapierre, L.A., Israel, D.A., Turner, J.R., and Peek, R.M., Jr. (2009). *Helicobacter pylori* dysregulation of gastric epithelial tight junctions by urease-mediated myosin II activation. Gastroenterology *136*, 236-246.

Wyle, F.A., Tarnawski, A., Schulman, D., and Dabros, W. (1990). Evidence for gastric mucosal cell invasion by *C. pylori*: an ultrastructural study. J Clin Gastroenterol *12 (Suppl 1)*, S92-98.

Xia, H.X., Buckley, M., Keane, C.T., and O'Morain, C.A. (1996). Clarithromycin resistance in *Helicobacter pylori*: prevalence in untreated dyspeptic patients and stability *in vitro*. J Antimicrob Chemother *37*, 473-481.

Xu, K., and Strauch, M.A. (1996). Identification, sequence, and expression of the gene encoding gamma-glutamyltranspeptidase in *Bacillus subtilis*. J Bacteriol *178*, 4319-4322.

Yahiro, K., Niidome, T., Kimura, M., Hatakeyama, T., Aoyagi, H., Kurazono, H., Imagawa, K., Wada, A., Moss, J., and Hirayama, T. (1999). Activation of *Helicobacter pylori* VacA toxin by alkaline or acid conditions increases its binding to a 250-kDa receptor protein-tyrosine phosphatase beta. J Biol Chem *274*, 36693-36699.

Yahiro, K., Wada, A., Nakayama, M., Kimura, T., Ogushi, K., Niidome, T., Aoyagi, H., Yoshino, K., Yonezawa, K., Moss, J., and Hirayama, T. (2003). Protein-tyrosine phosphatase alpha, RPTP alpha, is a *Helicobacter pylori* VacA receptor. J Biol Chem *278*, 19183-19189.

Yajima, N., Hiraishi, H., and Harada, T. (1995). Protection of cultured rat gastric cells against oxidant stress by iron chelation. Role of lipid peroxidation. Dig Dis Sci *40*, 879-886.

Yamaoka, Y. (2008). Increasing evidence of the role of *Helicobacter pylori* SabA in the pathogenesis of gastroduodenal disease. J Infect Dev Ctries *2*, 174-181.

Yamaoka, Y. (2010). Mechanisms of disease: *Helicobacter pylori* virulence factors. Nat Rev Gastroenterol Hepatol *7*, 629-641.

Yamaoka, Y., Kikuchi, S., el-Zimaity, H.M., Gutierrez, O., Osato, M.S., and Graham, D.Y. (2002a). Importance of *Helicobacter pylori oipA* in clinical presentation, gastric inflammation, and mucosal interleukin 8 production. Gastroenterology *123*, 414-424.

Yamaoka, Y., Kita, M., Kodama, T., Imamura, S., Ohno, T., Sawai, N., Ishimaru, A., Imanishi, J., and Graham, D.Y. (2002b). *Helicobacter pylori* infection in mice: Role of outer membrane proteins in colonization and inflammation. Gastroenterology *123*, 1992-2004.

Yamaoka, Y., Kita, M., Kodama, T., Sawai, N., and Imanishi, J. (1996). *Helicobacter pylori cagA* gene and expression of cytokine messenger RNA in gastric mucosa. Gastroenterology *110*, 1744-1752.

Yamaoka, Y., Kodama, T., Gutierrez, O., Kim, J.G., Kashima, K., and Graham, D.Y. (1999). Relationship between *Helicobacter pylori iceA*, *cagA*, and *vacA* status and clinical outcome: studies in four different countries. J Clin Microbiol *37*, 2274-2279.

Yamaoka, Y., Kwon, D.H., and Graham, D.Y. (2000). A M(r) 34,000 proinflammatory outer membrane protein (oipA) of *Helicobacter pylori*. Proc Natl Acad Sci U S A *97*, 7533-7538.

Yamaoka, Y., Ojo, O., Fujimoto, S., Odenbreit, S., Haas, R., Gutierrez, O., El-Zimaity, H.M., Reddy, R., Arnqvist, A., and Graham, D.Y. (2006). *Helicobacter pylori* outer membrane proteins and gastroduodenal disease. Gut *55*, 775-781.

Yamasaki, E., Wada, A., Kumatori, A., Nakagawa, I., Funao, J., Nakayama, M., Hisatsune, J., Kimura, M., Moss, J., and Hirayama, T. (2006). *Helicobacter pylori* vacuolating cytotoxin induces activation of the proapoptotic proteins Bax and Bak, leading to cytochrome c release and cell death, independent of vacuolation. J Biol Chem *281*, 11250-11259.

Yoshikawa, T., and Naito, Y. (2000). The role of neutrophils and inflammation in gastric mucosal injury. Free Radic Res *33*, 785-794.

Yu, J., Leung, W.K., Go, M.Y., Chan, M.C., To, K.F., Ng, E.K., Chan, F.K., Ling, T.K., Chung, S.C., and Sung, J.J. (2002). Relationship between *Helicobacter pylori babA2* status with gastric epithelial cell turnover and premalignant gastric lesions. Gut *51*, 480-484.

Zaterka, S., Eisig, J.N., Chinzon, D., and Rothstein, W. (2007). Factors related to *Helicobacter pylori* prevalence in an adult population in Brazil. Helicobacter *12*, 82-88.

Zhang, J., Johnston, G., Stebler, B., and Keller, E.T. (2001). Hydrogen peroxide activates NFkappaB and the interleukin-6 promoter through NFkappaB-inducing kinase. Antioxid Redox Signal *3*, 493-504.

Zhang, Q., Dawodu, J.B., Etolhi, G., Husain, A., Gemmell, C.G., and Russell, R.I. (1997). Relationship between the mucosal production of reactive oxygen radicals and density of *Helicobacter pylori* in patients with duodenal ulcer. Eur J Gastroenterol Hepatol *9*, 261-265.

Zheng, P.Y., Hua, J., Ng, H.C., and Ho, B. (1999). Unchanged characteristics of *Helicobacter pylori* during its morphological conversion. Microbios *98*, 51-64.

Zheng, P.Y., Hua, J., Yeoh, K.G., and Ho, B. (2000). Association of peptic ulcer with increased expression of Lewis antigens but not *cagA*, *iceA*, and *vacA* in *Helicobacter pylori* isolates in an Asian population. Gut *47*, 18-22.

APPENDICES

Note: “qsp” stands for “quantité suffisante pour” or “quantity sufficient for”.

Appendix 1

Chocolate blood agar

For a 500 ml preparation:

Blood agar base No. 2 (Oxoid)	20.0 g
Distilled water	475 ml
Horse blood (Quad Five)	25 ml

1. The blood agar base No. 2 and distilled water were mixed in a 500 ml bottle.
2. The mixture was then autoclaved at 121°C for 20 minutes.
3. The agar was cooled to 50°C before the horse blood was added aseptically.
4. The blood was lysed by immersing the bottle containing the molten agar in an 80°C water bath for 10 minutes with constant swirling.
5. The chocolate blood agar was subsequently cooled to 50°C before pouring into sterile petri dishes (Sterilin).
6. The plates were stored at 4°C until use.

Appendix 2

Medium for screening antibiotic resistant constructs

Kanamycin stock (20 mg/ml)

For a 10 ml preparation:

Kanamycin (Sigma-Aldrich)	200 mg
Distilled water	10 ml (qsp)

Chloramphenicol stock (15 mg/ml)

For a 10 ml preparation:

Chloramphenicol (Sigma-Aldrich)	150 mg
Absolute ethanol (Merck)	10 ml (qsp)

1. The respective antibiotic solutions were sterilized by filtering through a 0.22 µm filter (Millipore).
2. They were then kept as 500 µl aliquots at -20°C until use.

Chocolate blood agar + kanamycin (20 µg/ml) or chloramphenicol (15 µg/ml)

For a 500 ml preparation:

Blood agar base No. 2 (Oxoid)	20.0 g
Distilled water	475 ml
Horse blood (Quad Five)	25 ml

1. The blood agar base No. 2 and distilled water were mixed in a 500 ml bottle.
2. The mixture was then autoclaved at 121°C for 20 minutes.
3. The agar was then cooled to 50°C before the horse blood was added aseptically.
4. The blood was lysed by immersing the bottle containing the molten agar in an 80°C water bath for 10 minutes with constant swirling.
5. The chocolate blood agar was subsequently cooled to 50°C before addition of 500 µl kanamycin (20 mg/ml) or 500 µl chloramphenicol (15 mg/ml) and poured into sterile petri dishes (Sterilin).
6. The plates were stored at 4°C until use.

Appendix 3

Brain Heart Infusion broth with glycerol

For a 300 ml preparation:

Brain Heart Infusion (Oxoid)	11.4 g
Yeast Extract (Oxoid)	1.2 g
Glycerol	60 ml
Distilled water	210 ml
Horse serum (Gibco)	30 ml

1. The brain heart infusion, yeast extract, glycerol and distilled water were mixed.
2. The mixture was then autoclaved at 121°C for 20 minutes.
3. The medium was cooled before 30 ml of horse serum was added.

Appendix 4

0.01 M Tris-EDTA (TE) buffer

For a 1 litre preparation:

Tris-base (Merck)	1.211 g
EDTA (Sigma-Aldrich)	0.372 g
Distilled water	1000 ml (qsp)

Adjust to pH 8.0 using HCl.

Appendix 5

Reaction mixture for PCR amplification

For a 50 µl reaction mixture:

50 ng genomic DNA (working stock of 10 ng/µl)	5 µl
50 pmol primer (forward and reverse)	5 µl each
1 unit *Taq* DNA polymerase (Finnzymes)	0.5 µl
200 µM each of dATP, dGTP, dCTP, dTTP (Promega)	1 µl each
10× incubation buffer (Finnzymes)	5 µl
(10 mM Tris-HCl, 50 mM KCl, 2 mM $MgCl_2$, 0.01% gelatin)	
Sterile distilled water	25.5 µl

Appendix 6

6 × DNA Loading buffer

For a 100 ml preparation:

Bromophenol blue (Bio-Rad)	0.2 g
Xylene cyanol FF (Sigma-Aldrich)	0.2 g
Glycerol (QRec)	60 ml
EDTA (Sigma-Aldrich)	1.861 g
Distilled water	100 ml (qsp)

Appendix 7

Ethidium bromide

For preparation of a 10 mg/ml stock solution:

Ethidium bromide (Sigma-Aldrich)	100 mg
Distilled water	10 ml (qsp)

The solution was kept in the dark at room temperature until use.

Appendix 8

Tris-Acetate-EDTA (TAE) Buffer

For a 1 litre 50 × TAE buffer preparation:

Tris-base (Merck)	242.28 g
Glacial acetic acid (Schedelco)	57.1 ml
EDTA (Sigma-Aldrich)	37.22 g
Distilled water	1000 ml (qsp)

For a litre of 1× TAE buffer preparation:

To 20 ml of 50 × TAE buffer, add 980 ml of distilled water.

Appendix 9

Polyacrylamide gel reagents

Resolving gel buffer (1.5 M Tris-HCl, pH 8.8)

Tris-base (Merck)	90.86 g
Distilled water	500 ml (qsp)

Stacking gel buffer (0.5 M Tris-HCl, pH 6.8)

Tris-base (Merck)	30.29 g
Distilled water	500 ml (qsp)

10% Ammonium persulphate (APS)

Ammonium persulphate (Bio-Rad)	0.5 g
Distilled water	5 ml (qsp)

Only freshly-prepared APS solution was used.

The resolving and stacking gels were prepared as follows:

Resolving gel (12%)

For 1 gel (8.5 cm by 7.5 cm):

Resolving gel buffer	2.5 ml
40% acrylamide (Bio-Rad)	3.0 ml
10% SDS (Merck)	100 µl
TEMED (MP Biochemicals)	5 µl
10% APS (Bio-Rad)	50 µl
Distilled water	4.35 ml

Stacking gel (4%)

For 1 gel (8.5 cm by 7.5 cm):

Stacking gel buffer	1.26 ml
40% acrylamide (Bio-Rad)	0.5 ml
10% SDS (Merck)	50 µl
TEMED (MP Biochemicals)	5 µl
10% APS (Bio-Rad)	25 µl
Distilled water	3.18 ml

Appendix 10

5 × Reducing Loading Buffer

For a 10 ml preparation:

SDS (Merck)	1 g
1 M Tris (pH 6.8) (Merck)	1.563 ml
β-mercaptoethanol (Sigma-Aldrich)	1.25 ml
Glycerol (QRec)	2.5 ml
Bromophenol blue (Bio-Rad)	2.5 mg
Distilled water	10 ml (qsp)

The solution was kept at 4°C until use.

Appendix 11

SDS-PAGE Running Buffer

For 1 litre of 10 × SDS-PAGE running buffer:

Tris-base (Merck)	30.3 g
Glycine (Fisher Scientific)	150.14 g
SDS (Merck)	10 g
Distilled water	1000 ml (qsp)

Appendix 12

Coomassie blue solution (R-250)

Coomassie Blue R-250 (Bio-Rad)	0.6 g
Methanol (Schedelco)	250 ml
Glacial acetic acid (Schedelco)	50 ml
Distilled water	500 ml (qsp)

Appendix 13

Destaining solution

Methanol (Schedelco)	400 ml
Glacial acetic acid (Schedelco)	100 ml
Distilled water	1000 ml (qsp)

Appendix 14

LB (Luria-Bertani) Medium

For a 1 litre preparation:

Tryptone (Oxoid)	10 g
Yeast extract (Oxoid)	5 g
NaCl (Sigma-Aldrich)	10 g
Distilled water	1000 ml (qsp)

1. The solution was adjusted to pH 7.2 with 5 M NaOH.
2. The mixture was then autoclaved at 121°C for 20 minutes.

Appendix 15

LB (Luria-Bertani) Agar plate

For a 1 litre preparation:

Agar Technical (Agar No. 3) (Oxoid)	12 g
LB medium	1000 ml (qsp)

1. The mixture was then autoclaved at 121°C for 20 minutes.
2. It was then cooled to 50°C before pouring into sterile petri dishes.
3. The plates were stored at 4°C until use.

Appendix 16

Ampicillin Stock (50 mg/ml)

For a 10 ml preparation:

Ampicillin (sodium salt) (Sigma-Aldrich)	500 mg
Distilled water	10 ml (qsp)

1. The solution was sterilized by filtering through a 0.22 µm filter (Millipore).

2. It was then kept as 500 µl aliquots at -20°C until use.

LB + Ampicillin (50 µg/ml) Agar Plate

For a 1 litre preparation:

AgarTechnical (Agar No. 3) (Oxoid)	12 g
LB medium	1000 ml (qsp)

1. The mixture was then autoclaved at 121°C for 20 minutes.

2. It was then cooled to 50°C before 1 ml of ampicillin (50 mg/ml) was added.

3. The LB+Amp plates were stored at 4°C until use.

Appendix 17

1M $CaCl_2$

For a 200 ml preparation:

$CaCl_2.6H_2O$ (Merck)	43.82 g
Distilled water	200 ml (qsp)

1. The solution was sterilized by filtering through a 0.22 µm filter (Millipore).
2. It was then kept as 10 ml aliquots at -20°C until use.
3. When using, dilute with 90 ml of distilled water, filter through 0.45 µm filter (Millipore) and keep on ice.

Appendix 18

100 mM Isopropyl-*β*-D-thiogalactoside (IPTG) stock

IPTG (Bio-Rad)	0.24 g
Distilled water	10 ml (qsp)

Dispense into 1 ml aliquots and store at -20ºC.

X-galactosidase (X-Gal) (20 mg/ml)

5-bromo-4-chloro-3-indolyl-ß-D-galactoside (Bio-Rad)	20 mg
Dimethylformamide (Sigma-Aldrich)	1 ml

Wrap in aluminium foil and store at -20ºC.

LB + Ampicillin (50 µg/ml) + IPTG + X-Gal plate

On a LB + Ampicillin agar plate (Appendix 16), add:

100 mM IPTG (Bio-Rad)	40 µl
20 mg/ml X-Gal (Bio-Rad)	40 µl

Spread with a spreader and incubate at 37ºC for 30 minutes.

Appendix 19

Phosphate buffered saline (PBS)

For 1 litre of 10 × PBS preparation:

NaCl (Sigma-Aldrich)	80 g
KH_2PO_4 (Merck)	2.4 g
$Na_2HPO_4.2H_2O$ (Merck)	14.4 g
KCl (Merck)	2 g
Distilled water	1000 ml (qsp)

The solution was adjusted to pH 7.4 before use.

Appendix 20

His-tag affinity chromatography buffers

(A) 8 × Binding buffer

Imidazole (Sigma-Aldrich)	1.36 g
NaCl (Sigma-Aldrich)	116.88 g
Tris-base (Merck)	9.69 g
Distilled water	500 ml (qsp)

pH was adjusted to 7.9 using 5N HCl.

(B) 8 × Charge buffer

$NiSO_4.6H_2O$ (Merck)	52.57 g
Distilled water	500 ml (qsp)

(C) 8 × Wash buffer

Imidazole (Sigma-Aldrich)	16.34 g
NaCl (Sigma-Aldrich)	116.88 g
Tris-base (Merck)	9.69 g
Distilled water	500 ml (qsp)

pH was adjusted to 7.9 using 5N HCl.

(D) 4 × Elute buffer

Imidazole (Sigma-Aldrich)	27.23 g
NaCl (Sigma-Aldrich)	11.69 g
Tris-base (Merck)	0.97 g
Distilled water	100 ml (qsp)

pH was adjusted to 7.9 using 5N HCl.

(E) 4 × Strip buffer

EDTA (Sigma-Aldrich)	14.89 g
NaCl (Sigma-Aldrich)	11.69 g
Tris-base (Merck)	0.97 g
Distilled water	100 ml (qsp)

pH was adjusted to 7.9 using 5N HCl.

Appendix 21

GGT activity assay reagents

(A) Assay buffer solution

Tris-base (Merck)	1.21 g
Distilled water	100 ml

The solution was adjusted to pH 8.0 before use.

(B) Donor substrate solution (γ-glutamyl-ρ-nitroanilide)

γ-glutamyl-ρ-nitroanilide (Sigma-Aldrich)	80 mg
1M HCl (VWR)	1 ml
Distilled water	19 ml

1. The substrate was dissolved at room temperature by stirring.
2. 30 ml distilled water was added and pH was adjusted to 8.0 using 0.05-0.1 g Tris base.
3. Distilled water was further added to a final volume of 60 ml.
4. Solution was aliquoted and stored at -20°C until use.

(C) Acceptor solution (Glycyl-glycine)

Glycyl-glycine (Sigma-Aldrich)	0.66 g
Distilled water	50 ml

The solution was adjusted to pH 8.0 and stored at -20°C until use.

Appendix 22

Lysis buffer for *H. pylori*

For a 100 ml preparation:

Tris-base (pH 7.5) (Merck)	0.606 g
NaCl (Sigma-Aldrich)	0.584 g
Glycerol (QRec)	10 ml
Triton-X 100 (Bio-Rad)	1 ml
Distilled water	100 ml (qsp)

Appendix 23

Coating buffer (0.1 M Sodium carbonate, pH 9.5)

$NaHCO_3$ (Sigma-Aldrich)	7.13 g
Na_2CO_3 (Merck)	1.59 g
Distilled water	1000 ml (qsp)

Appendix 24

PBS-Tween buffer (0.05%)

For a 1 litre preparation:

Tween 20 (Merck)	0.5 ml
1× PBS	1000 ml

Appendix 25

Western blot transfer buffer (pH 9.2)

For a litre of 1 × transfer buffer:

Tris-base (Merck)	3 g
Glycine (Fisher Scientific)	14.4 g
Methanol (Schedelco)	200 ml
Distilled water	1000 ml (qsp)

Appendix 26

CNBr affinity chromatography reagents

(A) Coupling buffer

$NaHCO_3$ (Sigma-Aldrich)	0.84 g
NaCl (Sigma-Aldrich)	2.922 g
Distilled water	100 ml (qsp)

Solution was adjusted to pH 8.3 before use.

(B) Blocking buffer

Tris-base (Merck)	1.21 g
Distilled water	100 ml (qsp)

Solution was adjusted to pH 8.0 before use.

(C) Elution buffer

Glycine (Fisher Scientific)	0.375 g
Distilled water	100 ml (qsp)

Solution was adjusted to pH 2.5 before use.

(D) Neutralization buffer

Na_2HPO_4 (Merck)	3.55 g
Distilled water	100 ml (qsp)

Solution was adjusted to pH 10.3 before use.

Appendix 27

Urease Reagent (pH 6.8)

For a 500 ml preparation:

Urea (Bio-Rad)	10 g
$NaH_2PO_4.H_2O$ (Merck)	0.22 g
Na_2HPO_4 (Merck)	0.51 g
Phenol Red (Sigma-Aldrich)	750 µl
Distilled water	500 ml (qsp)

1. Urea, $NaH_2PO_4.H_2O$, Na_2HPO_4 and distilled water were mixed and adjusted to pH 6.8.
2. The solution was sterilized by filtration through a 0.22 µm filter (Millipore).
3. Phenol red that was sterilized by autoclaving at 121°C for 20 minutes was then added to the filtrate.
4. The reagent was stored at 4°C until use.

During testing, 0.5 ml of the culture was added to 0.5 ml of urease test reagent. A colour change from yellow to magenta indicates a positive reaction.

Appendix 28

Growth medium for AGS cells

For a 1 litre preparation:

Nutrient Mixture F-12 Ham Kaighn's Modification	11.3 g
$NaHCO_3$ (Sigma-Aldrich)	1.17 g
Fetal calf serum (HyClone)	100 ml
Nanopure water	1000 ml (qsp)

The medium was filtered through a 0.22 µm filter (Corning) and stored at 4°C until use.

Appendix 29

Growth medium for HeLa cells and primary human macrophages

For a 1 litre preparation:

RPMI-1640 (Invitrogen)	890 ml
L-glutamine (200 mM) (Gibco)	10 ml
Fetal calf serum (HyClone)	100 ml

1. Fetal calf serum was filtered through a 0.22 µm filter (Millipore).

2. The solution was mixed well and stored at 4°C until use.

Appendix 30

Growth medium for primary human gastric epithelial cells

(A) Leibovitz's L-15 medium

Leibovitz's L-15 (Sigma-Aldrich)	98 ml
Penicillin/Streptomycin (Gibco)	1 ml
Fungizone/Amphotericin B (Gibco)	1 ml

(B) Coating solution

Fibronectin (1 mg/ml) (Gibco)	1 ml
Type I rat tail collagen (5 mg/ml) (Gibco)	1 ml
BSA (1 mg/ml) (Merck)	1 ml
Leibovitz's L-15 medium (Gibco)	100 ml (qsp)

(C) Enzymatic isolation of gastric cells

Collagenase Type II (Gibco)	87 mg
Dispase (Gibco)	68.5 mg
Trypsin Inhibitor (Gibco)	1 mg
BSA (Merck)	125 mg
Leibovitz's L-15 medium	100 ml (qsp)

(D) Growth medium for primary gastric cells

Nutrient Mixture F-12 Ham Kaighn's Modification	88 ml
Fetal calf serum (HyClone)	10 ml
Penicillin/Streptomycin (Gibco)	1 ml
Fungizone/Amphotericin B (Gibco)	1 ml

Appendix 31

Cytosolic and nuclear protein extraction buffers

(A) Buffer A

HEPES (Sigma-Aldrich)	240 mg
KCl (Merck)	70 mg
EDTA (Sigma-Aldrich)	3.7 mg
$MgCl_2$ (Merck)	31 mg
Tween 20 (Sigma-Aldrich)	0.2 ml
DTT (Bio-Rad)	15.42 mg
PMSF (Merck)	8.71 mg
Distilled water	100 ml (qsp)

(B) Buffer C

HEPES (Sigma-Aldrich)	480 mg
NaCl (Sigma-Aldrich)	2.3 g
EDTA (Sigma-Aldrich)	3.7 mg
$MgCl_2$ (Merck)	31 mg
Glycerol (QRec)	25 ml
DTT (Bio-Rad)	15.42 mg
PMSF (Merck)	8.71 mg
Distilled water	100 ml (qsp)

Appendix 32

Cell Lysis buffer

For a 100 ml preparation:

Tris-base (pH 7.5) (Merck)	0.606 g
NaCl (Sigma-Aldrich)	0.584 g
Glycerol (QRec)	10 ml
Triton-X 100 (Bio-Rad)	1 ml
Protease inhibitor (Roche)	10 tablets
Distilled water	100 ml (qsp)

Appendix 33

MTT assay reagents

(A) MTT [3-(4, 5- dimethylthiazolyl-2)-2, 5-diphenyltetrazolium bromide] stock solution

MTT (Sigma-Aldrich)	25 mg
PBS buffer (pH 7.4)	5 ml

The solution was filter sterilized and stored at 4°C.

(B) Lysis solution

SDS (Merck)	10 g
Dimethyl sulfoxide (MP Biomedicals)	99.4 ml
Glacial acetic acid (Schedelco)	0.6 ml

Appendix 34

Neutral red dye uptake assay reagents

(A) BSA-PBS solution (0.3% w/v)

BSA (Merck)	0.3 g
PBS buffer (pH 7.4)	100 ml

(B) Neutral red dye solution (0.05% w/v)

Neutral red (BDH Chemicals)	0.05 g
BSA-PBS solution (0.3% w/v)	100 ml

The solution was filtered through a 0.22 µm filter before use.

(C) Neutral red dye extraction solution

Ethanol (Sigma-Aldrich)	70 ml
HCl (37%) (VWR)	1 ml
Distilled water	29 ml (qsp)

Appendix 35

Live-cell imaging of *H. pylori*-infected AGS cells

Video 1. AGS cells infected with *H. pylori* wild type for 24 hours.

Video 2. AGS cells infected with *H. pylori* Δ*ggt* for 24 hours.

Video 3. Uninfected AGS cells.